

GEOLOGICAL AND GEOTECHNICAL FACTORS RESPONSIBLE FOR LANDSLIDE  
SUSCEPTIBILITY OF THE KOPE FORMATION IN CINCINNATI, OHIO

A thesis submitted  
To Kent State University in partial  
Fulfillment of the requirements for the  
Degree of Masters of Science

by  
Michael P. Glassmeyer

December, 2014

Thesis written by

Michael Patrick Glassmeyer

B.S., Northern Kentucky University, 2009

M.S., Kent State University, 2014

Approved by

Dr. Abdul Shakoor, Advisor

Dr. Daniel Holm, Chair, Department of Geology

Dr. James Blank, Dean, College of Arts and Sciences

## TABLE OF CONTENTS

LIST OF FIGURES.....	vii
LIST OF TABLES.....	xiv
ACKNOWLEDGEMENTS.....	xv
ABSTRACT.....	1
CHAPTER	
1. INTRODUCTION.....	3
1.1 Background.....	3
1.2 Topography Geology of Cincinnati Area.....	5
1.2.1 Topography of the Cincinnati Area.....	5
1.2.2 Geology of the Cincinnati Area.....	5
1.2.2.1 Kope Formation and Associated Colluvium.....	6
1.2.2.2 Glacially Deposited Soils.....	9
1.3 Types of Slope Movement Associated with the Kope Formation.....	9
1.3.1 Rotational Landslides.....	10
1.3.2 Translational Landslides.....	12
1.3.3 Complex Landslides.....	12
1.3.4 Rapid Earth Flows.....	14

	1.4 Typical Methods of Remediation.....	14
	1.5 Study Objectives.....	15
2	PREVIOUS RESEARCH.....	16
3	METHODOLOGY.....	21
	3.1 Field Investigations.....	21
	3.1.1 Landslide Inventory Map.....	21
	3.1.2 Site Selection.....	23
	3.1.3 Field Data Collection.....	23
	3.1.4 Sampling.....	25
	3.2 Laboratory Investigations.....	29
	3.2.1 Natural Water Content.....	29
	3.2.2 Grain Size Distribution Analysis.....	29
	3.2.3 Atterberg Limits.....	30
	3.2.4 Direct Shear Test.....	30
	3.2.5 Slake Durability Test.....	31
	3.3 Stability Analysis Using the Slide Program.....	31
4	LABORATORY DATA PRESENTATION AND ANALYSIS.....	32
	4.1 Natural Water Content.....	32
	4.2 Grain Size Distribution.....	32
	4.3 Atterberg Limits.....	35
	4.4 Clay Content and Clay Mineralogy.....	35
	4.5 Slake Durability.....	38
	4.6 Strength Parameters.....	38



5	DESCRIPTION AND ANALYSIS OF SELECTED SLOPE FAILURES.....	41
	5.1 General Description of Sites Studied.....	41
	5.1.1 Rotational Failures.....	41
	5.1.2 Translational Slope Failures.....	43
	5.2 Stability Analysis.....	43
	5.2.1 Ten Mile Road Landslide Stability Analysis.....	43
	5.2.2 Wagner Road Landslide Stability Analysis.....	45
	5.2.3 Columbia Parkway Landslide Stability Analysis.....	45
6	DISCUSSION.....	49
	6.1 Landslide Inventory Map.....	49
	6.2 Factors Responsible for the Landslide Susceptibility of the Kope Formation.....	49
	6.2.1 Strength Parameters.....	49
	6.2.2 Groundwater.....	53
	6.2.3 Human Activity.....	56
	6.2.4 Disintegration and Erodability of the Bedrock.....	56
	6.2.5 Undercutting of the Slope Toe.....	58
	6.2.6 Steepness of Slopes.....	58
7	CONCLUSIONS AND RECOMENDATIONS.....	60
	7.1 Conclusions.....	60
	7.2 Recommendations.....	61
	REFERENCES CITED.....	62

## APPENDICIES

I:	Geologic Maps of the Cincinnati, OH Area.....	72
II:	LiDAR Derived Maps and Aerial Photographs.....	76
III:	Grain Size Distribution Analysis Results.....	82
IV:	Direct Shear Test Results.....	93
V:	Description and Analysis of Selected Slope Failures.....	99
VI:	LiDAR Derived Maps and Aerial Photographs of Selected Slope Failures.....	133
VII:	Borehole Logs for the Wagner Road Landslide.....	194

## LIST OF FIGURES

### Figure

1.1	Landslide susceptibility and incidence map of Ohio.....	4
1.2	Generalized geologic stratigraphic column of bedrock in the Cincinnati, Ohio area.....	7
1.3	Map showing the extent of the Kope Formation in the Cincinnati area.....	8
1.4	Cross section of a typical rotational landslide that occurs in colluvium derived from the Kope Formation.....	11
1.5	Cross section of a typical translational landslide that occurs in colluvium derived from the Kope Formation.....	13
3.1	Landslide inventory map for the Kope Formation and the colluvial soils derived from it within the Cincinnati area.....	22
3.2	Map showing the locations of the landslide sites selected for detailed study.....	24
3.3	Landslide features as defined by the International Association of Engineering Geology Commission on Landslides.....	26
3.4	Landslide geometry as defined by the International Association of Engineering Geology Commission on Landslides.....	28
4.1	Grain size distribution curve for the colluvial soil from the Eight Mile Road landslide site.....	34
4.2	Grain size distribution curve for the colluvial soil from the Columbia Parkway landslide site.....	34
4.3	Atterberg limits of the fine-grained fraction of the colluvial soil from the landslide sites, plotted on the Casagrande's plasticity chart.....	37
5.1	Map showing the locations of the landslide sites selected for detailed study.....	42

5.2	Critical surface for the minimum factor of safety for dry and saturated conditions for the Ten Mile Road landslide as determined by the Slide program.....	44
5.3	Critical Surface for the minimum factor of safety for wet and dry conditions for the Wagner Road landslide as determined by the Slide program.....	46
5.4	Critical Surface for the minimum factor of safety for wet and dry conditions as determined by the Slide program for the Columbia Parkway landslide.....	48
6.1	Relationship between cohesion and factor of safety for the Ten Mile Road landslide.....	50
6.2	Relationship between friction angle and factor of safety for the Ten Mile Road landslide.....	50
6.3	Relationship between cohesion and factor of safety for the Wagner Road landslide.....	51
6.4	Relationship between friction angle and factor of safety for the Wagner Road landslide.....	51
6.5	Relationship between cohesion and factor of safety for the Columbia Parkway landslide.....	52
6.6	Relationship between friction angle and factor of safety for the Columbia Parkway landslide.....	52
6.7	Relationship between water table location and factor of safety for the Ten Mile Road landslide.....	54
6.8	Relationship between water table location and factor of safety for the Wagner Road landslide.....	54
6.9	Relationship between water table location and factor of safety for the Columbia Parkway landslide.....	55
6.10	Relationship between load applied to the top of the slope and factor of safety for the Wagner Road landslide.....	57
6.11	Undercutting the toe of the slope at the Berkshire Road landslide.....	59
AI.1	Map showing the extent of the Kope Formation bedrock in the Cincinnati, Ohio area.....	73
AI.2	Map showing the surficial deposits of the Kope Formation in the Cincinnati, Ohio area.....	74

AI.3 Map showing the colluvium derived from the Kope Formation in the Cincinnati, Ohio area.....	75
AII.1 Slope map generated from LiDAR data of the Cincinnati, Ohio area.....	77
AII.2 Hillshade map generated from LiDAR Data of the Cincinnati, Ohio area.....	78
AII.3 DEM map generated from LiDAR Data of the Cincinnati, Ohio area.....	79
AII.4 Topographic map generated from LiDAR Data of the Cincinnati, Ohio area.....	80
AII.5 Aerial photograph of the Cincinnati, Ohio area.....	81
AIII.1 Eight Mile Road landslide grain size distribution analysis results.....	83
AIII.2 Nine Mile Road landslide grain size distribution analysis results.....	84
AIII.3 Ten Mile Road landslide grain size distribution analysis results.....	85
AIII.4 Berkshire Road landslide grain size distribution analysis results.....	86
AIII.5 Columbia Parkway landslide grain size distribution analysis results.....	87
AIII.6 Delhi Pike landslide grain size distribution analysis results.....	88
AIII.7 Elstun Road landslide grain size distribution analysis results.....	89
AIII.8 Nordyke Road landslide grain size distribution analysis results.....	90
AIII.9 Old US 52 landslide grain size distribution analysis results.....	91
AIII.10 Wagner Road landslide grain size distribution analysis results.....	92
AIV.1 Eight Mile Road landslide direct shear test results.....	94
AIV.2 Ten Mile Road landslide direct shear strength test results.....	94
AIV.3 Delhi Pike landslide direct shear strength test results.....	95
AIV.4 Elstun Road landslide direct shear strength test results.....	95
AIV.5 Nordyke Road landslide direct shear strength test results.....	96
AIV.6 Old US 52 landslide direct shear strength test results.....	96
AIV.7 Wagner Road landslide direct shear strength test results.....	97
AIV.8 Nine Mile Road landslide direct shear strength test results.....	97
AIV.9 Berkshire Road landslide direct shear strength test results.....	98

AIV.10	Columbia Parkway landslide direct shear strength test results.....	98
AV.1	Map showing the location of the Eight Mile Road landslide site.....	101
AV.2	View of the toe of the Eight Mile Road landslide.....	102
AV.3	Map showing the location of the Ten Mile Road landslide site.....	104
AV.4	The scarp face of the Ten Mile Road Landslide.....	105
AV.5	The toe of the Ten Mile Road landslide, undercut by a stream.....	105
AV.6	Map showing the location of the Delhi Pike landslide complex site.....	107
AV.7	Damage caused to Delhi Pike by the landslide.....	108
AV.8	Scarp face of one of the landslides at the Delhi Pike landslide complex site.....	108
AV.9	Toe of one of the landslides at the Delhi Pike landslide complex site.....	109
AV.10	Map showing the location of the Elstun Road Landslide site.....	111
AV.11	An example of the damage caused to Elstun Road as a result of landsliding.....	112
AV.12	The landslide toe (on right) of the Elstun Road landslide.....	112
AV.13	Map showing the location of the Nordyke Road landslide site.....	114
AV.14	Damage caused to Nordyke Road by landslide activity.....	115
AV.15	Head scarp of the Nordyke Road landslide.....	115
AV.16	Toe of the Nordyke Road landslide.....	116
AV.17	Map showing the location of the Old US 52 landslide site.....	118
AV.18	Scarp and toe the Old US52 landslide. Notice the small stream undercutting the toe.....	119
AV.19	Map showing the location of the Wagner Road landslide site.....	121
AV.20	Scarp and the associated displacement at the Wagner Road landslide site.....	122
AV.21	Toe at the Wagner Road landslide.....	122
AV.22	Remains of a retaining wall that had been constructed to stabilize Wagner Road.....	123
AV.23	Map showing the location of the 9 Mile Road landslide.....	125

AV.24	Scarp and toe of the 9 Mile Road landslide.....	126
AV.25	Map showing the location of the Berkshire Road landslide.....	128
AV.26	Scarp and toe of the Berkshire Road landslide. Notice the accumulation of landslide debris in the toe area.....	129
AV.27	Map showing the location of the Columbia Parkway landslide.....	131
AV.28	Head scarp of the Columbia Parkway landslide.....	132
AV.29	Toe of the Columbia Parkway landslide, emerging on the top of the retaining wall.....	132
AVI.1	Slope map of the Eight Mile Road landslide.....	134
AVI.2	Hillshade map of the Eight Mile Road landslide.....	135
AVI.3	Terrain map of the Eight Mile Road landslide.....	136
AVI.4	DEM map of the Eight Mile Road landslide.....	137
AVI.5	Topographic map of the Eight Mile Road landslide.....	138
AVI.6	Aerial photograph of the Eight Mile Road landslide. ....	139
AVI.7	Slope map of the Nine Mile Road landslide.....	140
AVI.8	Hillshade map of the Nine Mile Road landslide.....	141
AVI.9	Terrain map of the Nine Mile Road landslide.....	142
AVI.10	DEM map of the Nine Mile Road landslide.....	143
AVI.11	Topographic map of the Nine Mile Road landslide.....	144
AVI.12	Aerial photograph of the Nine Mile Road landslide.....	145
AVI.13	Slope map of the Ten Mile Road landslide.....	146
AVI.14	Hillshade map of the Ten Mile Road landslide.....	147
AVI.15	Terrain map of the Ten Mile Road landslide.....	148
AVI.16	DEM map of the Ten Mile Road landslide.....	149
AVI.17	Topographic map of the Ten Mile Road landslide.....	150
AVI.18	Aerial photograph of the Ten Mile Road landslide.....	151
AVI.19	Slope map of the Berkshire Road landslide.....	152

AVI.20	Slope map of the Berkshire Road landslide.....	153
AVI.21	Terrain map of the Berkshire Road landslide.....	154
AVI.22	Slope map of the Berkshire Road landslide.....	155
AVI.23	Topographic map of the Berkshire Road landslide.....	156
AVI.24	Aerial photograph of the Berkshire Road landslide.....	157
AVI.25	Slope map of the Columbia Parkway landslide.....	158
AVI.26	Hillshade map of the Columbia Parkway landslide.....	159
AVI.27	Terrain map of the Columbia Parkway landslide.....	160
AVI.28	DEM map of the Columbia Parkway landslide.....	161
AVI.29	Topographic map of the Columbia Parkway landslide.....	162
AVI.30	Aerial photograph of the Columbia Parkway landslide.....	163
AVI.31	Slope map of the Delhi Pike landslide.....	164
AVI.32	Hillshade map of the Delhi Pike landslide.....	165
AVI.33	Terrain map of the Delhi Pike landslide.....	166
AVI.34	DEM map of the Delhi Pike landslide.....	167
AVI.35	Topographic map of the Delhi Pike landslide.....	168
AVI.36	Aerial photograph of the Delhi Pike landslide.....	169
AVI.37	Slope map of the Elstun Road landslide.....	170
AVI.38	Hillshade map of the Elstun Road landslide.....	171
AVI.39	Terrain map of the Elstun Road landslide.....	172
AVI.40	DEM map of the Elstun Road landslide.....	173
AVI.41	Topographic map of the Elstun Road landslide.....	174
AVI.42	Aerial photograph of the Elstun Road landslide.....	175
AVI.43	Slope map of the Nordyke Road landslide.....	176
AVI.44	Hillshade map of the Nordyke Road landslide.....	177



AVI.45	Terrain map of the Nordyke Road landslide.....	178
AVI.46	DEM map of the Nordyke Road landslide.....	179
AVI.47	Topographic map of the Nordyke Road landslide.....	180
AVI.48	Aerial photograph of the Nordyke Road landslide.....	181
AVI.49	Slope map of the Old US 52 landslide.....	182
AVI.50	Hillshade map of the Old US 52 landslide.....	183
AVI.51	Terrain map of the Old US 52 landslide.....	184
AVI.52	DEM map of the Old US 52 landslide.....	185
AVI.53	Topographic map of the Old US 52 landslide.....	186
AVI.54	Aerial photograph of the Old US 52 landslide.....	187
AVI.55	Slope map of the Wagner Road landslide.....	188
AVI.56	Hillshade map of the Wagner Road landslide.....	189
AVI.57	Terrain map of the Wagner Road landslide.....	190
AVI.58	DEM map of the Wagner Road landslide.....	191
AVI.59	topographic map of the Wagner Road landslide.....	192
AVI.60	Aerial photograph of the Wagner Road landslide.....	193
AVII.1	Borehole log of the Wagner Road landslide.....	195
AVII.2	Borehole log of the Wagner Road landslide.....	196

## LIST OF TABLES

### Table

3.1 Definitions of landslide features as identified in Figure 3.3.....	27
3.2 Definitions of landslide geometric features as identified in Figure 3.4.....	28
4.1 Natural water content values for the colluvial soil samples from the landslide sites studied.....	33
4.2 Atterberg limits of the fine-grained fraction of the colluvial soil from the studied sites.....	36
4.3 Slake durability index test results for the bedrock samples from translational landslide sites.....	39
4.4 Shear strength parameters for the failure developing through the colluvial soil.....	40
4.5 Shear strength parameters for failure developing along the soil bedrock contact.....	40

## ACKNOWLEDGEMENTS

I would like to thank my adviser, Dr. Abdul Shakoor, who has been a constant source of support and guidance through my project. Over the years you have taught me so much. Thank you.

I would also like to thank my committee members Dr. Daniel Holm and Dr. David Hacker for their contributions.

I would like to thank the Hamilton County Engineers and the Clermont County Engineers offices for sharing landslide location data and for allowing me to access various landslide sites and for providing information regarding known landslides. I would also like to thank Terracon for sharing me subsurface data and remediation plans for the Wagner Road Landslide.

I would like to offer a special thanks to Scott Sinclair and Jim, I am grateful for all the sacrifices they made to assist me in the field. I would like to acknowledge the help and support I received from Nate Saraceno during the laboratory and data analysis portions of the project. I am grateful for all the support that I received from my family, friends and classmates that I received through this project.

## ABSTRACT

GLASSMEYER, MICHAEL PATRICK, M.S. DECEMBER 2014      GEOLOGY

GEOLOGICAL AND GEOTECHNICAL FACTORS RESPONSIBLE FOR  
LANDSLIDE SUSCEPTIBILITY OF THE KOPE FORMATION IN CINCINNATI,  
OHIO (196 pp.)

Thesis Advisor: Abdul Shakoor

The objective of this study was to determine the factors responsible for the high frequency of landslide occurrence in the Kope Formation and the overlying colluvial soil present in the Cincinnati area and to prepare a landslide inventory map. . The area around Cincinnati is one of the most landslide susceptible regions in the United States. Several million dollars are spent yearly by the government and private entities to repair landslide damage. Landslides within the Cincinnati area generally occur in colluvium derived from the Kope Formation. The Kope Formation consists of approximately 80% shale inter-bedded with 20% limestone. The colluvium that is formed from the weathering of the shale consists of a low plasticity clay. There are two main types of slope failures that occur in the Cincinnati area: rotational slides and translational slides.

An inventory map was created using LiDAR data of the landslides that occurred in the colluvium derived from the Kope Formation. From the landslide inventory

map, ten landslides were chosen for detailed study and undisturbed samples were collected from each site for laboratory testing. Of the ten landslide sites chosen, seven were rotational and three were translational in nature. One sample, representative of the slide material was collected from each rotational landslide. Two samples were collected from each translational landslide, one from the overlying colluvial soil and one from the underlying bedrock. Tests were conducted to determine natural water content, Atterberg limits, shear strength parameters, dry density, grain size distribution, and slake durability. For the translational landslides, strength parameters were determined by shearing the sample along the contact between the bedrock and the overlying colluvium.

Multiple factors were found to contribute to landslide susceptibility of the Kope Formation and the overlying colluvium. These factors include: low shear strength of the colluvial soil; development of pore water pressure within the slope; human activities such as the addition of weight to the top of the slopes or the removal of material from the base of the slope; low to very low durability of the bedrock that allows rapid disintegration of the bedrock and accumulation of colluvial soil; undercutting of the slope toe by stream water; and the steepness of slopes.

## CHAPTER 1

### INTRODUCTION

#### 1.1 Background

The Cincinnati area, including the Hamilton and Clermont Counties, is located in the southwest corner of Ohio and is characterized by extensive landslide activity (Ohio EMA, 2011). Landslides in the Cincinnati area occur in glacial soils, bedrock, and colluvial soils derived from bedrock (Fleming, 1975). Although a majority of these landslides are associated with the Kope Formation and the overlying colluvial soil, some landslides also occur in the colluvial soils that overlie the Fairview Formation. Most landslides in the Cincinnati area occur during late winter into early spring, but they may occur at any time throughout the year (Fleming, 1975).

The Cincinnati area is one of the most landslide susceptible areas in the United States (Ohio EMA, 2011). Figure 1.1 shows areas in Ohio that are most susceptible to landslides and have the highest landslide incidence. The red color in the figure indicates high landslide susceptibility and incidence, dark green indicates areas of high susceptibility and moderate incidence, light green indicates areas of high susceptibility and low incidence, yellow indicates areas of moderate susceptibility and moderate incidence, orange indicates areas of moderate susceptibility and low incidence, and tan indicates areas of low susceptibility and low incidence of landslides. The map also indicates the regional susceptibility and incidence of landslides with region 1 having an

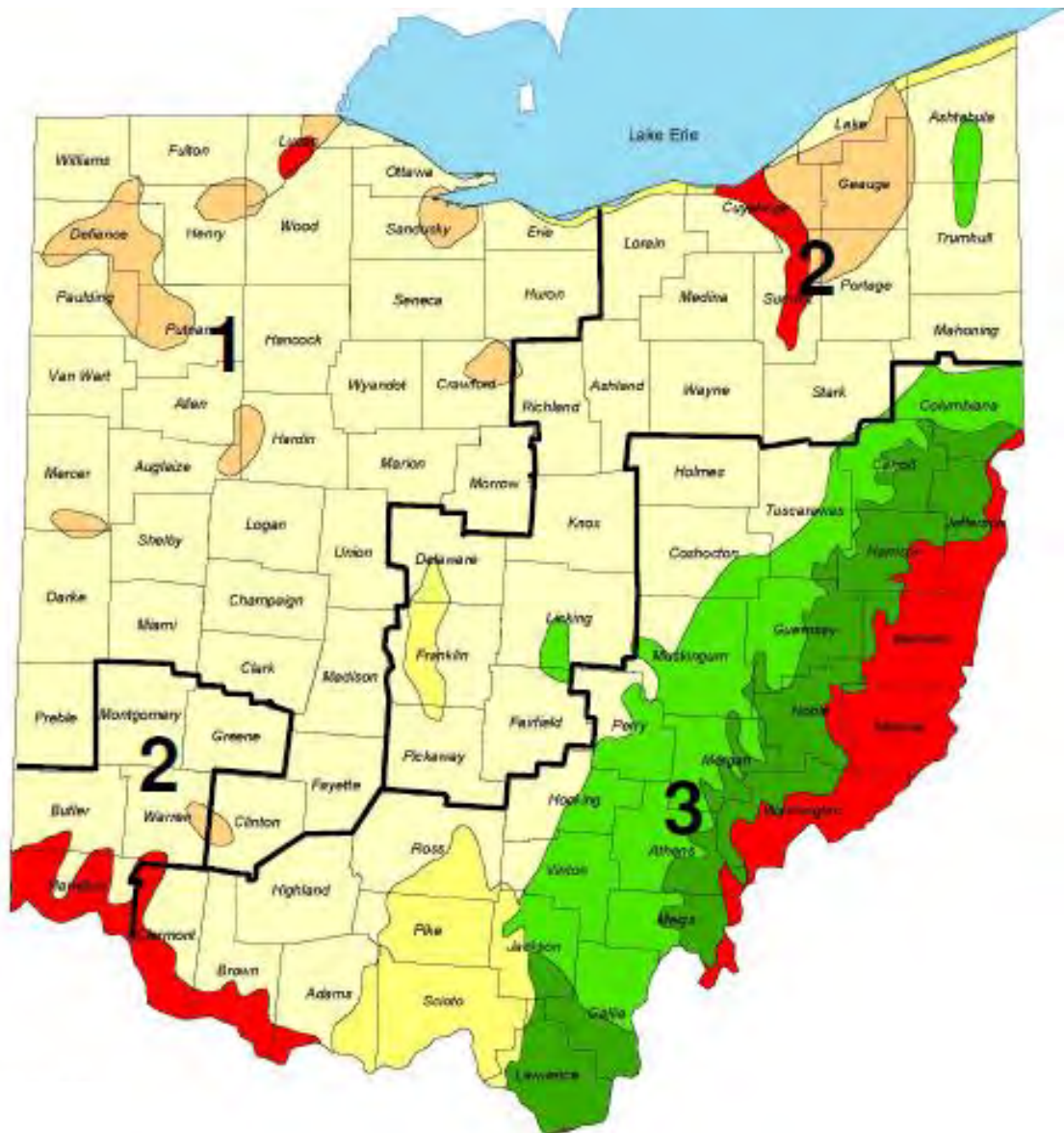


Figure 1.1: Landslide susceptibility and incidence map of Ohio, red indicates high landslide susceptibility and incidence, dark green represents areas of high susceptibility and moderate incidence, light green indicates areas of high susceptibility and low incidence, yellow indicates areas moderate susceptibility and moderate incidence, orange indicates areas of moderate susceptibility and low incidence, and tan indicates areas of low susceptibility and low incidence (Ohio EMA, 2011).

overall low susceptibility and low incidence, region 2 having primarily moderate susceptibility and low incidence of landslides with areas that are highly susceptible and areas that have a high incidence of landslides, and region 3 having a high susceptibility to landslides and low to high incidence of landslides (Ohio EMA, 2011).

Millions of dollars are spent each year on landslide damage and emergency road repairs in the Cincinnati area (Rockaway, 2002). The annual per capita cost for landslide damage in the Cincinnati area is \$5.80 in 1981 dollars, which is equivalent to \$17.00 in current dollars. This cost does not include the more than \$22 million in 1981 dollars, equivalent to \$64 million in current dollars, that was spent to stabilize a single landslide that occurred on Mount Adams during the construction of Interstate 471. One of the most costly time periods for landslide damage in the Cincinnati area occurred between 1973 and 1978 when, over a six-year period, an average of \$5.1 million in 1981 dollars, equivalent to \$14.9 million in current dollars, was spent per year to repair landslide damage (Schuster, 1996).

## 1.2 Topography and Geology of the Cincinnati Area

### 1.2.1 Topography of the Cincinnati Area

The Cincinnati area consists of an upland surface that is enveloped by the Illinoian age glacial deposits and has been dissected by ancient drainage systems as well as the modern Ohio River and its tributaries. Many of the tributaries are located in broad terraced valleys with steep slopes. The Cincinnati area has approximately 120 m (400 ft) of relief between the Ohio River and the hilltops (Baum and Johnson, 1996).

### 1.2.2 Geology of the Cincinnati Area

There are primarily two types of material in the Cincinnati area in which



landslides occur, the colluvium that is derived from the Kope Formation and glacial deposits from the Pre-Illinoian, the Illinoian, and the Wisconsinan glaciations. Glacial deposits mainly cover the upland areas of Cincinnati. The glacial deposits also form terraces along the Ohio River and its tributaries. Alluvium and outwash cover the valley floors and colluvium covers a majority of the hillsides. (Baum and Johnson, 1996). The Cincinnati area is located on the western flank of the Cincinnati Arch where the bedrock dips gently at about 1.5 to 2 meters (5 to 6.5 feet) per kilometer (0.7 mile), which amounts to less than 1 degree (Fleming, 1975). Figure 1.2 shows a generalized stratigraphic column of the bedrock in the Cincinnati area.

#### 1.2.2.1 Kope Formation and Associated Colluvium

The Kope Formation, Ordovician in age, is stratigraphically the lowest formation exposed in the Cincinnati area, and is overlain by the Fairview Formation. The contact between the two formations is at an elevation between 200 and 215 m (670 and 715 ft) (Gibbons, 1973). Figure 1.3 shows the extent of the Kope Formation in the Cincinnati area as indicated by the surficial geology map. The Kope Formation is more than 60 m (200 ft) thick and consists of inter-bedded, medium to dark grey, shale (80%) and coarse-grained fossiliferous limestone (20%) (Yahne, 1974; Fleming and Johnson, 1994). The shale is made up of illite, chlorite, calcite, and quartz (Yahne, 1974).

The limestone of the Kope Formation, which can be seen at any location in the Cincinnati area, contains three sets of near-vertical fractures occurring at regular spacing. The orientations of the fractures, however, vary between different locations (Hofman, 1966; Brett and Algeo, 2001; Brett et al., 2003). The shale of the Kope Formation also contains steeply dipping fractures (Richards, 1982; Baum, 1983). Fractures, small local

System	Series	KENTUCKY (U.S. Geological Survey)	OHIO (Ohio Department of Natural Resources)
ORDOVICIAN	Upper Ordovician	Bull Fork Formation 26+ m (85+ ft) 50% shale	Undifferentiated 0 - 41+ m (0-135+ ft) % shale varies
		Grant Lake Limestone (Bellevue tongue) 2 - 10 m (2-33 ft) 0% shale	Bellevue Limestone 0 - 8 m (0-25 ft) 0% shale
		Miamitown Shale of Ford (1967)	Miamitown Shale 0 - 11 m (0-35 ft) 90% shale
		Fairview Formation ~30 m (~100 ft) 45 - 60% shale	Fairview Formation ~21 - 100 m (~70-100 ft) 60 - 75% shale
		Kope Formation 61+ m (200+ ft) 80 - 85% shale	Kope Formation 61+ m (200+ ft) 70 - 80% shale
	Middle and Upper Ordovician	Point Pleasant Formation ~30 m (~100 ft) 30 - 50% shale	Not exposed

Figure 1.2: Generalized stratigraphic column of bedrock in the Cincinnati area (Fleming, 1975).

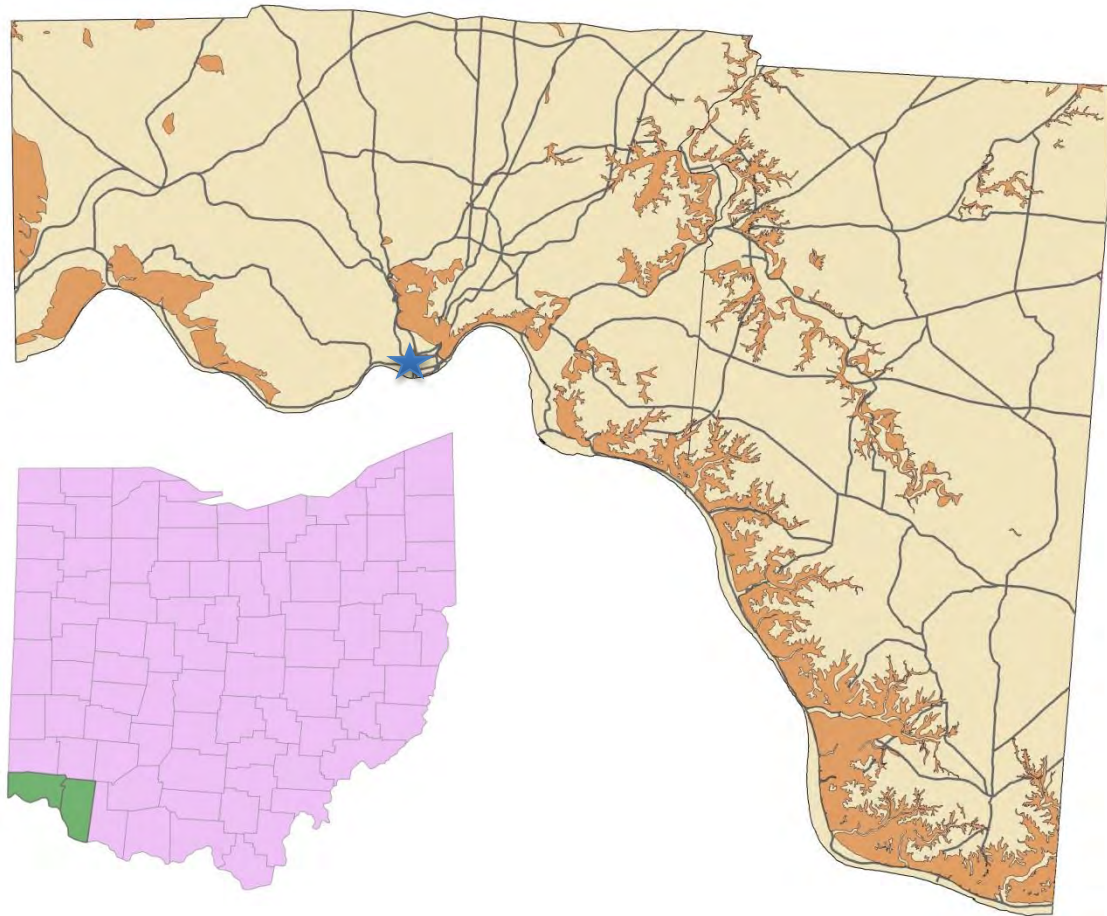


Figure 1.3: Map showing the extent of the Kope Formation in the Cincinnati area. The star indicates the location of downtown Cincinnati. The shaded area in the south west corner of the Ohio map shows Hamilton (left) and Clermont (right) counties.

solution channels, and nearly horizontal shale-limestone contacts are the main venues of groundwater movement within the bedrock (Fenneman, 1916).

The colluvium associated with the Kope Formation is classified as Eden silty clay loam according to the Hamilton county survey report and as clay of low plasticity (CL) according to the Unified Soil Classification System (USCS) (Lerch et al., 1982; Holtz et al., 2011). The colluvium ranges in thickness from a few centimeters up to 13 m (45 ft) (Fleming and Johnson, 1994) and covers many of the hillsides, especially the hillsides that been glaciated only during the pre-Illinoisan time. The colluvium is derived from weathered bedrock and consists of broken pieces of weathered limestone and a silty clay matrix (Fleming and Johnson, 1994).

#### 1.2.2.2 Glacially Deposited Soils

There are at least three major episodes of glaciations that have affected the Cincinnati area: the Pre-Illinoisan, Illinoisan, and the Wisconsinan glaciations. These glaciation episodes changed the drainage pattern within the Cincinnati area and left glacial deposits in the valleys, on the upland areas, and on the hillsides (Durrell, 1961, 1977; Pavey et al., 1992). Prior to glaciation the Cincinnati area was a gently rolling plain and had north flowing streams with approximately 45 m (150 ft) deep valley (Durrell, 1977; Potter, 2007).

### 1.3 Types of Slope Movement Associated with the Kope Formation

Landslides associated with the Kope Formation occur in both the bedrock and within the colluvial soil that covers the bedrock. Slides that occur within the colluvial soil or along the contact between the colluvial soil and the bedrock are much more common than the slides that occur within the bedrock of the Kope Formation. The types of slope

movement associated with the Kope Formation are rotational slides, translational slides, rapid earthflows, rockfalls, combination of rotational and translational slides (complex slides), and soil creep, with rotational landslides and translational landslides being the most common and rockfalls and creep being the least common. A brief description of the main types of slope movement that are associated with the Kope Formation is given below.

### 1.3.1 Rotational Landslides

A rotational landslide is a type of slope failure in which movement occurs along a curved and concaved surface (Cruden and Varnes, 1996). Rotational landslides are very common in the colluvium derived from the Kope Formation. Rotational landslides are generally 2 -15 m (6 ft - 50 ft) thick, 30 - 300 m (100 ft - 1000 ft) in width (measured perpendicular to the direction of sliding), and 30 -150 m (100 ft - 500 ft) in length (measured in the direction of sliding). They occur on slopes that are between 6 degrees and 15 degrees (Baum and Johnson, 1996). Figure 1.4 shows a cross section of a typical thick rotational slide in colluvium derived from the Kope Formation bedrock.

Some of the rotational slides that occur in the Kope Formation are due to natural processes, such as groundwater causing a buildup of pore pressure. However, a majority of the rotational slides are due to earthwork operations done in material that would be stable under normal conditions (Fleming and Johnson, 1994). Most of the rotational slides are characterized by a single major scarp, also known as the head scarp, and a few minor scarps. The lateral margins of the slides are often poorly defined (Baum and Johnson, 1996).

The presence of springs and local marshy ground at a rotational slide indicates

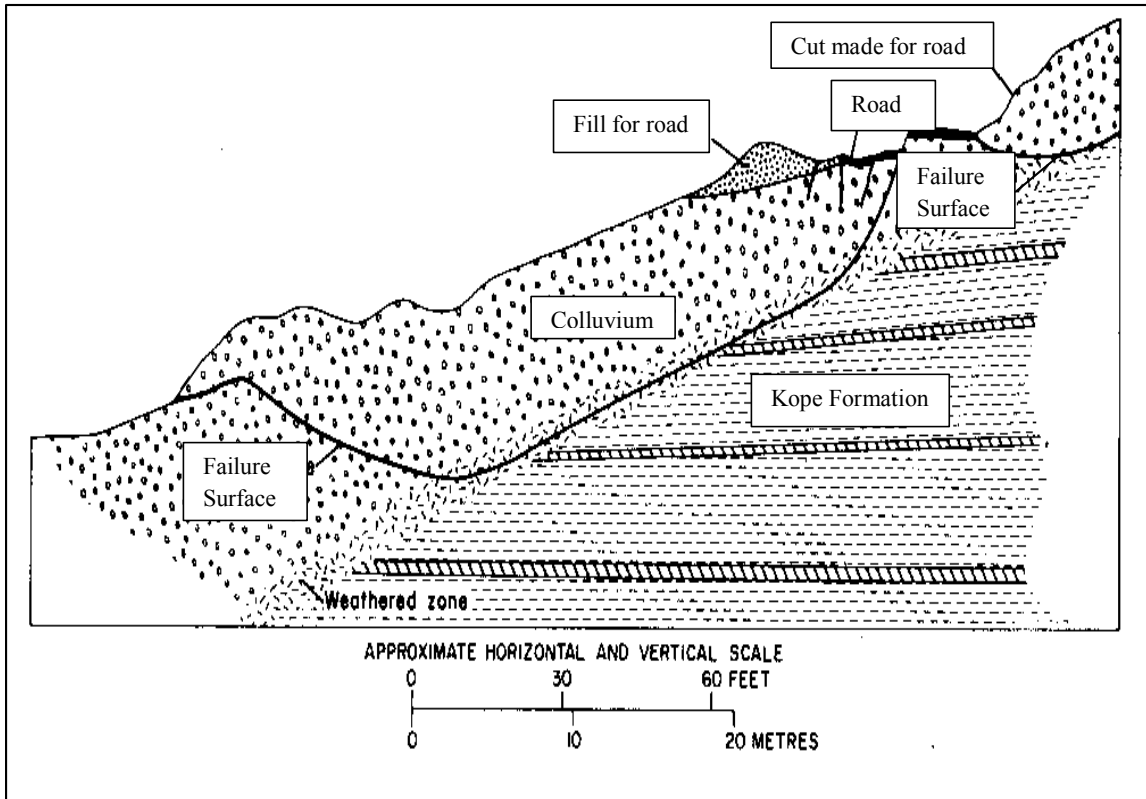


Figure 1.4: Cross section of a typical rotational landslide that occurs in colluvium derived from the Kope Formation (Fleming, 1975).

that a portion of the slide is saturated. The springs usually exist at the base of the toe of a landslide, and are indicated by the large amount of vegetation that can be seen in the toe areas of many landslides. Marshy areas are either at the base of the toe of a landslide or they are located on top of the toe (Fleming and Johnson, 1994).

### 1.3.2 Translational Landslides

A translational landslide is a type of slope movement where a mass of sliding material is displaced along a planar or undulating surface of rupture (Cruden and Varnes, 1996). Translational slides are very common in thin colluvial soils covering steep slopes. These slides are generally 10 - 150 m (33 – 500 ft) in width and 30 – 130 m (100 ft – 430 ft) in length. They occur on slopes that are 15 – 30 degrees. The translational slides can vary in shape from long and narrow to wide and short (Richards, 1982). Figure 1.5 shows the typical cross section of a translational landslide seen in the Cincinnati area. Translational slides generally occur during the spring because the slide material, the colluvium derived from the Kope Formation, is almost 100% saturated between the months of January and May (Haneberg, 1991).

The dominant form of deformation in translation slides is longitudinal stretching. A large majority of the translational slides have a number of scarps that face downhill, which is consistent with longitudinal stretching. The well-developed flanks of the slide are indicated by the presence of troughs or scarps. The failure plane is close to or is located along the irregular contact between the colluvium and the underlying bedrock (Baum and Johnson, 1996).

### 1.3.3 Complex Landslides

Complex landslides are made up of one or more thin slides, that are joined

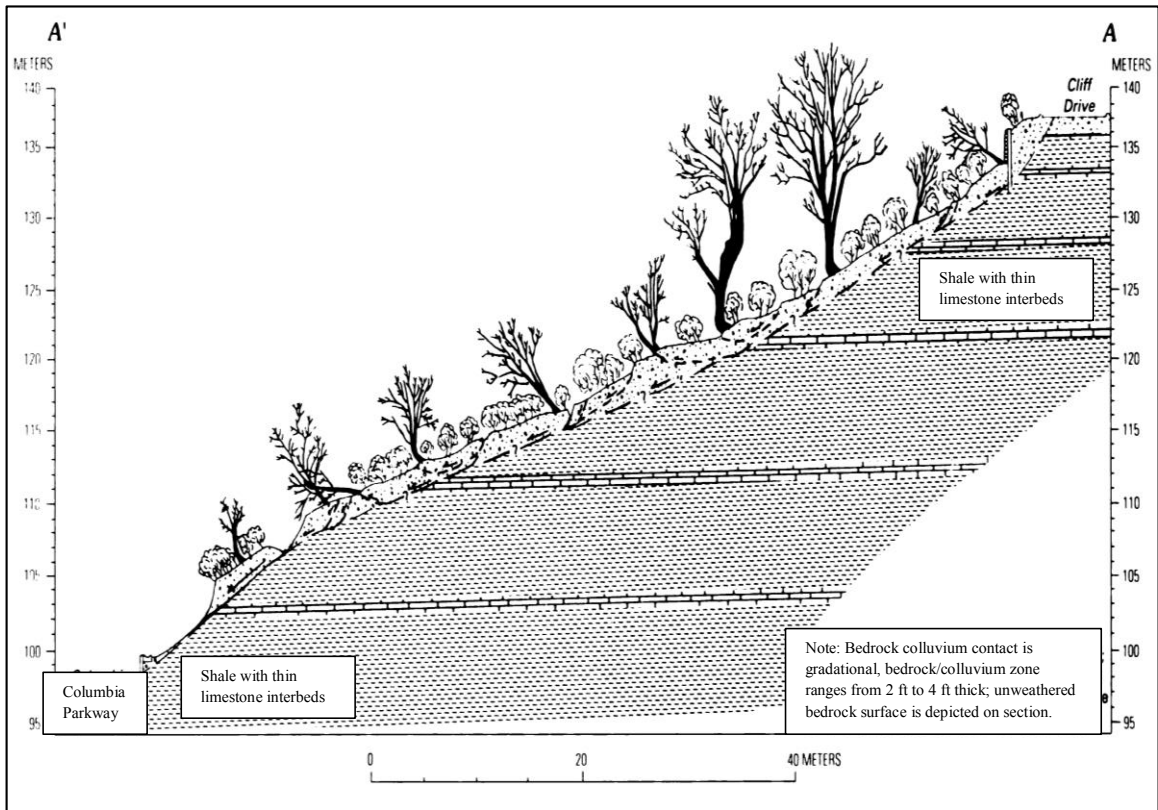


Figure 1.5: Cross section of a typical translational landslide that occurs in colluvium derived from the Kope Formation (Baum and Johnson, 1996).



together to make a thick landslide. The thin landslides are on the upper part of the hillside and contain a series of scarps; the thick landslides are confined to the lower portion of the hillside and will contain internal toes. The thin landslides usually act as the head and the thick landslides act as the toe of the landslide complex. The Delhi Pike Landslide complex is an example of a complex landslide (Baum and Johnson, 1996).

#### 1.3.4 Rapid Earth Flows

A rapid earthflow is a spatially continuous movement that contains surfaces of shear that are short-lived and that are closely spaced (Cruden and Varnes, 1996). Rapid earthflows occur on steeper slopes that are underlain by the Kope Formation and are common along the Columbia Parkway. In the Cincinnati area rapid earthflows are commonly referred to as mudslides. Rapid earthflows commonly spill on to roadways and disrupt traffic. They occur during wet periods in areas where the overlying colluvium is thin, < 2 meters (6.6 feet) and is clayey in nature (Pohana, 1983). Rapid earthflows involve the movement of the entire thickness of the colluvium, with the failure plane along the contact between the bedrock and the colluvium, which results in exposing the bedrock (Fleming, 1975; Richards, 1982; Riestenberg and Sovonik-Dunford, 1983).

#### 1.4 Typical Methods of Remediation

There are several methods of remediation that are used by both the county and the city government agencies. One of the most common methods used when a landslide causes damage to a road is to pave over the damaged section. This is done when it is determined that the movement of the slope is too slow for any permanent solution to be cost effective. There are several roads in the area where this method has been used for more than twenty years and has resulted in the pavement of some roads being in excess of

2.5 m (8 ft) thick. Another common method of remediation that is used is the pier retaining wall built to support the hillside. The placement of a pier wall is currently one of the most widely used methods of slope stabilization in the Cincinnati area. Another method is the placement of a crib wall or a concrete gravity retaining wall. Some less common methods include the use of soil nails or the placement of gabions.

### 1.5 Study Objectives

Although landslides in the Cincinnati area have been studied extensively, the susceptibility of the Kope Formation to landslide occurrence has not been investigated specifically. Thus, the main objective of this study was to investigate as to why the Kope Formation and the colluvium derived from it are so highly susceptible to landsliding.

The following tasks were chosen to accomplish the main objective:

- 1) Determine the engineering properties of the Kope Formation and the overlying colluvium.
- 2) Identify the types of slope movement that affect the Kope Formation.
- 3) Evaluate the triggering mechanisms of slope failures in the Kope Formation and the overlying colluvium.
- 4) Create a landslide inventory map for Kope Formation and the associated colluvium within the Cincinnati area.
- 5) Explain the susceptibility of the Kope Formation and the overlying colluvium in terms of engineering properties, slope characteristics, and hydrologic conditions.

## CHAPTER 2

### PREVIOUS RESEARCH

Most landslide investigations in the Cincinnati area did not begin until after the 1970's and the descriptions of the local geology prior to 1970 only briefly mention landslides (Baum and Johnson, 1996). The studies that have been conducted since the 1970's have either focused on the Delhi Pike landslide complex, or on a small specific area. Also, most of the previous studies on landslides did not discriminate between the type of material in which the slides occurred (e.g. colluvium derived from the Kope Formation, glacial deposits, or lake bed clays deposited during several glaciation events).

There have been two studies done to produce landslide susceptibility maps for the Cincinnati area. The first study was conducted by Hough and Fleming (1974) who divided the Cincinnati area into three categories based on landslide susceptibility. The first category includes areas critical with respect to stability. The second category includes areas which have the potential for slope instability. The third category includes areas of stable bedrock or areas of glacial deposits which may or may not be susceptible to slope instability. The second study was by Sowers and Daltymple (1980). In this study, the landslide prone areas were divided into four categories: least susceptible, moderately susceptible, moderately to highly susceptible, and highly susceptible to landslides respectively.

In 1978 Dr. Arvid Johnson of the Department of Geology, the University of

Cincinnati, started a program to create detailed engineering geologic maps of portions of the Cincinnati area. Consequently eight engineering geology and related slope stability maps were created for areas in Hamilton County as a part of Masters' thesis mapping projects. These maps identified landslide areas and areas that had the potential for landsliding. The purpose of these maps was for the planning and development of specific areas in Hamilton County. These reports can also be used by geotechnical engineers and engineering geologists who may be interested in performing a detailed investigation within an area of a proposed development. In preparing these reports, Baum (1983) looked at the stability of the Fay Apartments and a section of the Mount Airy Forest area, Brockman (1983) looked at the stability Dry Run Creek area, Geiger (1983) looked at the stability of sections of Newport, Bellevue, and Fort Thomas, Kentucky, Lion (1983) studied the stability of a part of the Springfield Township area for the development of the hillsides, Pohana (1983) studied a part of the Anderson Township area, Richards (1983) studied the stability of Mount Adams and portions of Walnut Hills and Columbia Parkway, Rodriguez-Molina (1983) studied the stability of areas within Avondale, and Olson (1988) studied the stability around Sawyer Place.

In addition to the eight maps mentioned above, several theses and dissertations written at the University of Cincinnati on landslide mechanisms. Yahne (1974) conducted a preliminary study of landslides in Cincinnati, Ohio. McCandless (1976) studied the bulking of landslides by looking at the topography and density changes in landslide debris. Riestenberg (1981) studied the effect that vegetation has on the stability of slopes in the Cincinnati area, especially the increase in stability in thin colluvium caused by the roots of sugar maple and white ash. Murdock (1987) studied pore-water pressures and

unsaturated flow during infiltration at the Delhi Pike landslide complex. Gokce (1989) described the mechanisms of landsliding. Haneberg (1989) studied the effects of water in thin colluvium in Delhi Township.

Besides the studies that were conducted at the University of Cincinnati there are also several U.S.G.S. publications that deal with landslides in the Cincinnati area. Fleming and Taylor (1980) performed a study on estimating the cost of landslide damage. Baum (1994) looked at the contribution of artesian water pressure on progressive failure at the Delhi Pike landslide complex in detail. Fleming and Johnson (1994) studied the Delhi Pike landslide complex. Haneberg and Gokce (1994) studied the effects of rapid water level fluctuations in thin colluvium at the Delhi Pike landslide complex. Riestenberg (1994) studied the effect of sugar maple roots on the stability of slopes in the Cincinnati area. Baum and Johnson (1996) performed a study about the landslide problems, research, and mitigation methods in the Cincinnati area.

Other research examining landslides in the Cincinnati area includes the following studies: Exon (1929) did a senior thesis on the Riverside landslide, Von Schlichten (1935) studied landslides that were in the vicinity of Cincinnati, Scheper (1973) developed a report of landslide investigations in the Cincinnati area, Fleming (1975) and Hough (1978) performed overview studies of landslides in the Cincinnati area, and Fleming, Johnson, and Hough (1981) studied the engineering geology of the Cincinnati area for the 1981 Geological Society of America (GSA) field trip guide book. Taylor, Fleming, and Durrell (1981) studied the seasonal movements of landslides in the Cincinnati area. Riestenberg and Sovonik-Dunford (1983) studied the role that woody vegetation plays in the stabilization of hillside in the Cincinnati area. Bernkopf et al

(1985) studied the economics of landslide mitigation strategies. Bernknopf et al (1988) looked at a probabilistic approach to hazard mapping with applications for economic evaluation. Haneberg (1991) studied the pore pressure fluctuations in thin colluvium. Behringer and Shakoor (1992) looked at selected landslides and their relation to human activity. Gokce (1992) studied extrusion landslides in Cincinnati lake bed clays. Haneberg (1992) developed a mass balance model of the hydrologic response of fine-grained hillside soils to rainfall. Haneberg et al (1992) studied the geologic environment of Cincinnati for the development of a field trip guide book. Hutto (1992) performed a stability analysis on a landslide along Interstate 275. Pohana (1992) performed an overview study of landslides for the Hillside Trust. Pohana (1992) also evaluated the landslide prevention and remediation techniques used by the City of Cincinnati. Riestenberg (1992) studied the effect of two tree species interplanted in colluvium on the hillsides of Cincinnati. Pohana and Jamison (1993) looked at the remediation and prevention of landslides in the Cincinnati area.

There have also been several city and county reports on landsliding in the Cincinnati area. H.C. Nutting and Co. (1967) studied the physical features of the Cincinnati area in an unpublished report for Hamilton County. The Cincinnati City Planning Commission (1970) developed a plan and a program for the developing Cincinnati hillsides. Merritt (1975) performed a hillside development study to identify areas of critical environmental impact. The Hamilton County Regional Planning Commission (1976) studied the development of the hillsides and the effects of development on landslides in the Cincinnati area. The Earth Movement Task Force (1982) gave recommendations to mitigate the hazard that is associated with landslides in

the developed and undeveloped areas of Hamilton County in an unpublished report. The Earth Surface Process Group (1987) prepared a report and gave recommendations for the maintenance and repair of deteriorating retaining wall and streets that have been damaged by landslides. Smale (1987) looked at the infrastructure of the City of Cincinnati. The Cincinnati Hillside Trust studied the economic impact that landslides have on Cincinnati and Hamilton County. The Cincinnati Hillside Trust (1991) developed a hillside protection plan for the Cincinnati area that involved an overview study of the hillsides, identification of hillsides sensitive to sliding, and guidelines for development of the Greater Cincinnati hillsides.

## CHAPTER 3

### METHODOLOGY

#### 3.1 Field Investigations

##### 3.1.1 Landslide Inventory Map

In preparation for the field investigations, a landslide inventory map was developed for the Kope Formation and the overlying colluvial soils. Landslide data was collected from multiple sources including LiDAR (light detection and ranging) imagery, field observations, and city and county agencies. Three different layers were used to define the area mapped on the LiDAR maps. These layers included the extent of the Kope Formation in the Cincinnati area, as defined by the Ohio Department of Natural Resources (ODNR) bedrock geology map, the extent of the Kope Formation as defined by the ODNR surficial geology map, and the extent of the colluvium as defined by the ODNR soil survey. Appendix I provides the details of the three layers used. Landslides that were identified using the LiDAR derived maps were verified through field observations. Figure 3.1 shows the landslide inventory map.

The LiDAR data and aerial photographs were obtained from the Ohio Geographically Referenced Information Program (OGRIP). The LiDAR data were collected from 2006-2008 as a part of the Ohio Statewide Imagery Program I (OSIP I). The LiDAR data were collected with Leica ALS50 digital LiDAR systems. The average post spacing between LiDAR points was 2.1 m (7 ft) and the flying altitude was 2225 m



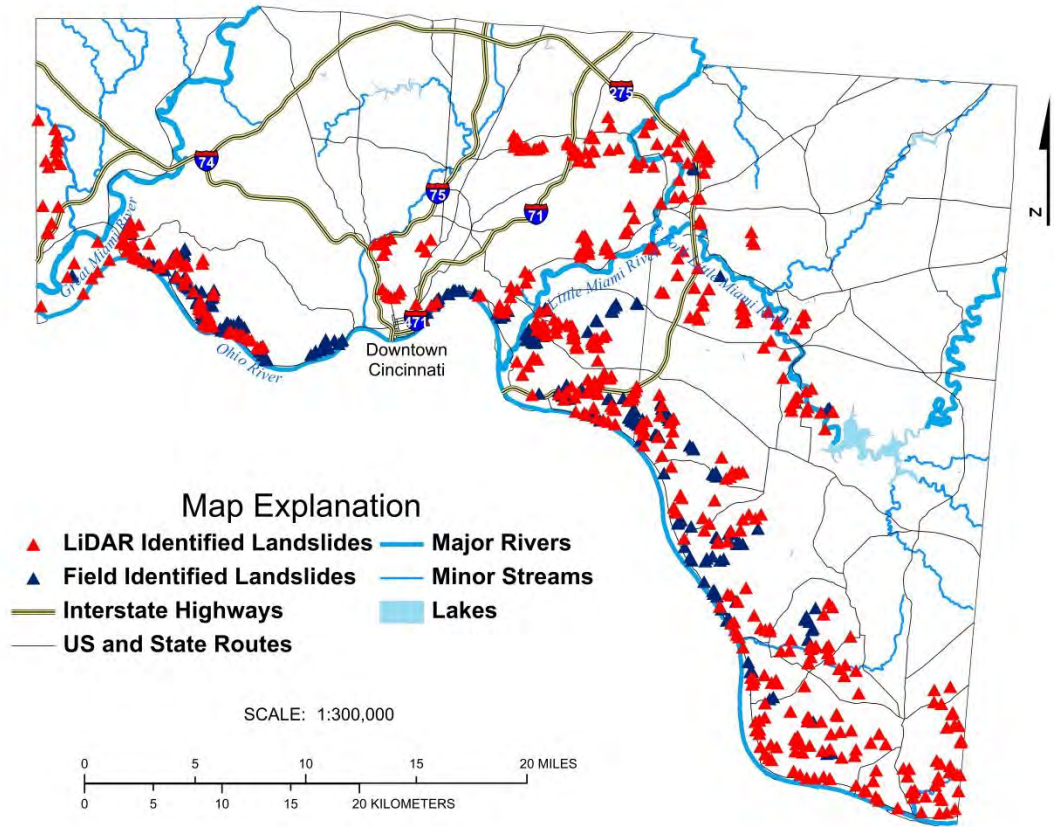


Figure 3.1: Landslide inventory map for the Kope Formation and the colluvial soils derived from it within the Cincinnati area.

(7,300 ft) at 170 knots (Ohio Office of Information Technology, 2007). The data for each county was divided up into tiles that were 1524 m (5000 ft) by 1524 m (5000 ft) square. The data is accurate to within 0.33 m (1 ft) (Ohio Office of Information Technology, 2006).

Since LiDAR data is a las, a blob point file, the data had to be converted into usable maps through the use of ArcGIS. The files had to be first converted from multipoint file to an ASCII files. The ASCII files were then converted to raster files. Once the raster files were created, a variety of different map types were developed including a slope map, a hillshade map, a DEM map, and a topography map, as shown in Appendix II.

Each map that was created was studied to look for landslide related features such as scarp or the toe bulges. The landslides that were identified from the LiDAR and aerial photographs were randomly verified through field observations. Verification of the landslides was done using the GPS.

### 3.1.2 Site Selection for Detailed Study

From the landslide inventory map ten landslide sites were chosen for detailed study. The sites were selected so to encompass a range of landslide sizes, landslide types, and geographic locations across the Cincinnati area. Figure 3.2 shows the landslide sites selected for detailed study.

### 3.1.3 Field Data Collection

Field data collected at each site included the thickness of the colluvium, the location of the failure plane with respect to slope face and whether the slide occurred in colluvium or within the bedrock, slope geometry including the slope height, slope angle,

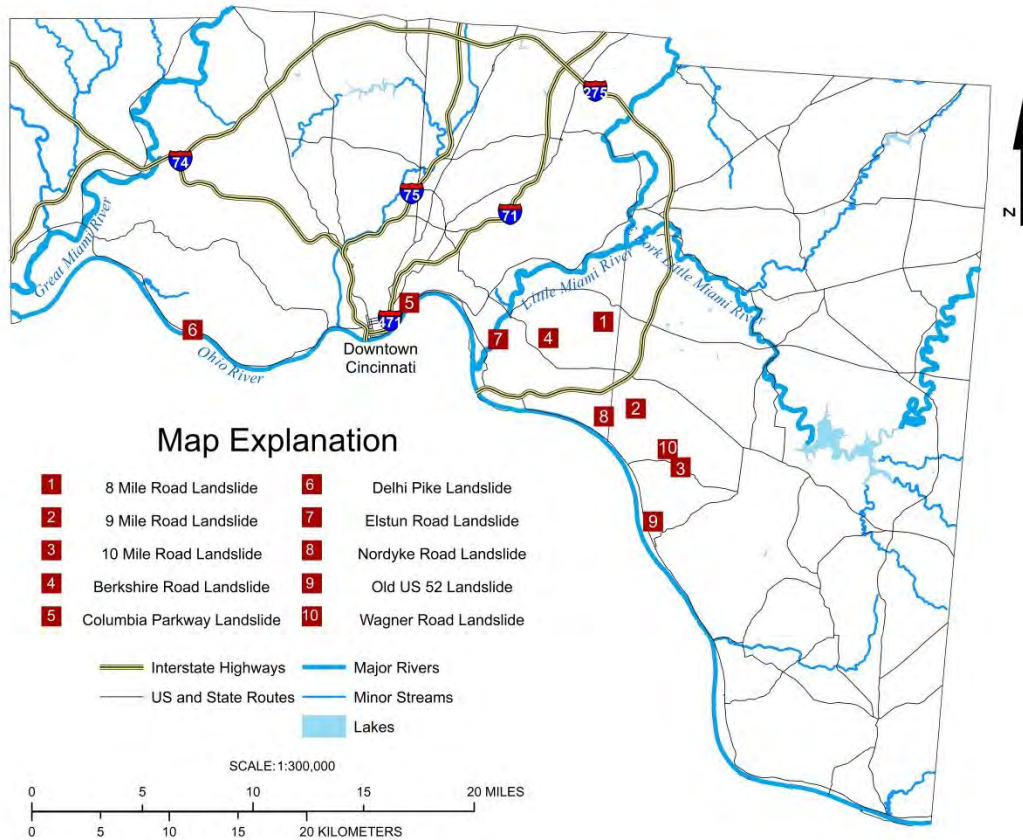


Figure 3.2: Map showing the locations of the landslide sites selected for detailed study.

and slope length, and landslide dimensions including the length and width of each slide. The type of slope movement was identified at each site in accordance with the Cruden and Varnes classification system (Cruden and Varnes, 1996). Where possible, information about the hydrogeologic conditions was obtained.

In order to properly describe the various types of landslide features at the selected sites, the standardized terminology recommended by the International Association of Engineering Geology (IAEG) Commission on Landslides (1990) was used, as shown in Figure 3.3 and defined in Table 3.1. The IAEG Commission on Landslides (1990) also provides the definitions for landslide dimensions as shown in Figure 3.4 and Table 3.2. The landslide dimensions were measured in accordance with the definitions provided in Figure 3.4 and Table 3.2.

#### 3.1.4 Sampling

An attempt was made to obtain undisturbed Shelby tube samples from local government agencies and also from local geotechnical companies. However, no undisturbed Shelby tube samples were available for any of the landslide sites. Therefore, undisturbed chunk samples were collected for laboratory testing. At least 5 kg (11 lb) of material, representative of the slide material was collected for each of the rotational and translational slides that were studied in detail. Additionally, 5 kg (11 lbs) of a bedrock sample was collected for each of the translational landslide sites. The collected samples were immediately sealed in air tight bags and then placed in five gallon plastic buckets. This was done to ensure that the natural water content of each sample was preserved and so that the sample would not slake.

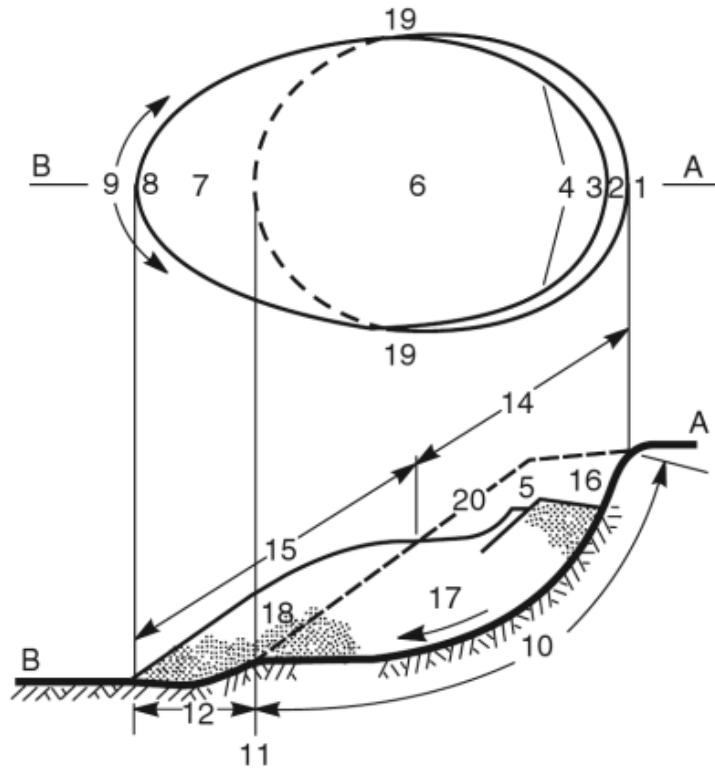


Figure 3.3: Landslide features as defined by the International Association of Engineering Geology Commission on Landslides (1990), the features are defined in Table 3.1.

Table 3.1: Definitions of landslide features as identified in Figure 3.3 (International Association of Engineering Geology Commission on Landslides, 1990).

Number	Name	Definition
1	Crown	Practically undisplaced material adjacent to highest parts of main scarp
2	Main scarp	Steep surface on undisturbed ground at upper edge of landslide caused by movement of displaced material (13, stippled area) away from undisturbed ground; it is visible part of surface of rupture (10)
3	Top	Highest point of contact between displaced material (13) and main scarp (2)
4	Head	Upper parts of landslide along contact between displaced material and main scarp (2)
5	Minor scarp	Steep surface on displaced material of landslide produced by differential movement within displaced material
6	Main body	Part of displaced material of landslide that overlies surface of rupture between main scarp (2) and toe of surface of rupture (11)
7	Foot	Portion of landslide that has moved beyond toe of surface of rupture (11) and overlies original ground surface (20)
8	Tip	Point on toe (9) farthest from top (3) of landslide
9	Toe	Lower, usually curved margin of displaced material of a landslide, most distant from main scarp (2)
10	Surface of rupture	Surface that forms (or that has formed) lower boundary of displaced material (13) below original ground surface (20)
11	Toe of surface of rupture	Intersection (usually buried) between lower part of surface of rupture (10) of a landslide and original ground surface (20)
12	Surface of separation	Part of original ground surface (20) now overlain by foot (7) of landslide
13	Displaced material	Material displaced from its original position on slope by movement in landslide; forms both depleted mass (17) and accumulation (18)
14	Zone of depletion	Area of landslide within which displaced material (13) lies below original ground surface (20)
15	Zone of accumulation	Area of landslide within which displaced material lies above original ground surface (20)
16	Depletion	Volume bounded by main scarp (2), depleted mass (17), and original ground surface (20)
17	Depletion mass	Volume of displaced material that overlies surface of rupture (10) but underlies original ground surface (20)
18	Accumulation	Volume of displaced material (13) that lies above original ground surface (20)
19	Flank	Undisplaced material adjacent to sides of surface of rupture; compass directions are preferable in describing flanks, but if left and right are used, they refer to flanks as viewed from crown
20	Original ground surface	Surface of slope that existed before landslide took place

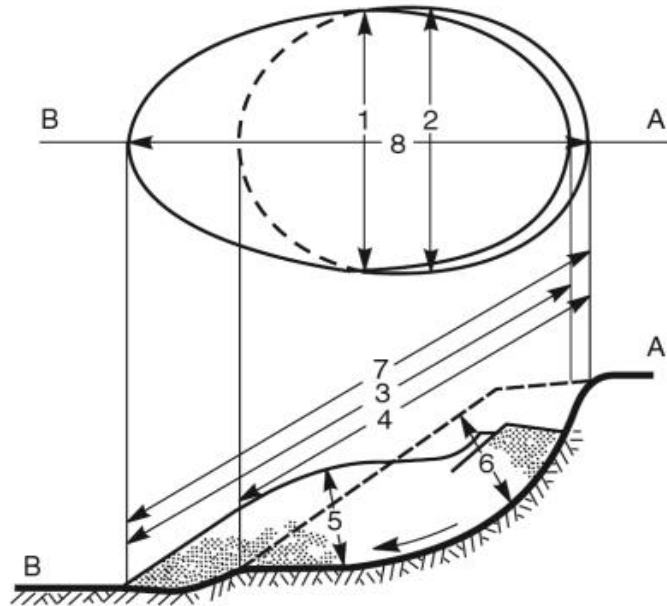


Figure 3.4: Landslide geometry as defined by the International Association of Engineering Geology Commission on Landslides (1990), features are defined in table 2.

Table 3.2: Definitions of landslide geometric features as identified in Figure 3.4 (International Association of Engineering Geology Commission on Landslides, 1990).

Number	Name	Definition
1	Width of displaced mass, $W_d$	Maximum width of displaced mass perpendicular to length, $L_d$
2	Width of surface rupture, $W_r$	Maximum width between flanks of landslide perpendicular to length, $L_r$
3	Length of displaced mass, $L_d$	Minimum distance from tip to top
4	Length of surface rupture, $L_r$	Minimum distance from toe of surface of rupture to crown
5	Depth of displaced mass, $D_d$	Maximum depth of displaced mass measured perpendicular to plane containing $W_d$ and $L_d$
6	Depth of surface of rupture, $D_r$	Maximum depth of surface of rupture below original ground surface measured perpendicular to plane containing $W_r$ and $L_r$
7	Total length, $L$	Minimum distance from tip of landslide to crown
8	Length of center line, $L_{cl}$	Distance from crown to tip of landslide through points on original ground surface equidistant from lateral margins of surface of rupture and displaced material

## 3.2 Laboratory Investigations

Laboratory tests were conducted to determine the geological and geotechnical properties of the Kope Formation bedrock and the colluvial soils derived from it. All tests were conducted in accordance with the American Society for Testing and Materials (ASTM) specifications (ASTM, 1996). The tests performed include natural water content, grain size distribution, Atterberg limits, direct shear test, and slake durability test.

### 3.2.1 Natural Water Content Test

The natural water content of each sample was determined in accordance with ASTM method D2216 as soon as the sample was brought to the laboratory. The natural water content is a reflection of the void ratio of a soil and a general indicator of its engineering behavior.

### 3.2.2 Grain Size Distribution Analysis

ASTM method D422 (sieve analysis) was used to determine the grain size distribution of oven dried samples of colluvial soil. For material passing the #200 sieve (<0.074mm), hydrometer analysis (ASTM 422) was performed to determine the grain size distribution. The purpose of grain size distribution analysis was to classify the soil at each site according to the Unified Soil Classification System (USCS) (Casagrande, 1948; Holtz et al., 2011).

### 3.2.3 Atterberg Limits Test

Atterberg limits were determined in accordance with ASTM methods D2487 and D4318. This test was conducted only on fine grained material that passed the #200 sieve to determine the liquid limit, plastic limit, and the plasticity index. Atterberg limits were



used to classify the fine grained material according to the USCS (Casagrande, 1948; Holtz et al., 2011).

### 3.2.4 Direct Shear Test

Direct shear testing was performed in accordance with ASTM method D6528. Two versions of the direct shear test were conducted: the first was with the failure plane passing completely through the soil to simulate failure conditions in case of rotational type landslides, and the second was with the failure plane along the contact between the bedrock and the overlying colluvial soil to simulate failure conditions in the case of translational landslides. The direct shear test was conducted to determine the strength parameters of the soils (cohesion and friction angle) for use in stability analysis.

### 3.2.5 Slake Durability Test

ASTM method D4644 was used to perform the slake durability test on the shale layers within the Kope Formation to evaluate their susceptibility to weathering. The slake durability test was performed on the bedrock samples that were collected from the 9 Mile Road landslide, Berkshire Road landslide, and Columbia Parkway landslide sites. Two cycles of the test were performed on each sample and the second-cycle slake durability index ( $Id_2$ ) was calculated as follows:

$$Id_2 = \frac{\text{Dry weight after second cycle}}{\text{Initial weight of sample}} (100)$$

Based on the second-cycle slake durability index values the samples were classified according to Gamble's (1971) classification as follows: high durability ( $Id_2 > 95\%$ ); medium durability ( $Id_2$  85% to 95%); low durability ( $Id_2$  60% to 85%); and very low durability ( $Id_2$  0% to 60%).

### 3.3 Stability Analysis Using the Slide 6.0 Program

Slide 6.0 is a limit equilibrium slope stability program that was developed by RocScience, University of Toronto. It is used for determining the factor of for circular (rotational) or non-circular (translational) failures in both soil and rock. It uses the vertical slice equilibrium method to analyze the stability of a slide. The Slide program was used to perform a detailed stability analysis on the Nine Mile Road site, the Columbia Parkway site, and the Wagner Road site.

## CHAPTER 4

### LABORATORY DATA PRESENTATION AND ANALYSIS

#### 4.1 Natural Water Content

The water content of a soil is the ratio of the mass of water in the soil to the dry mass of the soil (Holtz and Kovacs, 2011). The water content is one of the most important index properties of a soil and has been correlated to many other soil properties. Table 4.1 shows that natural water content values for colluvial soils from the ten landslides sites ranges from 13.1% to 27.1% with a mean value of 20.4%. These relatively high water content values suggest the presence of a high percentage of fine-grained clayey material in the colluvial soils at the landslide sites which will promote buildup of pore pressure and reduction in shear strength during wet periods. The high water content values also indicate the potential for flow type movement.

#### 4.2 Grain Size Distribution

Figures 4.1 and 4.2 show the grain size distribution curves for the Eight Mile Road landslide site and the Columbia Parkway landslide site, respectively. The grain size distribution curves for all of the sites can be seen in Appendix III. The distribution of particle sizes in soil mass is defined by the coefficient of uniformity,  $C_u$ , and coefficient of curvature,  $C_c$ , with well graded soils exhibiting  $C_u$  values greater than 4 and  $C_c$  values between 1 and 3.

Based on the results of grain size distribution analysis and the Unified Soil

Table 4.1: Natural water content values for the colluvial soil samples from the landslide sites studied.

Sample Locations	Natural Water Content
8 Mile Road Landslide	13.1%
9 Mile Road Landslide	27.1%
10 Mile Road Landslide	13.9%
Berkshire Road Landslide	23.8%
Columbia Parkway Landslide	23.0%
Delhi Pike Landslide	25.6%
Elstun Road Landslide	18.9%
Nordyke Road Landslide	13.6%
Old US 52 Landslide	21.1%
Wagner Road Landslide	23.5%
Mean	20.4%
Median	22.0%

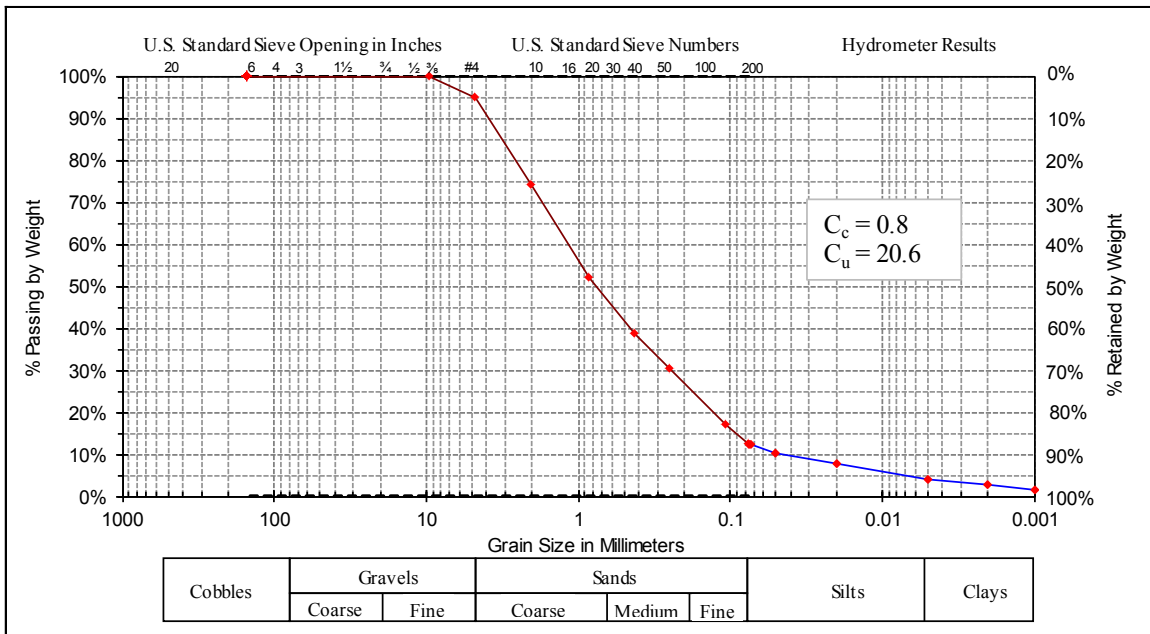


Figure 4.1: Grain size distribution curve for the colluvial soil from the Eight Mile Road landslide site.

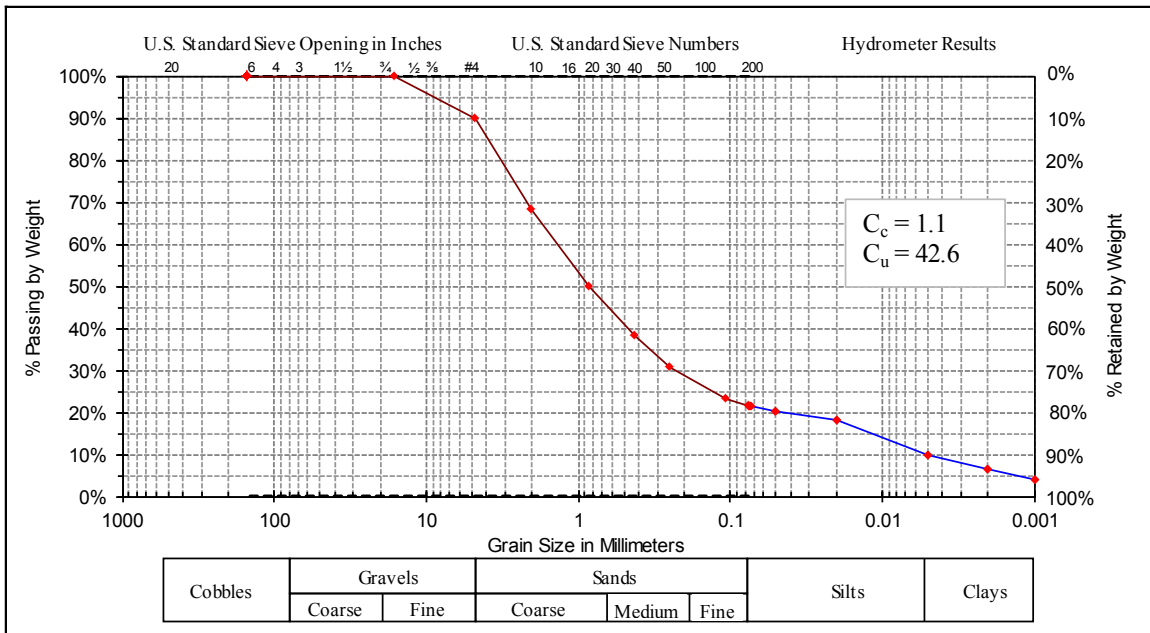


Figure 4.2: Grain size distribution curve for the colluvial soil from the Columbia Parkway landslide site.

Classification System (USCS), the colluvial soil derived from the Kope Formation can be classified as clayey sand (SC). The sand size particles consist predominantly of broken pieces of bedrock and fossils. Although the colluvial soil classifies as clayey sand, its engineering behavior during landslide activity is controlled primarily by the fine-grained clay matrix.

#### 4.3 Atterberg Limits

Table 4.2 shows the Atterberg limits test results for the studied soils. The table also lists the liquidity index (LI) values. The liquidity index compares the natural water content with the Atterberg limits and indicates how a soil will behave when sheared. If LI is more than 1, the soil will behave as a viscous liquid when sheared, if it ranges from 0-1, the soil will behave as a plastic material on shearing, and if it is less than zero, the soil will behave as a brittle material. The LI values in Table 4.2 indicate a plastic behavior of colluvial soils during landsliding.

Figure 4.3 shows Atterberg limits plotted on the Casagrande's plasticity chart. The plot shows that the fine-grained fraction of the colluvial soils classifies as clay of low plasticity (PL).

#### 4.4 Clay Content and Clay Mineralogy

According to Sarman (1991), Dick (1992), and Hajdarwish (2006) who performed x-ray diffraction analysis on samples from the Kope Formation, the clay in the Kope Formation is composed of chlorite, kaolinite, and illite. The mineral chlorite is subject to swelling when exposed to moisture (Holtz et al., 2011). Swelling clays are known to facilitate landsliding (Sarman, 1991).

Table 4.2: Atterberg limits of the fine-grained fraction of the colluvial soil from the studied sites.

Sample Locations	Liquid Limit	Plastic Limit	Plasticity Index	Liquidity Index
Eight Mile Road Landslide	23.6	10.9	12.7	0.2
Nine Mile Road Landslide	41.9	20.1	21.8	0.3
Ten Mile Road Landslide	23.0	12.3	10.7	0.2
Berkshire Road Landslide	40.0	23.3	16.8	0.03
Columbia Parkway Landslide	42.6	22.5	20.1	0.02
Delhi Pike Landslide	44.0	19.8	24.2	0.2
Elstun Road Landslide	37.8	18.5	19.3	0.02
Nordyke Road Landslide	24.4	11.6	12.8	0.2
Old US 52 Landslide	37.2	18.5	18.7	0.1
Wagner Road Landslide	34.1	18.4	15.7	0.3
Mean	34.9	17.6	17.3	0.2
Median	37.5	18.5	17.8	0.2

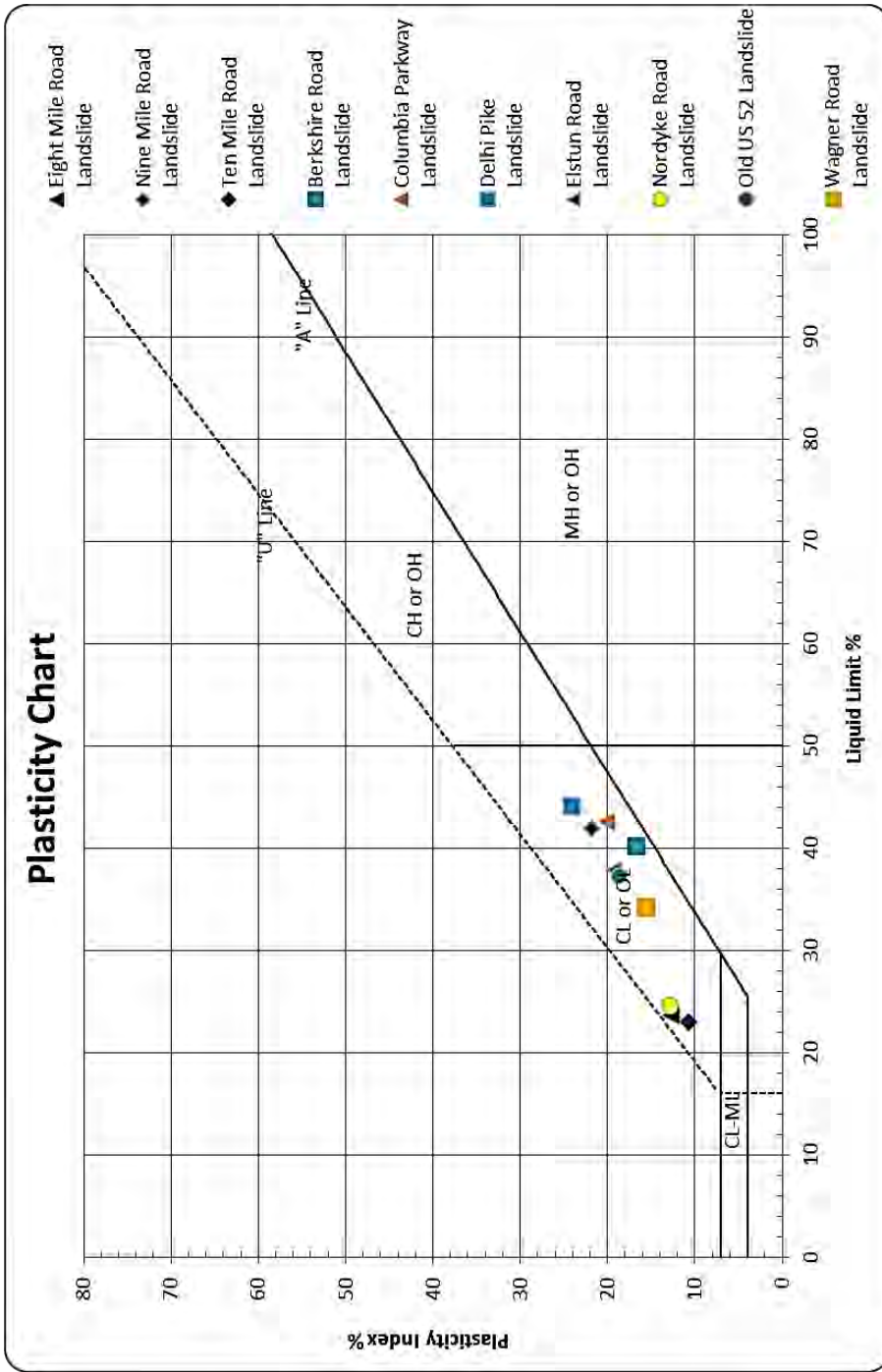


Figure 4.3: Atterberg limits of the fine-grained fraction of the colluvial soil from the landslide sites, plotted on the Casagrande's plasticity chart.



#### 4.5 Slake Durability

The slake durability index was measured for bedrock samples collected from each site where a translational failure occurred. Table 4.3 provides the results of the slake durability index test. The second-cycle slake durability index ( $Id_2$ ) ranges from 7.1% (very low durability) for the Columbia Parkway Landslide to 39.9% (low durability) for the 9 Mile Road Landslide.

The slake durability index is a measure of a rock's durability and resistance to weathering and erosion. The durability properties of argillaceous rocks are important in slope stability because of the reduction in strength properties as a result of weathering (Dick and Shakoor, 1995). The low to very low durability of the Kope Formation also explains the thick accumulation of colluvial soil that overlies it at many places.

#### 4.6 Strength Parameters

The strength parameters of a soil, which include both cohesion and friction angle, are the most important engineering property of a soil in terms of the stability of a slope. Table 4.4 shows the strength parameters for a failure plane developing within the colluvial soil, whereas Table 4.5 shows the strength parameters for a failure plane developing along the contact between the colluvial soil and the bedrock. Appendix IV shows the normal force versus the shear force for the direct shear test results for each landslide site. According to the stability analysis results, discussed later in the document, the shear strength parameters for both types of failure are well below those required for the slopes to be stable, especially upon buildup of pore pressure during the spring season.

Table 4.3: Slake durability index test results for the bedrock samples from translational landslide sites.

Location	Slake Durability Index Id <sub>1</sub> (%)	Slake Durability Index Id <sub>2</sub> (%)	Durability Rating
Berkshire Road Landslide	73.3%	28.5%	Very Low
Columbia Parkway Landslide	51.9%	7.1%	Very Low
Nine Mile Road Landslide	71.4%	39.9%	Low

Table 4.4: Shear strength parameters for the failure developing through the colluvial soil.

Sample Locations	Peak Cohesion (Kpa)	Residual Cohesion (Kpa)	Peak Friction Angle (degrees)	Residual Friction Angle (degrees)
Eight Mile Road Landslide	24.5	23.3	31.0	20.8
Ten Mile Road Landslide	27.5	22.5	33.8	15.6
Delhi Pike Landslide	33.4	24.0	23.8	17.8
Elstun Road Landslide	26.4	24.5	50.4	19.8
Nordyke Road Landslide	47.7	38.9	22.8	17.8
Old US 52 Landslide	35.2	32.7	39.4	20.3
Wagner Road Landslide	27.7	22.2	27.5	18.3
Mean	31.8	26.9	32.7	18.6
Median	27.7	24.0	31.0	18.3

Table 4.5: Shear strength parameters for failure developing along the soil bedrock contact.

Sample Locations	Residual Cohesion (Kpa)	Residual Friction Angle (degrees)
Nine Mile Road Landslide	11.8	14.0
Berkshire Road Landslide	13.0	8.0
Columbia Parkway Landslide	6.8	14.6
Mean	10.5	12.2
Median	11.8	14.0

## CHAPTER 5

### DESCRIPTION AND ANALYSIS OF SELECTED SLOPE FAILURES

#### 5.1 General Description of Sites Studied

Ten landslide sites were chosen for detailed study. Seven of the landslide sites were classified as rotational landslides and named on the basis of their location as the Eight Mile Road landslide site, Ten Mile Road landslide site, Delhi Pike landslide complex, Elstun Road landslide site, Nordyke Road landslide site, Old US 52 landslide site, and Wagner Road landslide site. Three of the landslide sites were classified as translational landslides and were named as the Nine Mile Road landslide site, Berkshire Road landslide site, and the Columbia Parkway landslide site. The location of each landslide site can be seen in Figure 5.1. Detailed descriptions of each site, including figures, can be seen in Appendix V.

##### 5.1.1 Rotational Landslides

Rotational landslides constitute the most common type of slope failure in the colluvial soil derived from the Kope Formation. All of the rotational landslides that were studied occurred in clay of low plasticity with abundant Ordovician age fossils. Rotational landslides occur where the soil material is 2 m – 15 m (6 ft – 50 ft) thick. The rotational landslides were caused by low shear strength parameters, poor drainage, buildup of pore pressure, over steepening of slopes during constructions, the addition of weight to the top of the slope, and undercutting of the toe by the stream water.

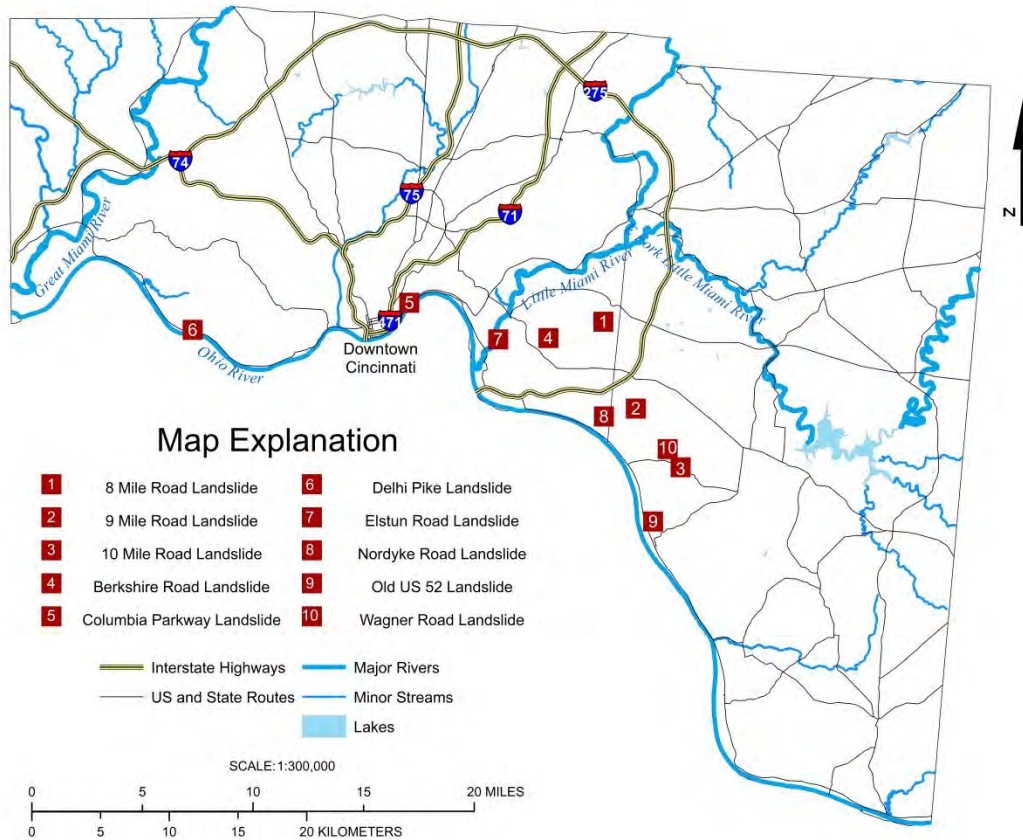


Figure 5.1: Map showing the locations of the landslide sites selected for detailed study.

### 5.1.2 Translational Landslides

Translational landslides are the second most common type of failure in the colluvial soil derived from the Kope Formation. Translational landslides tend to occur in complexes, affecting wide spread areas. The failure plane for a translational slide is located along the contact between the colluvial soil and the underlying bedrock. The sliding mass for all of the translational slides consisted of clay of low plasticity with abundant Ordovician age fossils. The thickness of colluvial soil at the locations of translational slides was found to be approximately 1.5 m to 3.0 m (5 ft to 10 ft).

The causes of translational landslides include low shear strength of the soil, undercutting of the toe of the slope by the stream, steepness of the slope and sliding surface, constant removal of material from the toe of the slope, and pore pressure developing during wet periods.

## 5.2 Stability Analysis

A stability analysis was performed on the Ten Mile Road landslide, the Wagner Road landslide, and the Columbia Parkway landslide using the Slide software program RocScience, 2012.

### 5.2.1 Ten Mile Road Landslide Stability Analysis

For the Ten Mile Road landslide the critical surface with the lowest factor of safety can be seen in Figure 5.2. The location of the critical surface, determined by the Slide Program, matches the failure surface location observed in the field. The minimum factor of safety for the dry condition is 0.83, and that for the saturated condition is 0.79.

The results of the stability analysis show that the cohesion of the soil would need to be 61.2 Kpa (1287 lb/ft<sup>2</sup>), instead of 27.5 Kpa (575 lb/ft<sup>2</sup>) for the landslide site at the

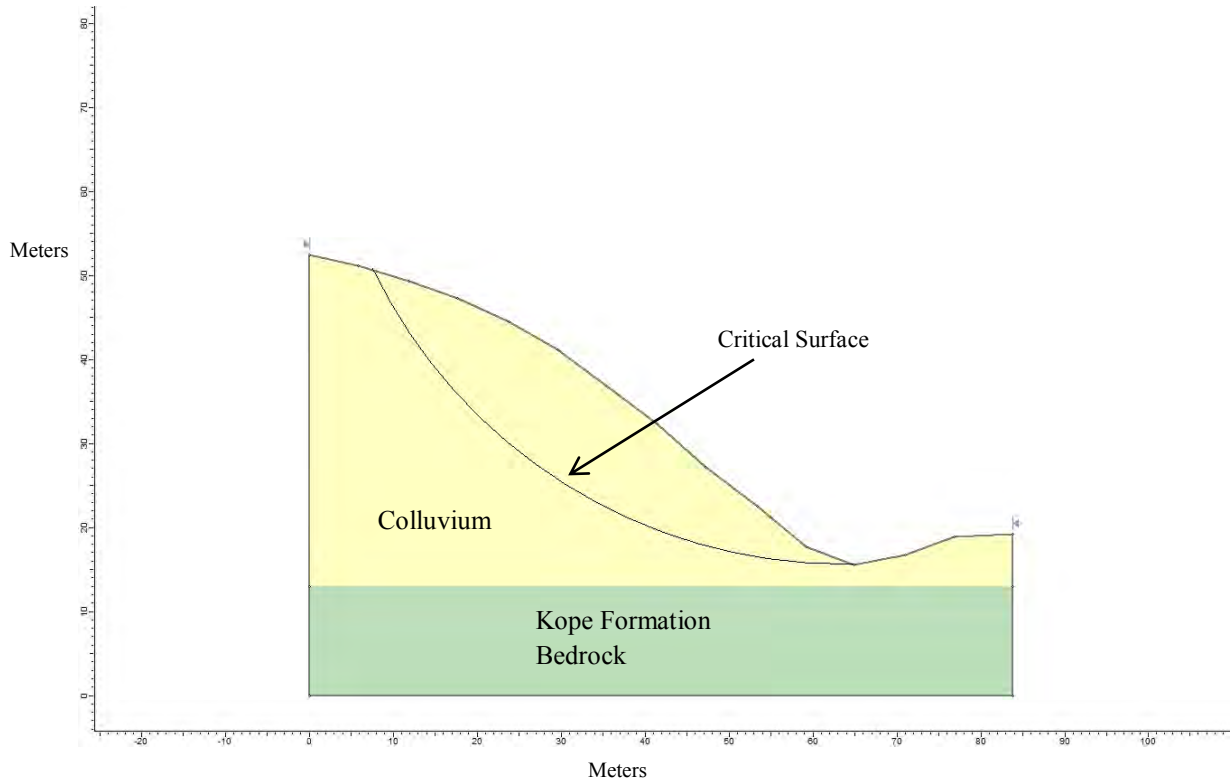


Figure 5.2: Critical surface for the minimum factor of safety for dry and saturated conditions for the Ten Mile Road landslide as determined by the Slide program.

10 Mile Road landslide to achieve a factor of safety equal to 1 if the friction angle remains constant (31°). The stability analysis also shows that for the 10 Mile Road landslide would need to have a residual friction angle of approximately 22° instead of 16° to have a factor of safety equal to 1 if the cohesion remains constant.

### 5.2.2 Wagner Road Landslide Stability Analysis

In performing the stability analysis on the Wagner Road landslide a linear load equivalent to 0.3 m (1 ft) thick concrete layer, was added to the top of the slope to account for the road. The critical surface with the lowest factor of safety, as determined by the Slide software, is shown in Figure 5.3.

The results of the stability analysis show a factor of safety of 0.95 for the dry slope and 0.62 for the saturated slope. The stability analysis results show that when the the water table is located at the position as determined from the boring logs, obtained from H.C. Nutting Co., the factor of safety is further reduced to 0.82.

The results of the stability analysis show that the soil would need to have a friction angle of approximately 24.5° for the slope to have a factor of safety equal to 1 if the cohesion remains constant. The stability analysis also show that the soil would need to have cohesion of 24.7 Kpa (515 lb/ft<sup>2</sup>) for the slope to have a factor of safety equal to 1 if the friction angle remains constant.

### 5.2.3 Columbia Parkway Landslide Stability Analysis

A stability analysis was performed on the Columbia Parkway landslide using the Slide program. The critical surface as determined by the Slide program is located along the contact between the colluvial soil and the underlying bedrock. The critical surface initiates at the top of the slope and progresses along the contact and emerges at the top of



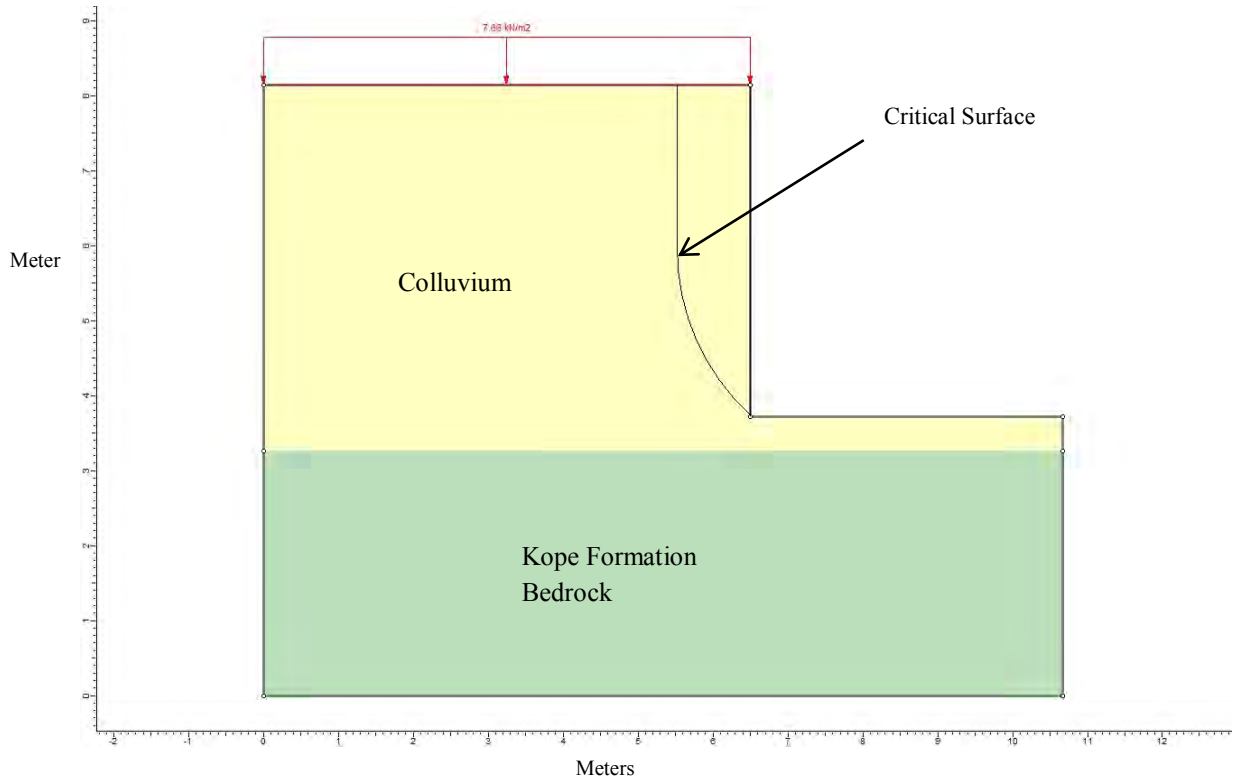


Figure 5.3: Critical Surface for the minimum factor of safety for wet and dry conditions for the Wagner Road landslide as determined by the Slide program.

the retaining wall at the base of the slope and can be seen in Figure 5.4.

The minimum factor of safety for the dry condition is 1.04, when the colluvium is at its natural water content, the factor of safety is 0.95, and when the colluvium is saturated the factor of safety is 0.94. If the water table is located in the middle of the colluvium, 1 m (3.3 ft) below the ground surface, the factor of safety is reduced to 0.77 and if the water table is located at the ground surface the factor of safety is reduced to 0.68. The results of the stability analysis show that the soil-rock friction angle need to be  $18^\circ$  instead of  $15^\circ$  (Table 4.5) to have a factor of safety equal to 1, if the cohesion remains constant (6.8 Kpa (142 lb/ft<sup>2</sup>)). The stability analysis also shows that the slope would need to have cohesion equal to 8.9 Kpa (185 lb/ft<sup>2</sup>) for the slope to have a factor of safety equal to 1 if the friction angle remains constant ( $15^\circ$ ).

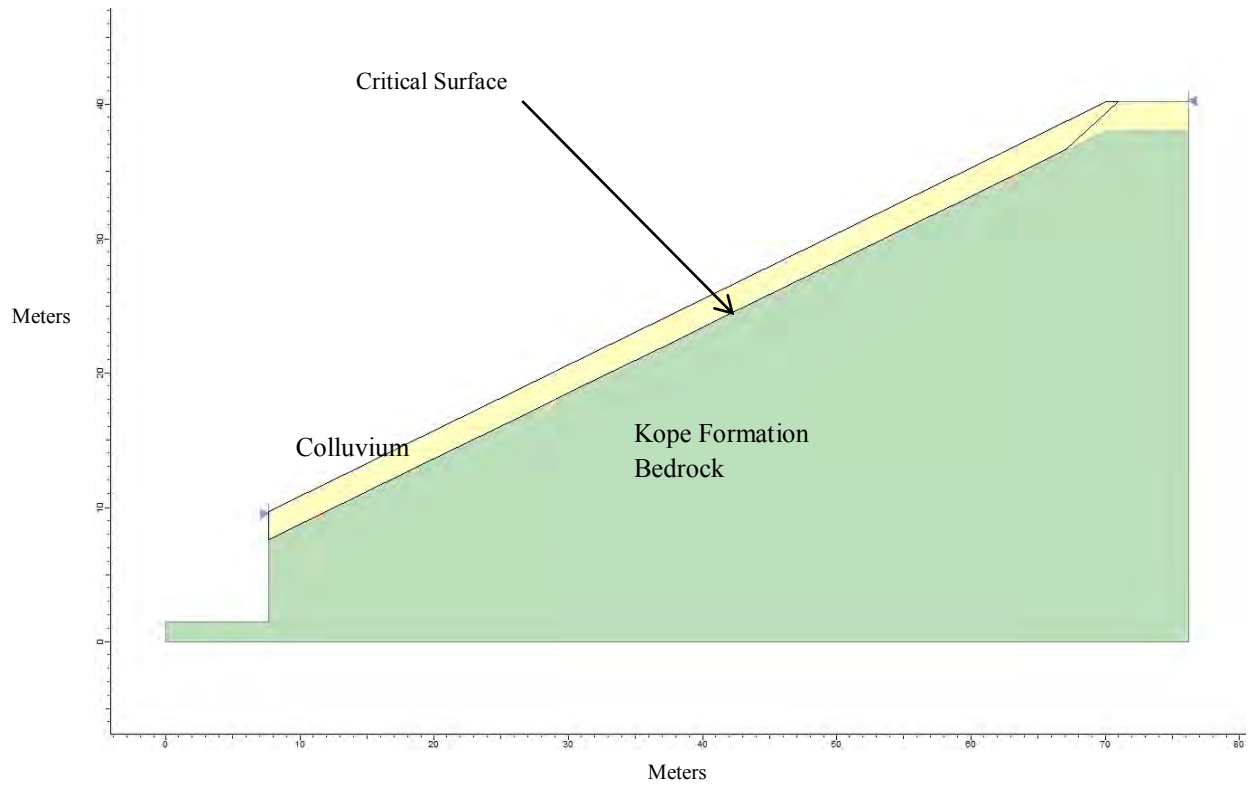


Figure 5.4: Critical Surface for the minimum factor of safety for wet and dry conditions as determined by the Slide program for the Columbia Parkway landslide.

## CHAPTER 6

### DISCUSSION

#### 6.1 Landslide Inventory Map

In preparing the landslide inventory map, a total of 842 landslides were identified in the colluvial soil derived from the Kope Formation. Of these, 542 landslides were identified using the LiDAR derived maps and 300 were identified through field observations and data obtained from county and city governments.

#### 6.2 Factors Responsible for Landslide Susceptibility of the Kope Formation

##### 6.2.1 Strength Parameters

The residual strength parameters are more important than the peak strength parameters for the long term stability of slopes comprised of colluvial soil derived from the Kope Formation. This is because many of the landslides in the Kope Formation have developed progressively or occur slowly over a long period of time. Figures 6.1 through 6.6 show the relationships between factor of safety and the residual strength parameters of cohesion and friction angle for the Ten Mile Road, Wagner Road, and Columbia Parkway landslides, respectively. A comparison of these plots with the residual strength parameters provided in Tables 4.4 and 4.5 shows that the residual cohesion and residual friction angle values for both types of failure (rotational and translational) are not high enough to support the slopes. Thus, the low shear strength of the colluvial soil and soil-bedrock contact is an important factor contributing to landslide susceptibility of the Kope

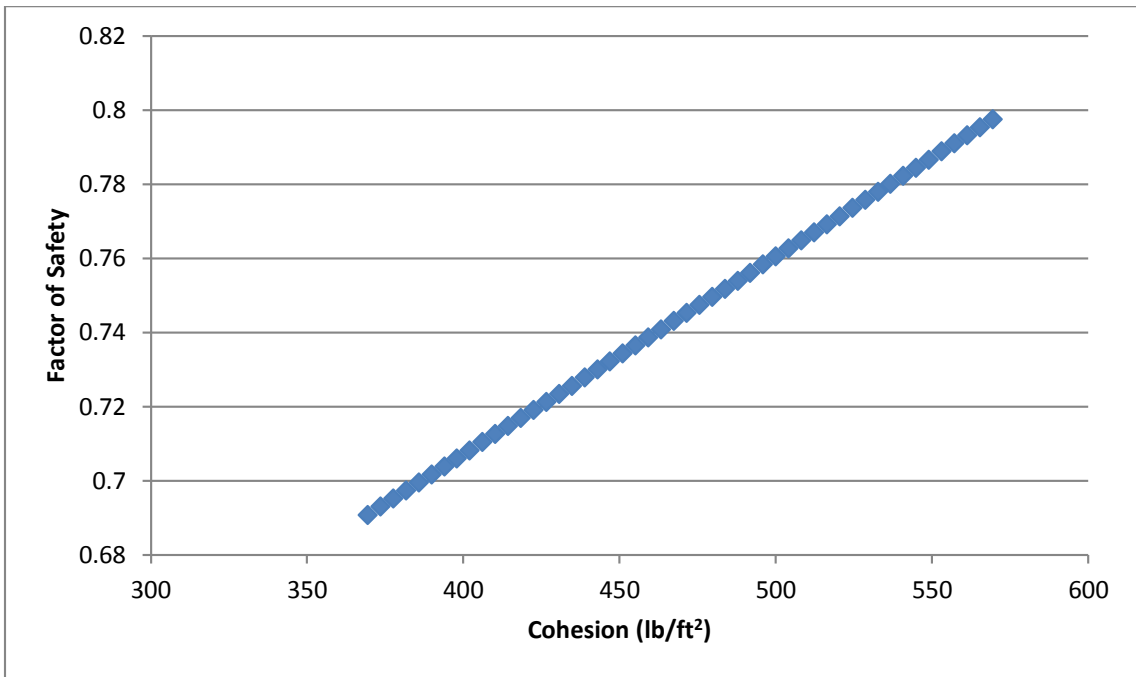


Figure 6.1: Relationship between cohesion and factor of safety for the Ten Mile Road landslide.

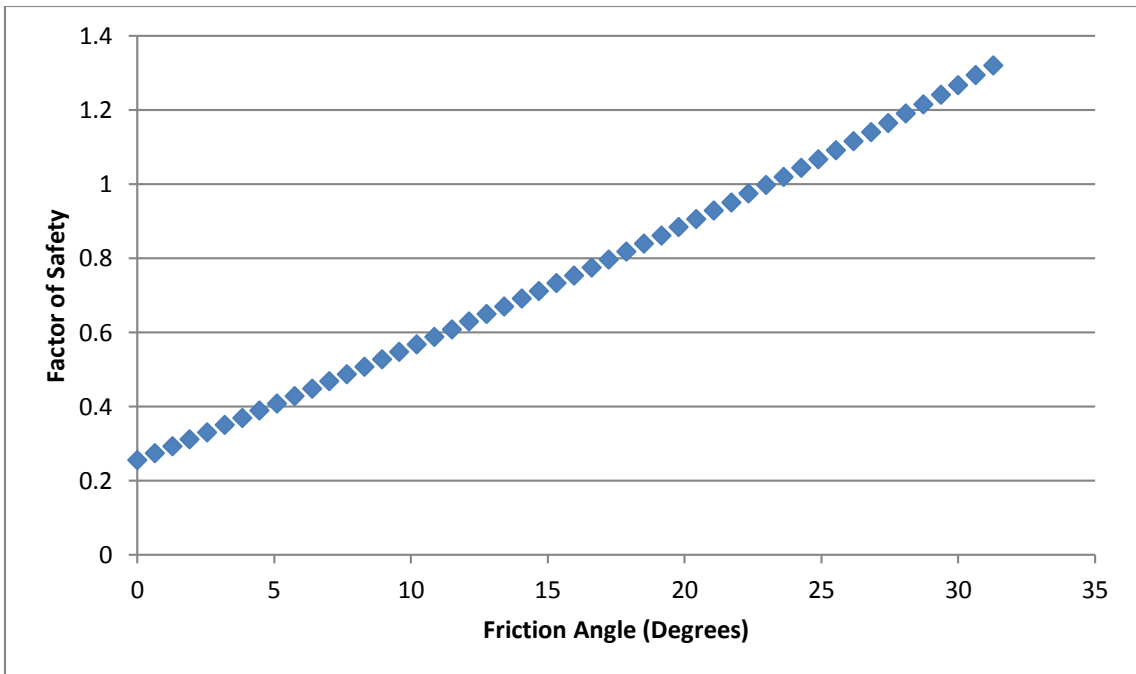


Figure 6.2: Relationship between friction angle and factor of safety for the Ten Mile Road landslide.

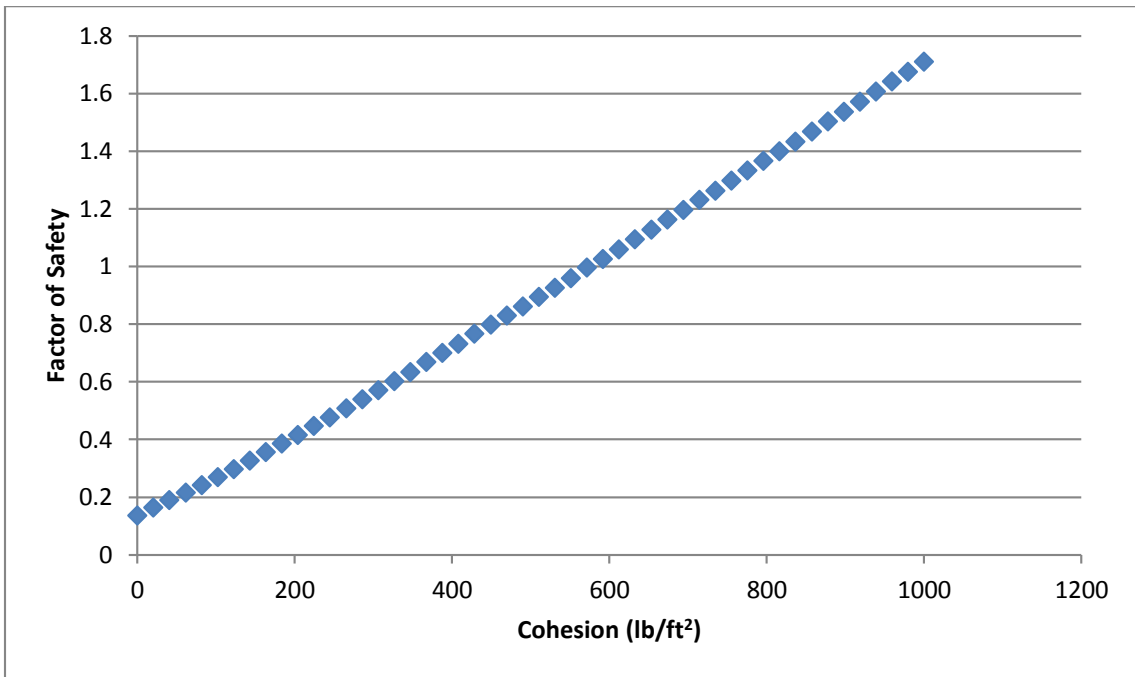


Figure 6.3: Relationship between cohesion and factor of safety for the Wagner Road landslide.

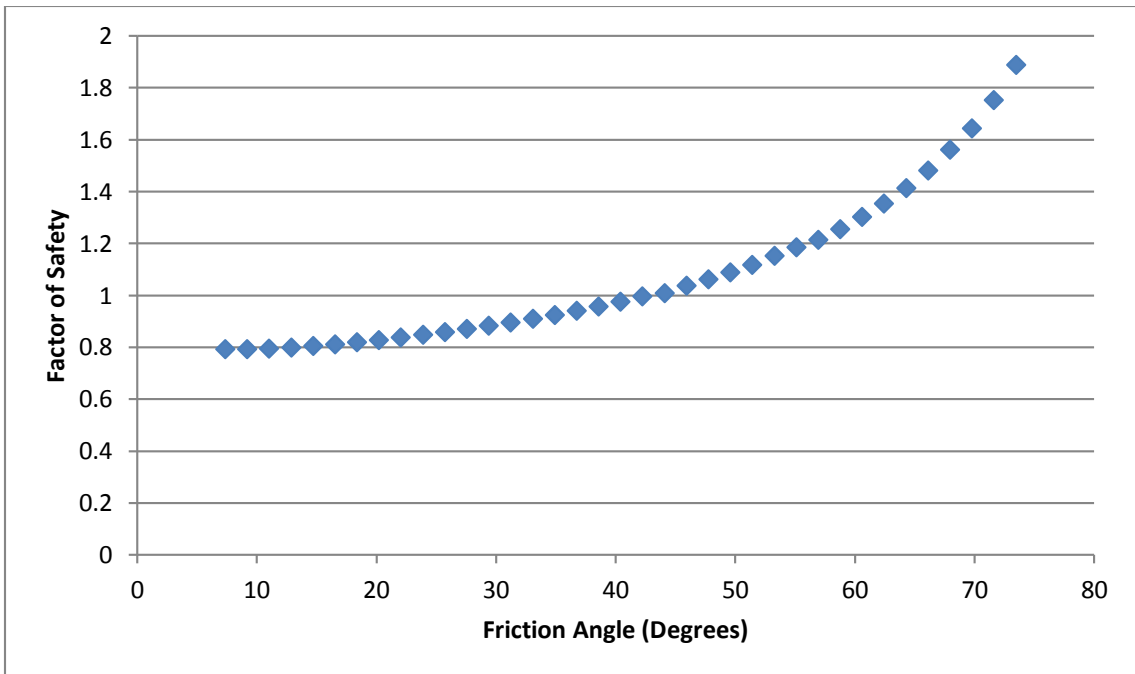


Figure 6.4: Relationship between friction angle and factor of safety for the Wagner Road landslide.

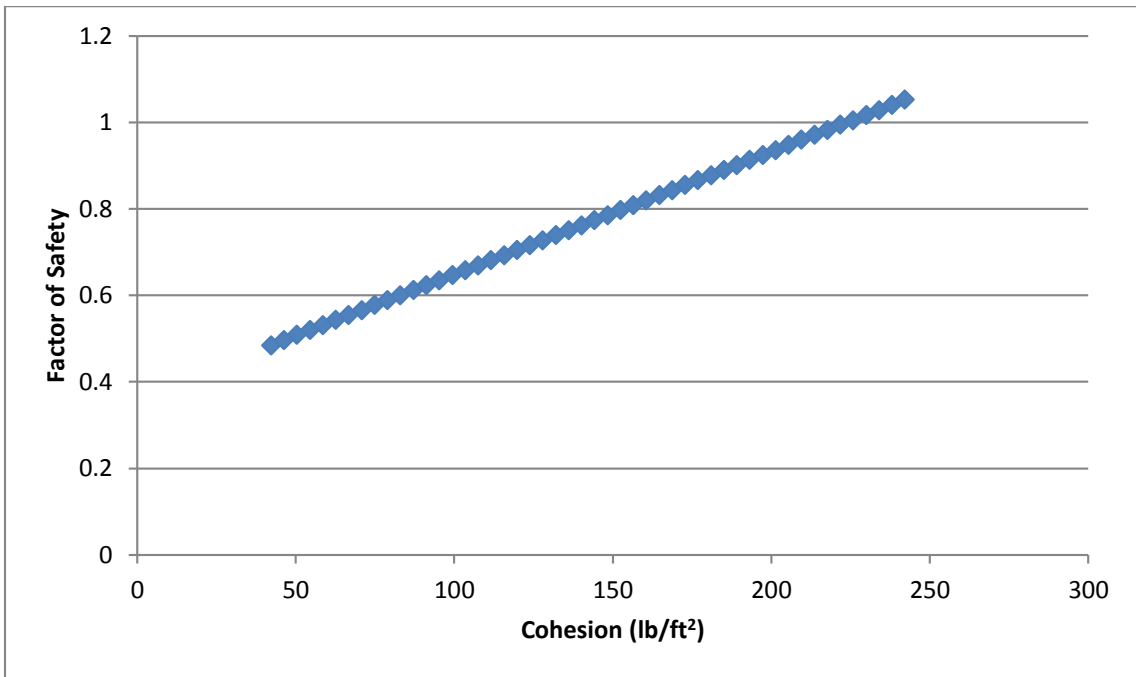


Figure 6.5: Relationship between cohesion and factor of safety for the Columbia Parkway landslide.

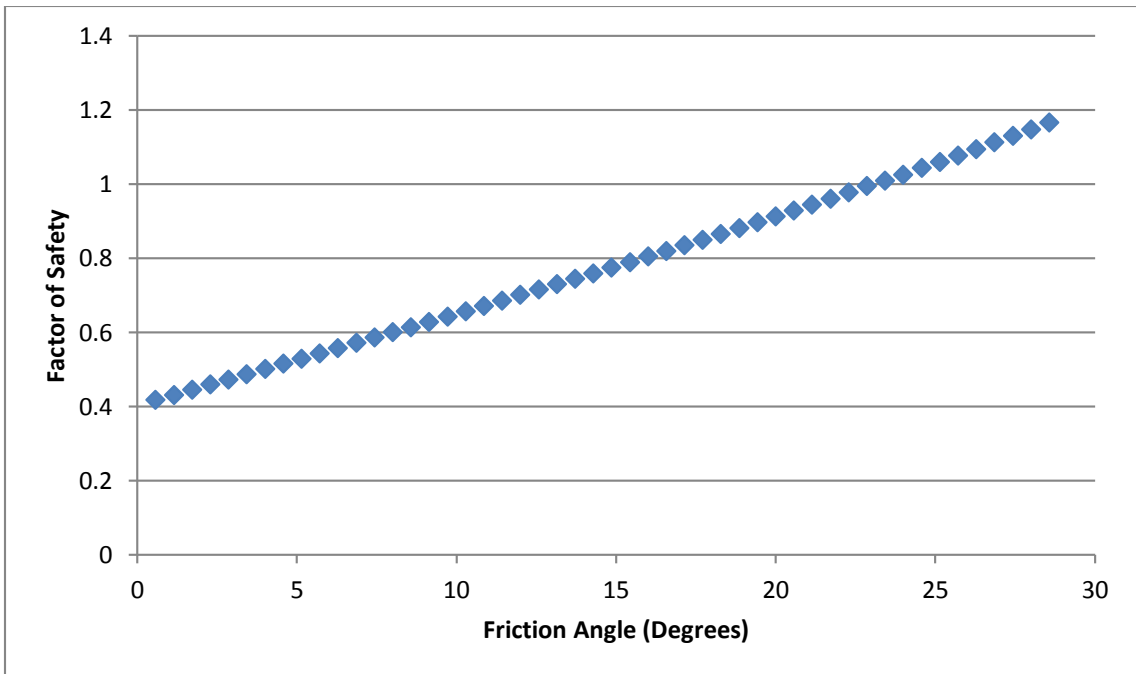


Figure 6.6: Relationship between friction angle and factor of safety for the Columbia Parkway landslide Formation.

### 6.2.2 Groundwater

The presence of water within a slope can cause a significant decrease in the stability of a slope. Since the slide material is silty, clayey sand for all of the landslides studied, it can be assumed that the material has low permeability and poor drainage characteristics (Holtz et al., 2011). This can lead to buildup of pore water pressure within the slope during prolonged periods of rainfall and snow melt, reducing shear strength and contributing to slope failure. Figures 6.7 through 6.9 show the relationship between the location of the water table and the factor of safety for the slopes for the Ten Mile Road, Wagner Road, and Columbia Parkway landslides, respectively. Where 0 represents the water table being located at the bedrock and 1 represents the water table being just below the ground surface and values in between represent the relative elevation of the water table along a vertical line from the bedrock to the ground surface.

The plots in Figures 6.7 through 6.9 and the results of the stability analysis (Chapter 5) show that as the water table within the slope rises the factor of safety of the slope gradually begins to decrease. The factor of safety is at its lowest point when the water table is just below the ground surface. When the water table is just below the ground surface, i.e. the soil is saturated, the factor of safety for the slope decreases by approximately 1/3 of its original. However, only partial saturation of the slope is required to cause failure as the slopes already have a factor of safety below 1.

The presence of groundwater in many of the slopes is evident from the continually flowing water or water seeps that can be observed throughout the year. Water seeps were frequently observed in the scarp areas of the landslides investigated in this study. Thus, development of pore pressure is another important factor that explains



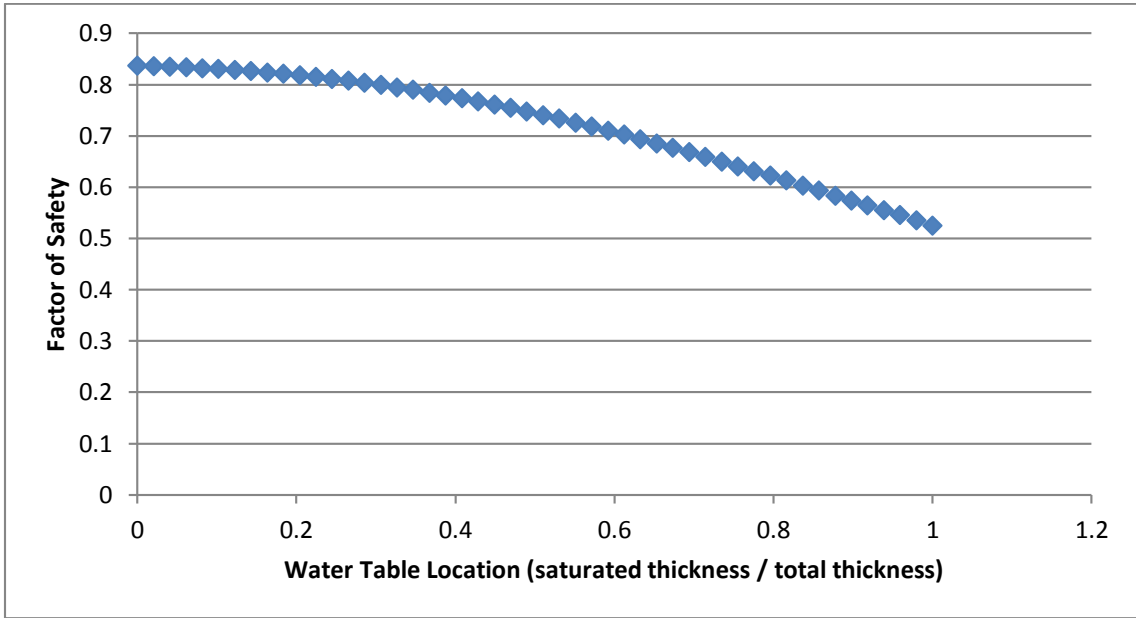


Figure 6.7: Relationship between water table location and factor of safety for the Ten Mile Road landslide, 1 indicates the water table is just below the ground surface and 0 represents the water table being located on the bedrock.

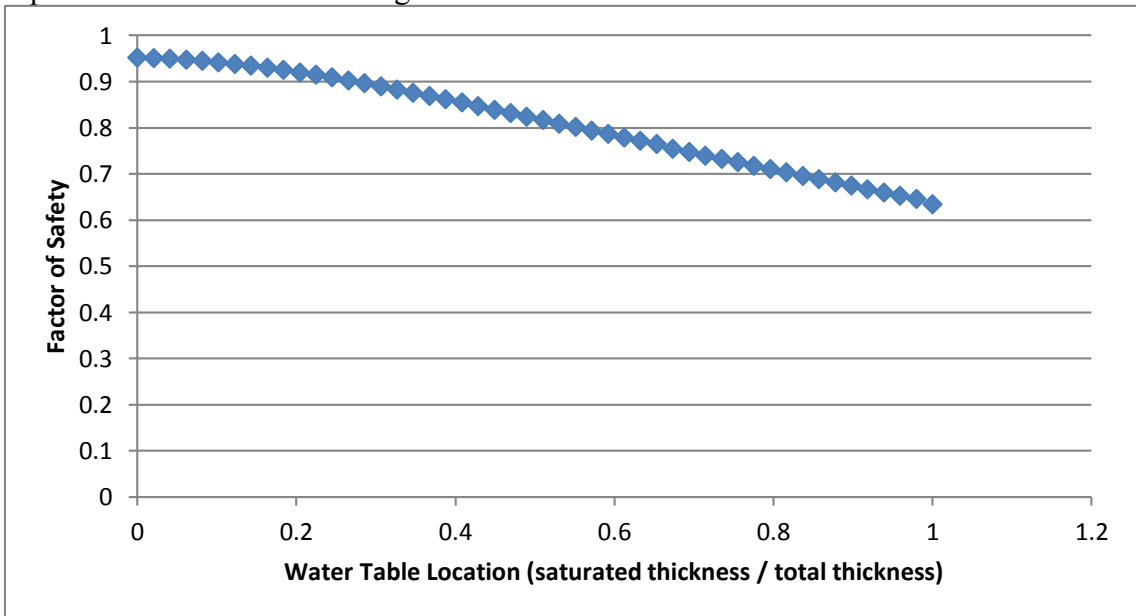


Figure 6.8: Relationship between water table location and factor of safety for the Wagner Road landslide, 1 indicates the water table is just below the ground surface and 0 represents the water table being located on the bedrock.

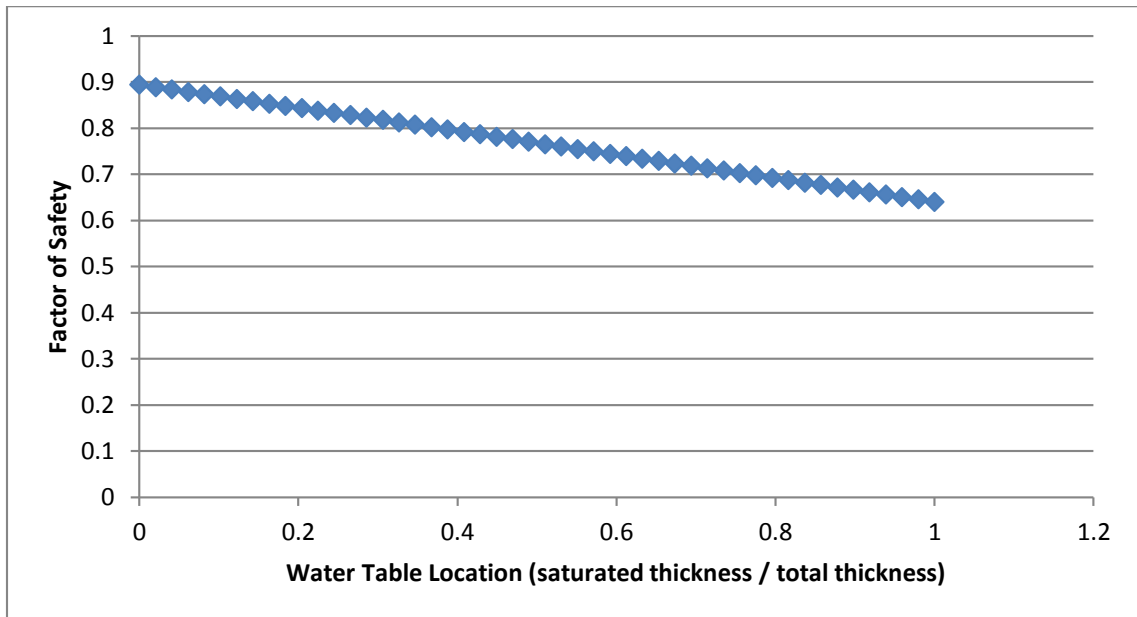


Figure 6.9: Relationship between water table location and factor of safety for the Columbia Parkway landslide, 1 indicates the water table is just below the ground surface and 0 represents the water table being located on the bedrock.

the high susceptibility of the Kope Formation derived colluvial soils to landsliding.

### 6.2.3 Human Activity

Human activity is an important factor in the stability of many slopes in the Cincinnati area. Construction activities alter the stability of a slope in two ways: (i) by adding weight to the top of the slope, and (ii) by removing lateral support the toe of the slope. Figure 6.10 shows the relationship between the load applied to the top of the slope and the factor of safety for the Wagner Road landslide.

The results of the stability analysis show that if the road was not on the top of the slope, the factor of safety for the slope would be just above 1.0, meaning a barely stable slope or a slope in a state of limit equilibrium. However, when load equivalent to 0.3 m (1 ft) thick pavement layer is imposed on the slope, the factor of safety decreases to 0.9, meaning an unstable slope.

Due to the topography of the Cincinnati area, many of the roads are either built on tops of hillsides, cut into hillsides, or built in the toe areas by partial removal of the slopes. By building on top of the slopes the driving forces acting to cause failure increase. By cutting out the hillsides and the toes of the slopes the resisting forces decrease. Thus, human activity adds to the potential for a slope to fail.

### 6.2.4 Disintegration and Erodibility of the Bedrock

The Kope Formation is a clay-bearing rock of low to very low durability against slaking ( $I_d = 7.1\% - 39.9\%$ ) because of which it easily disintegrates and erodes. It is the easy disintegration of the Kope Formation that leads to thick accumulation of the colluvial soil on top of bedrock. The weak nature of the Kope Formation and the colluvial soil derived from it make these materials susceptible to landsliding.

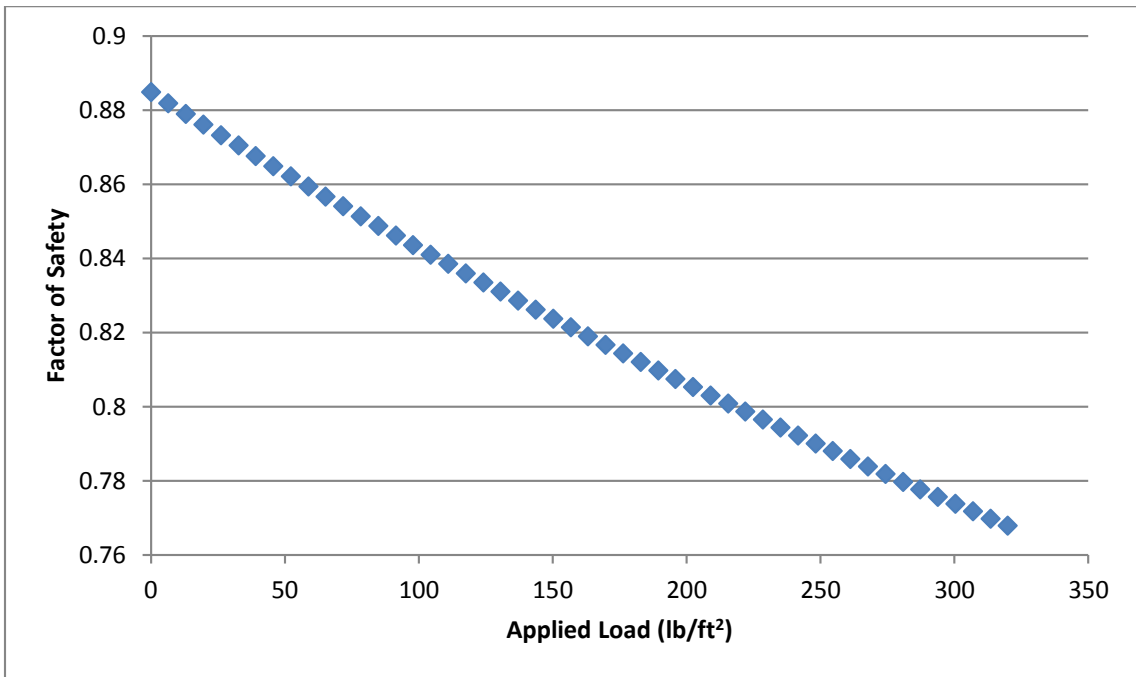


Figure 6.10: Relationship between load applied to the top of the slope and factor of safety for the Wagner Road landslide.

### 6.2.5 Undercutting of the Slope Toe

Many slopes in the Cincinnati area are subject to erosion of the slope toe by a stream. The erosion of the toe removes the lateral support, reducing the resisting forces. Thus, undercutting of the slope toe, facilitated by the low durability of the Kope Formation is a very important factor responsible for the high susceptibility of the Kope Formation to landsliding. Figure 6.11 shows a small stream removing material from the base of a slope by undercutting the toe at the Berkshire Road landslide..

### 6.2.6 Steepness of Slopes

The steepness of the hillsides in the Cincinnati area is one of the contributing factors to the landslide susceptibility of the colluvium that is associated with the Kope Formation. Many of the hillsides have been over-steepened as a result of the rapidly eroding streams. Again, the low to very low durability of the bedrock results in rapid down cutting of the valleys, giving rise to steep slopes. The hillsides have also been over-steepened as a result of human activities. The slope angles in the Cincinnati area range between 20° and 40°, which is generally higher than the residual friction angle values. The results of the stability analysis show that slopes steeper than 15° will not have an adequate factor of safety against failure under wet conditions.

The above discussion shows that there are multiple factors which, either individually or in combination, contribute to the high susceptibility of the Kope Formation to landsliding.



Figure 6.11: Undercutting the toe of the slope at the Berkshire Road landslide.

## CHAPTER 7

### CONCLUSIONS AND RECOMENDATIONS

#### 7.1 Conclusions

From the results of this study the following conclusion can be drawn:

- 1) Rotational and translational landslides are the main types of movement affecting the slopes comprised of colluvial soil derived from the Kope Formation. Once a failure has been initiated, both types of movement may transform into earthflows with the addition of water and occasionally into mudflows.
- 2) There are multiple factors that contribute to the high susceptibility of the colluvial soil to landsliding, including:
  - a. Low shear strength parameters of the colluvial soil. The shear strength of the soil is not high enough to prevent the failure of most slopes under varying drainage conditions.
  - b. Development of pore water pressure within the slopes that causes a significant reduction in the factor of safety.
  - c. Human activities, such as addition of weight to the top of the slopes and removal of material at the base of the slopes, increase the driving forces and decrease the resisting forces thereby increasing the landslide potential.

- d. Low to very low durability of the bedrock that allows rapid disintegration of the bedrock and accumulation of colluvial soil of varying thicknesses, depending upon the original slope of the bedrock.
- e. Undercutting of the slope toe by stream water.
- f. Steepness of the slopes.

## 7.2 Recommendations

Based on the results of this research the following recommendations are made:

- 1) Zoning laws governing the development on and around hillsides should be implemented to limit the development on unstable slopes for all types of future development. These zoning laws should require that a detailed geotechnical study be performed on all hillsides where a future development is planned.
- 2) Education of the citizens of the Cincinnati, Ohio area is needed so that the public can be aware of the landslide hazard. This will require communicating information about recognition of the conditions that make a slope susceptible to landsliding. This should also include how to recognize the signs of the past and the currently active slope failures.



## REFERENCES CITED

- ASTM Digital Library, 1996, ASTM International, American Society for Testing and Materials, 27 Dec 2010. <<http://www.astm.org/>>
- Baum R.L., 1983, Engineering geology and relative slope stability in the area of the Fay Apartments and in part of Mount Airy Forest, Cincinnati, Ohio: Cincinnati, Ohio, University of Cincinnati M.S. thesis, p. 74.
- Baum R.L., 1994, Contribution of artesian water to progressive failure of the upper part of the Delhi Pike landslide complex: U.S. Geological Survey Bulletin 2059-D, Washington DC, United States Government Printing Office, p. 14.
- Baum R.L. and Johnson, A.M., 1996, Overview of landslide problem, research, and mitigation, Cincinnati, Ohio, Area: U.S. Geological Survey Bulletin 2059-D, Washington DC, United States Government Printing Office, p. 33.
- Behringer, D.W., and Shakoor, Abdul, 1992, A study of selected landslides in the Cincinnati area in relation to human activity: Geological Society of America Abstracts with Programs, v. 24, no. 7, p. 294.
- Bernkopf, R.L., Brookshire, D.S., Campbell, H.C., Shapiro, C.D., and Fleming, R.W., 1985, The economics of landslide mitigation strategies in Cincinnati, Ohio – A methodology for benefit-cost analysis, Chapter D of Feasibility of a nationwide program for the identification and delineation of hazards from mudflows and landslides: United State Geological Society Open-File Report 85-276-D, p. 35.

- Bernknopf, R.L., Campbell, R.H., Brookshire, D.S. and Shapiro, C.D., 1988, A probabilistic approach to landslide hazard mapping in Cincinnati, Ohio, with applications for economic evaluation: Association of Engineering Geologists Bulletin, v. 25, no.1, p. 39-56.
- Brett, C. E., and Algeo, T. J., 2001, Stratigraphy of the Upper Ordovician Kope Formation in its type area (northern Kentucky), including a revised nomenclature. Algeo, T.J. and Brett, C.E., eds., Sequence, cycle and event stratigraphy of the Upper Ordovician and Silurian strata of the Cincinnati Arch region., Kentucky Geological Survey, series 12, Guidebook 1, p. 47-64.
- Brett, C.E., Algeo, T.J., and McLaughlin, P.J., 2003, Use of event beds and sedimentary cycles in high resolution stratigraphic correlation of lithologically repetitive successions: The Upper Ordovician Kope Formation of northern Kentucky and southwestern Ohio, in Harries, P., ed., High-resolution approaches in stratigraphic paleontology. Amsterdam, Plenum Press, p. 315-350.
- Brockman, C.S., 1983, The engineering geology, relative stability and Pleistocene History of the Dry Run Creek area, Hamilton County, Ohio: Cincinnati, Ohio, University of Cincinnati M.S. thesis, p. 147.
- Casagrande, A., 1948, Classification and identification of soils, Transactions, ASCE, Vol. 113, p. 901-930
- Cincinnati City Planning Commission, 1970, The plan and program for the Cincinnati hillsides: Cincinnati City Planning Commission, Cincinnati, Ohio, p. 61.

- Cruden DM, Varnes DJ. 1996. Landslide types and processes. In *Landslides: Investigation and Mitigation*, Turner AK, Schuster RL (Eds.). National Academy Press: Washington DC; p. 36-75.
- Dick, J.C., 1992, Relationship between durability and lithologic characteristics of mudrocks, Ph.D. dissertation, Kent, Ohio, Kent State University, p. 243.
- Dick, J. C., and Shakoor, A., 1995, Characterizing durability of mudrocks for slope stability purposes. *Reviews in Engineering Geology*, vol. 10, p. 121-130.
- Durrell, R.H., 1961, The Pleistocene geology of the Cincinnati area-Guidebook for field trips: Geological Society of America, Annual Meeting, Cincinnati, 1961, p. 47-57.
- Durrell, R.H., 1977, A recycled landscape: Cincinnati, Ohio, Cincinnati Museum of Natural History, p. 8.
- Earth Movement Task Force, 1982, Final Report: Unpublished report to Hamilton County, Cincinnati, Ohio, September, p. 38.
- Earth Surface Processes Group, 1987, Report and Recommendations on maintenance and repair Deteriorating retaining Walls and Streets Damaged by Landslides: City of Cincinnati, Cincinnati, Ohio, University of Cincinnati Department of Geology, unpublished report to Smale Commission, July, p. 48.
- Exon, A. H., 1929, Thesis on Riverside Landslide [Senior Thesis]: Cincinnati, Ohio, University of Cincinnati Department of Civil Engineering, p. 22.
- Fenneman, N.M., 1916, Geology of Cincinnati and vicinity: Ohio Geological Survey, Fourth Series, Bulletin 19, p. 207.
- Fleming, R.W., 1975, Geologic perspectives - The Cincinnati example, Ohio Valley Soils Seminar Proceedings, 6th, Ft. Mitchell, Ky., October 17, 1975, p. 22.

- Fleming, R.W., and Johnson, A.M., 1994, Landslides in colluvium: U.S. Geological Survey Bulletin 2059-D, Washington DC, United States Government Printing Office, p. 24.
- Fleming, R. W., and Taylor, F. A., 1980, Estimating the costs of landslide damage in the United States. U.S. Geological Survey Circular 832, p. 21.
- Fleming, R.W., Johnson, A.M., and Hough, J.E., 1981, Engineering Geology of the Cincinnati Area, with contributions by Gokce, A.O., and Lion, T.E., in volume 3 of Roberts, T.G., ed., Geological Society of America Cincinnati '81 Field Trip Guidebooks: Falls Church, Va. American Geological Institute, p. 543-570.
- Geiger, K.J., 1983, The engineering geology and relative stability of parts of Newport, Bellevue, and Fort Thomas, Kentucky: Cincinnati, Ohio, University of Cincinnati M.S. thesis, p. 66.
- Gibbons, A.B., 1973, Geologic map of parts of the Newport and Withamsville Quadrangles, Campsville and Kenton Counties, Kentucky, Washington D.C., United States Geologic Survey
- Gokce, O. A., 1989, Mechanisms of landsliding in Cincinnati area, Ohio: Cincinnati, Ohio, University of Cincinnati Ph. D. dissertation, p. 502.
- Gokce, A.O., 1992, Extrusion landslides in Cincinnati lake clays: Geological Society of America Abstracts with Programs, v. 24, no. 7, p. 204.
- Hajdarwish, A., 2006, Geologic Controls of Shear Strength Behavior of Mudrocks, Ph.D. dissertation, Kent State University, p. 258.
- Hamilton County Regional Planning Commission, 1976, Hillside Development Study: Plan and Strategy, Cincinnati, Ohio.

- Haneberg, W.C., 1989, Hydrology and drainage of a thin colluvium hillside in Delhi Township, Ohio: Cincinnati, Ohio, Ohio, University of Cincinnati Ph. D. dissertation, p. 232.
- Haneberg, W.C., 1991, Observation and analysis of pore pressure fluctuations in a thin colluvium landslide complex near Cincinnati, Ohio: *Engineering Geology*, v. 31, p. 159-184.
- Haneberg, W.C., 1992, A mass balance model for the hydrologic response of fine-grained hillside soils to rainfall: *Geological Society of America Abstracts with Programs*, v. 24, no. 7, p. 203.
- Haneberg, W.C., Riestenberg, M.M., Pohana, R.E., and Diekmeyer, S.C., 1992, Cincinnati's geologic environment, a trip for secondary school science teachers: *Ohio Division of Geological Survey Guidebook 9*, p. 23.
- Haneberg, W.C. and Gökce, A.Ö., 1994, Rapid water-level fluctuations in a thin colluvium landslide west of Cincinnati, Ohio: *U.S. Geological Survey Bulletin* 2059-C, p. 16.
- Hillside Trust, 1991, A hillside protection strategy for Greater Cincinnati – 1 - Overview: Cincinnati, Hillside Trust, p. 23., map, scale [1:126,720].
- Hillside Trust, 1991, A hillside protection strategy for Greater Cincinnati – 2 – Identifying Greater Cincinnati's sensitive hillsides: Cincinnati, Hillside Trust, 36 p. 7 maps, scale [1:126,720], [1:6486].

- Hillside Trust, 1991, A hillside protection strategy for Greater Cincinnati – 3 –  
Development guidelines for Greater Cincinnati's hillsides: Cincinnati, Hillside Trust, p. 131.
- Hofman, H.J., 1966, Deformational structures near Cincinnati, Ohio: Geological Society of America Bulletin, v. 77, no. 5, p. 533-548.
- Holtz, R.D. and Kovacs, W.D., 2011, An introduction to geotechnical engineering, Prentice-Hall, Inc., p. 13.
- Hough, J.E., 1978, Landsliding in Greater Cincinnati: Cincinnati, Ohio, James E. Hough, pamphlet, p. 35.
- Hough, J.E., and Fleming, R.W., 1974, Landslide-prone bedrock hillsides within the city of Cincinnati, Hamilton County, Ohio, Cincinnati, Ohio, Cincinnati Institute, map (1:24,000) with text.
- Hutto, Chloe, 1992, Stability analysis of a landslide along westbound I-275. Hamilton County, Ohio, Miami, Ohio: Miami University, p. 121.
- IAEG Commission on Landslides, 1990, Suggested nomenclature for landslides, Bulletin of the International Association of Engineering Geology, No. 41, p. 13-16.
- Lerch, N.K., Hale, W.F., and Lemaster, D.D., 1982, Soil Survey of Hamilton County, Ohio, U.S. Soil Conservation Service, p. 219.
- Lion, T.E., 1983, Engineering geology and relative stability of ground for hillside development in part of Springfield Township, Hamilton County, Ohio: Cincinnati, Ohio, University of Cincinnati M.S. thesis, p. 157.

- McCandless, R.M., 1976, Measurement of bulking in landslides on the basis of topographic form and density changes in landslide debris: Cincinnati, Ohio, University of Cincinnati M.S. thesis, p. 63.
- Merritt, R., 1975, Hillside Development Study - Identification of Critical Environmental Impact Areas: Cincinnati, Ohio, Hamilton County Regional Planning Commission, p. 65.
- Murdoch, L.C., III, 1987, Pore-water pressures and unsaturated flow during infiltration into colluvial soils at the Delhi Pike landslide, Cincinnati, Ohio: Cincinnati, Ohio, University of Cincinnati M.S. thesis, p. 133.
- Nutting, H.C. and Co., 1967, Physical features of the Ohio-Indiana area: Cincinnati, Ohio, unpublished report to Hamilton County Regional Planning Commission. Scale 1:16,000.
- Ohio Emergency Management Agency (Ohio EMA), 2011, State of Ohio emergency hazard mitigation plan: Ohio Department of Public Safety, p. 345.
- Ohio Office of Information Technology (OIT), 2006, Ohio Geographically Referenced Information Program (OGRIP): Ohio Statewide Imagery Program (OSIP).
- Ohio Office of Information Technology (OIT), 2007, Ohio Geographically Referenced Information Program (OGRIP): Ohio Statewide Imagery Program (OSIP), Metadata.
- Olson, R.L., 1988, Engineering geology and relative stability of ground adjacent to Sawyer Place, Cincinnati, Ohio: Cincinnati, Ohio, University of Cincinnati M.S. thesis, p. 102.

- Pavey, R.R., Goldthwait, R.P., Brockman, C.S., Hull, D.N., and Van Horn, R.G., 1992, The new Quaternary map of Ohio: Geological Society of America Abstracts with Programs, v. 24, no. 7, p. 314.
- Pohana, R. E., 1983, The Engineering geologic and relative stability analysis of a portion of Anderson Township: Cincinnati, Ohio, University of Cincinnati M.S. thesis, p. 132.
- Pohana, R.E., 1992, City of Cincinnati, geotechnical office: The Hillside Trust Outlook, v.11, no. 1 [spring], p.1-2.
- Pohana, R.E., 1992, Landslide remediation and prevention by the City of Cincinnati: Geological Society of America Abstracts with Programs, v. 24, no. 7, p. 204.
- Pohana, R.E., and Jamison, T.M., 1993, Landslide remediation and prevention by the City of Cincinnati: Ohio Valley Soils Seminar Proceedings, 24th, Ft. Mitchell, Ky., October 15, 1993, p.1-18.
- Potter, P. E., 2007, Exploring the geology of the Cincinnati/Northern Kentucky region. Kentucky Geological Survey, Special Publication 8, Series XII, University of Kentucky. p 56-65.
- Richards, K.A., 1982, The Engineering geology and relative stability of Mt. Adams, and parts of Walnut Hills and Columbia Parkway, Cincinnati, Ohio: Cincinnati, Ohio, University of Cincinnati M.S. thesis, p. 111.
- Riestenberg, M.M., 1981, The effect of woody vegetation on stabilizing slopes in the Cincinnati Area, Ohio: Cincinnati, Ohio, University of Cincinnati M.S. thesis, p. 79.



- Riestenberg, M.M., 1981, Anchoring of thin colluvium on hill slopes in Cincinnati by roots of Sugar Maple and White Ash Cincinnati, Ohio, University of Cincinnati Ph.D. dissertation, p. 366.
- Riestenberg, M.M., 1992, A study of two tree species interplanted in colluvium on hillsides in Cincinnati, Ohio: Geological Society of America Abstracts with Programs, v. 24, no. 7, p. 204.
- Riestenberg, M.M., 1994, Anchoring of thin colluvium by roots of sugar maple and white ash on hill slopes in Cincinnati: U.S. Geological Survey Bulletin 2059-E, p. 25.
- Riestenberg, M.M. and Sovonik-Dunford, S., 1983, The role of woody vegetation in stabilizing slopes in the Cincinnati area, Ohio: Geological Society of America Bulletin, v. 94, p. 506-518
- Rockaway, John, 2002, Southwestern Ohio landslide documentation investigation report, United States Geological Survey, Denver: USGS, p. 2 - 3.
- RocScience, 2012, Slide, <http://www.roscience.com/products/8/Slide>
- Rodriguez-Molina, C. 1983, Engineering geology and relative stability of parts of Avondale, Cincinnati, Ohio: Cincinnati, Ohio, University of Cincinnati M.S. thesis, p. 86.
- Sarman, R., 1991, A multiple regression approach to predict swelling in mudrocks, Ph.D. dissertation, Kent State University, p. 365.
- Scheper, R.J., 1973, Report of a landslide investigations: Cincinnati, Ohio, University of Cincinnati, Geology Library, graduate student report, p. 20.
- Schuster, R.L., 1996, Socioeconomic significance of landslides, Landslides Investigation and Mitigation, Transportation Research Board Special Report 247, p. 12-35.

- Smale, J.G. 1987, City of Cincinnati Infrastructure Report. p. 51.
- Sowers and Dalrymple, Consulting Engineers, 1980, Landslide susceptibility map of Cincinnati, Ohio: Unpublished report to the City of Cincinnati, May, maps (scale 1:24,000 and 1:9,600) with text.
- Taylor, F.A., Fleming, R.W., and Durrell, R., 1981, Seasonal movements of landslides near Cincinnati, Ohio, in Geological Survey Research 1981: U.S. Geological Survey Professional Paper 1275, p. 223.
- Von Schlichten, O. C., 1935, Landslides in the Vicinity of Cincinnati: The Compass, Sigma Gamma Epsilon, v. 15, no. 3, p. 151-154.
- Yahne, Gerald, 1974, A preliminary study of landslides in Cincinnati, Ohio, Cincinnati, Ohio: Department of Geology, University of Cincinnati, p.7.

## APPENDIX I

### Geologic Maps of the Cincinnati, OH Area

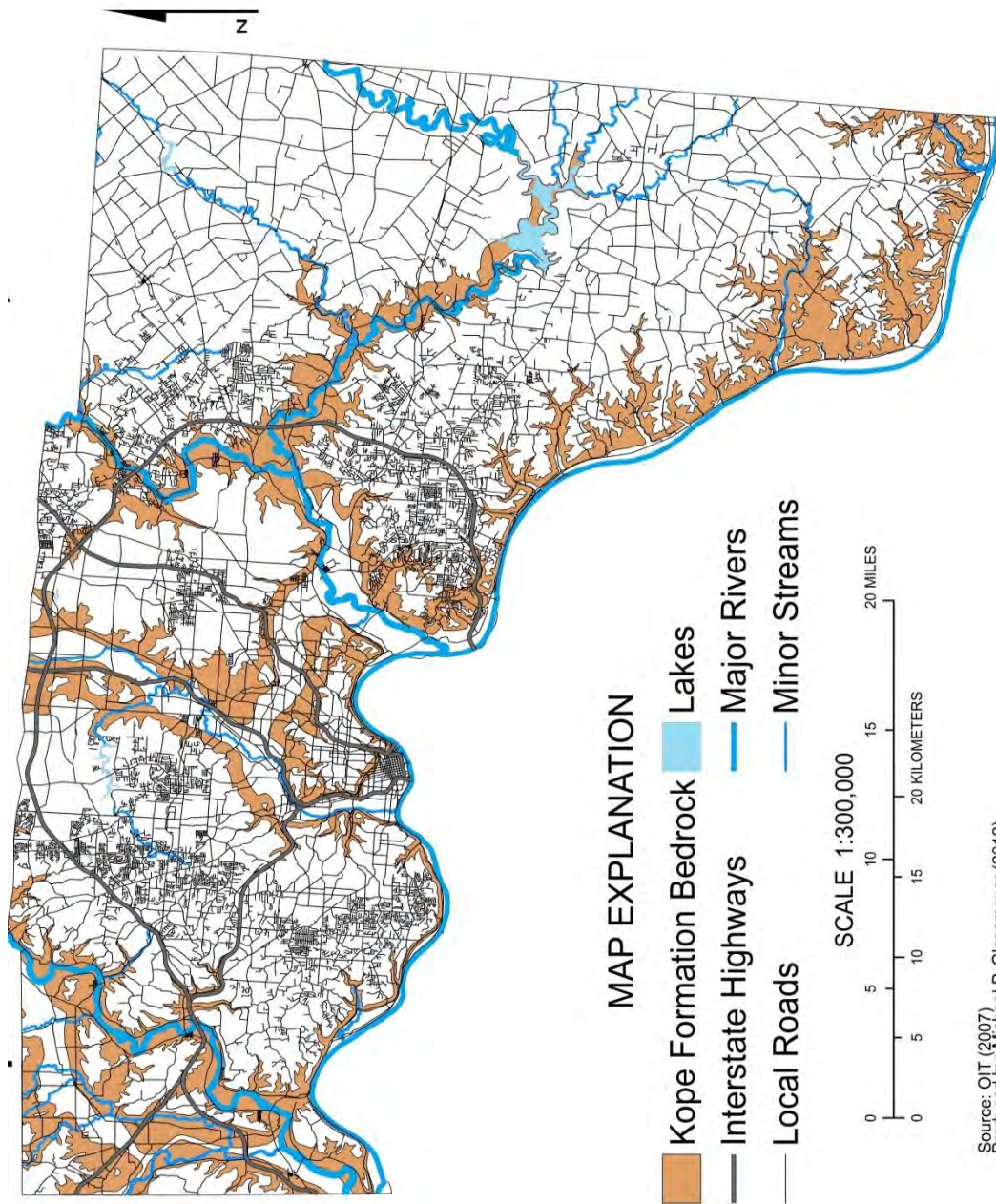


Figure AI.1: Map showing the extent of the Kope Formation bedrock in the Cincinnati, Ohio area.

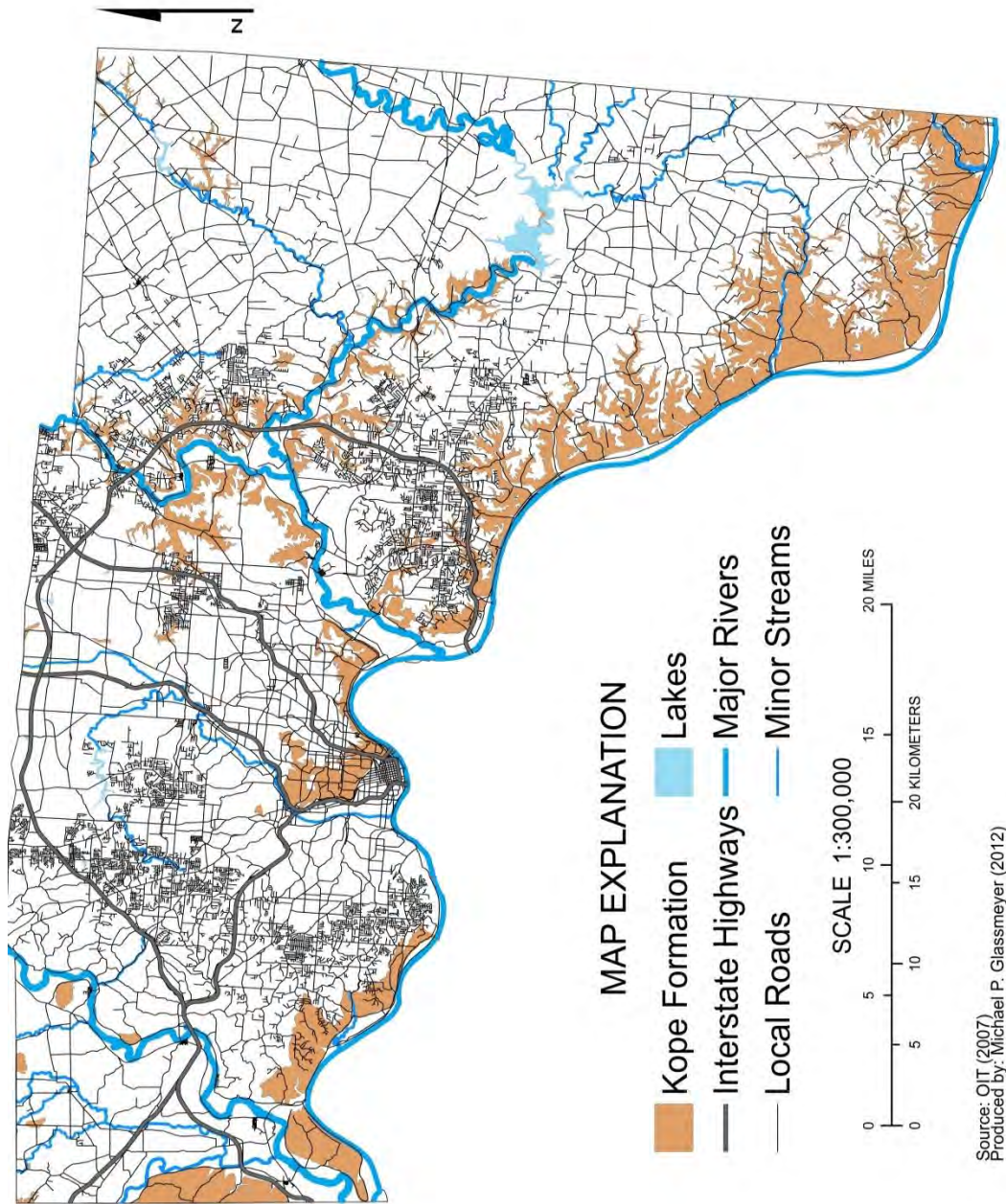


Figure AI.2: Map showing the surficial deposits of the Kope Formation in the Cincinnati, Ohio area.



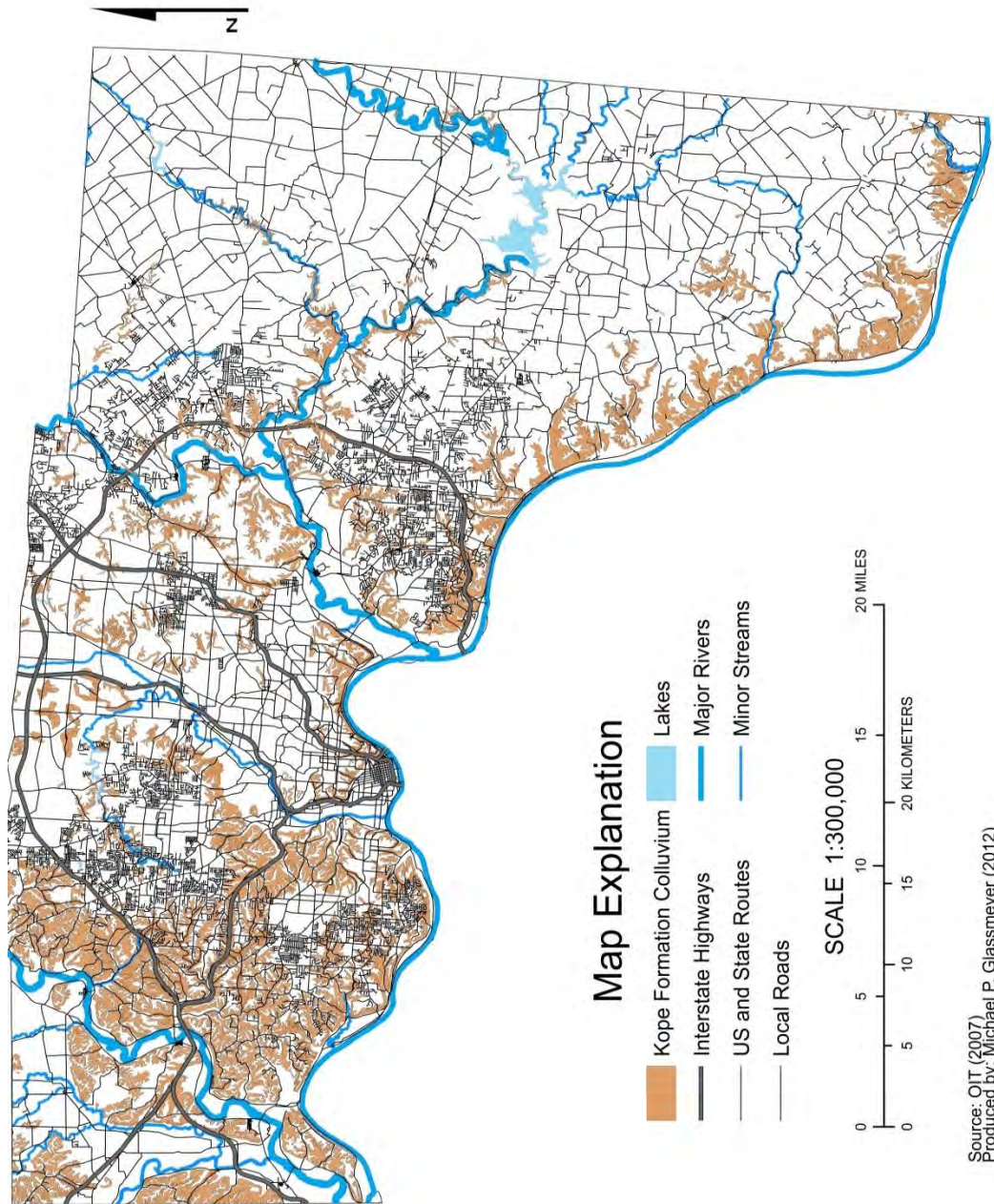


Figure AI.3: Map showing the colluvium derived from the Kope Formation in the Cincinnati, Ohio area.

## APPENDIX II

### LiDAR Derived Maps and Aerial Photographs

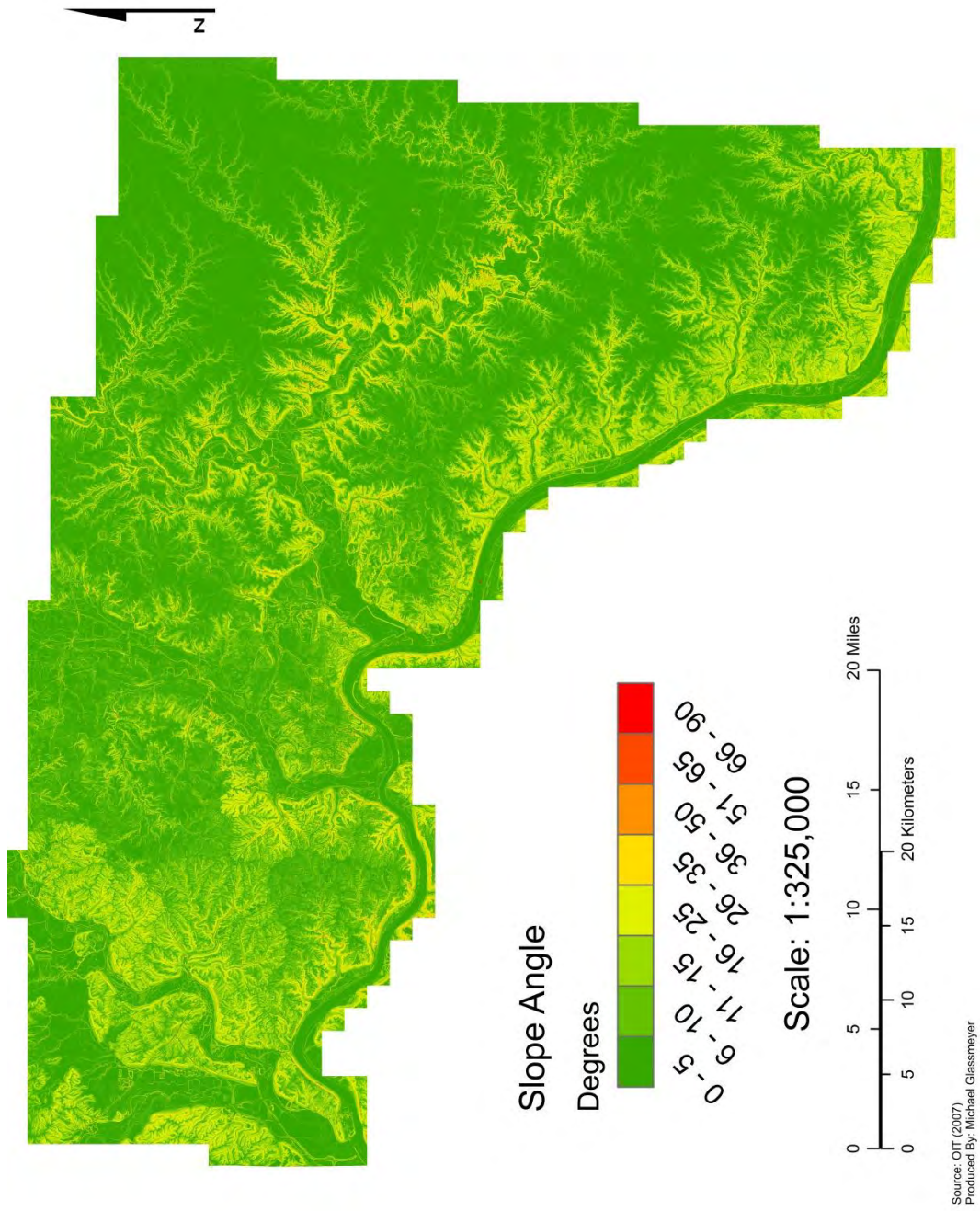
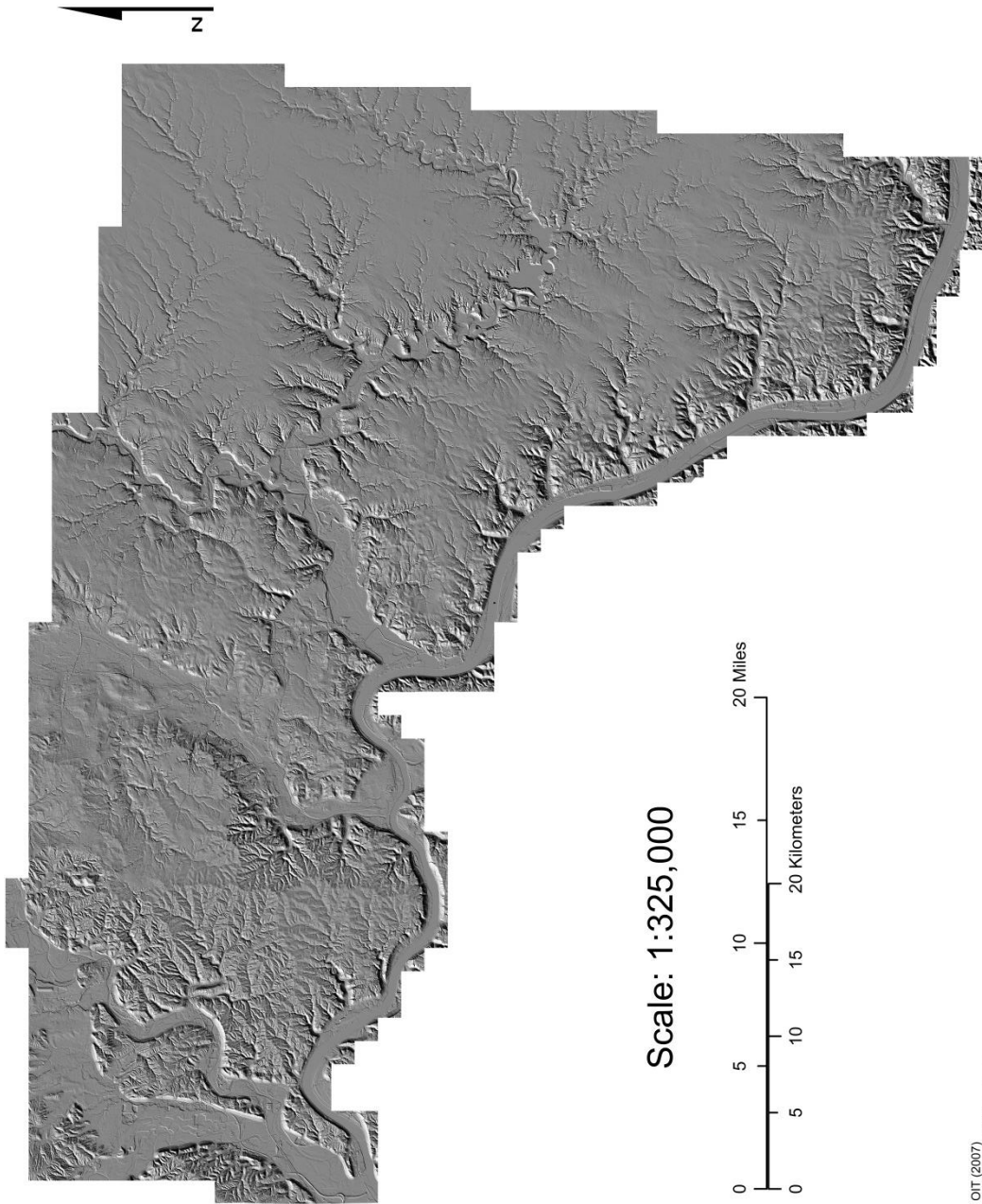


Figure AII.1: Slope map generated from LiDAR data of the Cincinnati, Ohio area.





Source: OIT (2007)  
Produced By: Michael Glassmeyer

Figure AII.2: Hillshade map generated from LiDAR Data of the Cincinnati, Ohio area.

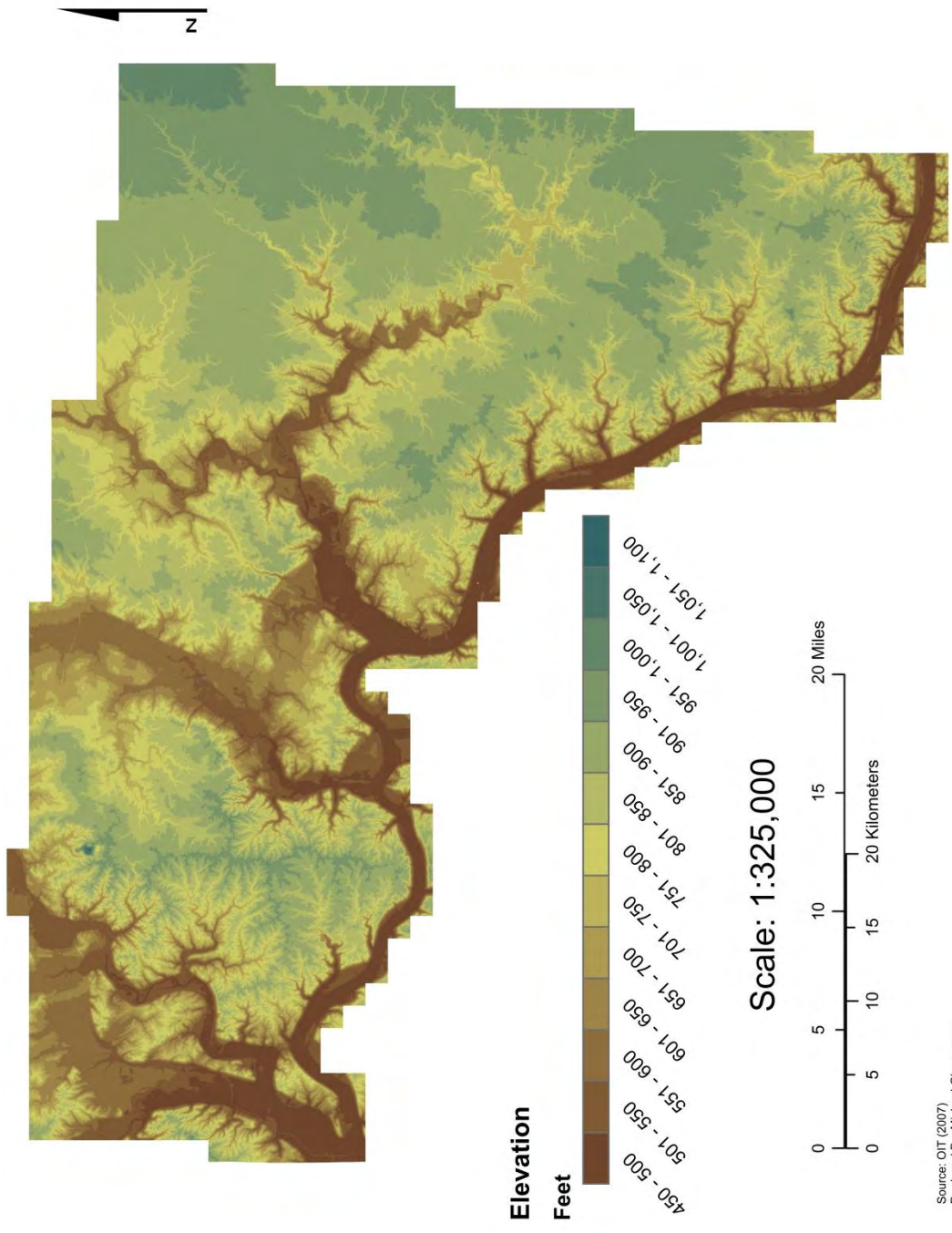


Figure AII.3: DEM map generated from LiDAR Data of the Cincinnati, Ohio area.

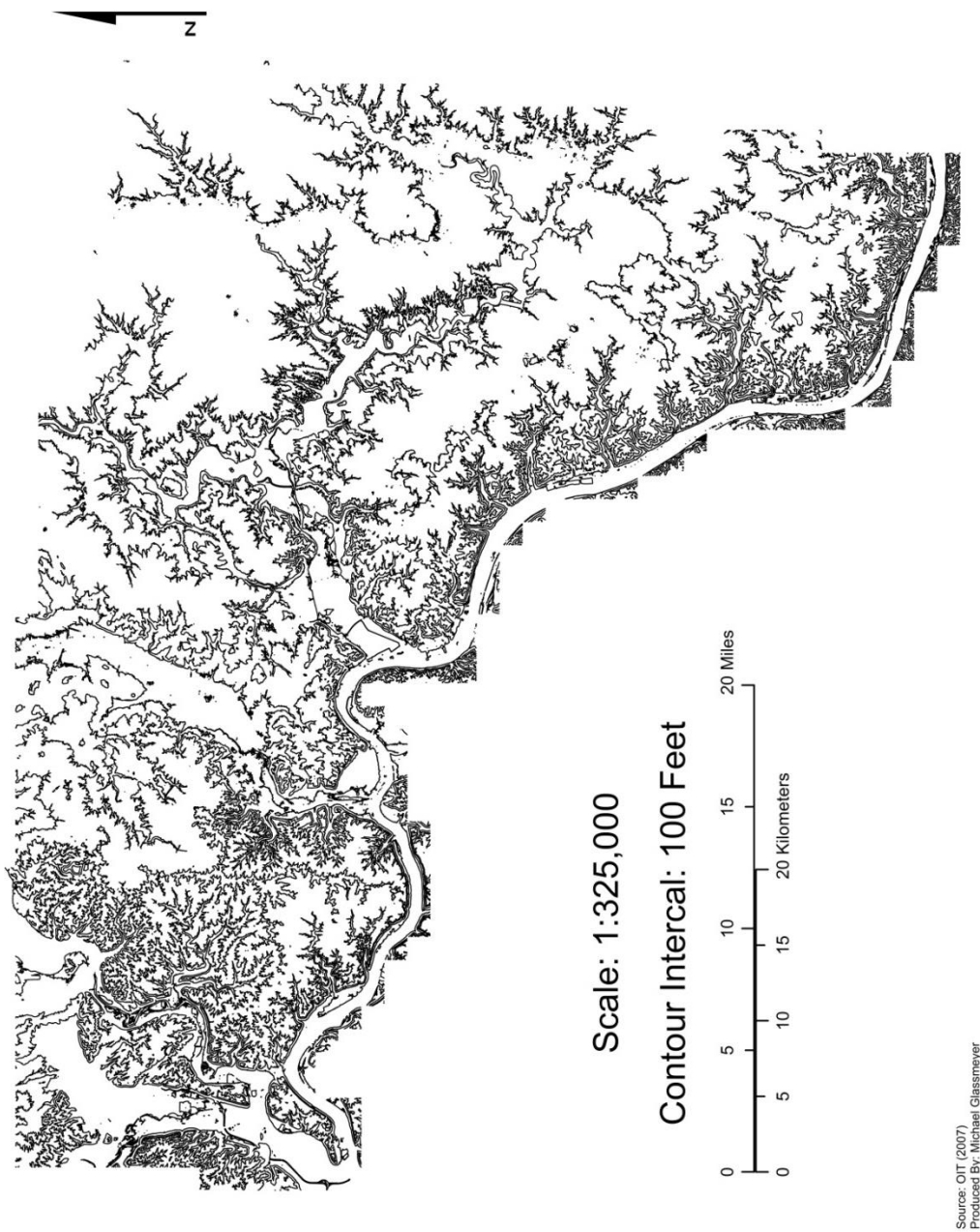
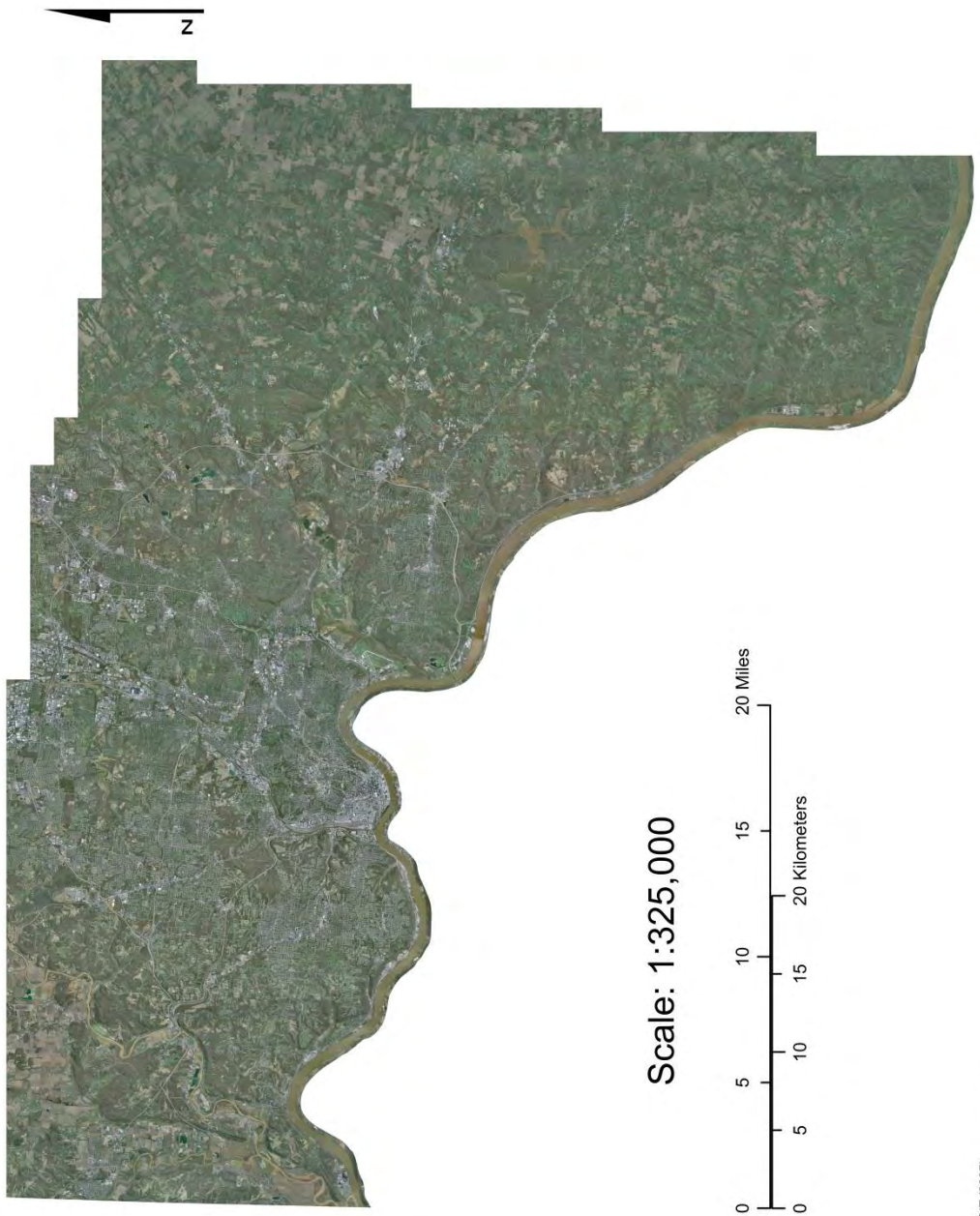


Figure AII.4: Topographic map generated from LiDAR Data of the Cincinnati, Ohio area.



Source: OIT (2007)  
Produced By: Michael Glassmeyer

Figure AII.5: Aerial photograph of the Cincinnati, Ohio area.

## APPENDIX III

### Grain Size Distribution Analysis Results

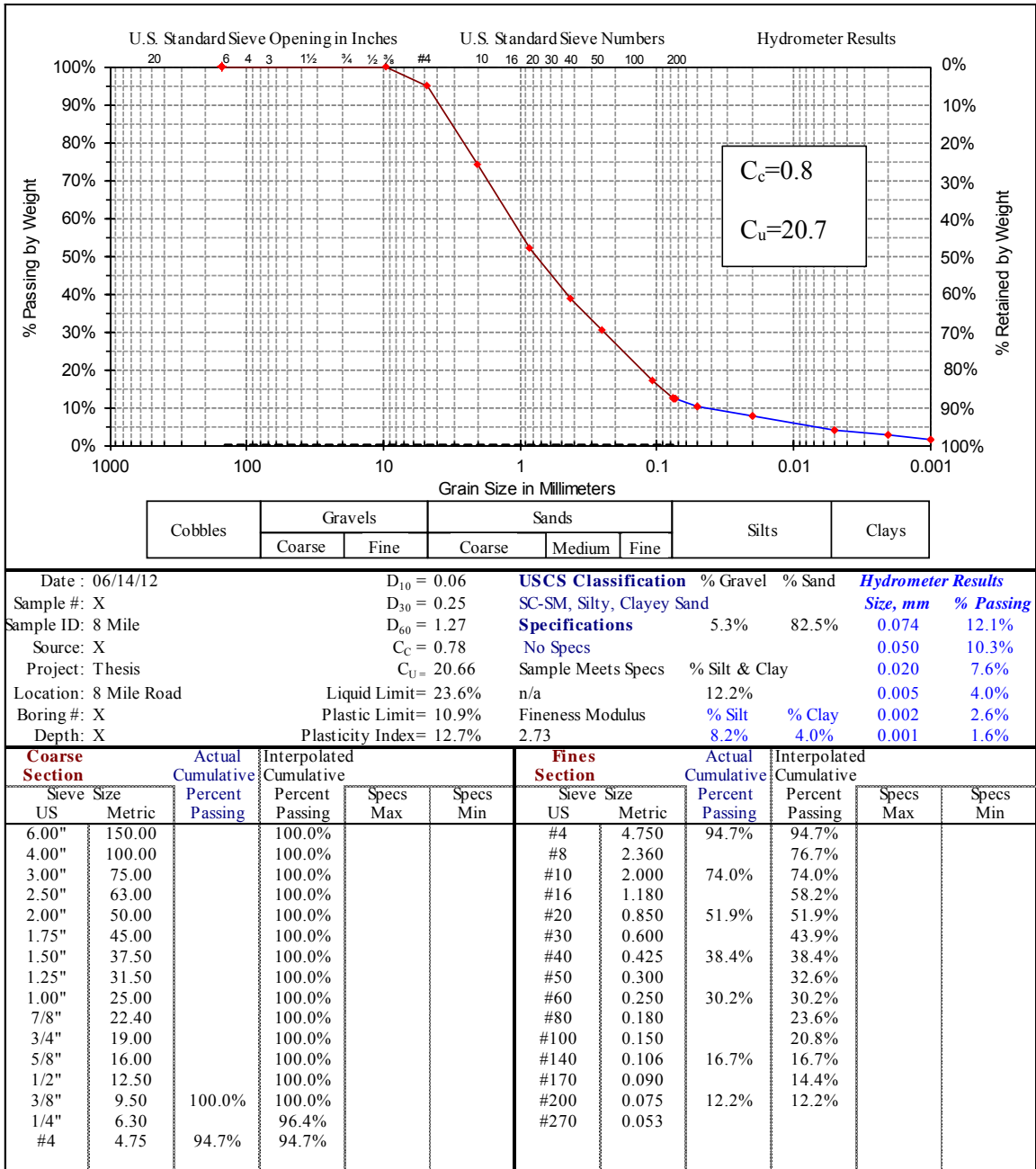


Figure AIII.1: Eight Mile Road landslide grain size distribution analysis results.



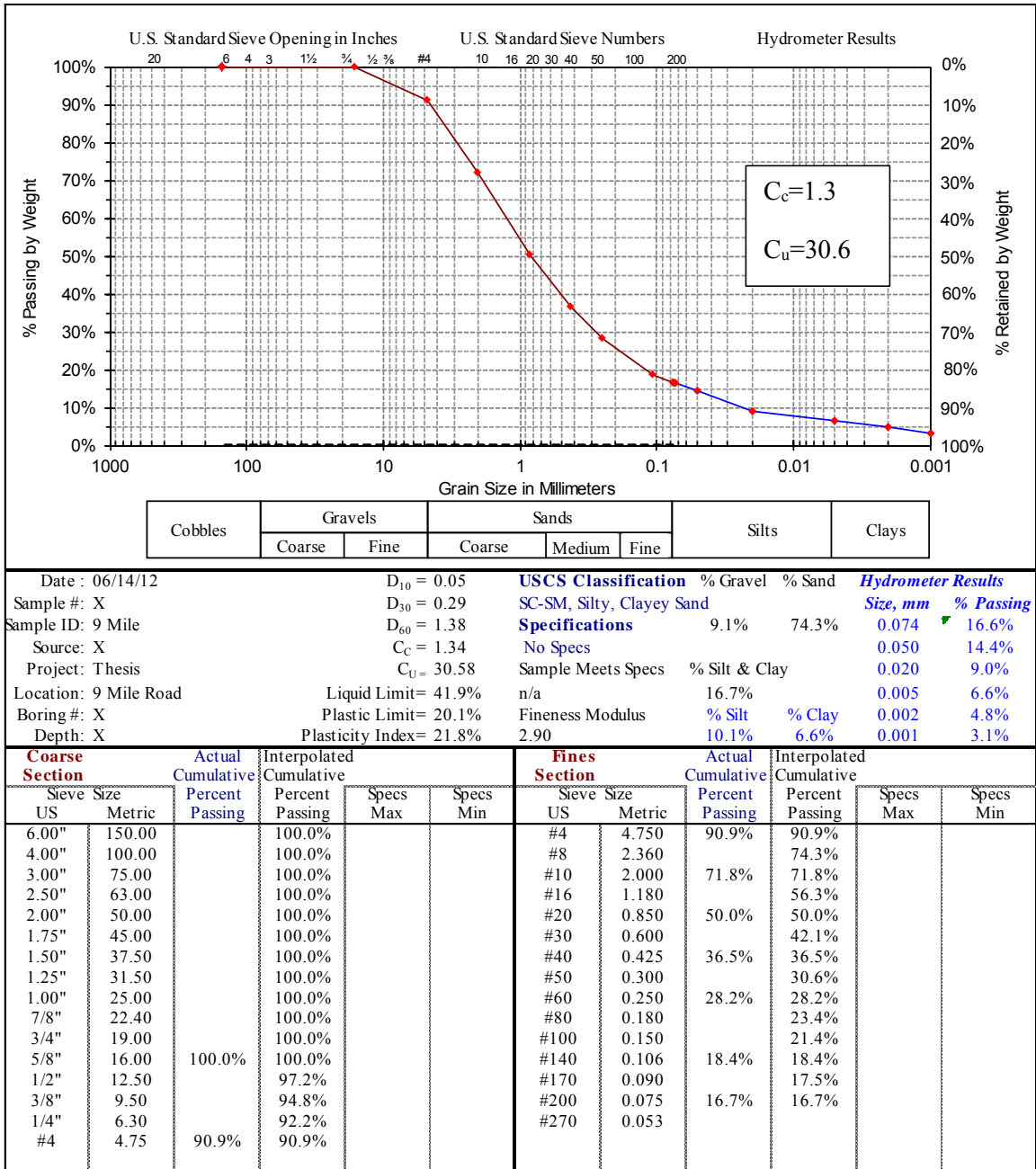


Figure AIII.2: Nine Mile Road landslide grain size distribution analysis results.

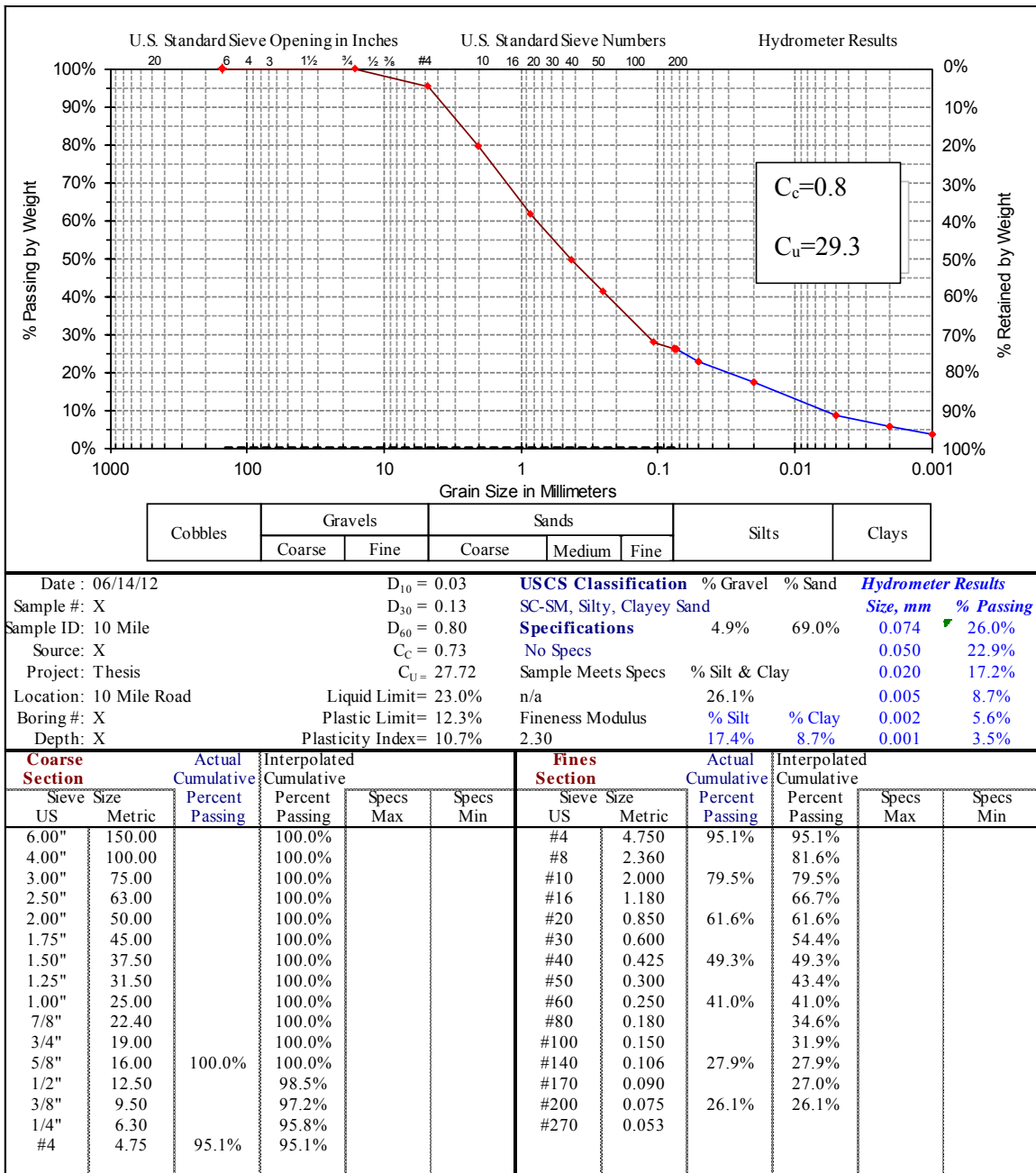


Figure AIII.3: Ten Mile Road landslide grain size distribution analysis results.



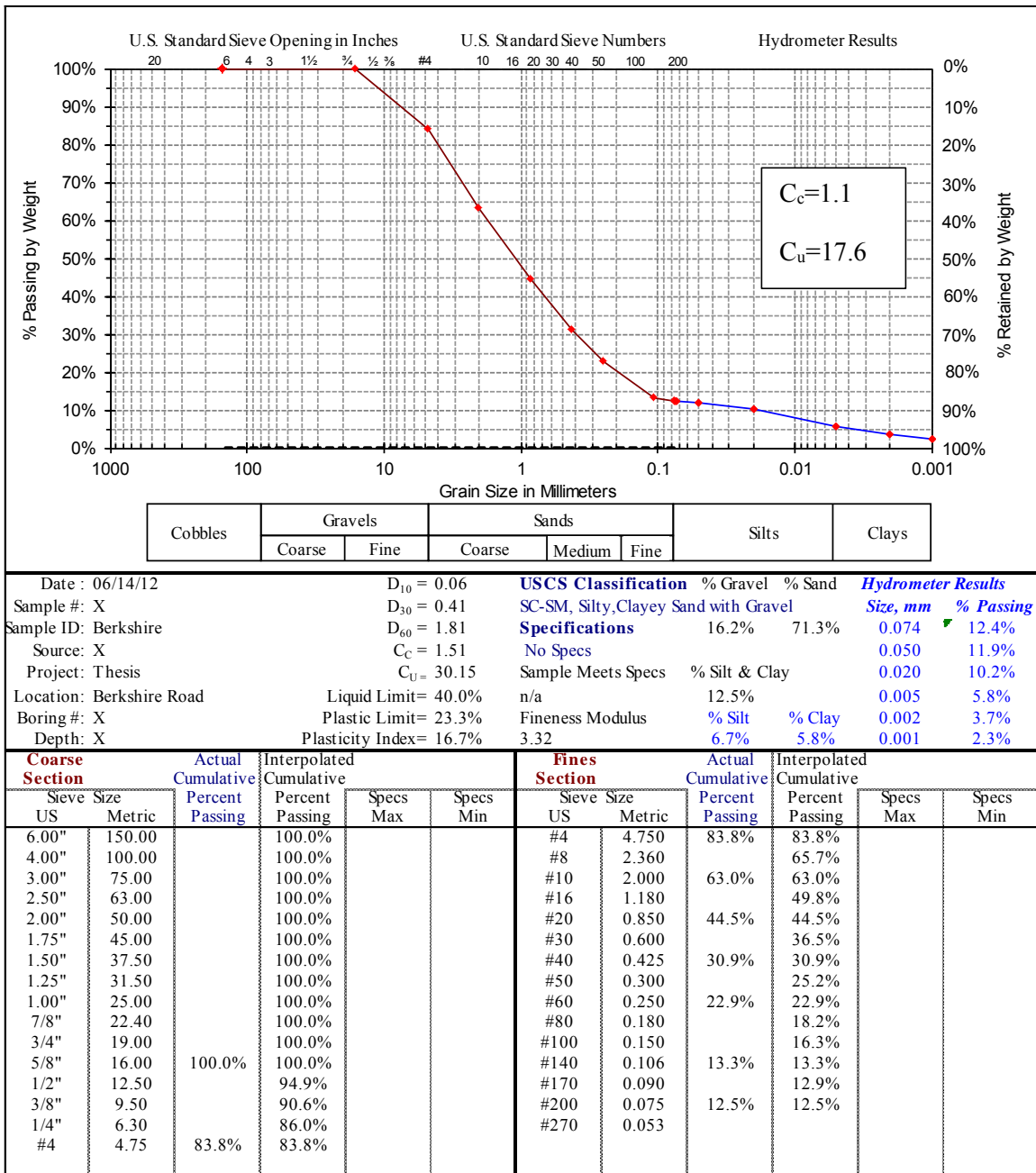


Figure AIII.4: Berkshire Road landslide grain size distribution analysis results.

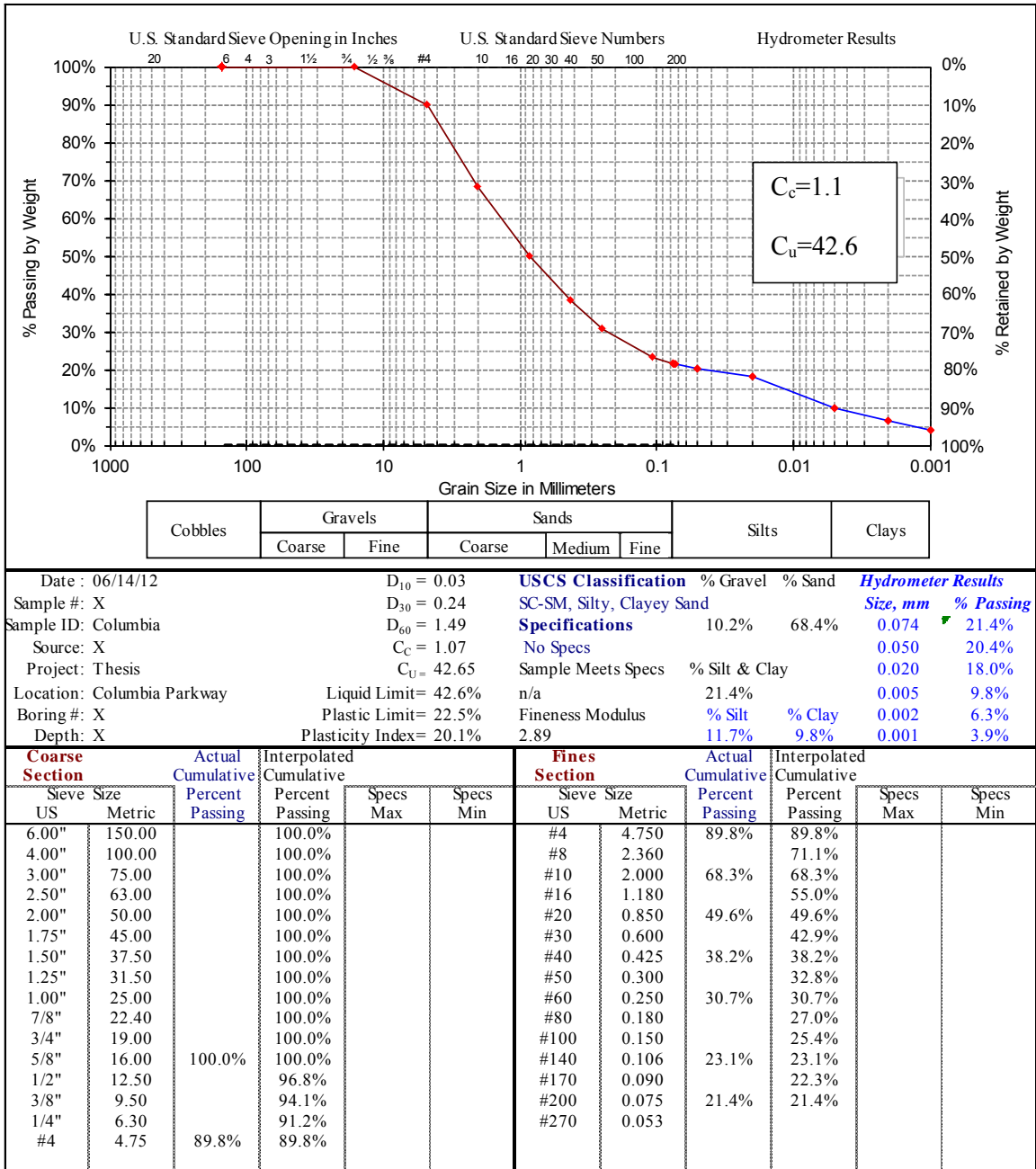


Figure AIII.5: Columbia Parkway landslide grain size distribution analysis results.

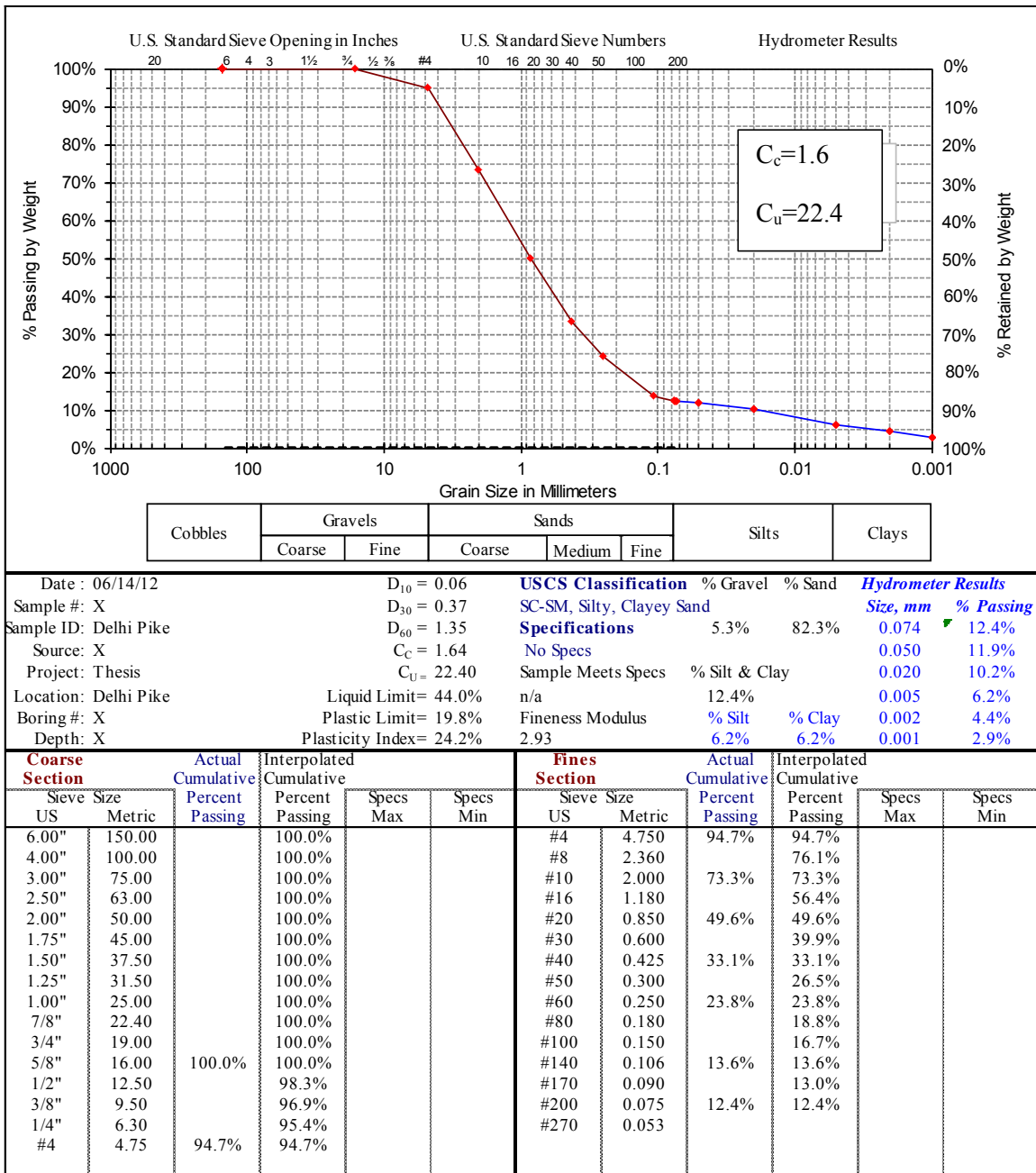


Figure AIII.6: Delhi Pike landslide grain size distribution analysis results.

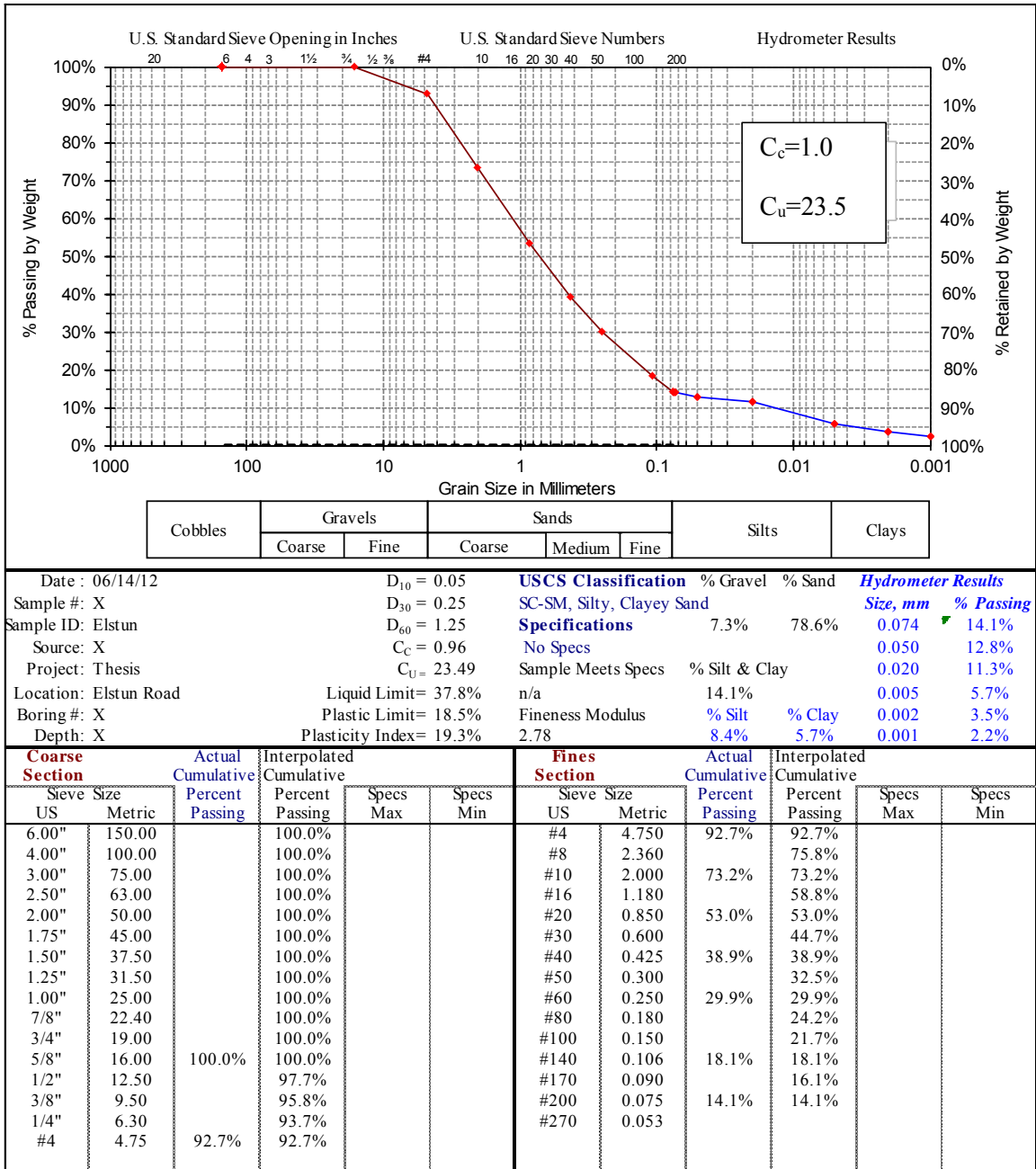


Figure AIII.7: Elstun Road landslide grain size distribution analysis results.

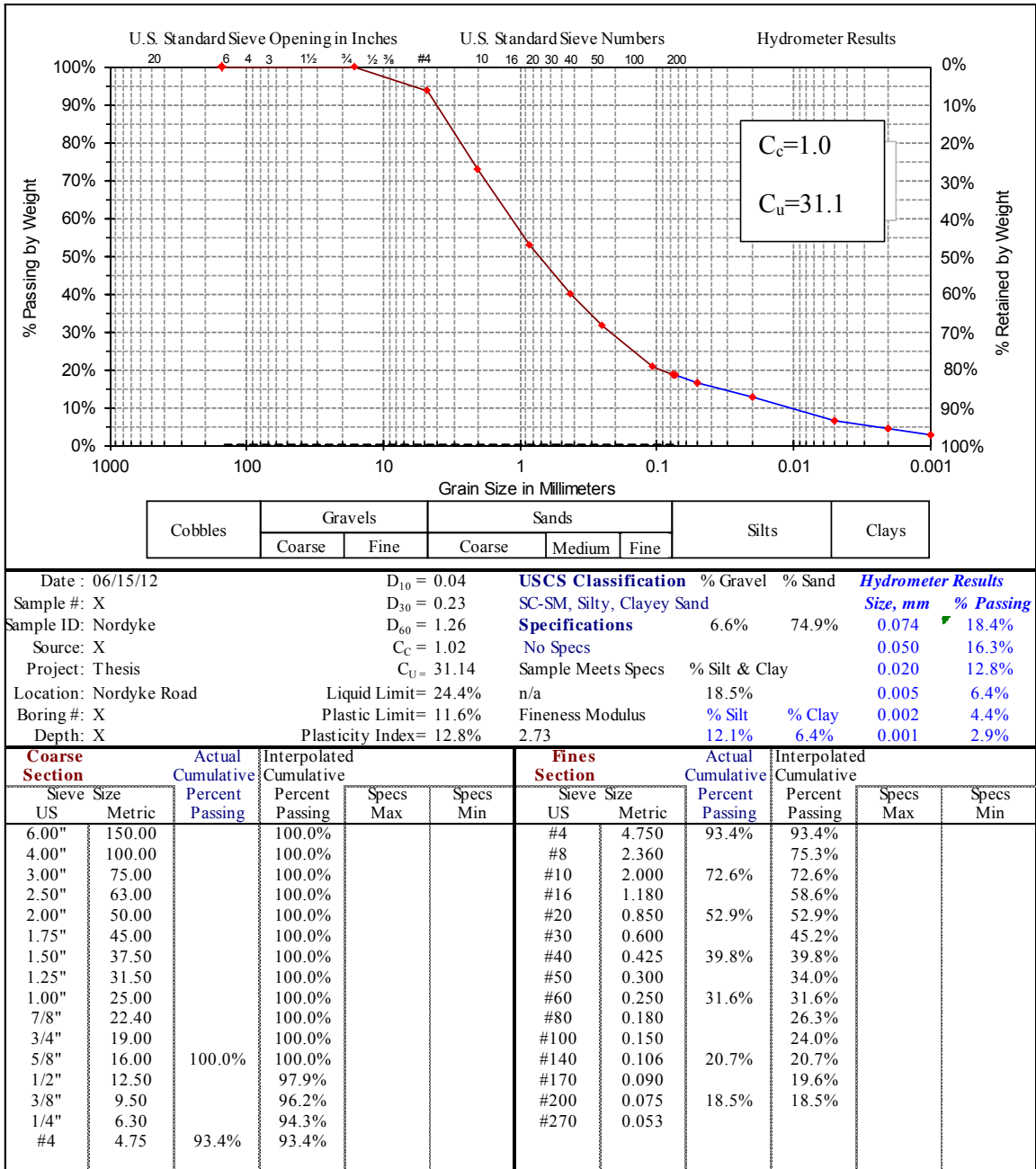


Figure AIII.8: Nordyke Road landslide grain size distribution analysis results.

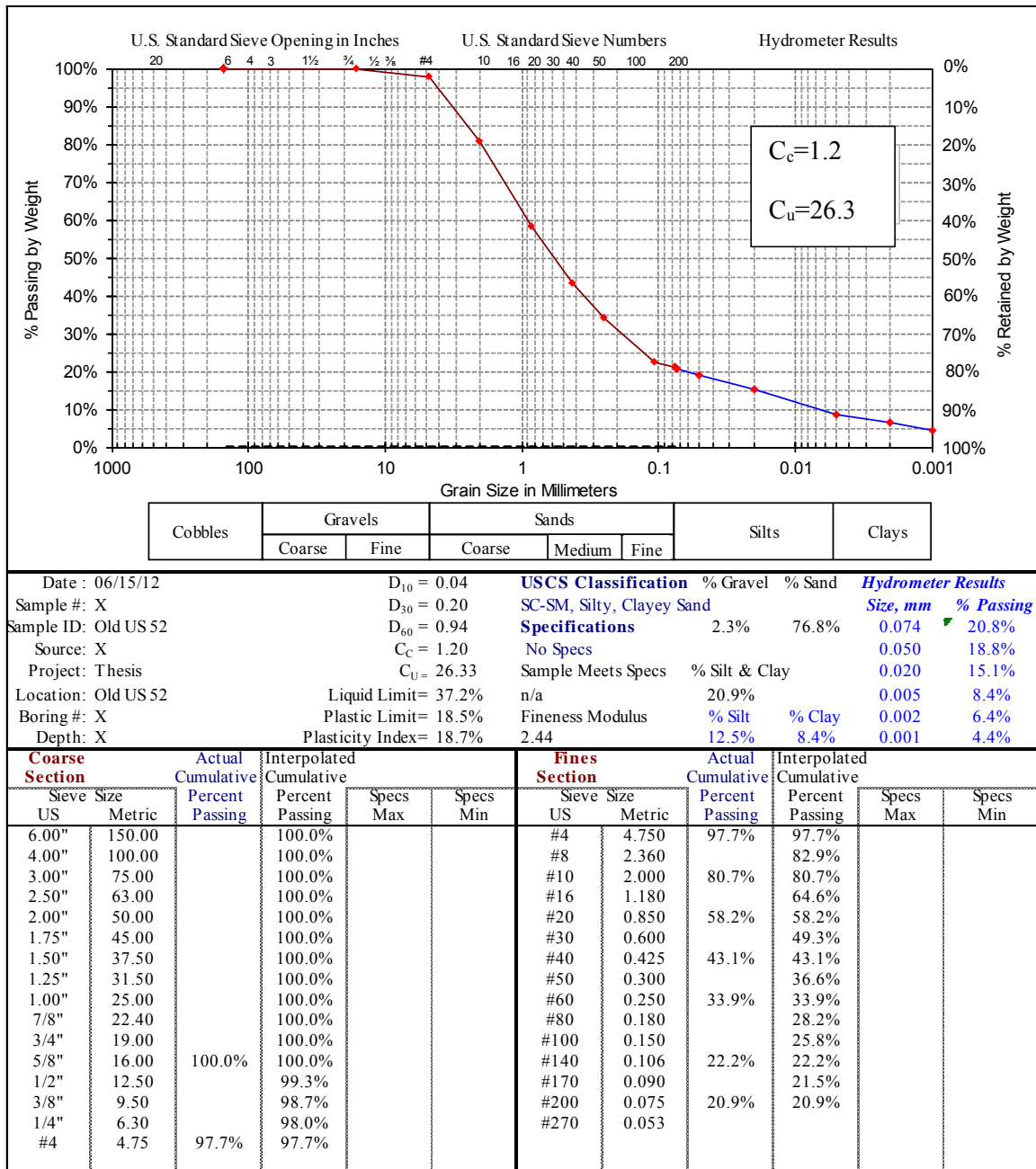


Figure AIII.9: Old US 52 landslide grain size distribution analysis results.

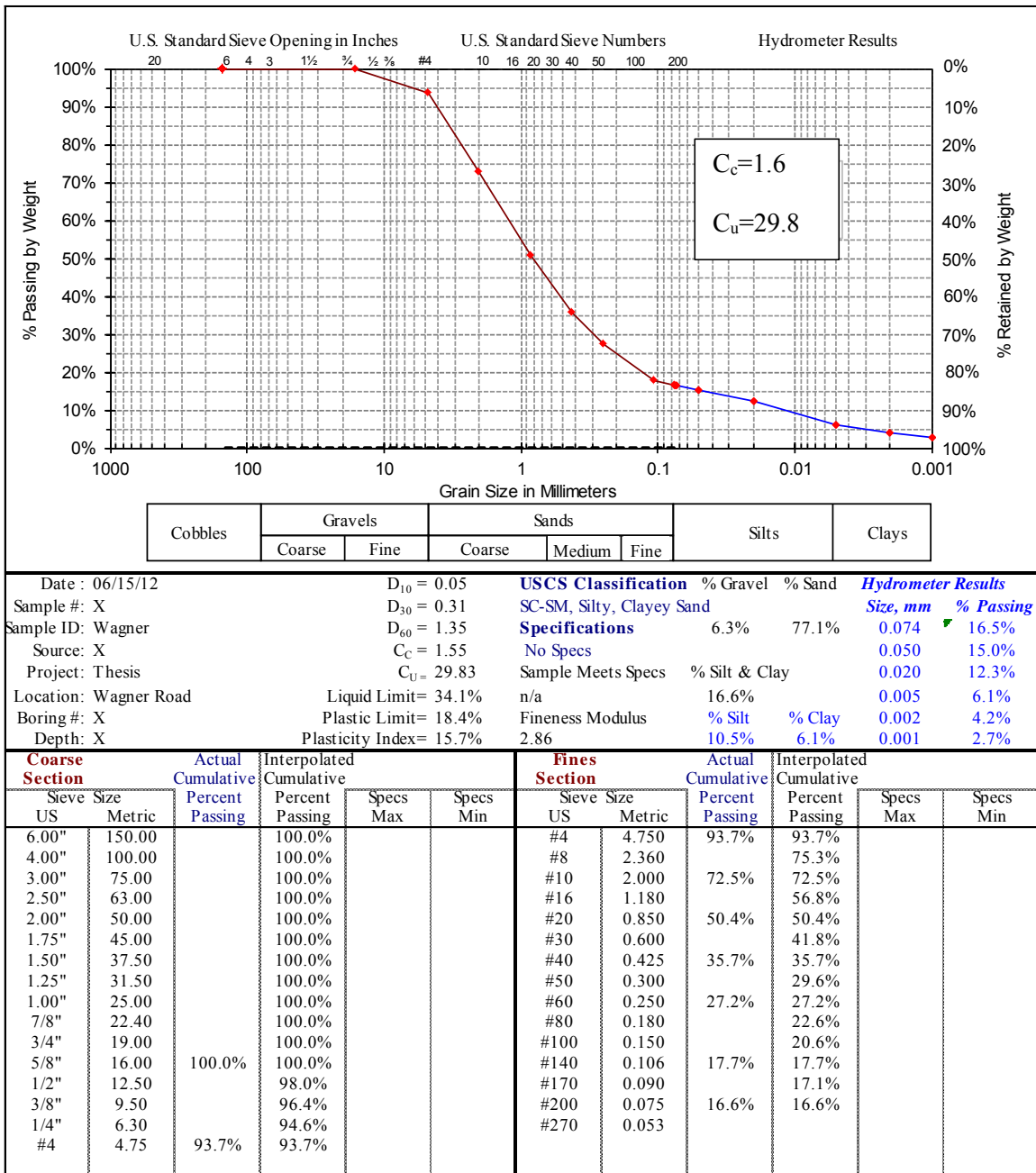


Figure AIII.10: Wagner Road landslide grain size distribution analysis results.

## APPENDIX IV

### Direct Shear Test Results



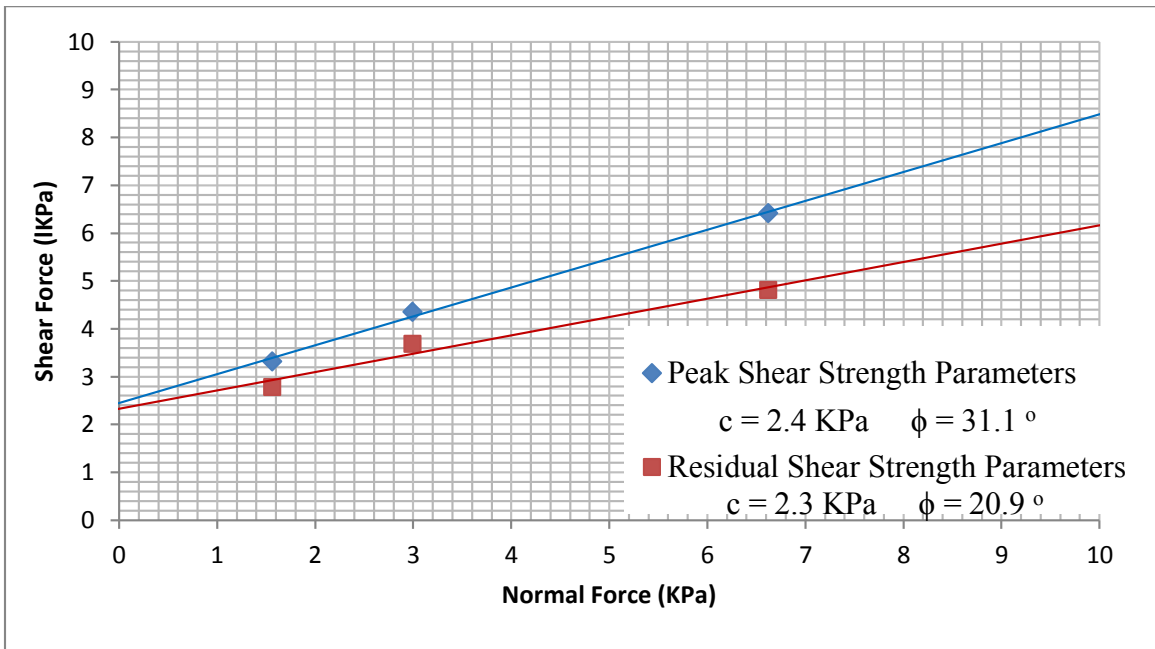


Figure AIV.1: Eight Mile Road landslide direct shear test results.

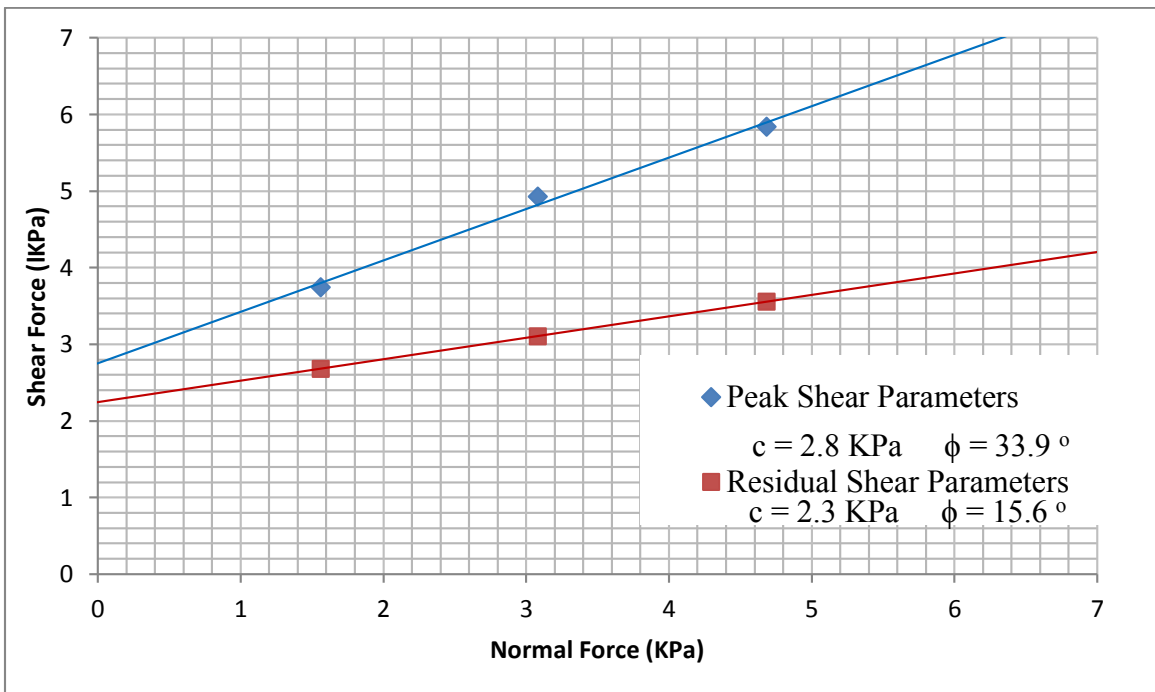


Figure AIV.2: Ten Mile Road landslide direct shear strength test results.

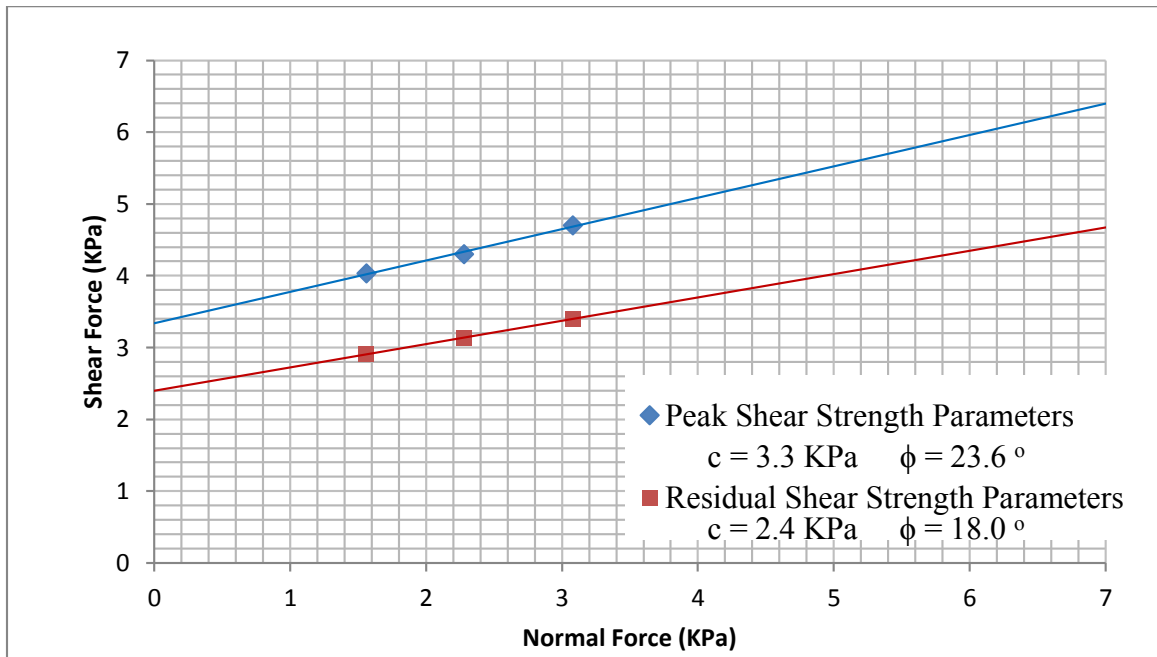


Figure AIV.3: Delhi Pike landslide direct shear strength test results.

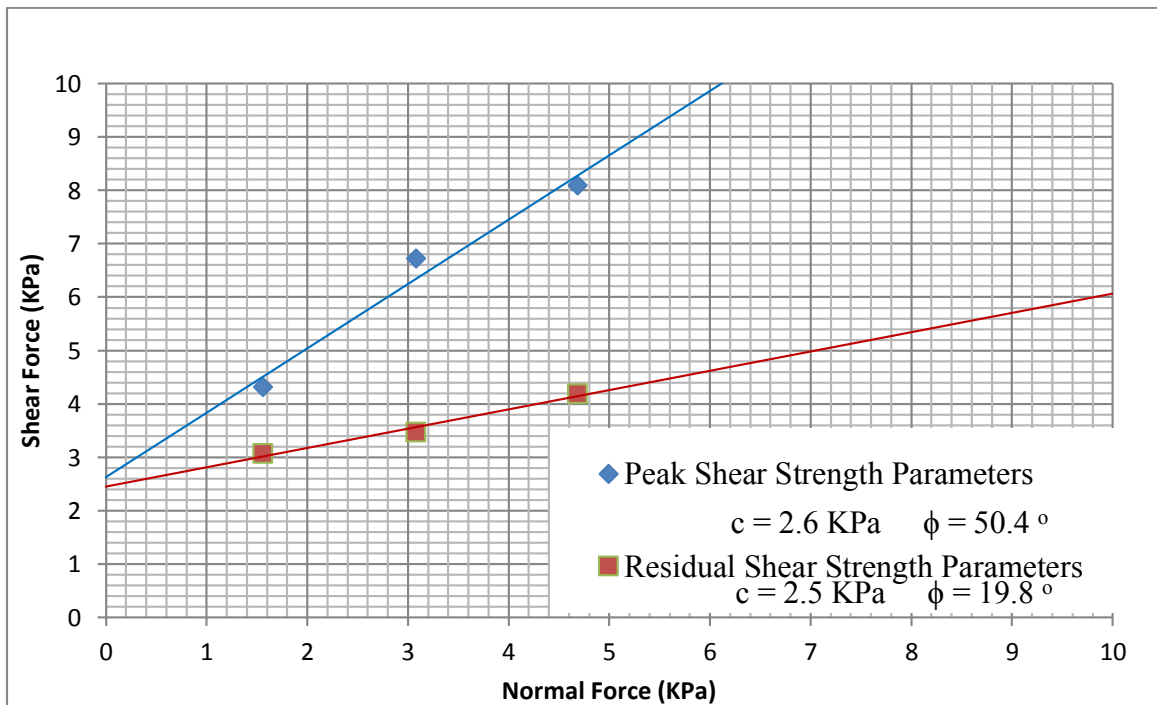


Figure AIV.4: Elstun Road landslide direct shear strength test results.

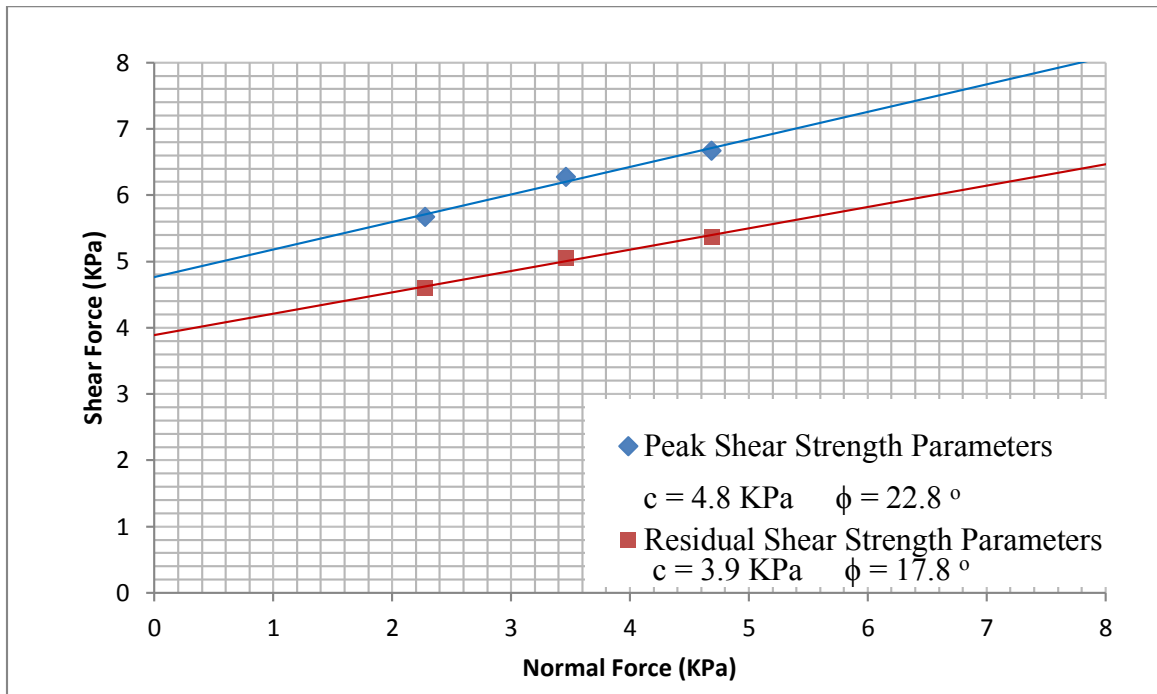


Figure AIV.5: Nordyke Road landslide direct shear strength test results.

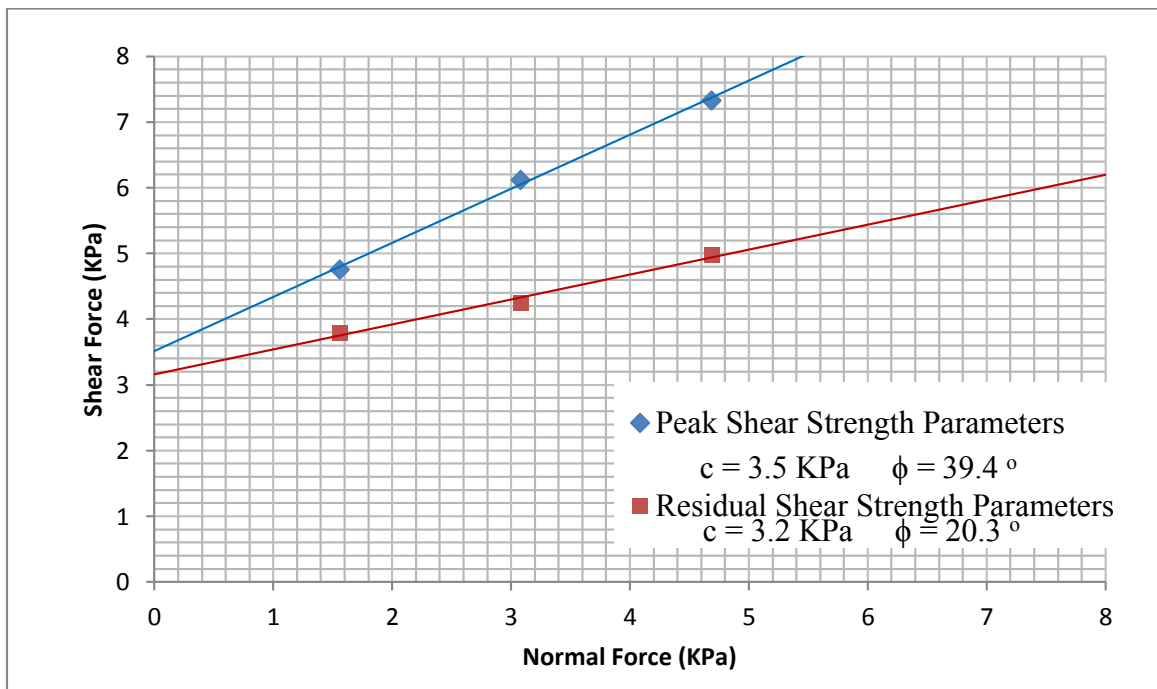


Figure AIV.6: Old US 52 landslide direct shear strength test results.

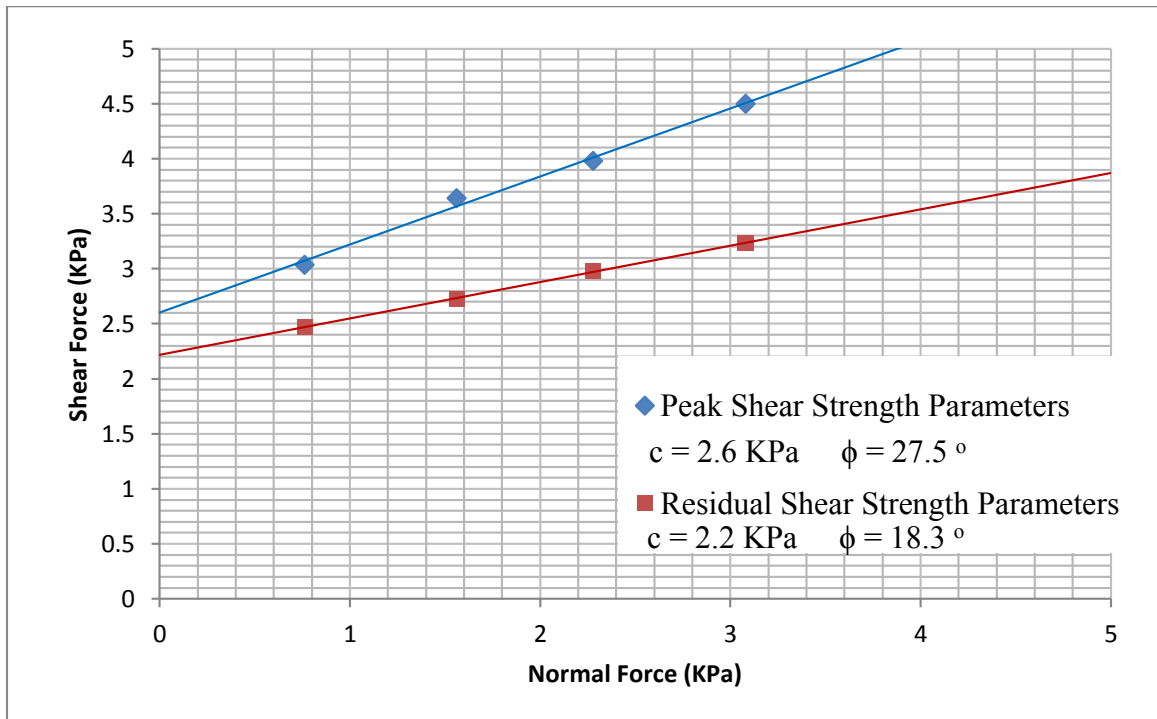


Figure AIV.7: Wagner Road landslide direct shear strength test results.

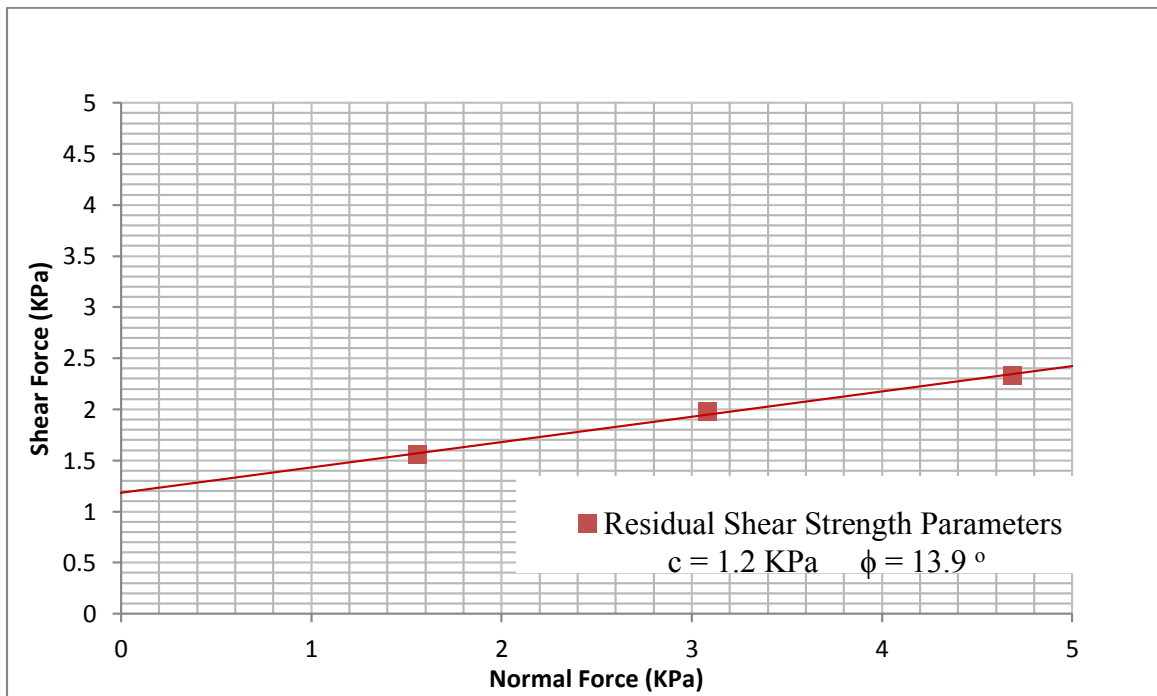


Figure AIV.8: Nine Mile Road landslide direct shear strength test results.

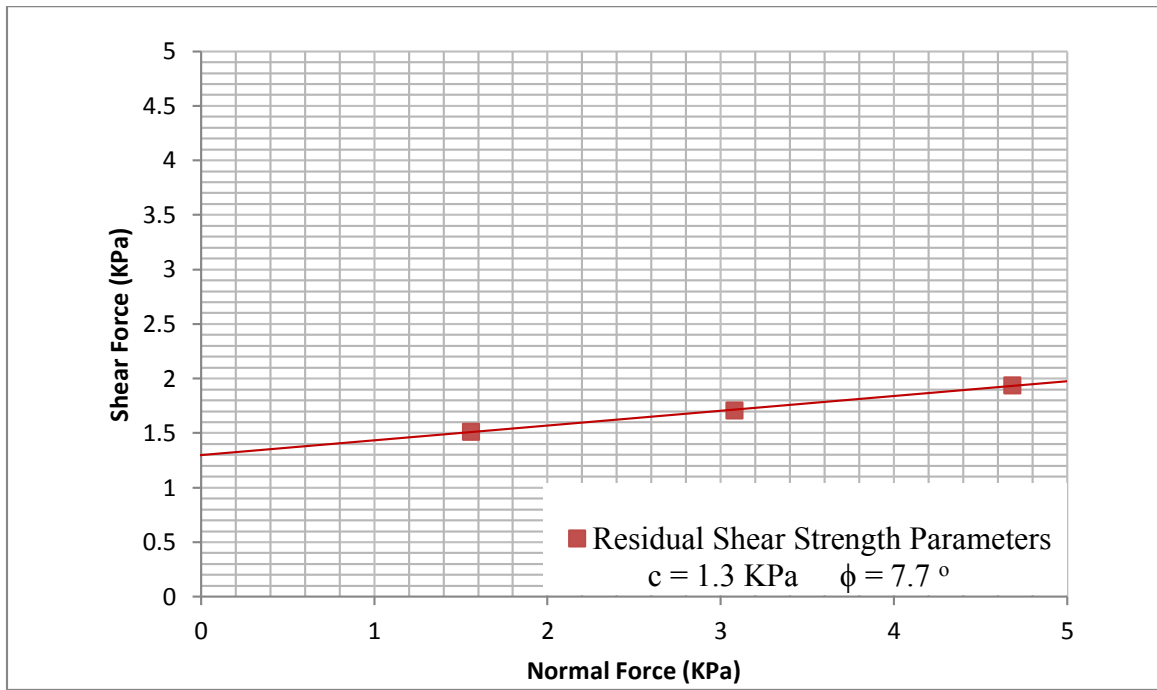


Figure AIV.9: Berkshire Road landslide direct shear strength test results.

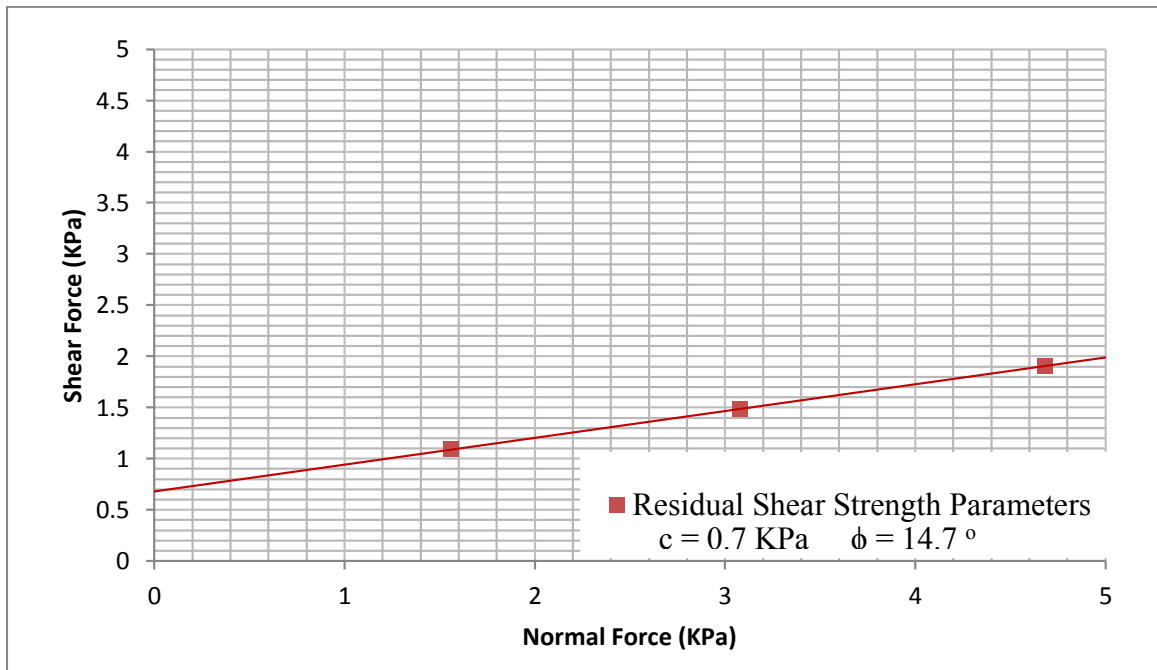


Figure AIV.10: Columbia Parkway landslide direct shear strength test results.

## APPENDIX V

### Description and Analysis of Selected Slope Failures

### Eight Mile Road Landslide

The Eight Mile Road landslide is located 16 km (10 miles) east of downtown Cincinnati. The failure occurred on the western side of Eight Mile Road approximately 0.8 km (0.5 miles) south of its intersection with the Bridle Road and 8 Mile Road (Figure AV.1). This landslide was identified from LiDAR derived maps as well as aerial photographs as can be seen in Appendix VI. The hillside at this site is 30 m (98 ft) high and prior to failure had a slope angle of 30°. The landslide is 26 m (85 ft) long, 39 m (127 ft) wide, and has a 3.7 m (12 ft) of displacement along the scarp. The toe of the landslide is located along the bank of a small stream (Figure AV.2).

According to the Unified Soil Classification System (USCS), the landslide material at the Eight Mile Road site is a silty, clayey sand. The bedrock is not seen at the Eight Mile Road landslide site.

The soil contains Ordovician age fossils, and limestone fragments ranging in size from 0.2 m to 0.6 m (0.5 ft to 2 ft). The soil has a peak friction angle of 31°, a peak cohesion of 2.4 KPa (512 lb/ft<sup>2</sup>), a residual friction angle is 21°, and a residual cohesion of 2.3 KPa (487 lb/ft<sup>2</sup>) (Table 4.4).

The probable cause of the Eight Mile Road landslide is the low shear strength of the soil and the development of pore water pressure within the hillside. The initial slope angle of the hillside is too steep for the slope to remain stable given the low strength parameters and buildup of pore pressure. Undercutting of the slope toe by the stream also appears to have contributed to the failure.

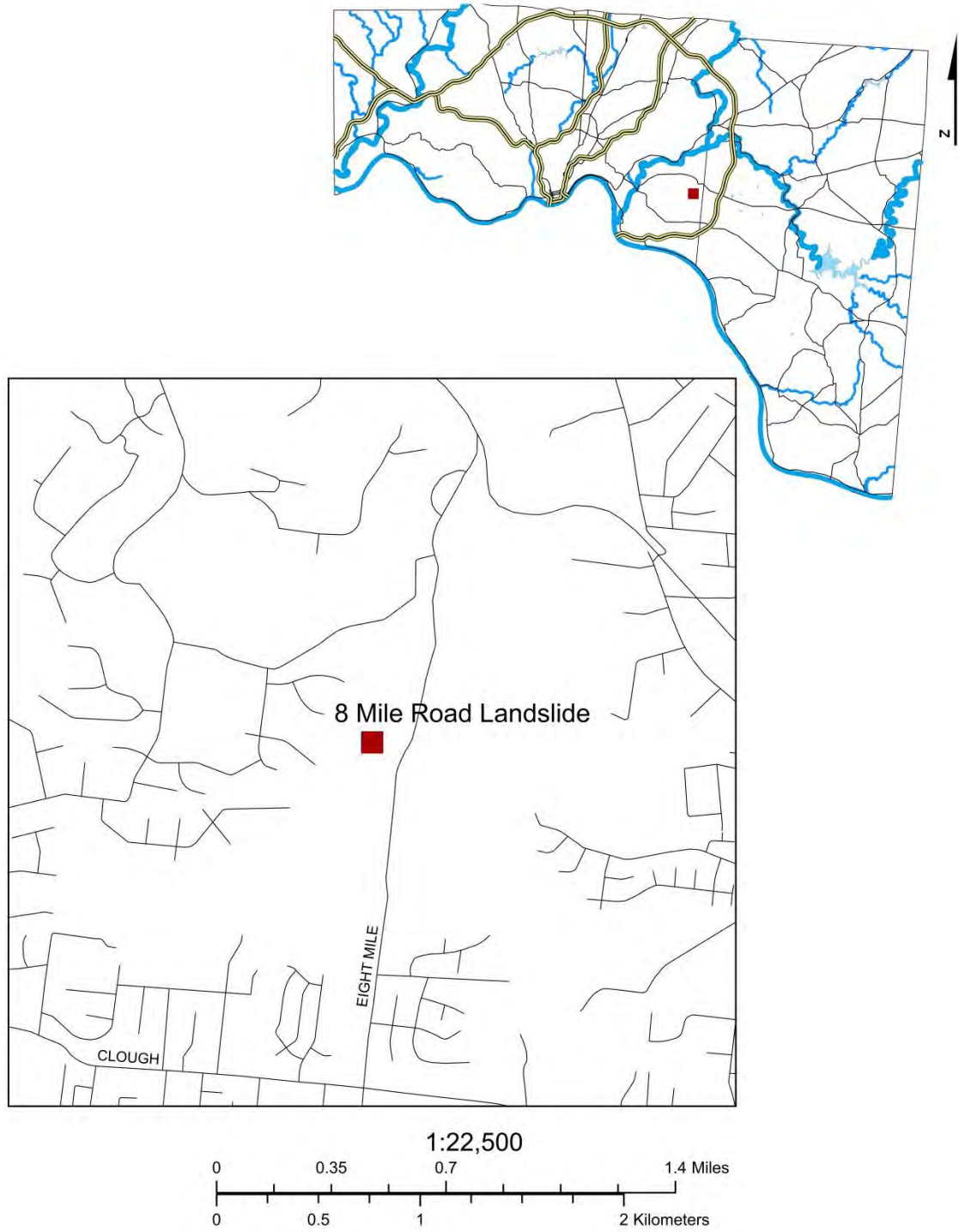


Figure AV.1: Map showing the location of the Eight Mile Road landslide site.



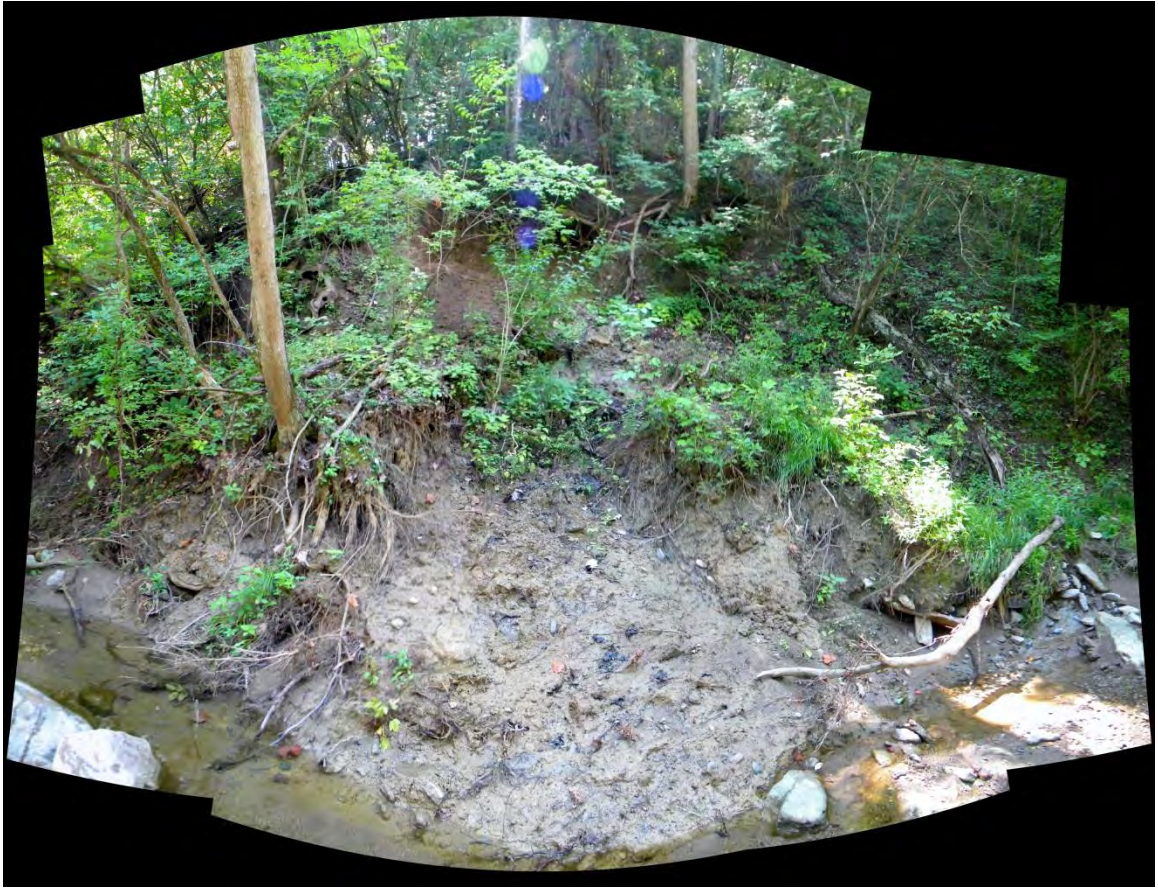


Figure AV.2: View of the toe of the Eight Mile Road landslide.

### Ten Mile Road Landslide

The Ten Mile Road landslide is located 24 km (15 miles) east of downtown Cincinnati. The failure occurred on the eastern side of Ten Mile Road approximately 100 m (330 ft) north of the intersection of Pond Run Road and Ten Mile Road (Figure AV.3). This slope failure was identified from LiDAR derived maps Appendix VI. The landslide is 43 m (141 ft) long, and 13 m (45 ft) wide. The scarp face is 3 m (10 ft) high (Figure AV.4). The toe of the landslide is located along the bank of a small stream (Figure AV.5).

The Ten Mile Road landslide silty, clayey sand according to the grain size distribution results and the USCS. It has a peak friction angle of  $34^{\circ}$ , peak cohesion of 2.8 KPa (575 lb/ft<sup>2</sup>), a residual friction angle of  $16^{\circ}$ , and a residual angle cohesion of 2.3 KPa (470 lb/ft<sup>2</sup>) (Table 4.4). The bedrock was not observed at the Ten Mile Road Landslide.

Similar to the Eight Mile Road landslide, low shear strength parameters, buildup of pore pressure, and undercutting of the toe by the stream water appear to be the probably causes of landslide at the Ten Mile Road site.

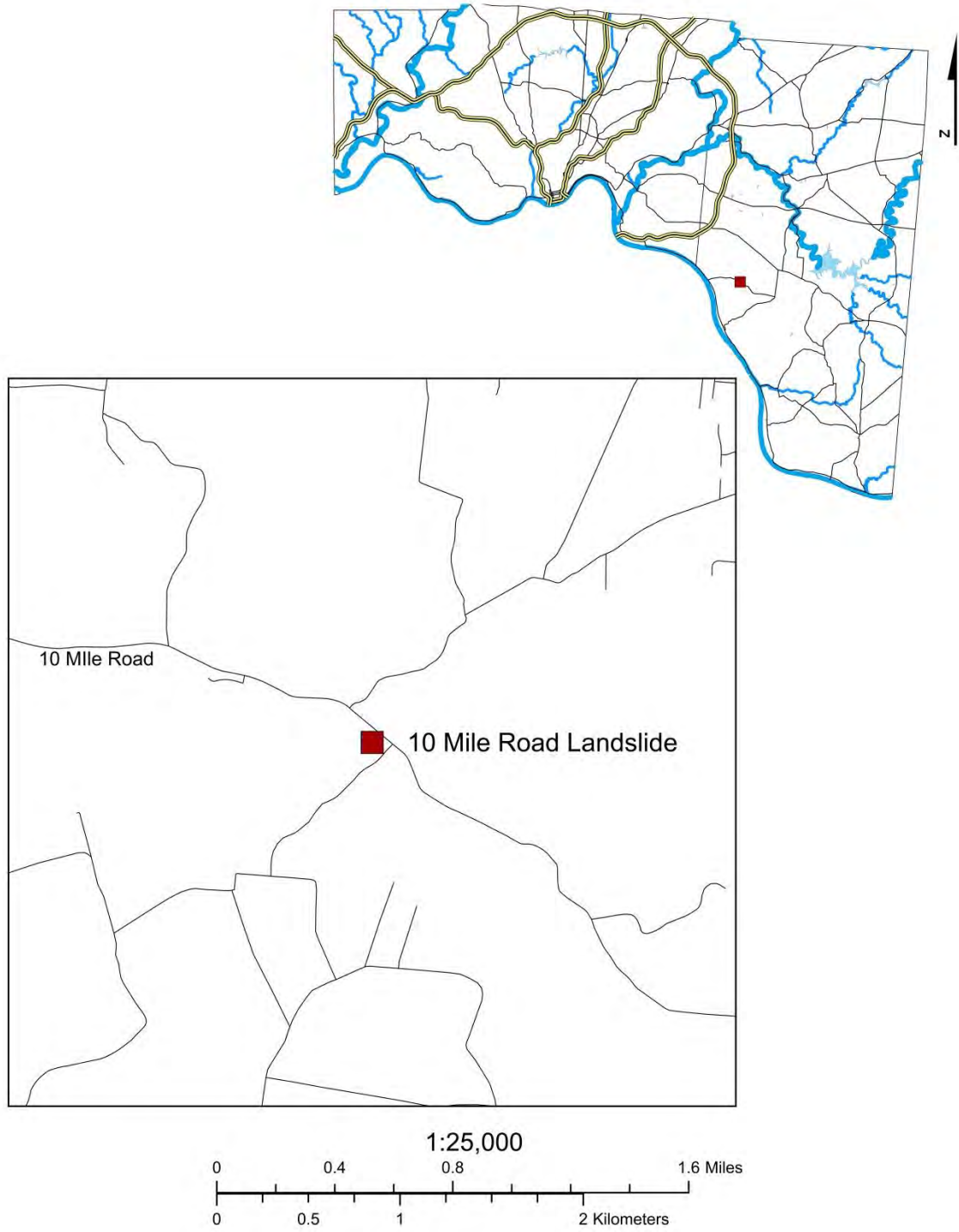


Figure AV.3: Map showing the location of the Ten Mile Road landslide site.





Figure AV.4: The scarp face of the Ten Mile Road Landslide.



Figure AV.5: The toe of the Ten Mile Road landslide, undercut by a stream.

### Delhi Pike Landslide

The Delhi Pike landslide complex, consisting of several landslides, is located approximately 13 km (8 miles) west of downtown Cincinnati (Figure AV.6). In 1973, Delhi Pike was closed permanently due to severe damage caused by landsliding. Failures had occurred both above and below roadway. The landslide complex is described in previous literature {Landslides in Colluvium (Fleming and Johnson, 1994) and is visible on the LiDAR derived maps and aerial photographs (Appendix VI). The landslide is 97.5 m (320 ft) long, 64 m (210 ft) wide, and has a 5.5 m (18 ft) high scarp. Figure AV.7 shows some of the damage caused by the Delhi Pike landslide. Figure AV.8 shows the scarp face, and Figure AV.9 shows the toe of one of the landslides at the Delhi Pike landslide site.

The slide material at the Delhi Pike landslide complex consists of silty, clayey sand according to the grain size distribution results and the USCS. The soil has a peak friction angle of  $24^{\circ}$ , a peak cohesion of 3.3 Kpa ( $700 \text{ lb/ft}^2$ ), a residual friction angle is  $18^{\circ}$  and a residual cohesion of 2.4 Kpa ( $500 \text{ lb/ft}^2$ ) (Table 4.4). The bedrock is not visible at the Delhi Pike landslide site.

The series of failures that comprise the Delhi Pike landslide complex are caused by a combination of factors including the low strength properties of the soil, over steepening of slope during the construction of the Delhi Pike, poor drainage, and the addition of weight to the slope from the road and the houses.

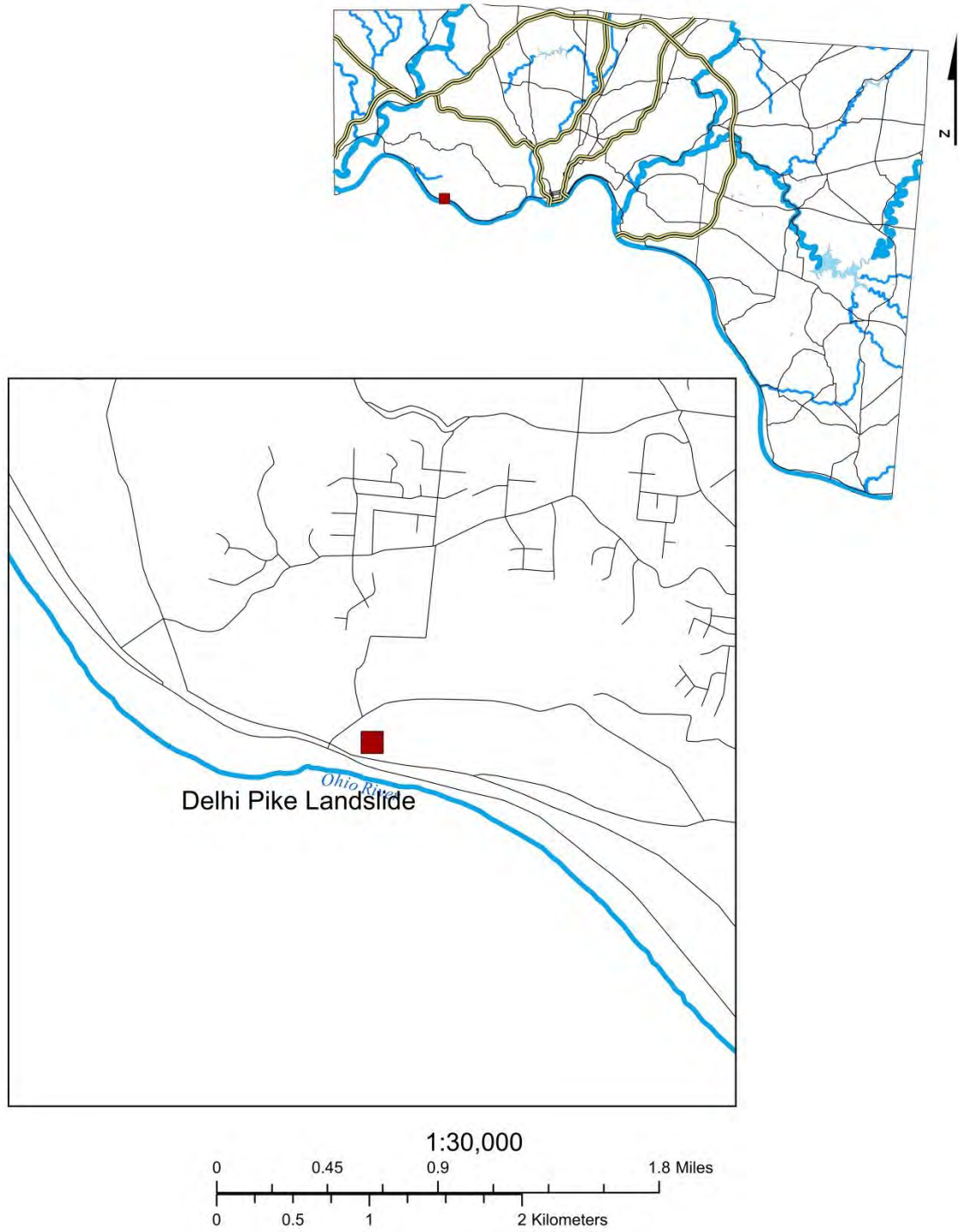


Figure AV.6: Map showing the location of the Delhi Pike landslide complex site.





Figure AV.7: Damage caused to Delhi Pike by the landslide.



Figure AV.8: Scarp face of one of the landslides at the Delhi Pike landslide complex site.





Figure AV.9: Toe of one of the landslides at the Delhi Pike landslide complex site.



### Elstun Road Landslide

The Elstun Road landslide site is located approximately 10 km (6 miles) east of downtown Cincinnati (Figure AV.10). Failures have occurred all along Elstun Road, even in an undeveloped area of the road. The landslides were identified from the information provided by Hamilton County Engineers office and also from LiDAR derived maps as well as aerial photographs (Appendix VI). One of the landslides along the Elstun Road has caused damaged to a 300 m (1000 ft) long stretch of the road resulting in its temporary closing. Along the roadway there is up to 0.3 m (1 ft) of vertical displacement of the pavement (Figure AV.11).

The landslide that was chosen for detailed study from the Elstun Road landslide site is 27.4 m (90 ft) long and 10.1 m (33 ft) wide, with a 2.4 m (8 ft) of displacement along the scarp. The toe of the landslide is located along the bank of a small stream (Figure AV.12).

Soil material at the Elstun Road landslide is a silty, clayey sand. It has a peak friction angle of  $50^{\circ}$ , a peak cohesion of 2.6 KPa (550 lb/ft<sup>2</sup>), a residual friction angle of  $20^{\circ}$ , and a residual cohesion value of 2.5 KPa (512 lb/ft<sup>2</sup>) (Table 4.4). The bedrock is not observed at the Elstun Road landslide site.

A combination of low residual shear strength, addition of weight on top of slope, and undercutting of the slope toe by the stream appears to be have contributed to the continual landslide problem along Elstun Road.

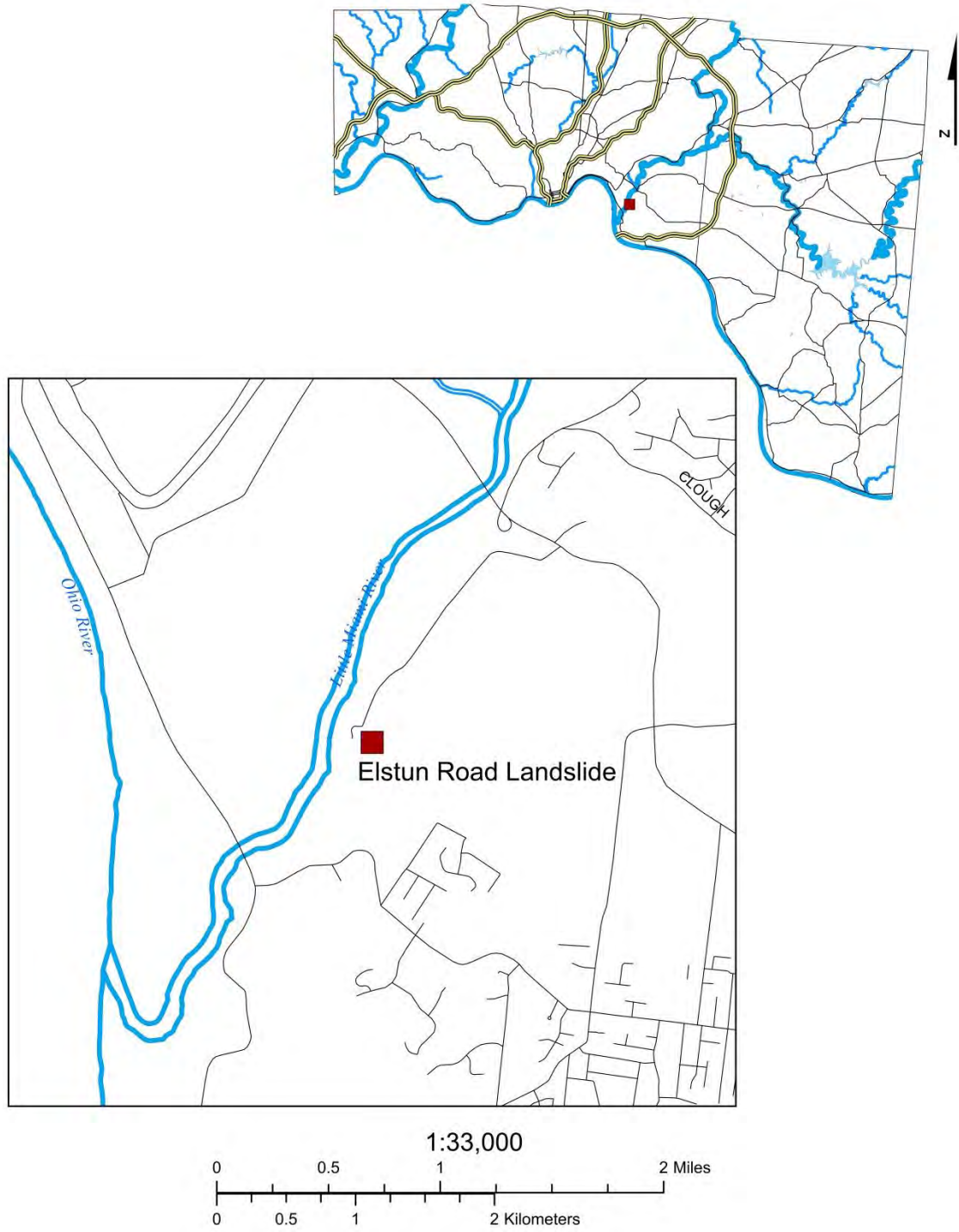


Figure AV.10: Map showing the location of the Elstun Road Landslide site.





Figure AV.11: An example of the damage caused to Elstun Road as a result of landsliding.



Figure AV.12: The landslide toe (on right) of the Elstun Road landslide.

### Nordyke Road Landslide

The Nordyke Road landslide site is located approximately 18 km (11 miles) east of downtown Cincinnati (Figure AV.13). Rotational landslides have occurred along the Nordyke Road as well as along a creek located downslope from Nordyke Road.

Appendix VI shows the use of LiDAR and aerial photographs in identifying landslides along the Nordyke Road. Figure AV.14 shows the damage to Nordyke Road as a result of landslide activity. The landslide studied is 12.8 m (42 ft) long, 11.9 m (39 ft) wide, and caused 3 m (10 ft) of displacement along the head scarp (Figure AV.15). Figure AV.16 shows the toe of the landslide.

Similar to the other sites, the colluvial soil at the Nordyke Road landslide site is silty, clayey sand with fossils and limestone fragments. The soil has a peak friction angle of  $23^{\circ}$ , a peak cohesion of 4.8 KPa (995 lb/ft<sup>2</sup>), a residual friction angle of  $18^{\circ}$ , and a residual cohesion of 3.9 KPa (813 lb/ft<sup>2</sup>) (Table 4.4). The bedrock was not observed at the Nordyke Road landslide site.

The Nordyke Road landslide is the combined effect of low shear strength of the soil, the undercutting of the toe by the stream, and pore pressure buildup.



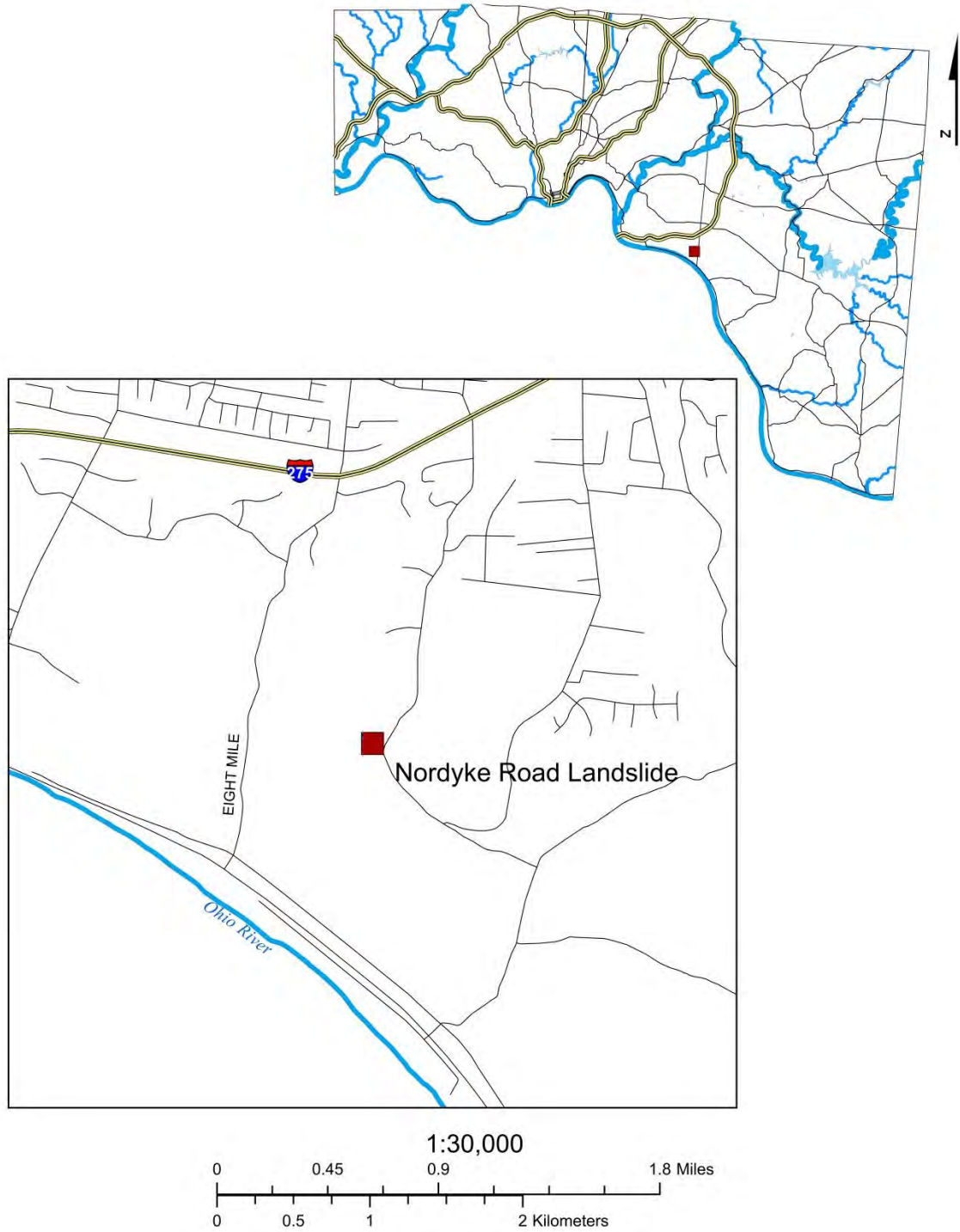


Figure AV.13: Map showing the location of the Nordyke Road landslide site.



Figure AV.14: Damage caused to Nordyke Road by landslide activity.



Figure AV.15: Head scarp of the Nordyke Road landslide.





Figure AV.16: Toe of the Nordyke Road landslide.

### Old US 52 Landslide

The Old US 52 landslide site is located approximately 24 km (15 miles) west of downtown Cincinnati (Figure AV.17). The landslide can be seen on LiDAR derived maps as well as aerial photographs (Appendix VI). The landslide is 6.7 m (22 ft) long, and 7.6 m (25 ft) wide, with a 1.5 m (5 ft) of displacement along the scarp face. The toe of the landslide is located along the bank of a small stream (Figure AV.18).

The soil has a peak friction angle of  $39^\circ$ , a peak cohesion of 3.5 KPa (734 lb/ft<sup>2</sup>), a residual friction angle of  $20^\circ$ , and a residual cohesion of 3.2 KPa (683 lb/ft<sup>2</sup>) (Table 4.4). The bedrock is not visible at the Old US 52 landslide site.

Similar to most of the other sites, the failure at the Old US 52 landslide site is the result of a combination of low shear strength of the soil, undercutting of the toe of the slope by a stream, and development of pore pressure during wet periods.



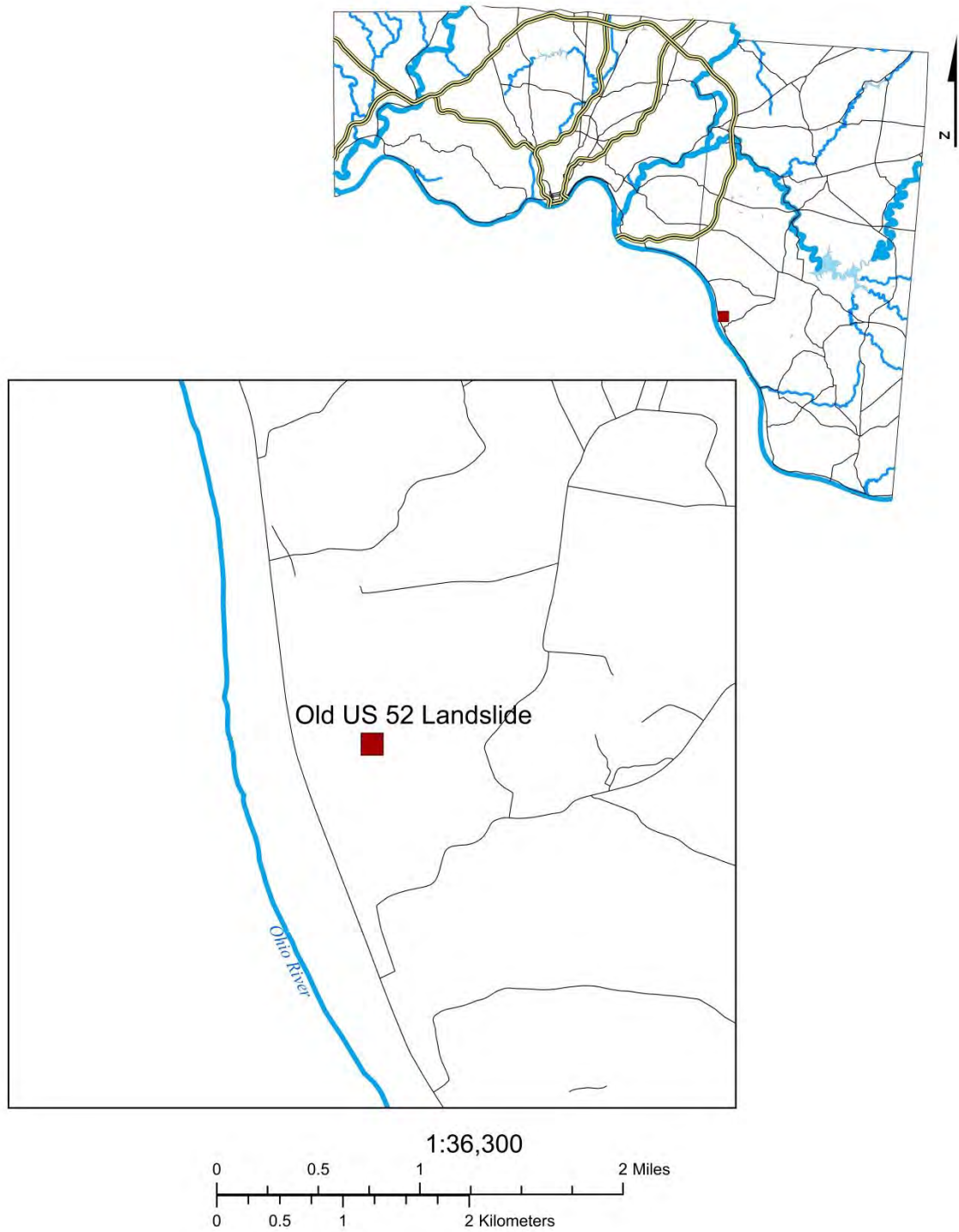


Figure AV.17: Map showing the location of the Old US 52 landslide site.



Figure AV.18: Scarp and toe the Old US52 landslide. Notice the small stream undercutting the toe.

### Wagner Road Landslide

The Wagner Road landslide complex is located approximately 22.5 km (14 miles) east of downtown Cincinnati (Figure AV.19). The Wagner Road landslide was identified from field observations and Clermont County records. It is also identifiable from LiDAR derived maps and aerial photographs (Appendix VI). The landslide is 6.1 m (20 ft) long and 24.1 m (79 ft) wide. The main scarp shows 1 m (3.3 ft) of vertical displacement of the road towards the creek (Figure AV.20). Figures AV.21 and AV.22 show, respectively, the toe of the landslide and the retaining wall that was constructed to support the slope.

The soil at the Wagner Road landslide site has a peak friction of  $28^{\circ}$ , a peak cohesion of 2.6 KPa (578 lb/ft<sup>2</sup>), a residual friction angle of  $18^{\circ}$ , and a residual cohesion of 2.2 KPa (463 lb/ft<sup>2</sup>) (Table 4.4). According to the boring logs obtained from Terracon Company (Appendix VII), the bedrock is located at 4.6 m (15 ft) depth.

The failure along the Wagner Road is the result of a combination of toe undercutting by a stream, steepness of the slope, the added weight of the road to top of slope, and the low shear strength of the soil

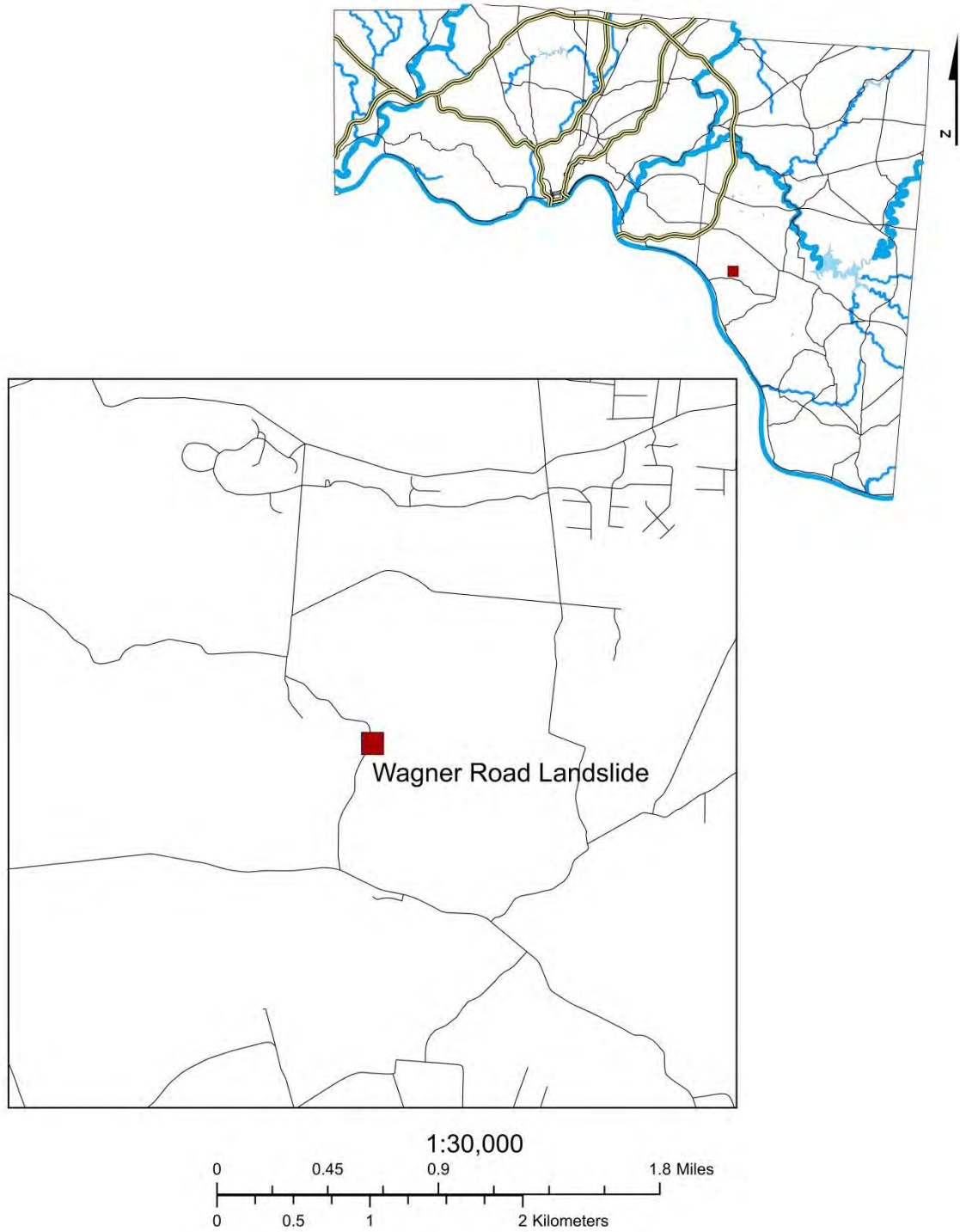


Figure AV.19: Map showing the location of the Wagner Road landslide site.





Figure AV.20: Scarp and the associated displacement at the Wagner Road landslide site.



Figure AV.21: Toe at the Wagner Road landslide.





Figure AV.22: Remains of a retaining wall that had been constructed to stabilize Wagner Road.

### Nine Mile Road Landslide

The Nine Mile Road landslide complex is located approximately 19 km (12 miles) east of downtown Cincinnati (Figure AV.23). Appendix VI includes the LiDAR derived maps and aerial photographs showing the Nine Mile Road landslide. The landslide is 15.3 m (50 ft) long and 6.1 m (20 ft) wide, with a 3.4 m (11 ft) of displacement along the main scarp. Thickness of the sliding mass was observed to be 1.5 m (5 ft). The toe of the landslide is located along the bank of a small stream (Figure AV.24).

The slide material at the 9 Mile Road landslide is similar to the other sites, a silty and clayey sand. The residual friction angle for the soil rock contact is  $14^{\circ}$  and a residual cohesion is 1.2 KPa (250 lb/ft<sup>2</sup>) (Table 4.5).

The low shear strength of the soil, undercutting of the toe of the slope by the stream, and pore pressure developing during wet periods, in combination, are the factors responsible for the Nine Mile Road landslide.

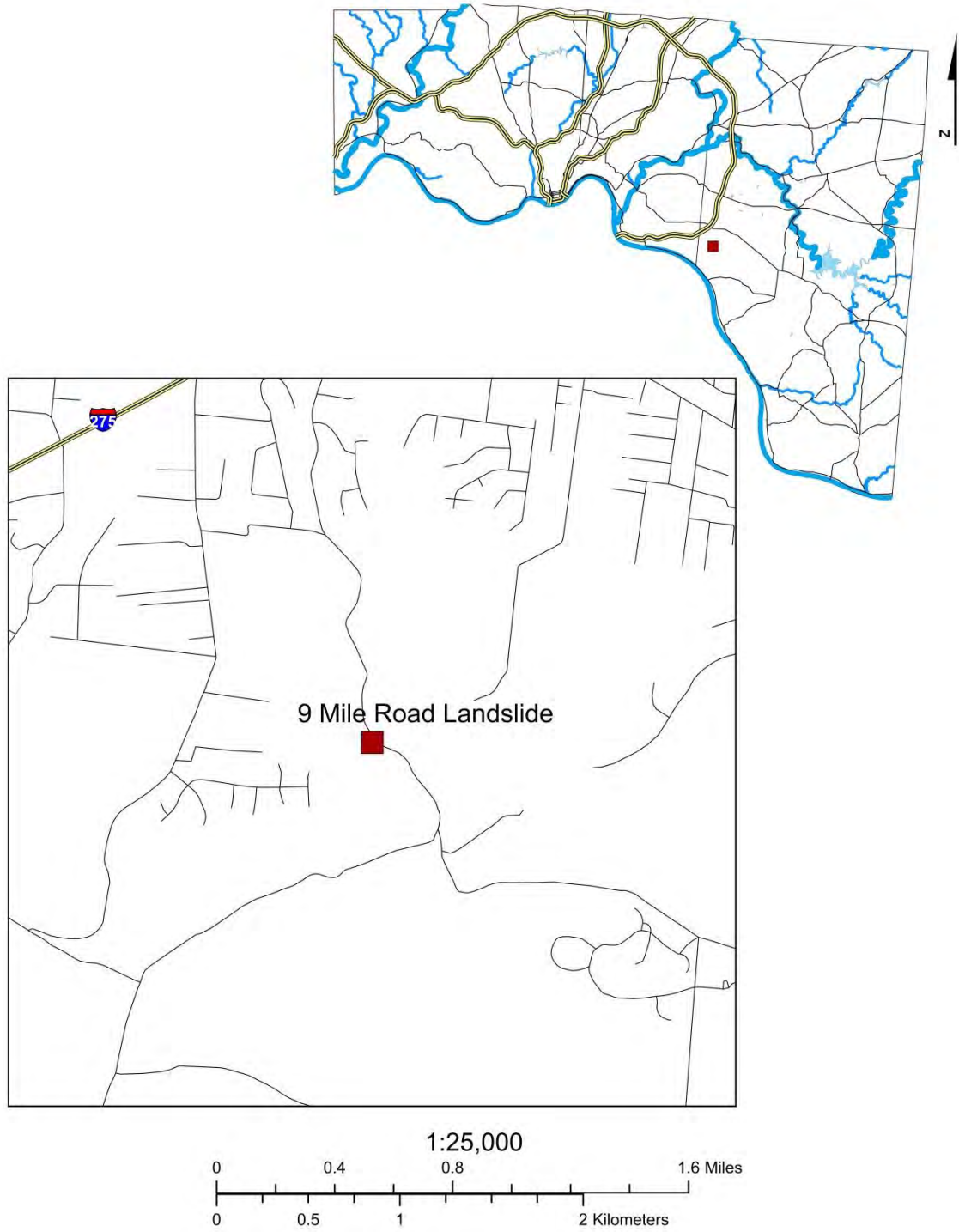


Figure AV.23: Map showing the location of the 9 Mile Road landslide.





Figure AV.24: Scarp and toe of the 9 Mile Road landslide.

### Berkshire Road Landslide

The Berkshire Road landslide complex is located approximately 13 km (8 miles) east of downtown Cincinnati (Figure AV.25). Appendix VI shows how the landslide appears on the slope map, hillshade map, terrain map, DEM map, topography map and aerial photos. The Berkshire Road landslide was also identified from field observations. The landslide is 9.1 m (30 ft) long, 3 m (10 ft) wide, and has a 4.6 m (15 ft) of displacement along the scarp face. The failure plane is inclined at 50° and the thickness of the sliding mass of soil is 1.5 m (5 ft). The toe of the landslide is located along the bank of a small stream (Figure AV.26).

The soil-rock contact at the Berkshire Road landslide has a residual friction angle of 8° and a residual cohesion of 1.3 KPa (271 lb/ft<sup>2</sup>) (Table 4.5).

The landslide at the Berkshire Road is the result of low shear strength of the soil, undercutting of the slope toe by stream water, and the steepness of the slope and the sliding surface.

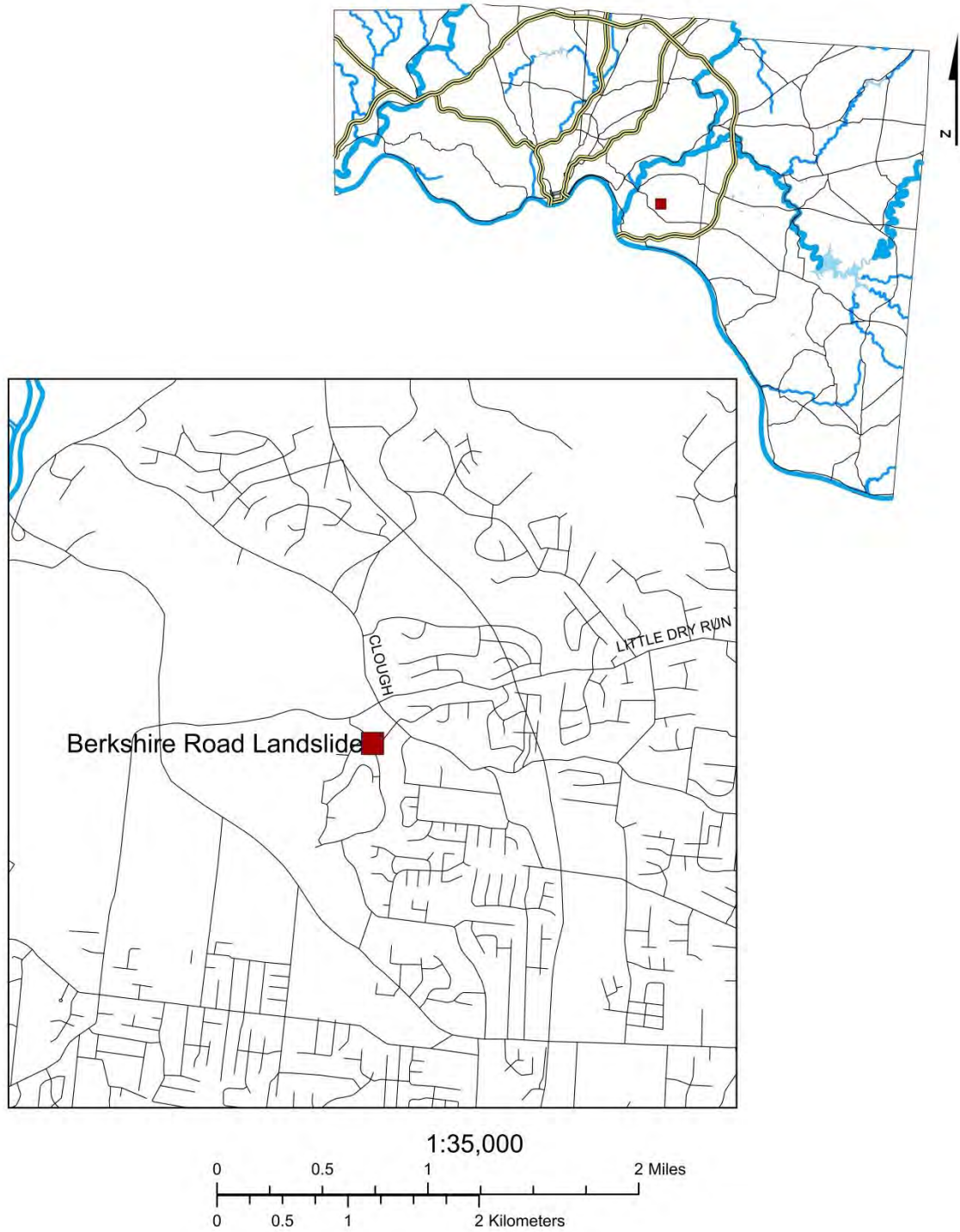


Figure AV.25: Map showing the location of the Berkshire Road landslide.





Figure AV.26: Scarp and toe of the Berkshire Road landslide. Notice the accumulation of landslide debris in the toe area.

### Columbia Parkway Landslide Complex

The Columbia Parkway landslide complex is located approximately 2.8 km (1.75 miles) east of downtown Cincinnati (Figure AV.27). The landslide complex was identified from field observations, landslide data from Hamilton County and from LiDAR derived maps (Appendix VI). The landslide is 58 m (190 ft) long, 12 m (40 ft) wide, and resulted in 0.75 m (2.5 ft) of displacement along the scarp face. The sliding soil mass is 2.1 m (7 ft) thick. The slope and the failure plane are parallel to each other and are inclined at an angle of 30°. The head scarp is located along the edge of Columbia Parkway (Figure AV.28) and the toe of the landslide is located at the top of a retaining wall along the Riverside Road (Figure AV.29).

The residual friction angle for the soil-rock contact at the Columbia Parkway site is 15° and the residual cohesion is 0.7 KPa (142 lb/ft<sup>2</sup>) (Table 4.5).

The factors responsible for the Columbia Parkway landslide complex include the low shear strength of the soil, the constant removal of material at the toe of the slope by the City of Cincinnati, and development of pore pressure.

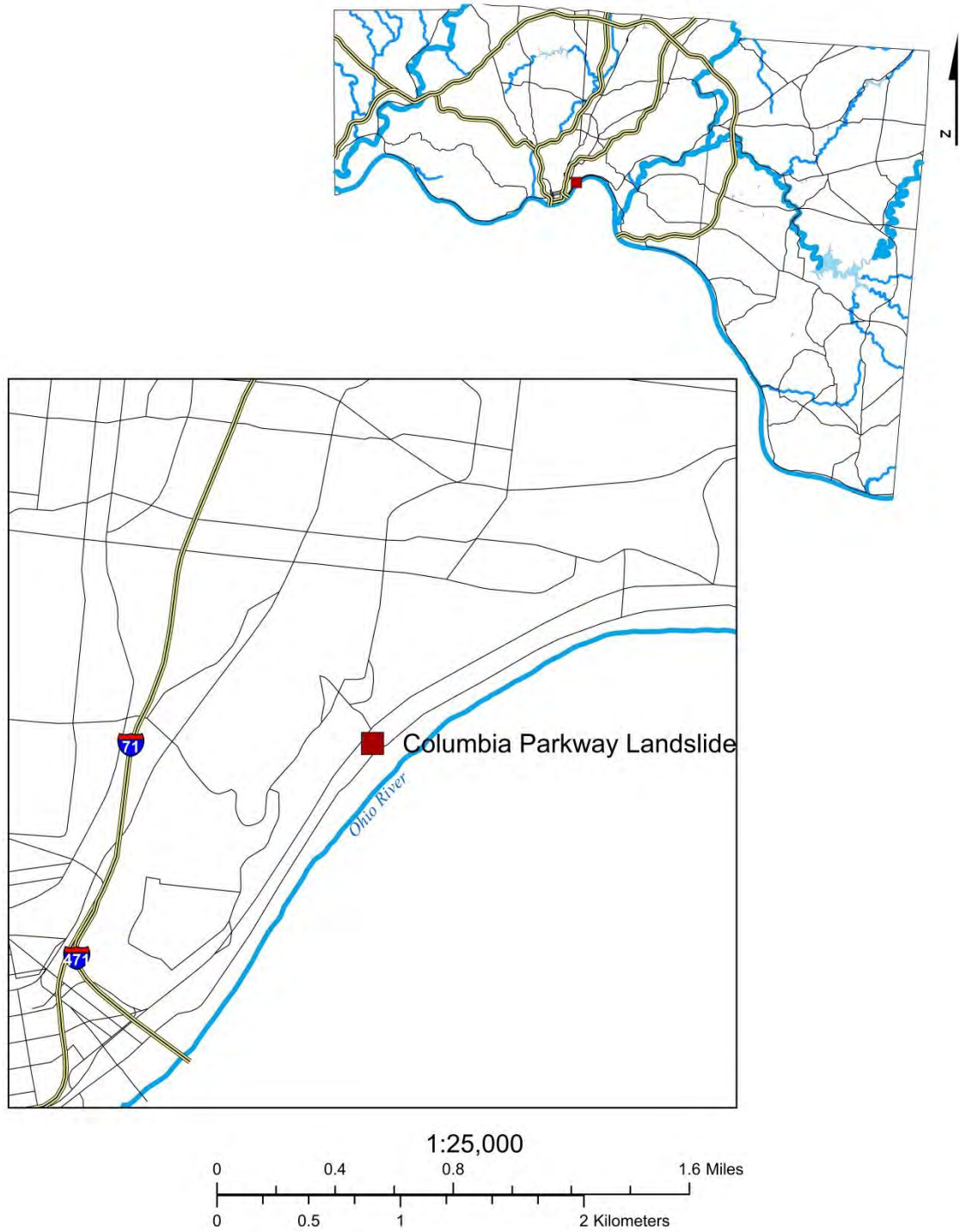


Figure AV.27: Map showing the location of the Columbia Parkway landslide.





Figure AV.28: Head scarp of the Columbia Parkway landslide.



Figure AV.29: Toe of the Columbia Parkway landslide, emerging on the top of the retaining wall.

## APPENDIX VI

### LiDAR Derived Maps and Aerial Photographs of Selected Slope Failures



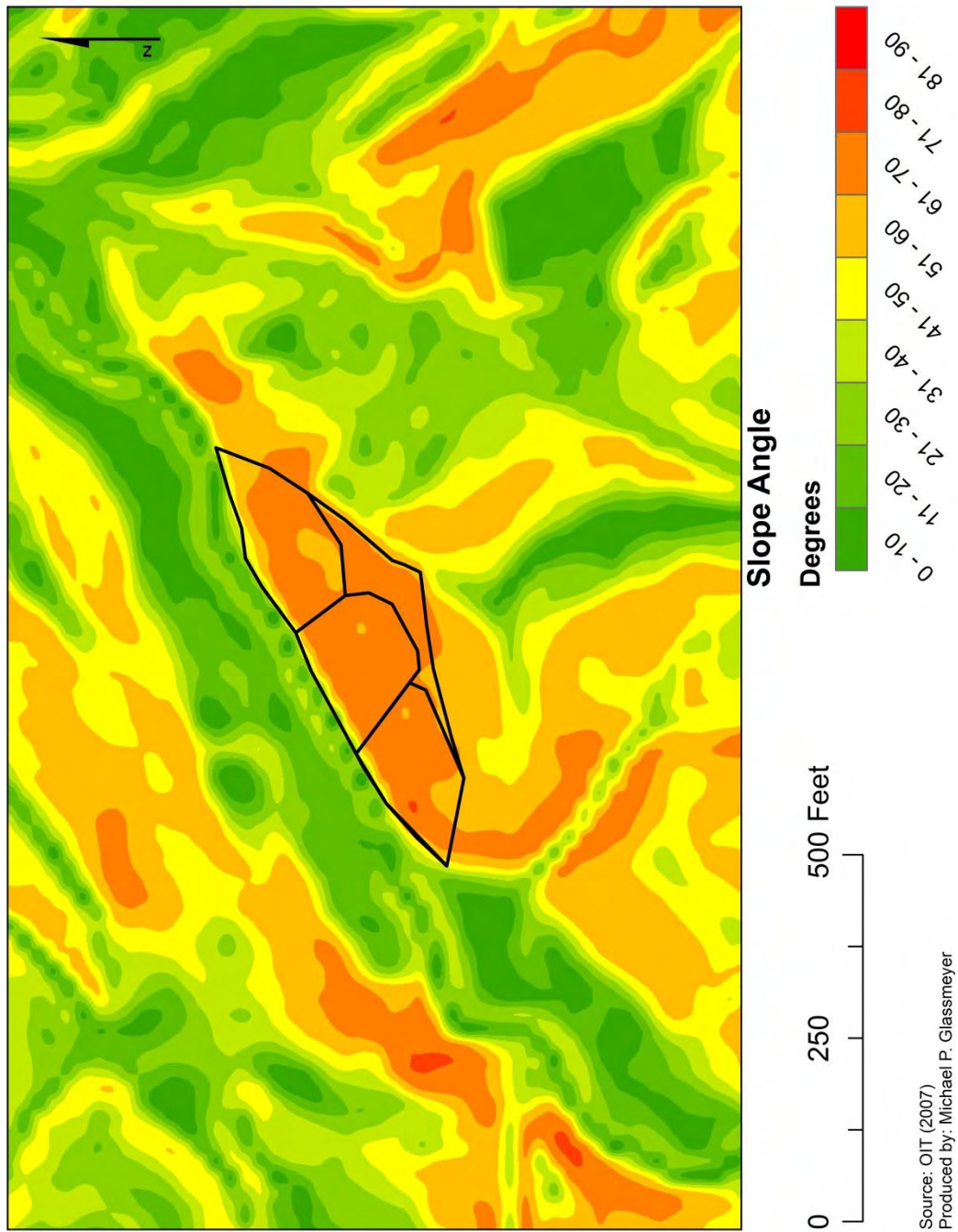
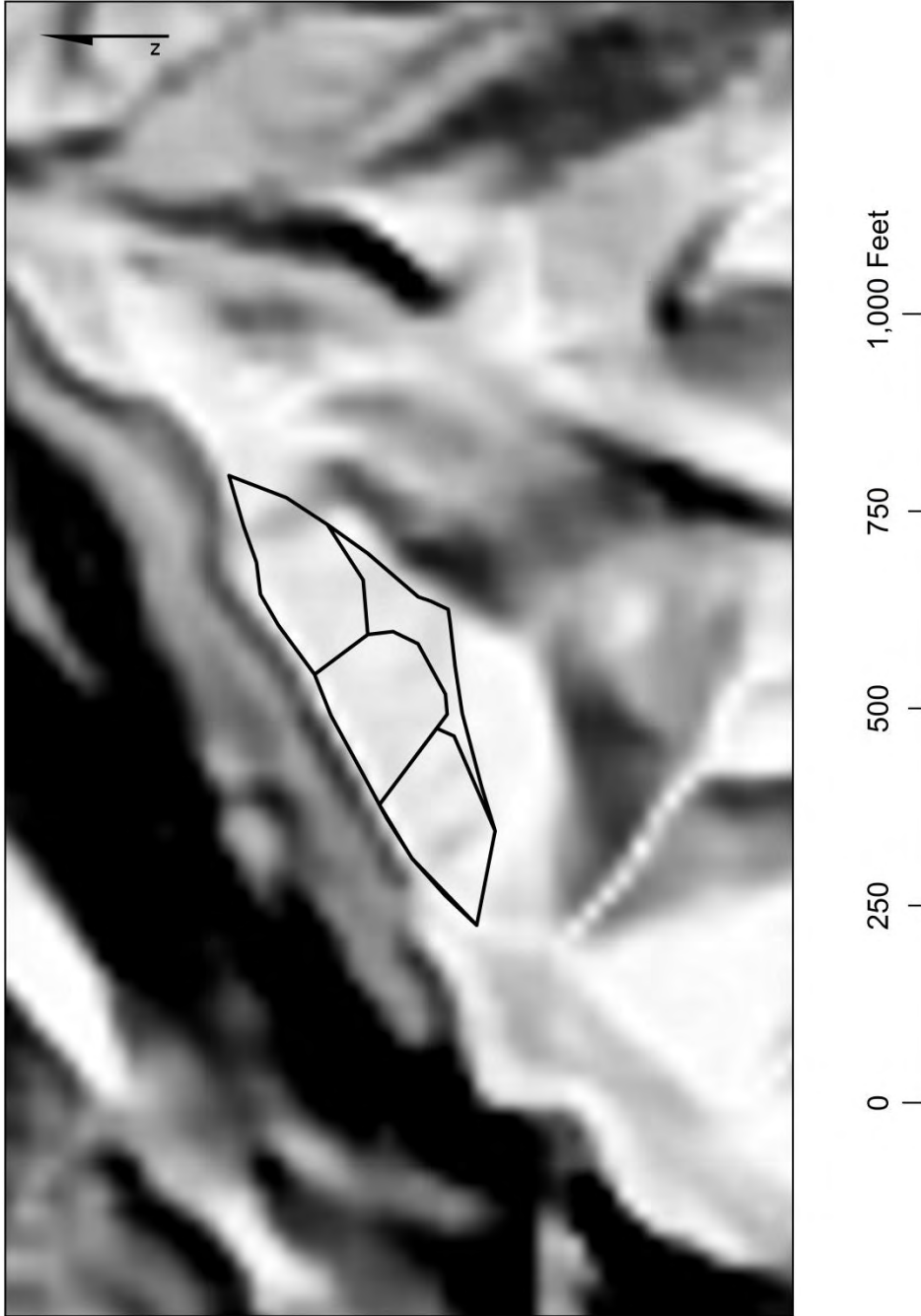


Figure AVI.1: Slope map of the 8 Mile Road landslide.



Source: OIT (2007)  
Produced by: Michael P. Glassmeyer

Figure AVI.2: Hillshade map of the 8 Mile Road landslide.

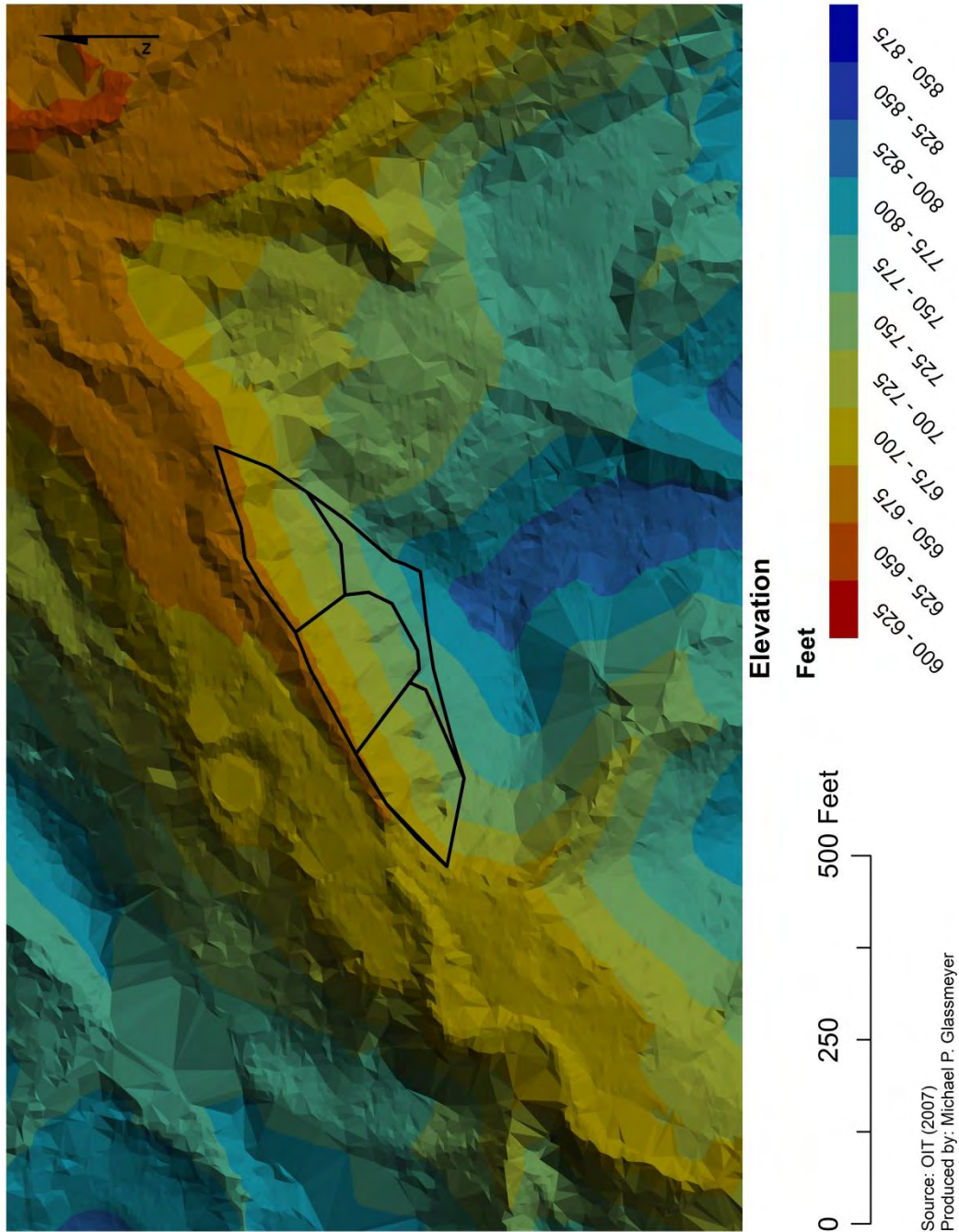
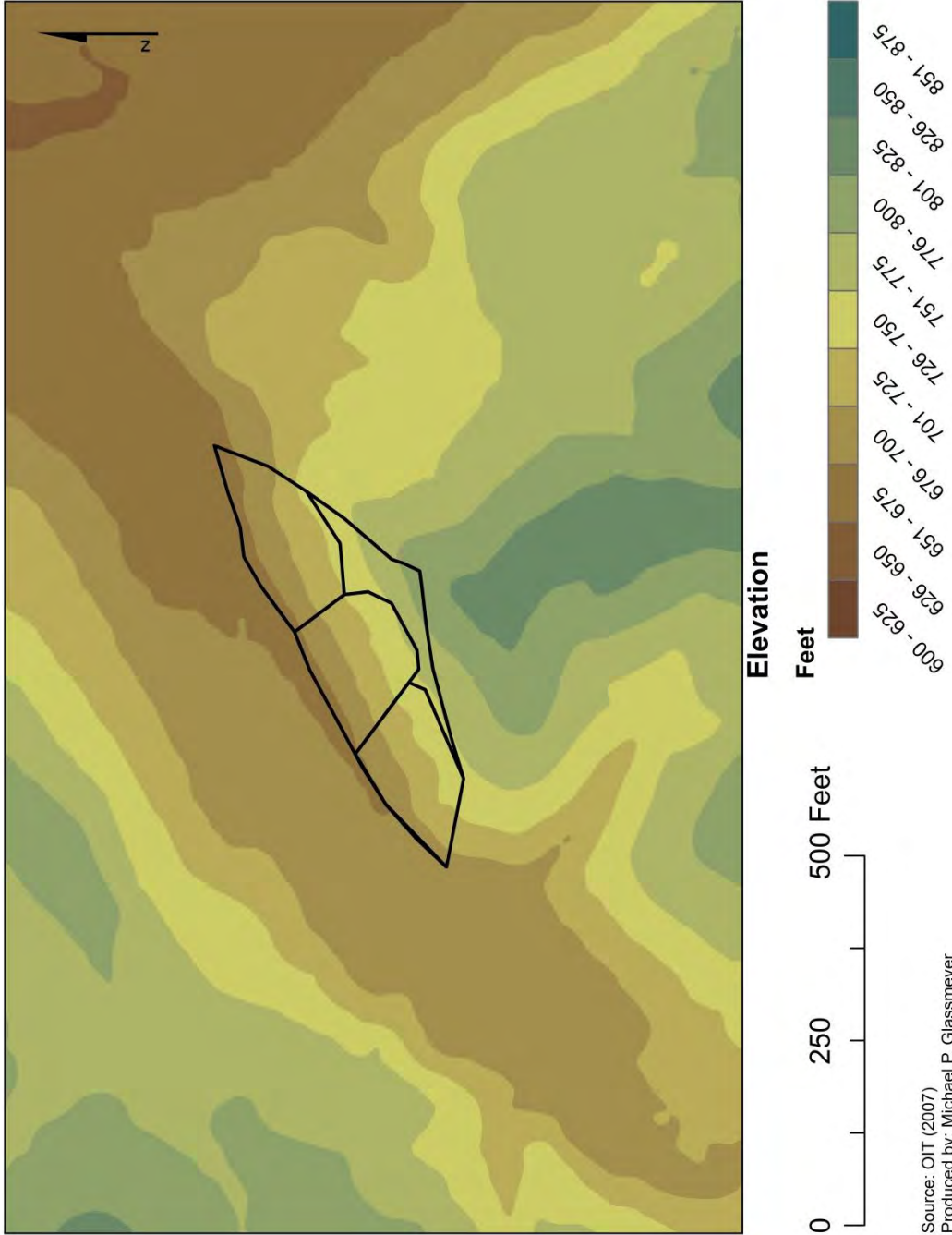


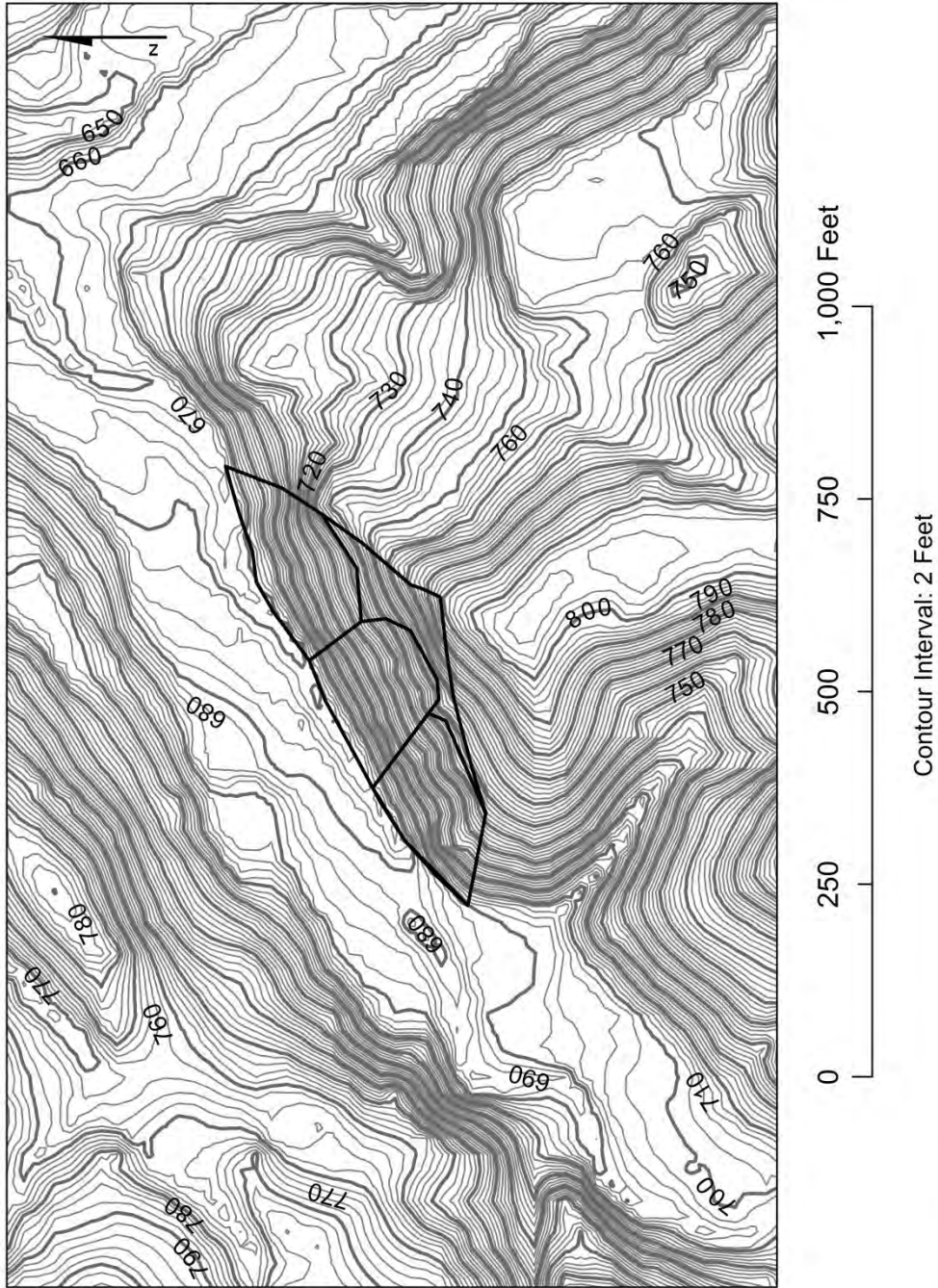
Figure AVI.3: Terrain map of the 8 Mile Road landslide.



Source: OIT (2007)  
 Produced by: Michael P. Glassmeyer

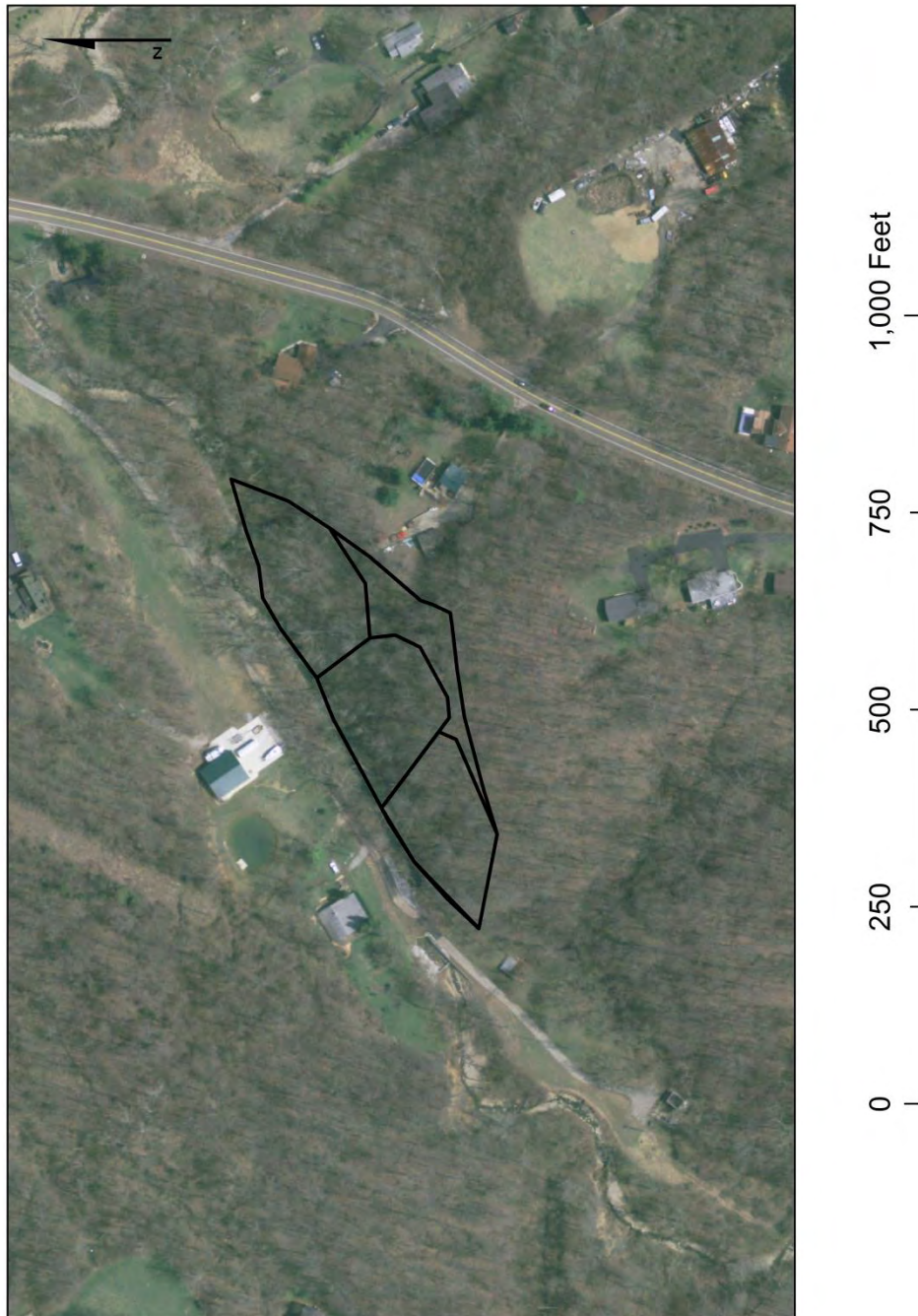


Figure AVI.4: DEM map of the 8 Mile Road landslide.



Source: OIT (2007)  
Produced by: Michael P. Glassmeyer

Figure AVI.5: Topographic map of the 8 Mile Road landslide.



Source: OIT (2007)  
Produced by: Michael P. Glassmeyer

Figure AVI.6: Aerial photograph of the 8 Mile Road landslide.

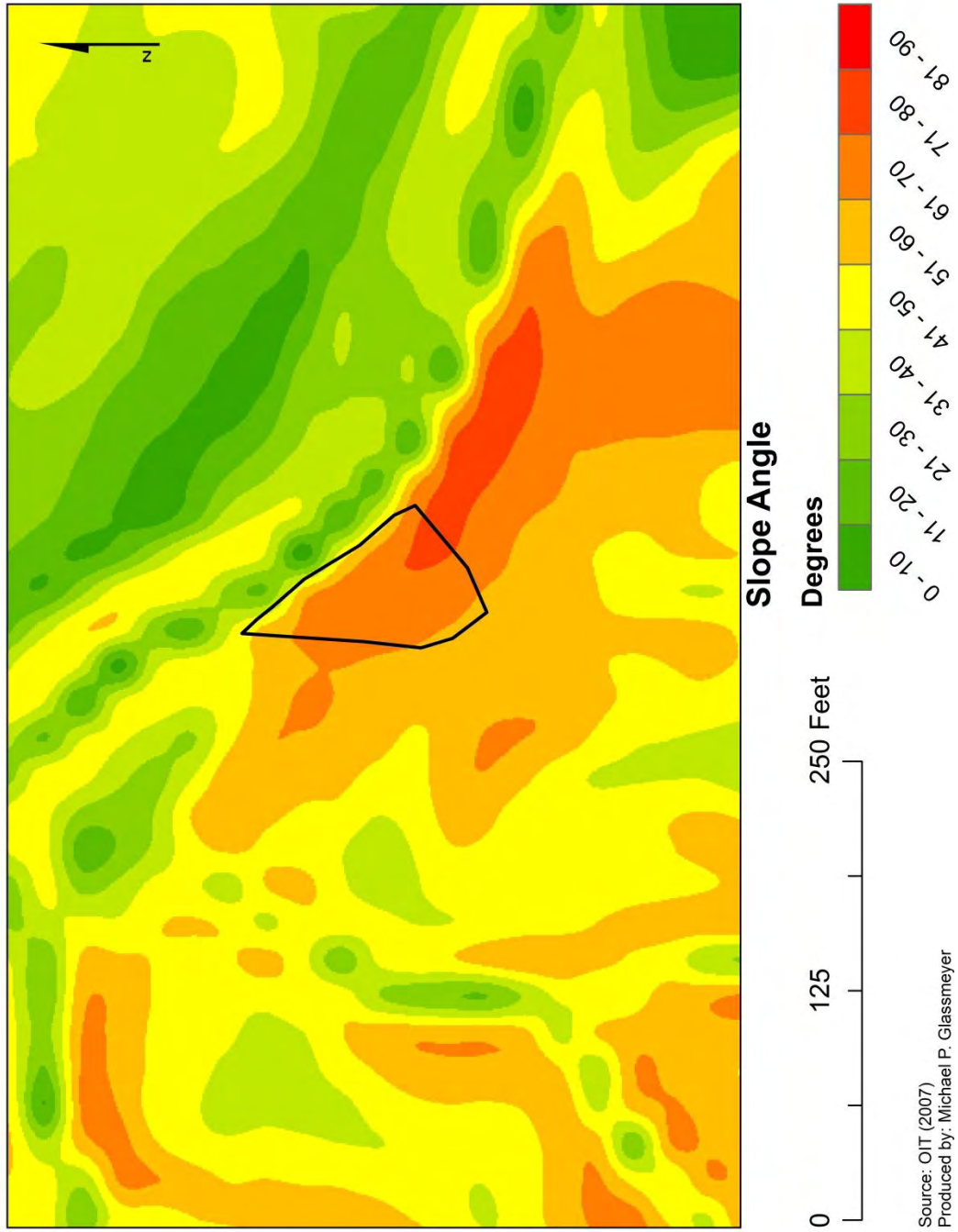
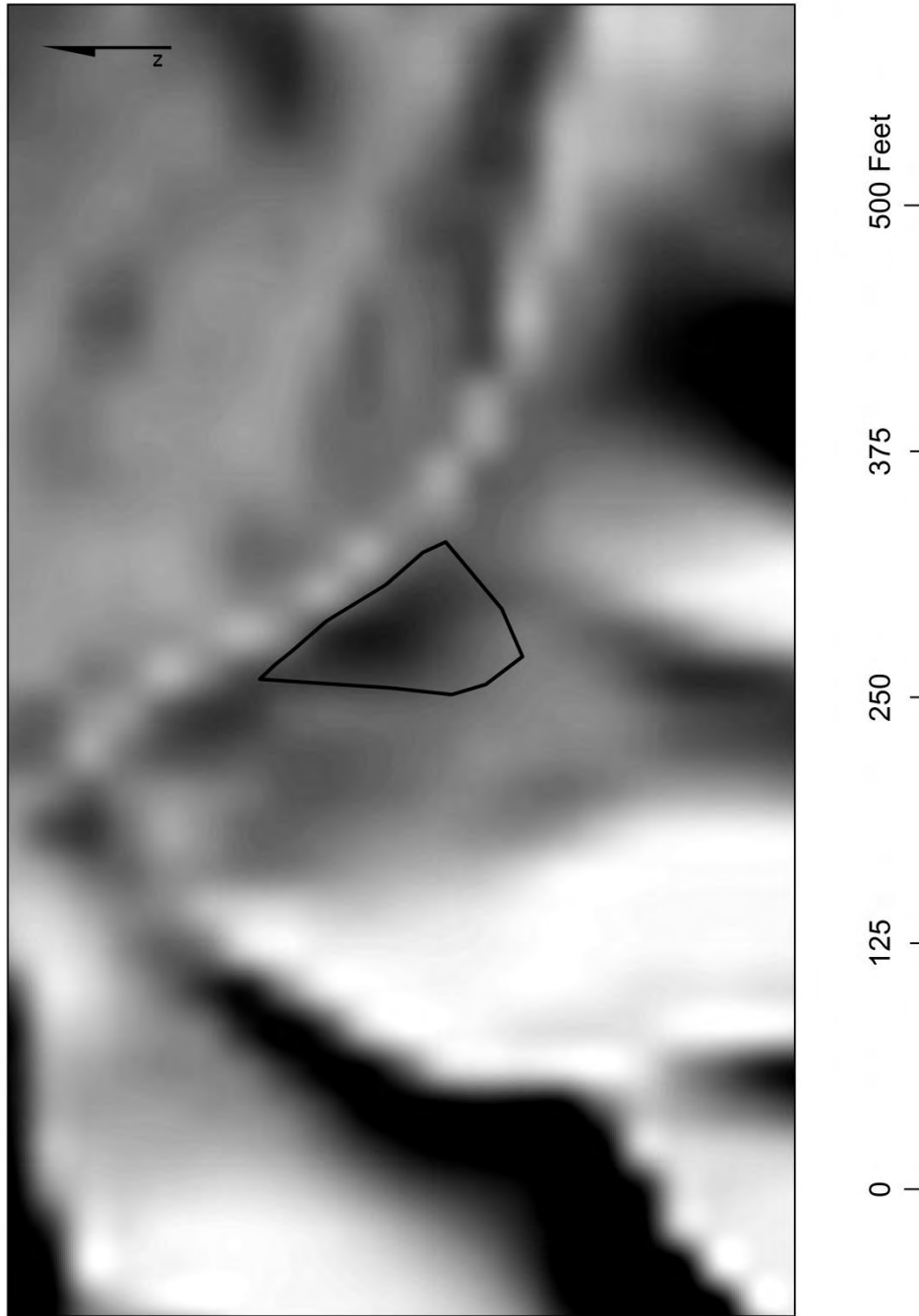




Figure AVI.7: Slope map of the 9 Mile Road landslide.



Source: OIT (2007)  
Produced by: Michael P. Glassmeyer

Figure AVI.8: Hillshade map of the 9 Mile Road landslide.

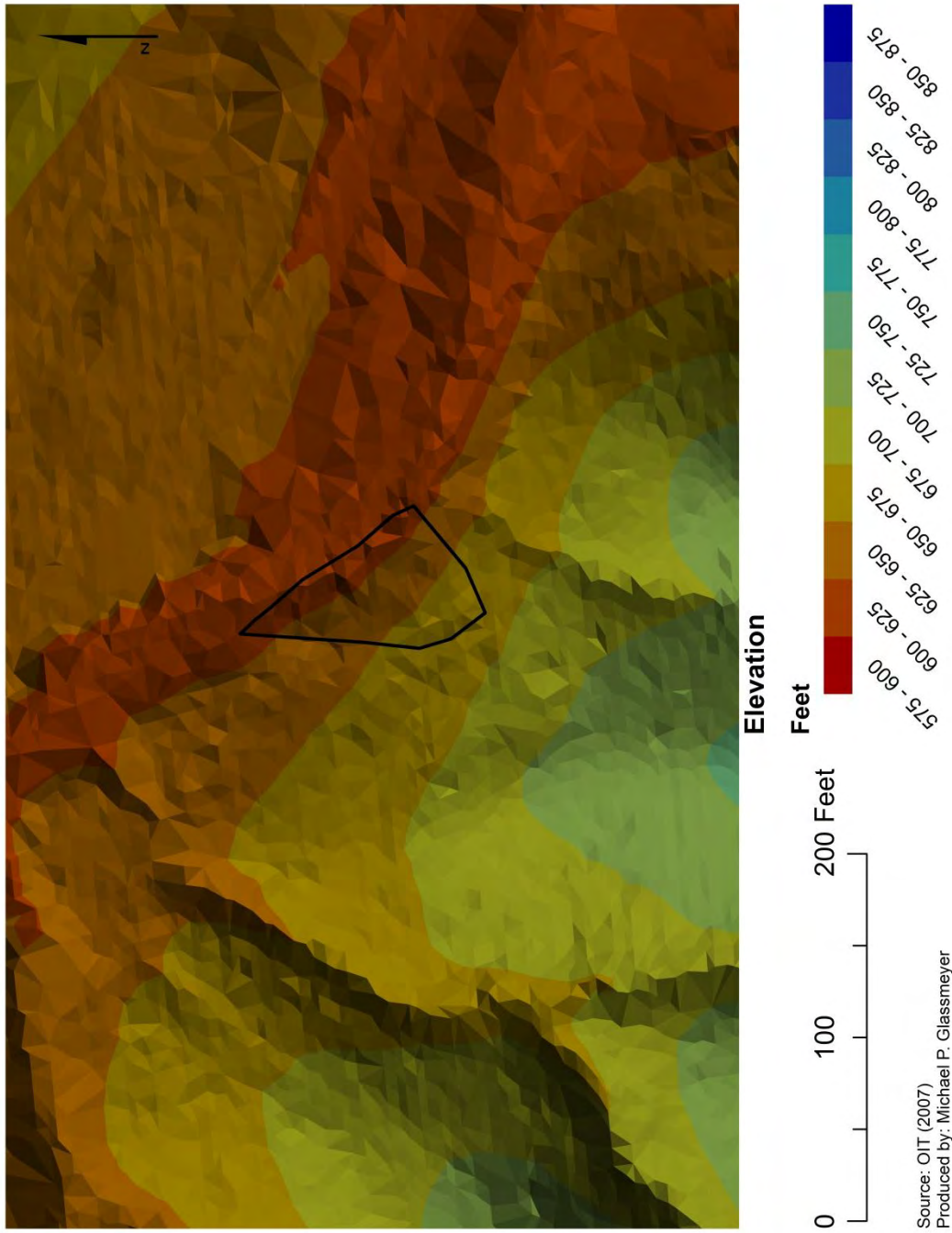


Figure AVI.9: Terrain map of the 9 Mile Road landslide.

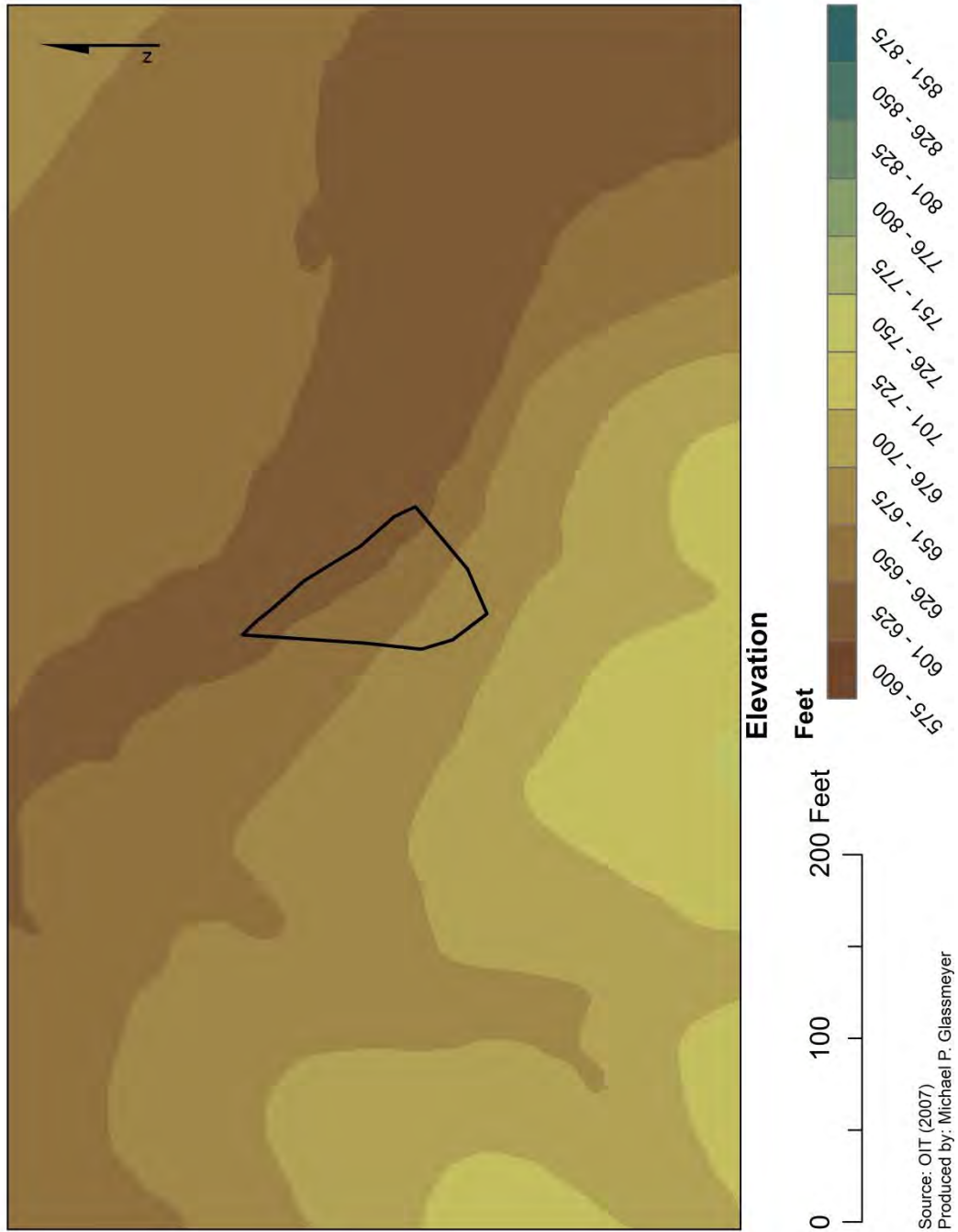


Figure AVI.10: DEM map of the 9 Mile Road landslide.

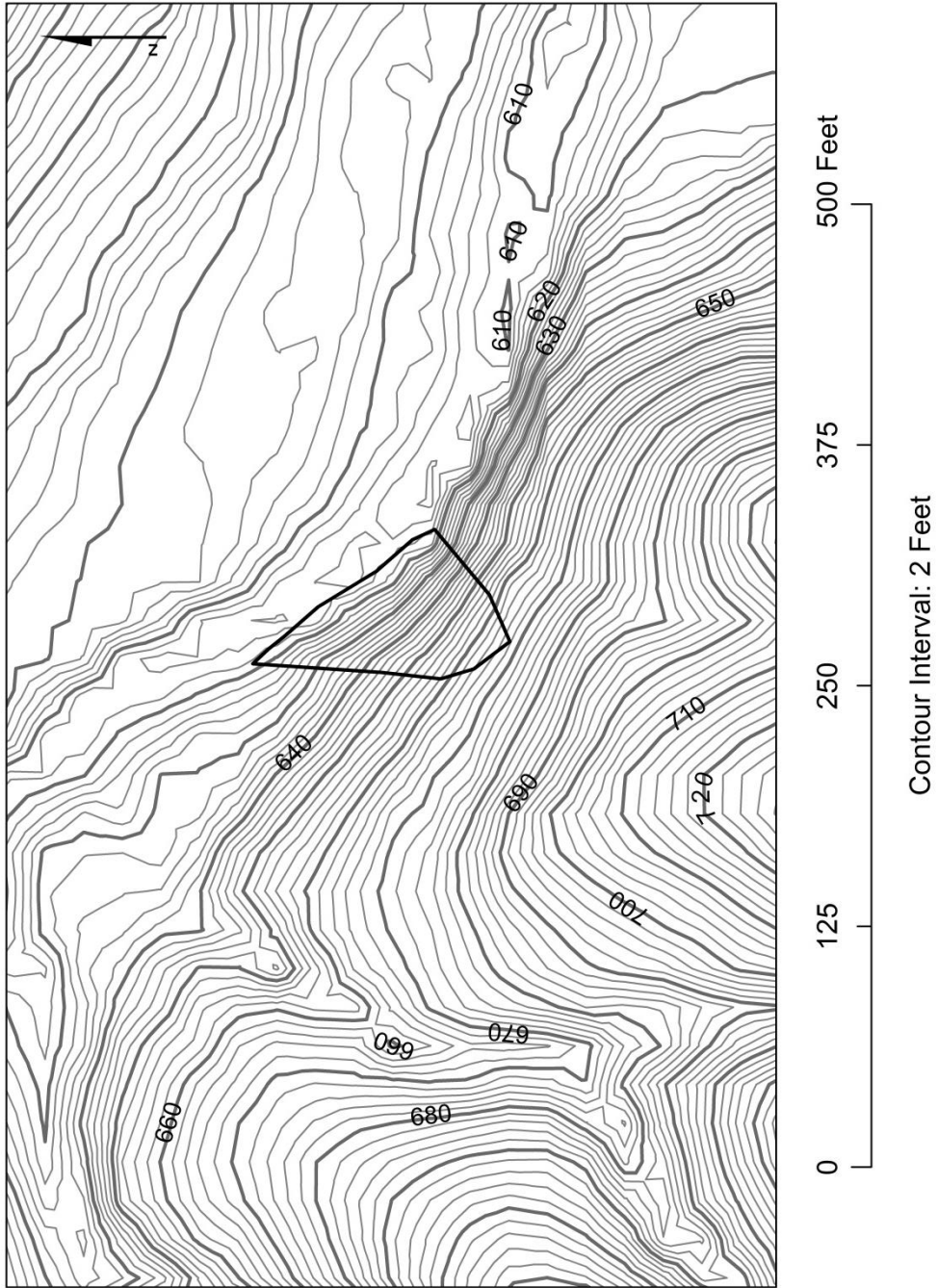


Figure AVI.11: Topographic map of the 9 Mile Road landslide.



Source: OIT (2007)  
Produced by: Michael P. Glassmeyer



Figure AVI.12: Aerial photograph of the 9 Mile Road landslide.

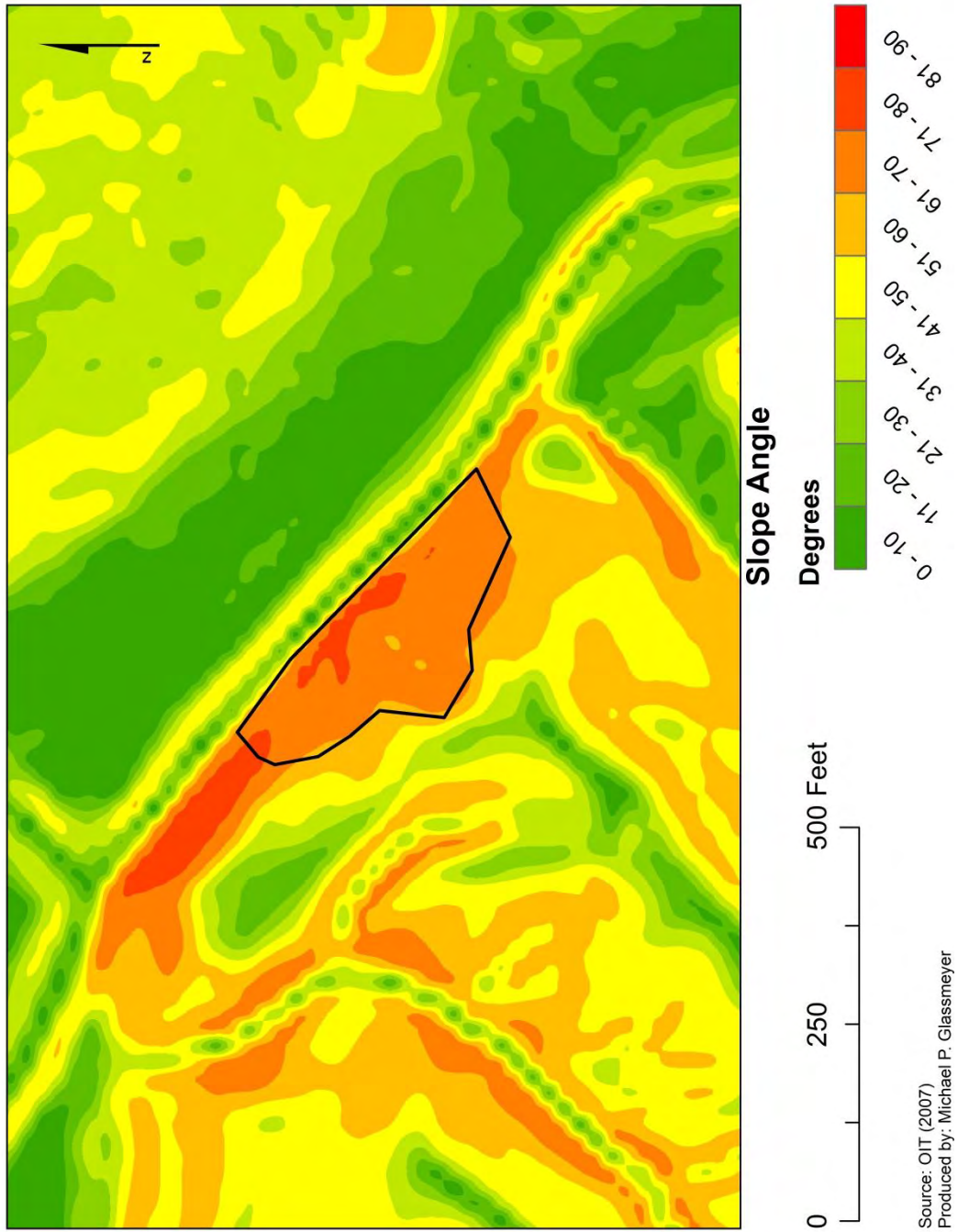
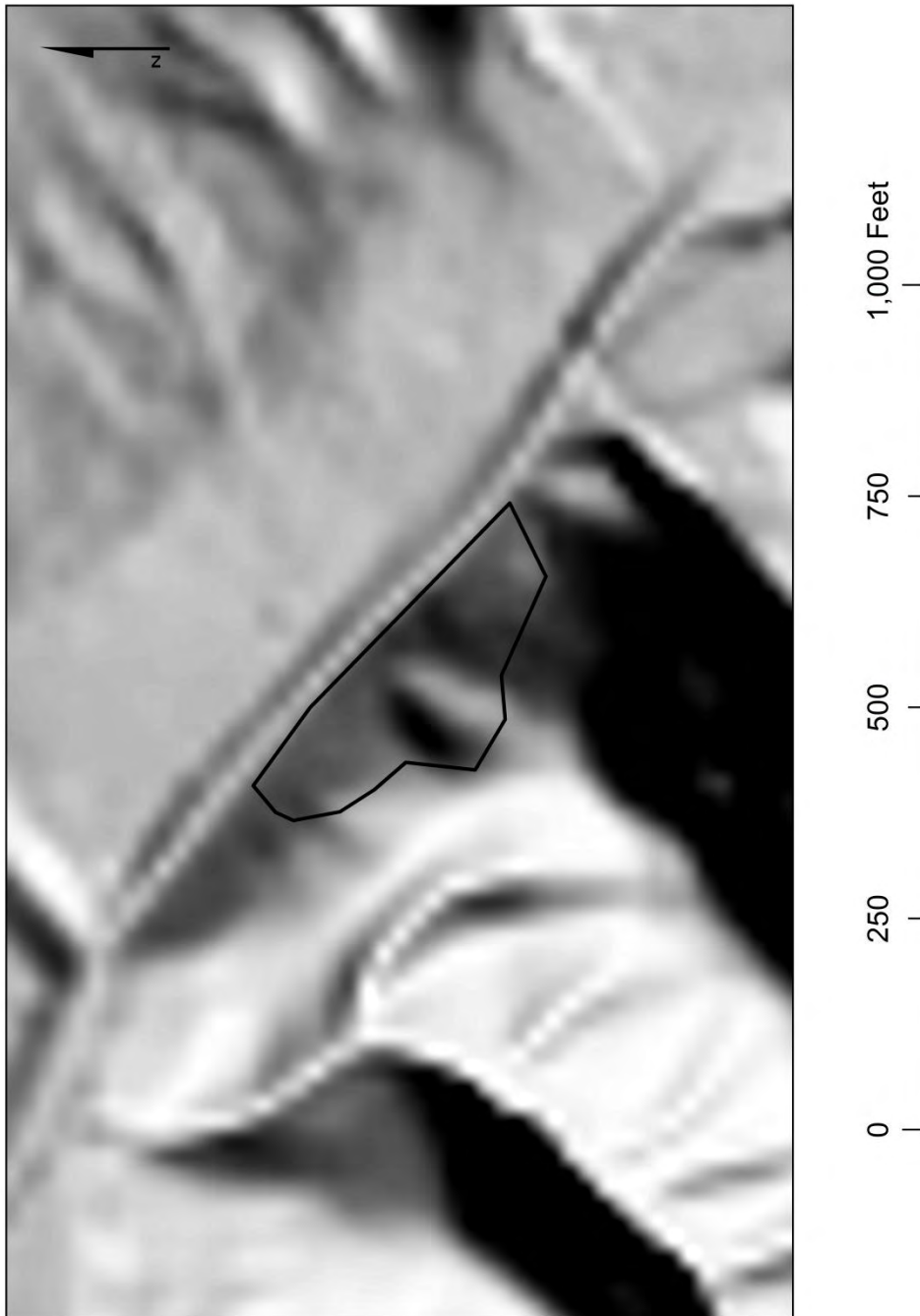


Figure AVI.13: Slope map of the 10 Mile Road landslide.



Source: OIT (2007)  
Produced by: Michael P. Glassmeyer



Figure AVI.14: Hillshade map of the 10 Mile Road landslide.

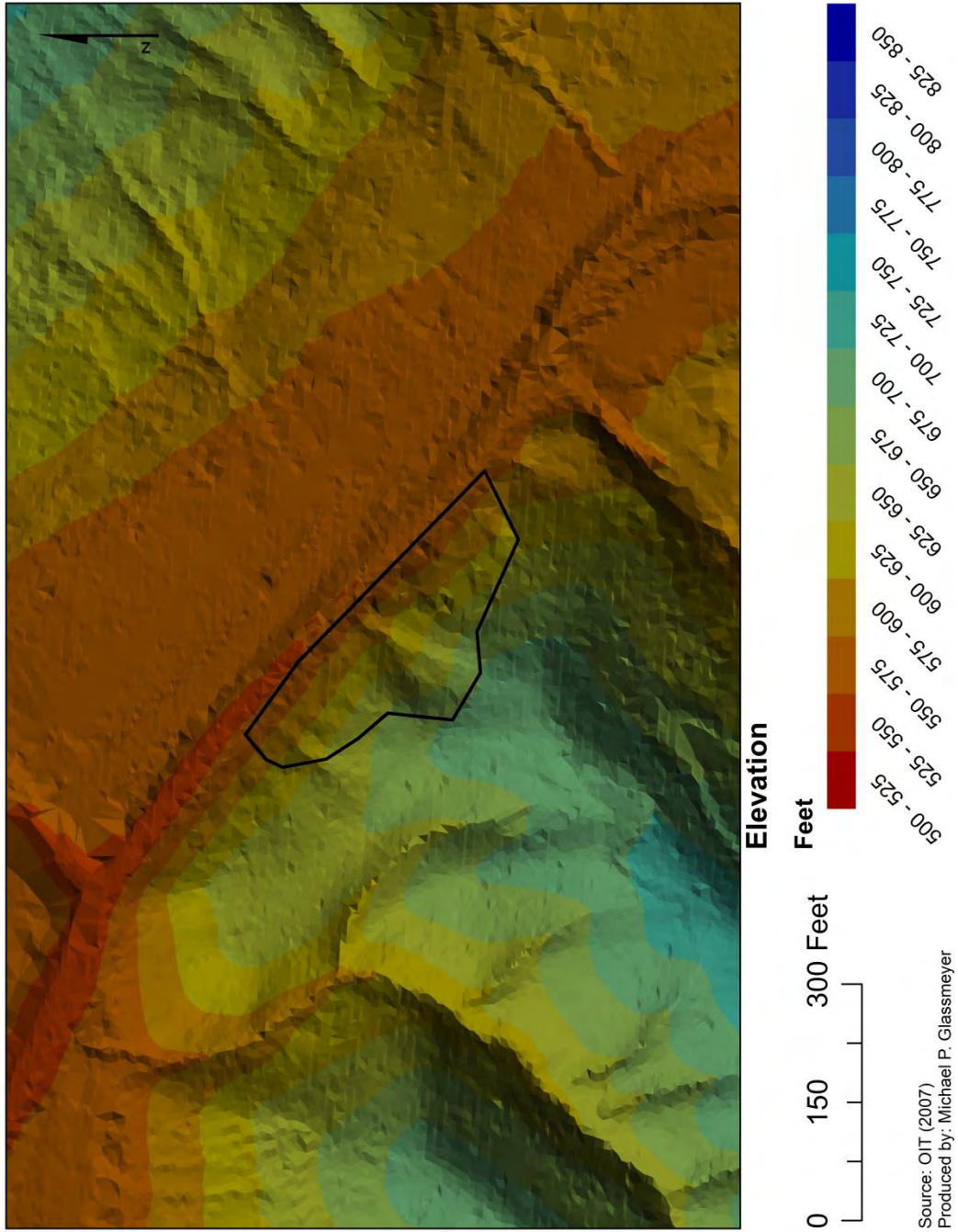


Figure AVI.15: Terrain map of the 10 Mile Road landslide.

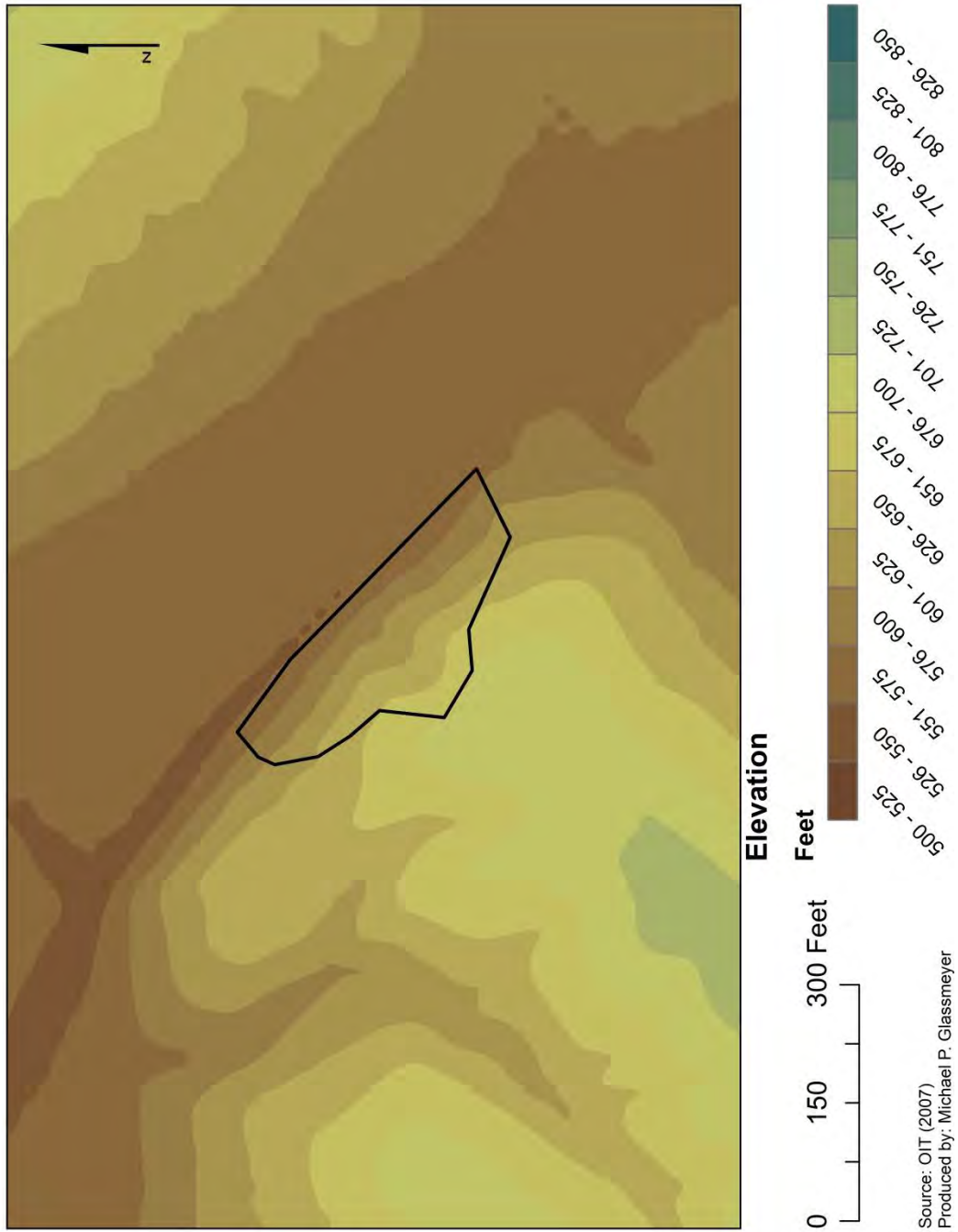


Figure AVI.16: DEM map of the 10 Mile Road landslide.

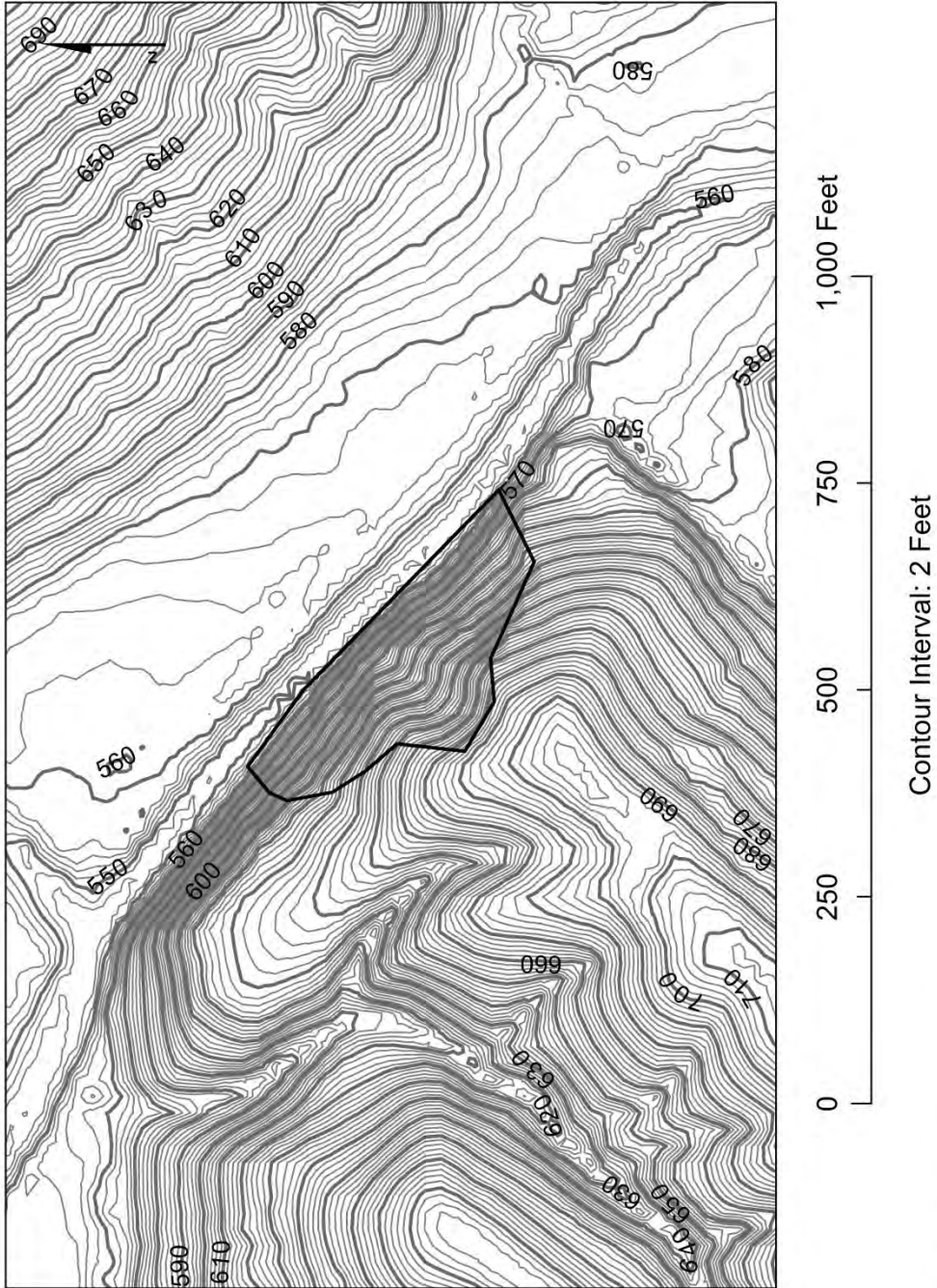
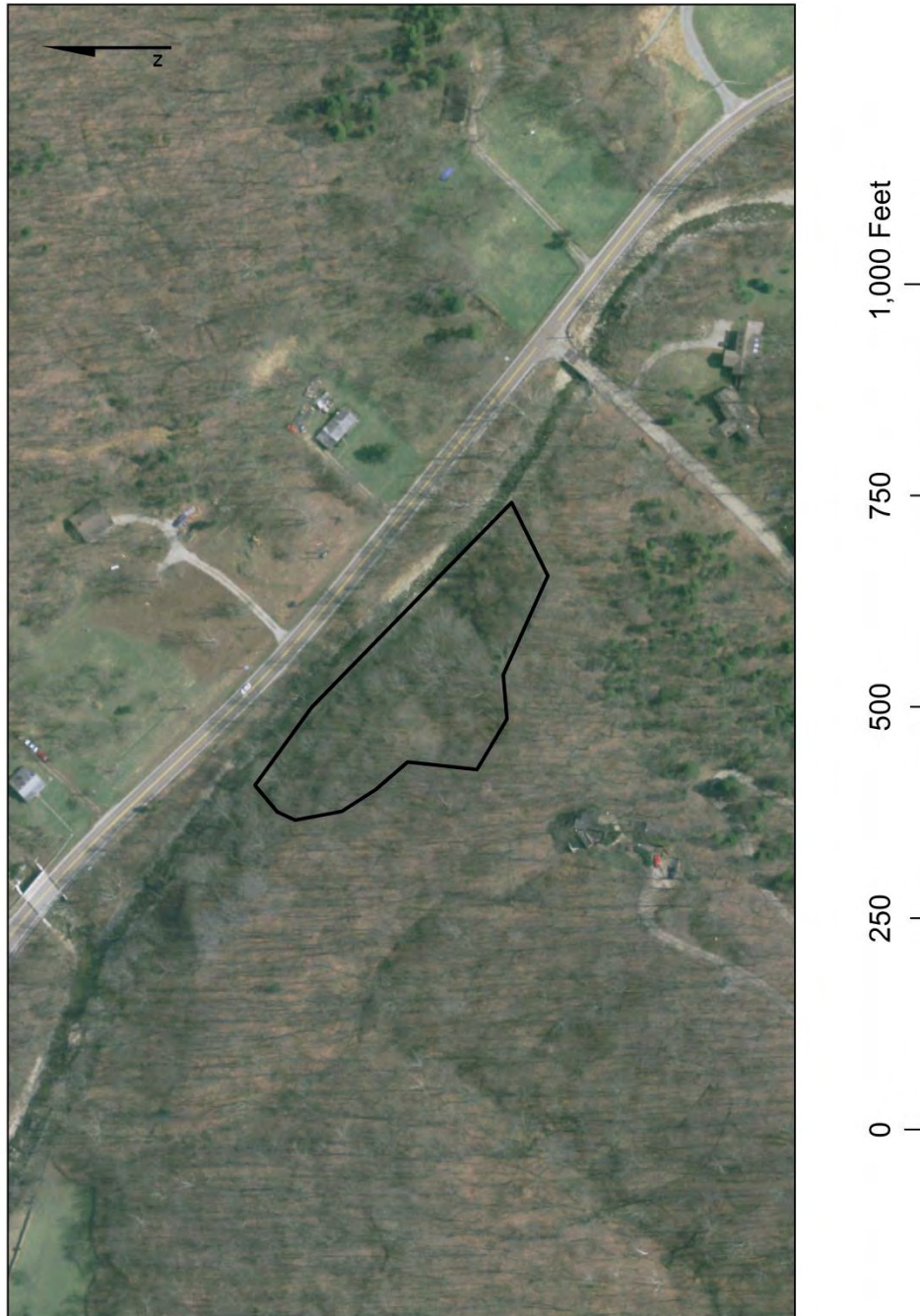




Figure AVI.17: Topographic map of the 10 Mile Road landslide.



Source: OIT (2007)  
Produced by: Michael P. Glassmeyer

Figure AVI.18: Aerial photograph of the 10 Mile Road landslide.

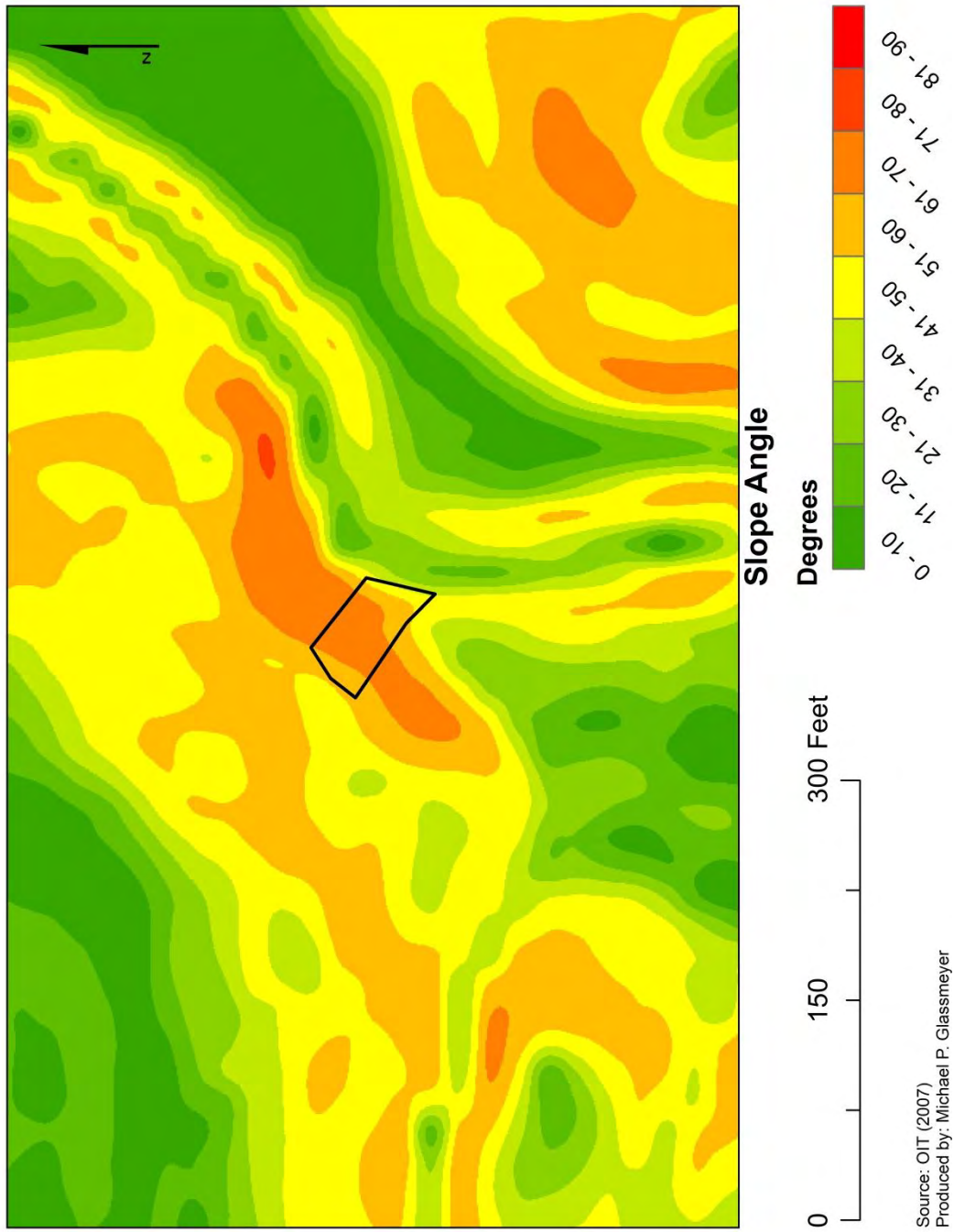
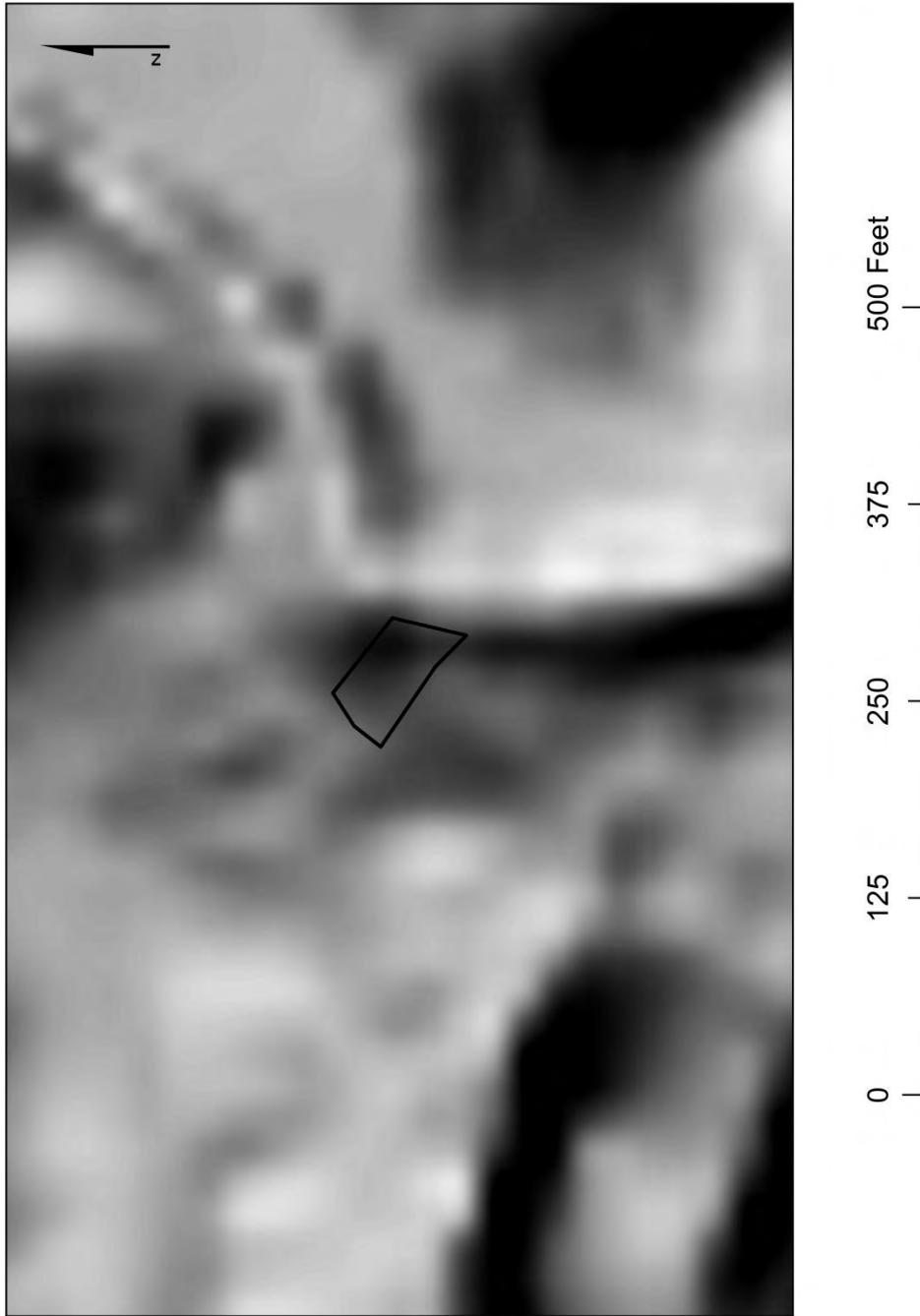


Figure AVI.19: Slope map of the Berkshire Road landslide.



Source: OIT (2007)  
Produced by: Michael P. Glassmeyer

Figure AVI.20: Slope map of the Berkshire Road landslide.

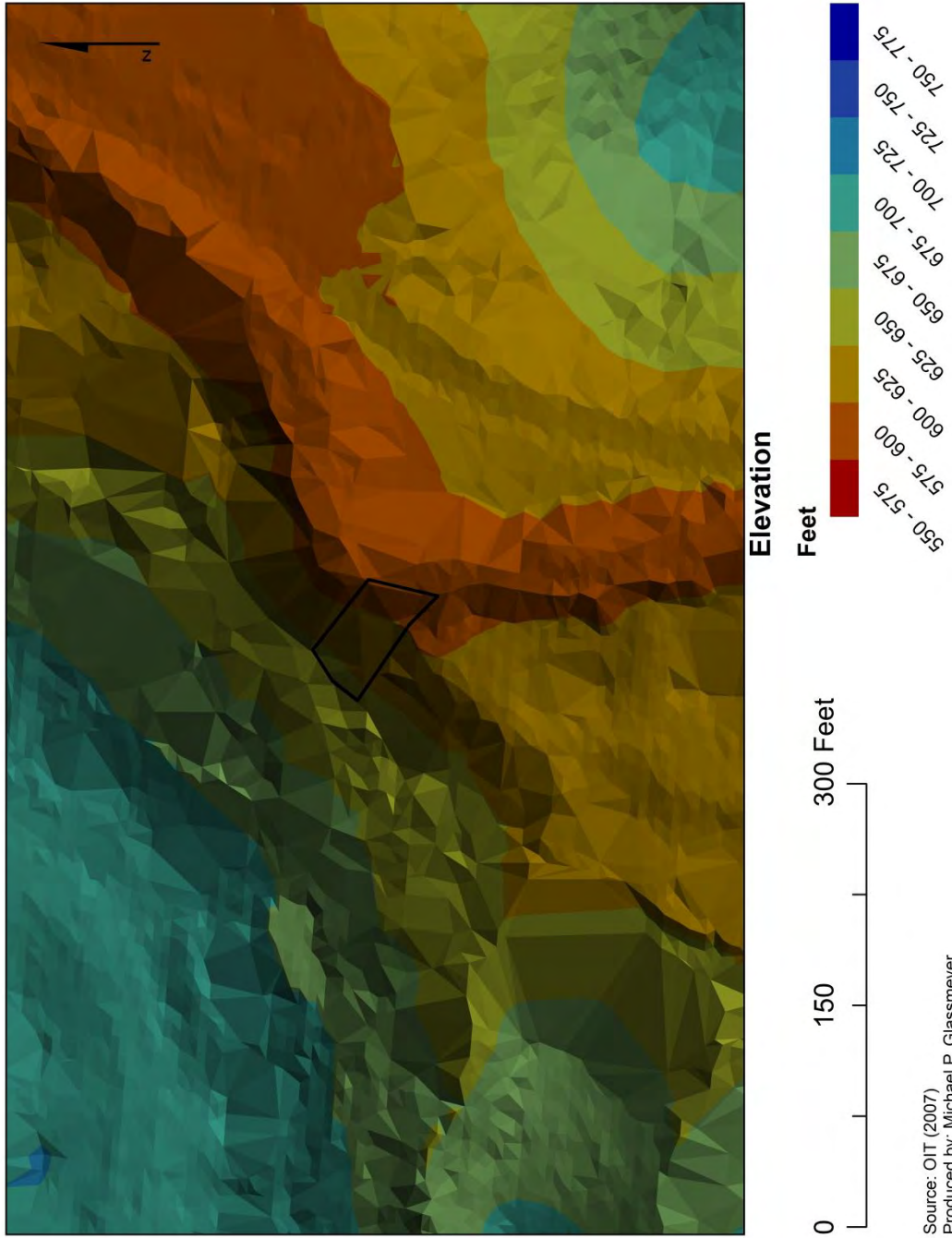




Figure AVI.21: Terrain map of the Berkshire Road landslide.

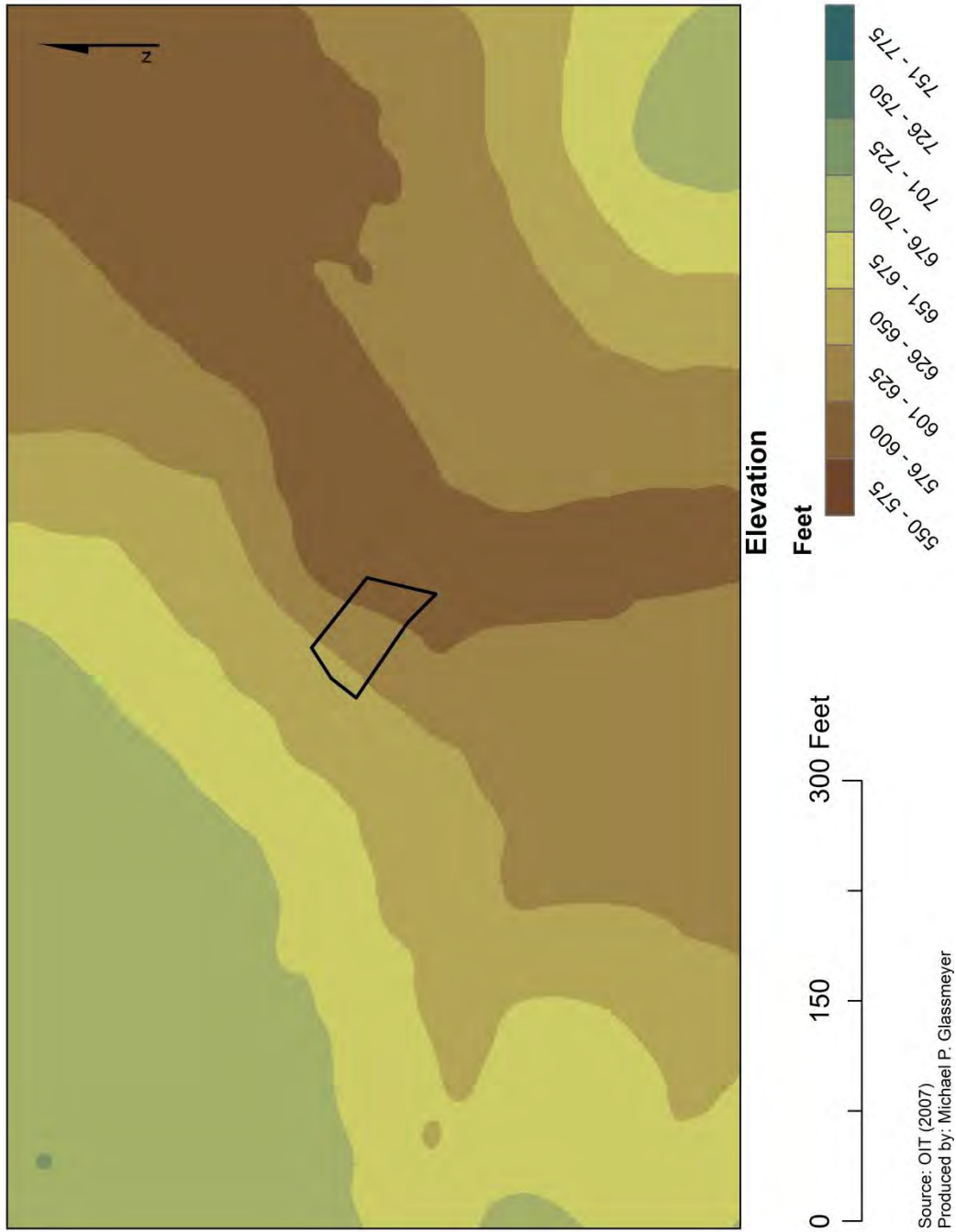
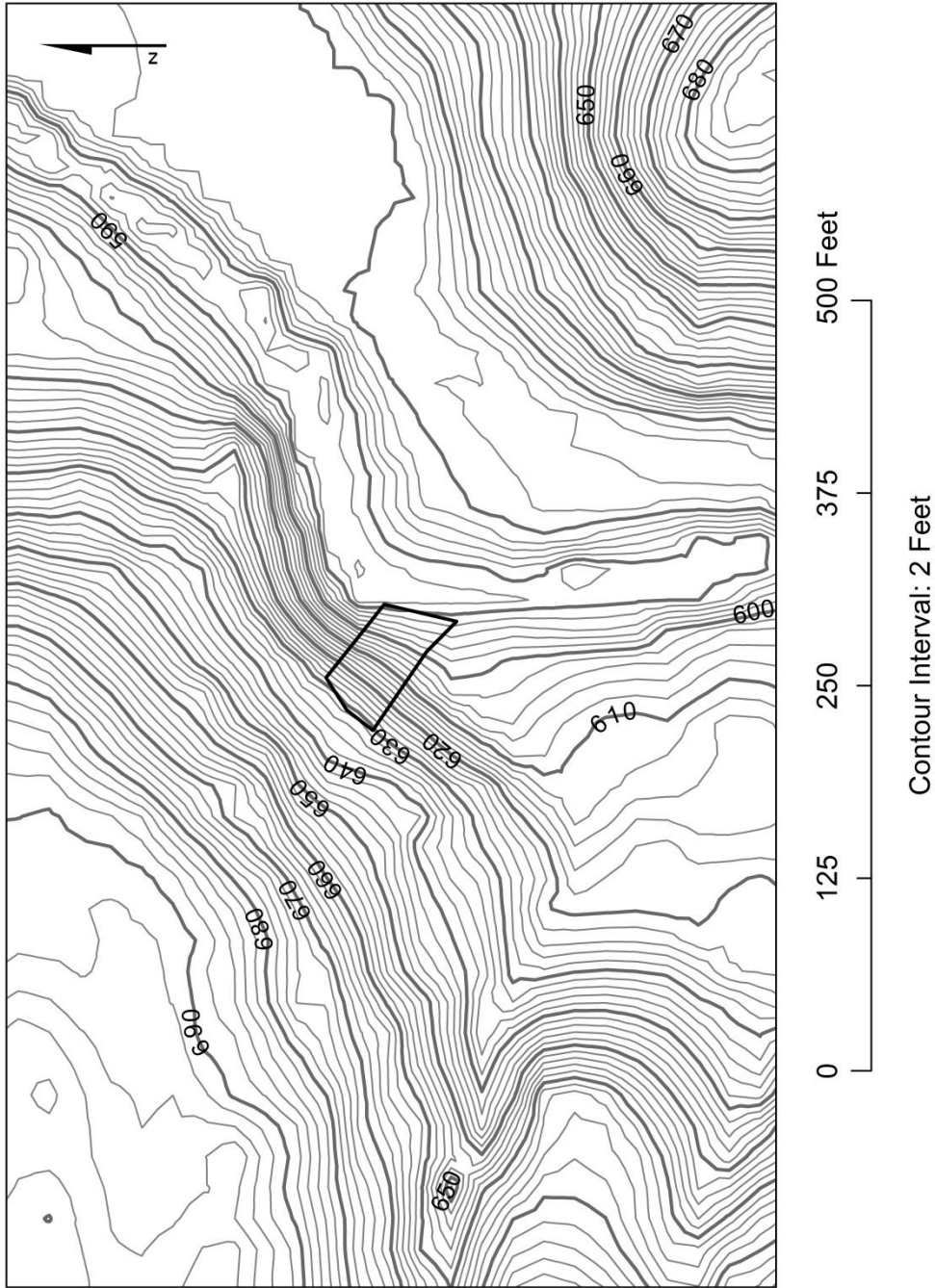


Figure AVI.22: Slope map of the Berkshire Road landslide.



Source: OIT (2007)  
Produced by: Michael P. Glassmeyer

Figure AVI.23: Topographic map of the Berkshire Road landslide.



Source: OIT (2007)  
Produced by: Michael P. Glassmeyer

Figure AVI.24: Aerial photograph of the Berkshire Road landslide.

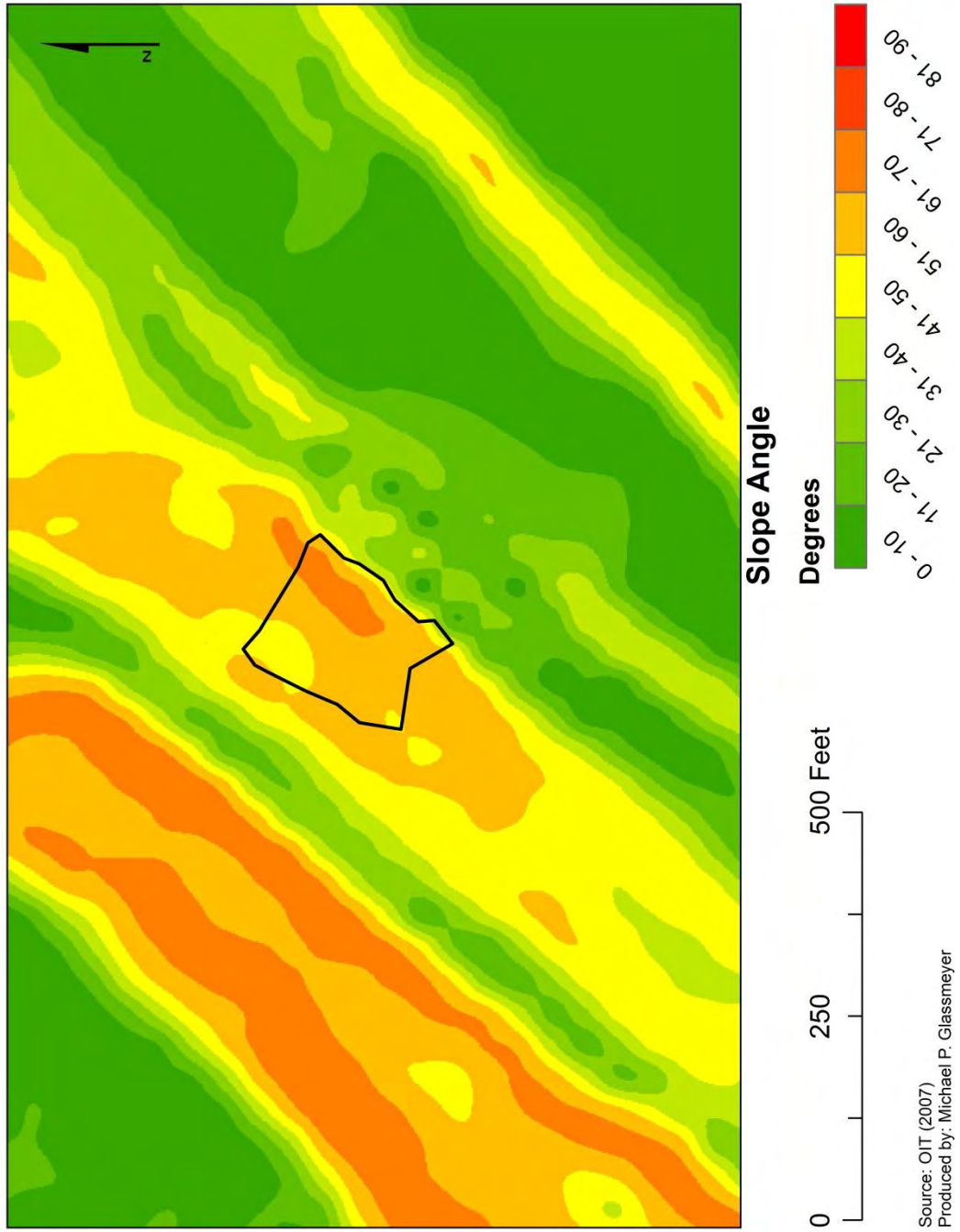
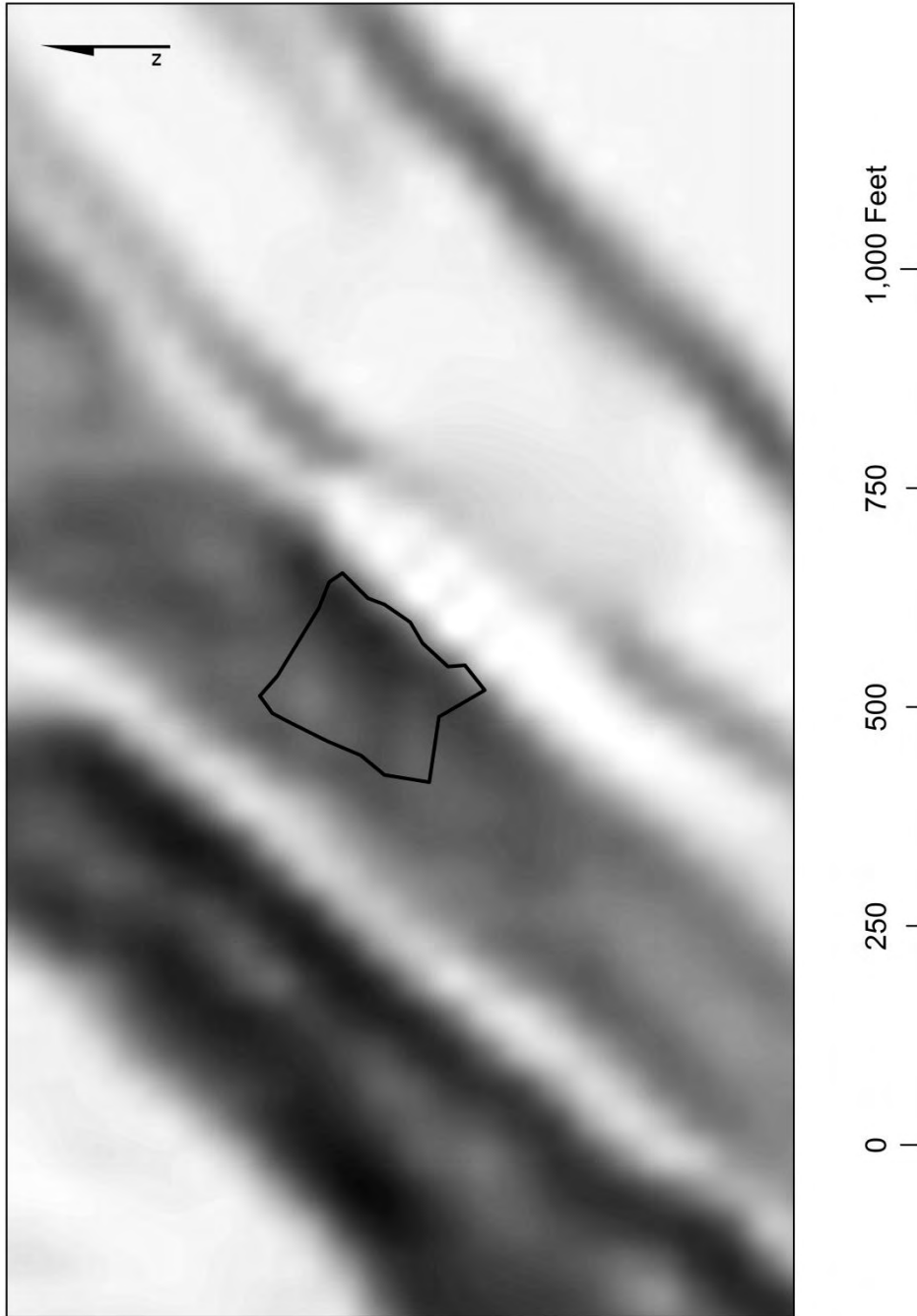


Figure AVI.25: Slope map of the Columbia Parkway landslide.



Source: OIT (2007)  
Produced by: Michael P. Glassmeyer



Figure AVI.26: Hillshade map of the Columbia Parkway landslide.

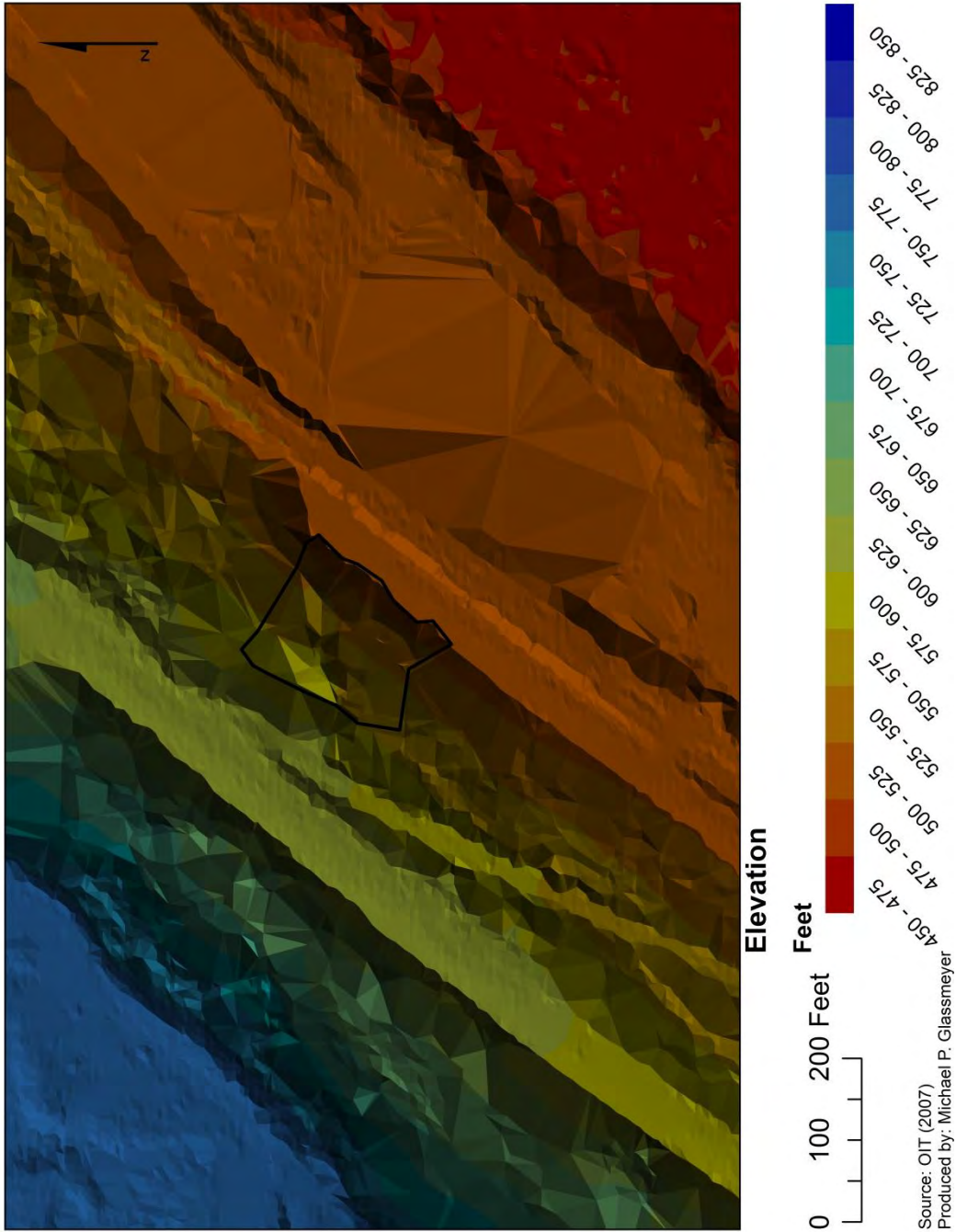


Figure AVI.27: Terrain map of the Columbia Parkway landslide.

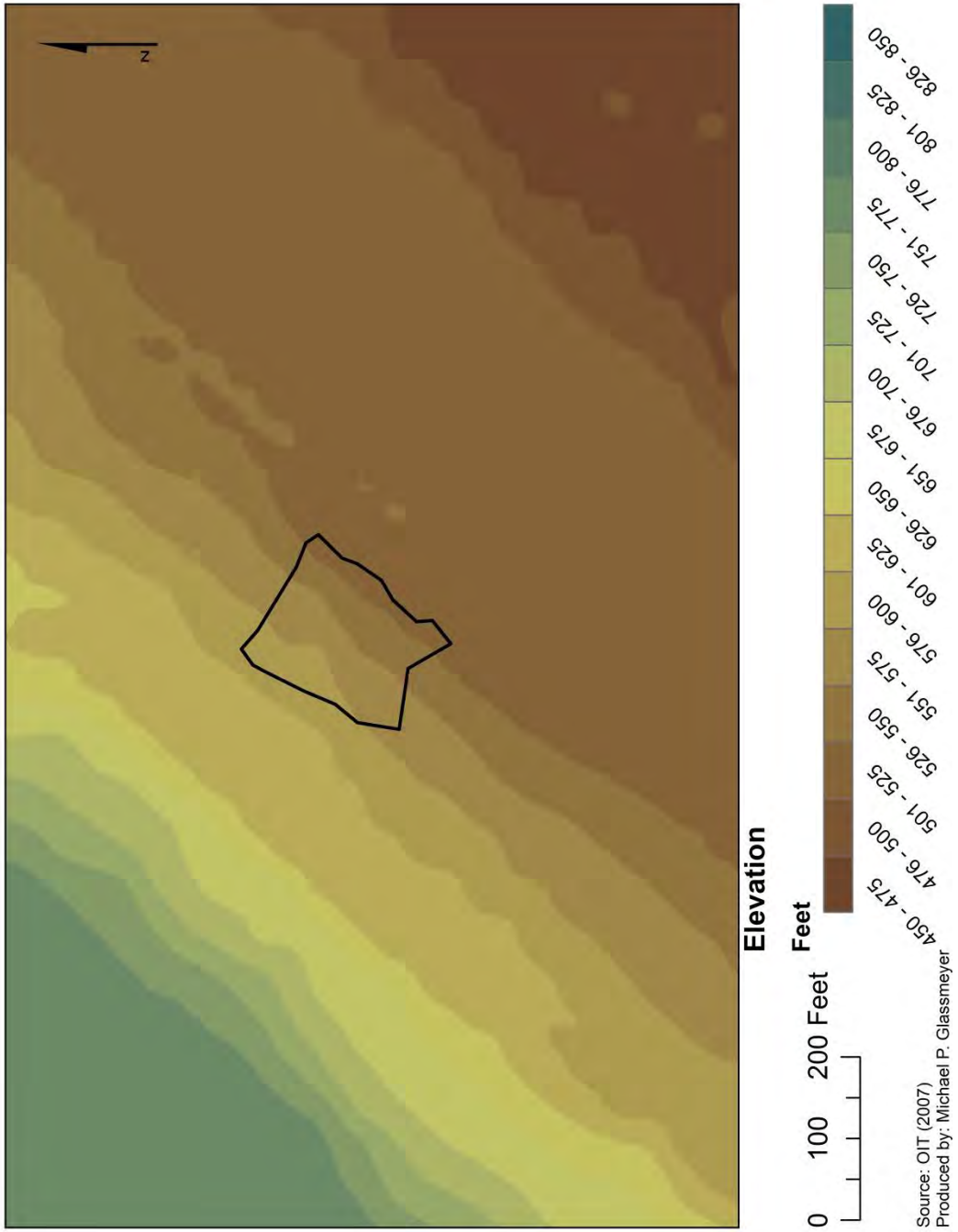




Figure AVI.28: DEM map of the Columbia Parkway landslide.

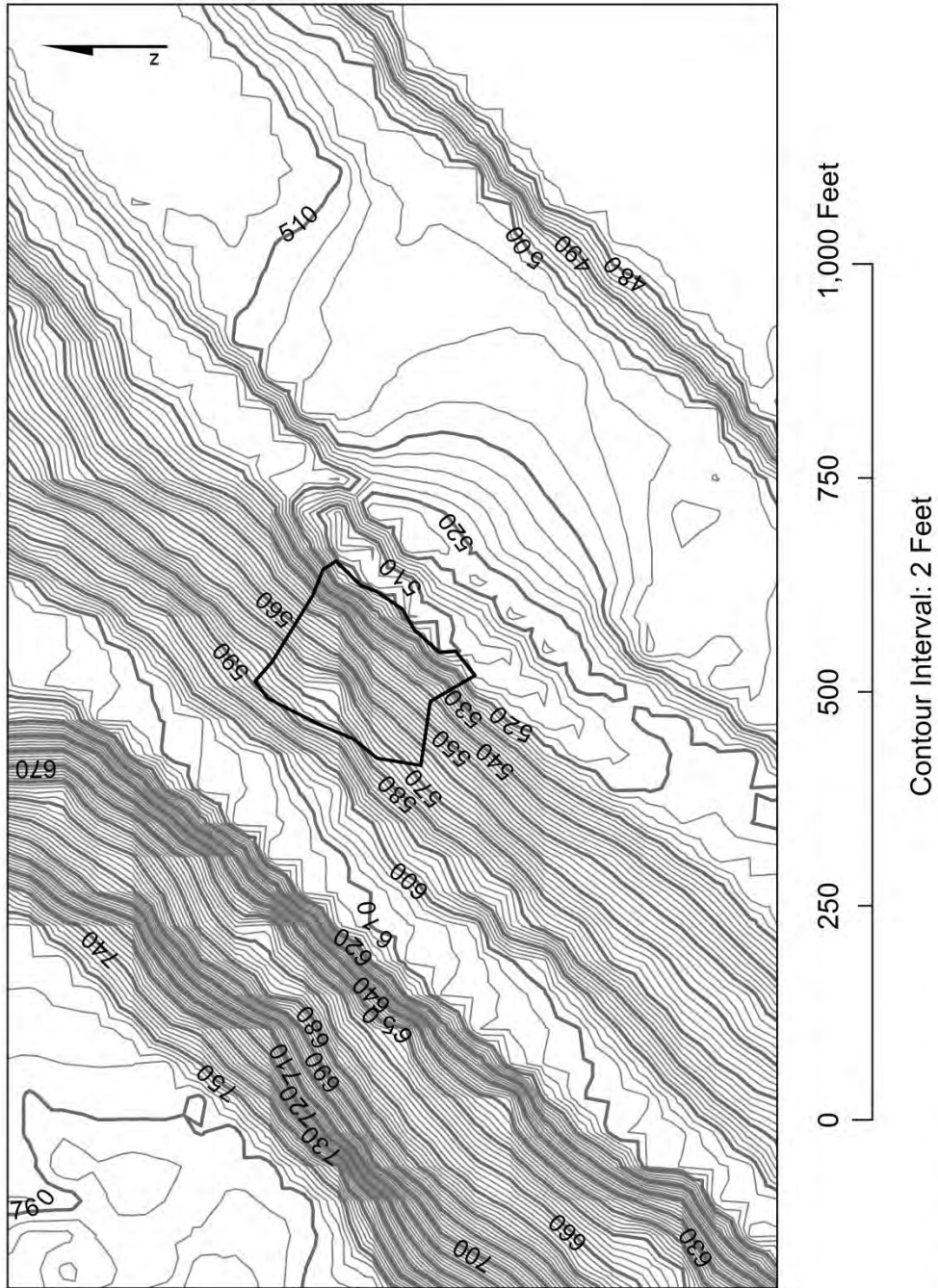


Figure AVI.29: Topographic map of the Columbia Parkway landslide.



Source: OJT (2007)  
Produced by: Michael P. Glassmeyer

Figure AVI.30: Aerial photograph of the Columbia Parkway landslide.

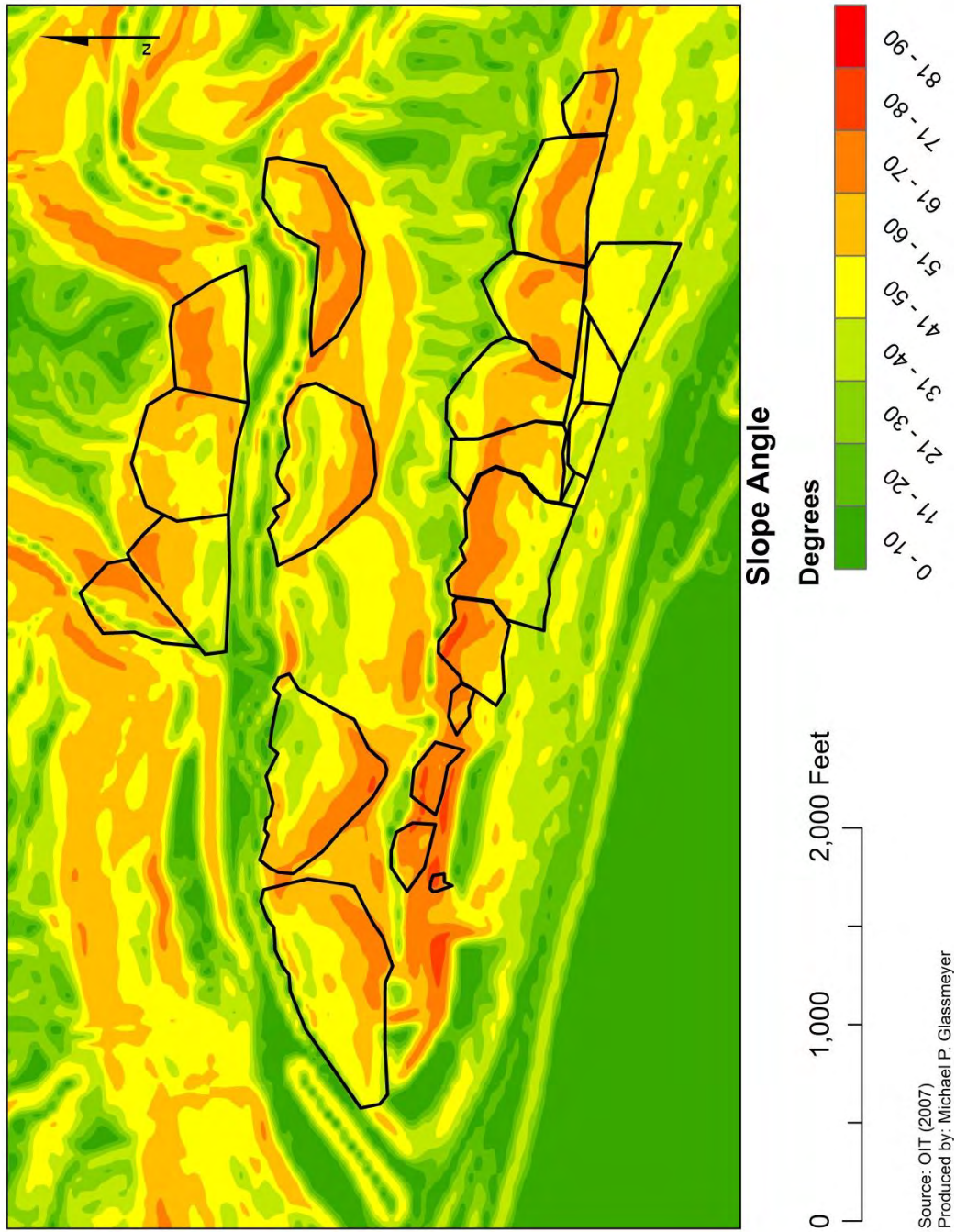
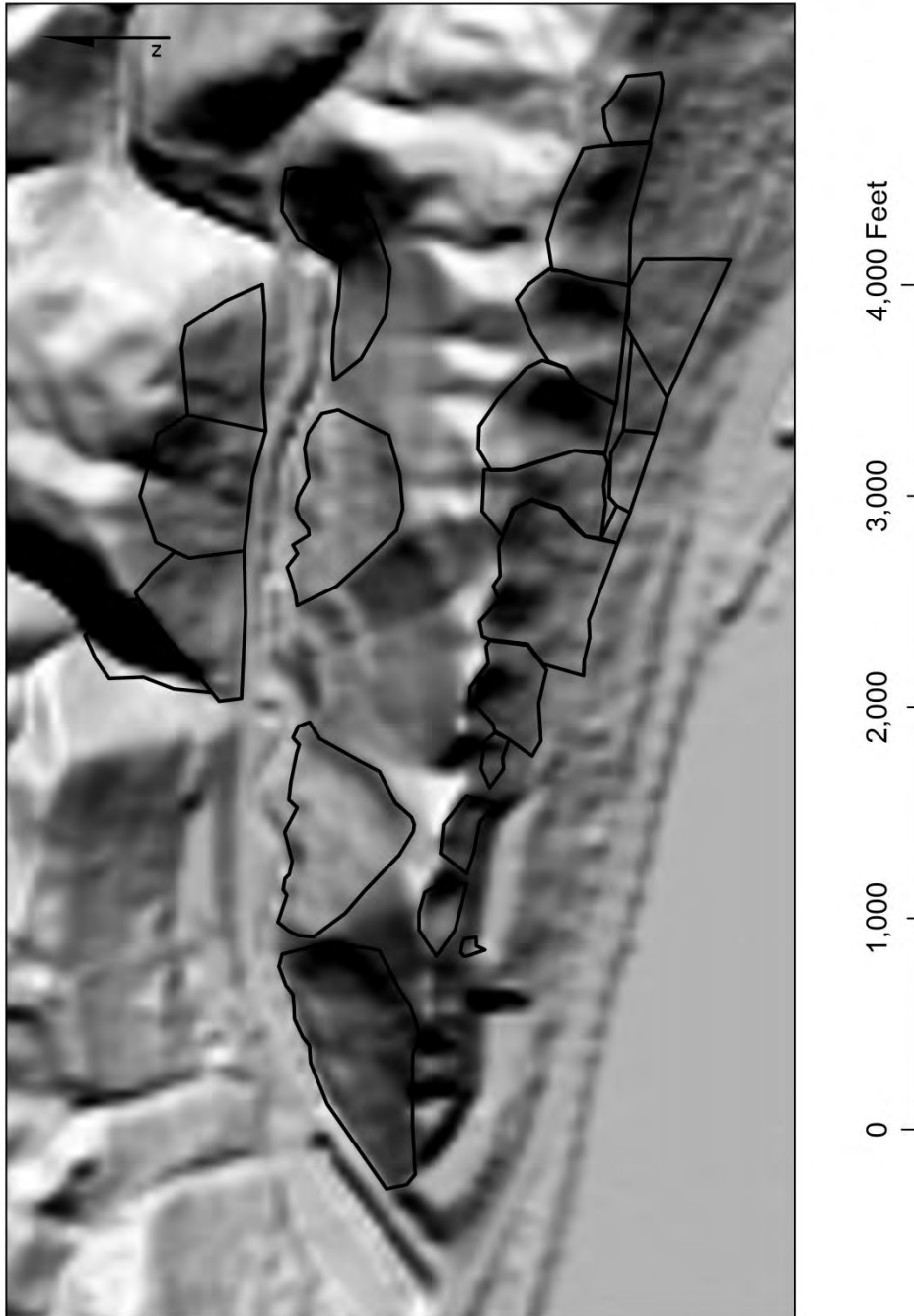


Figure AVI.31: Slope map of the Delhi Pike landslide.



Source: OIT (2007)  
Produced by: Michael P. Glassmeyer

Figure AVI.32: Hillshade map of the Delhi Pike landslide.



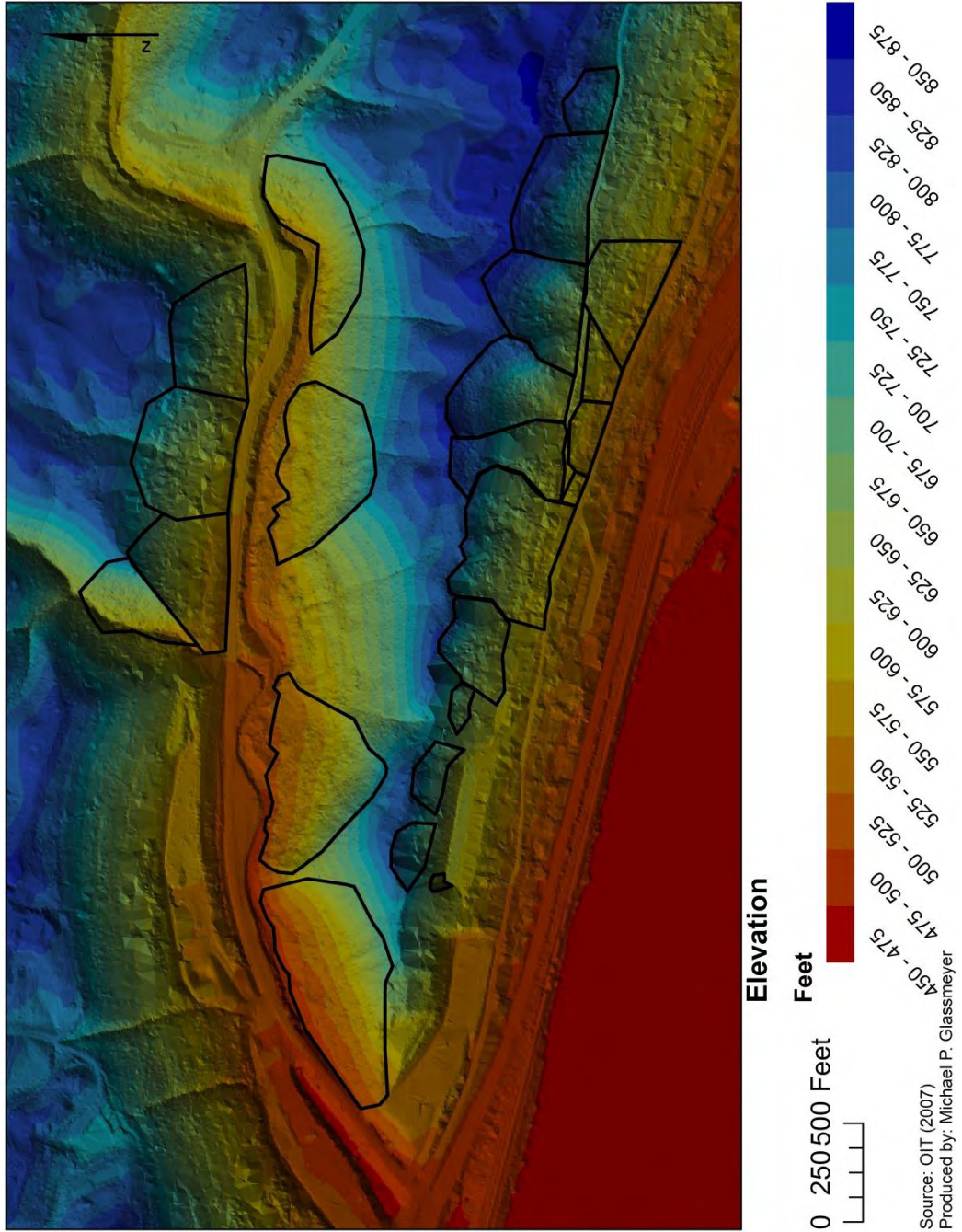


Figure AVI.33: Terrain map of the Delhi Pike landslide.

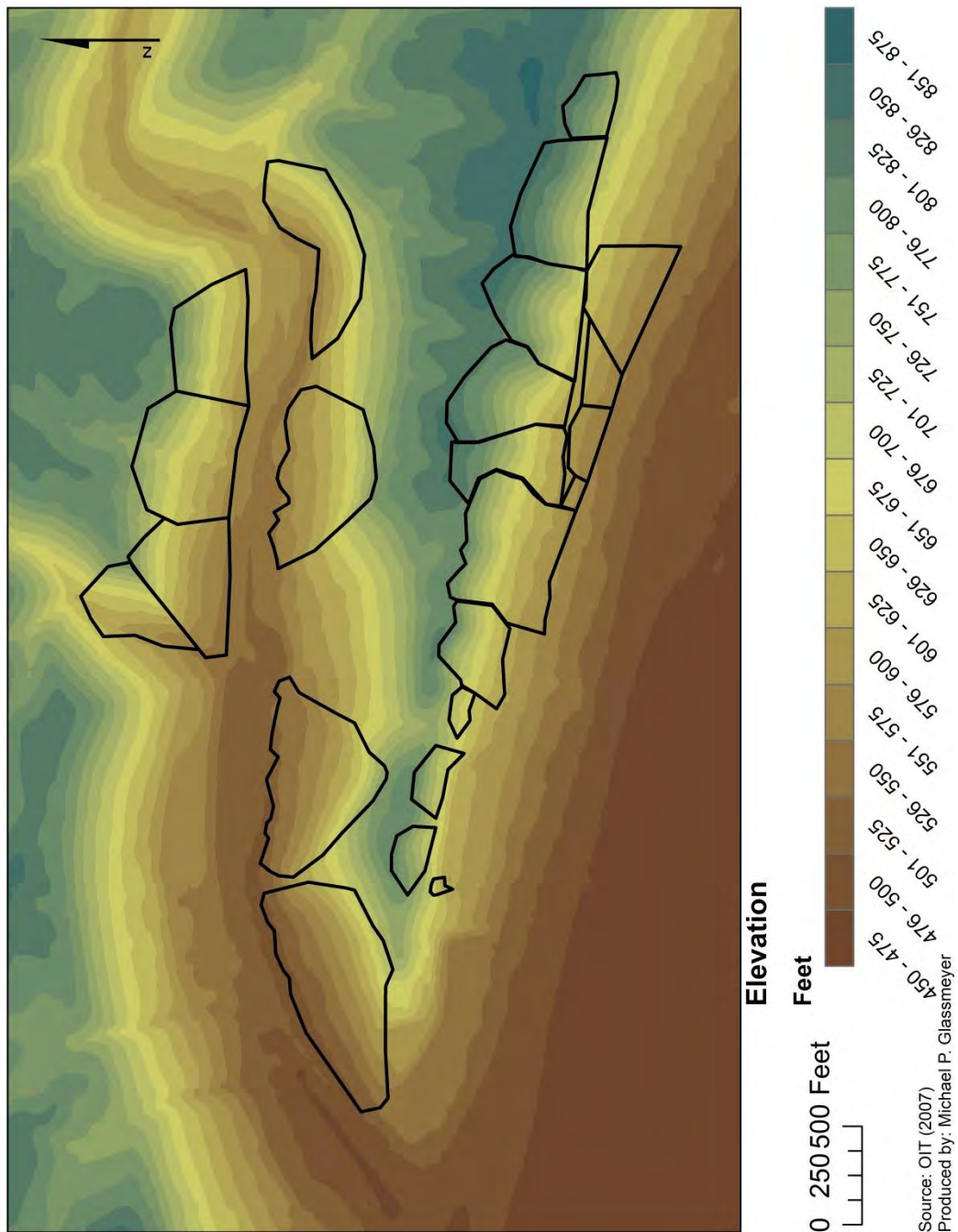
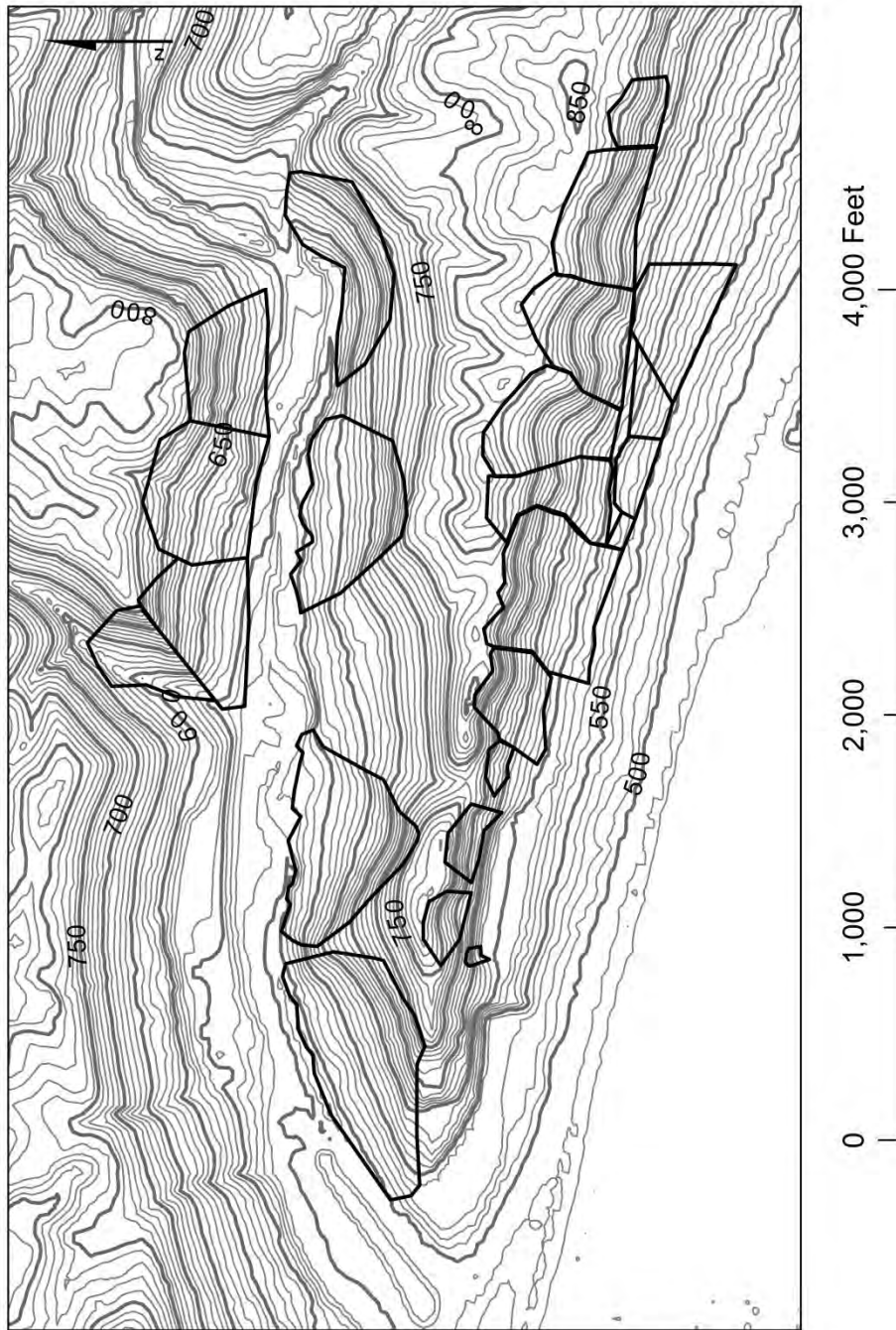


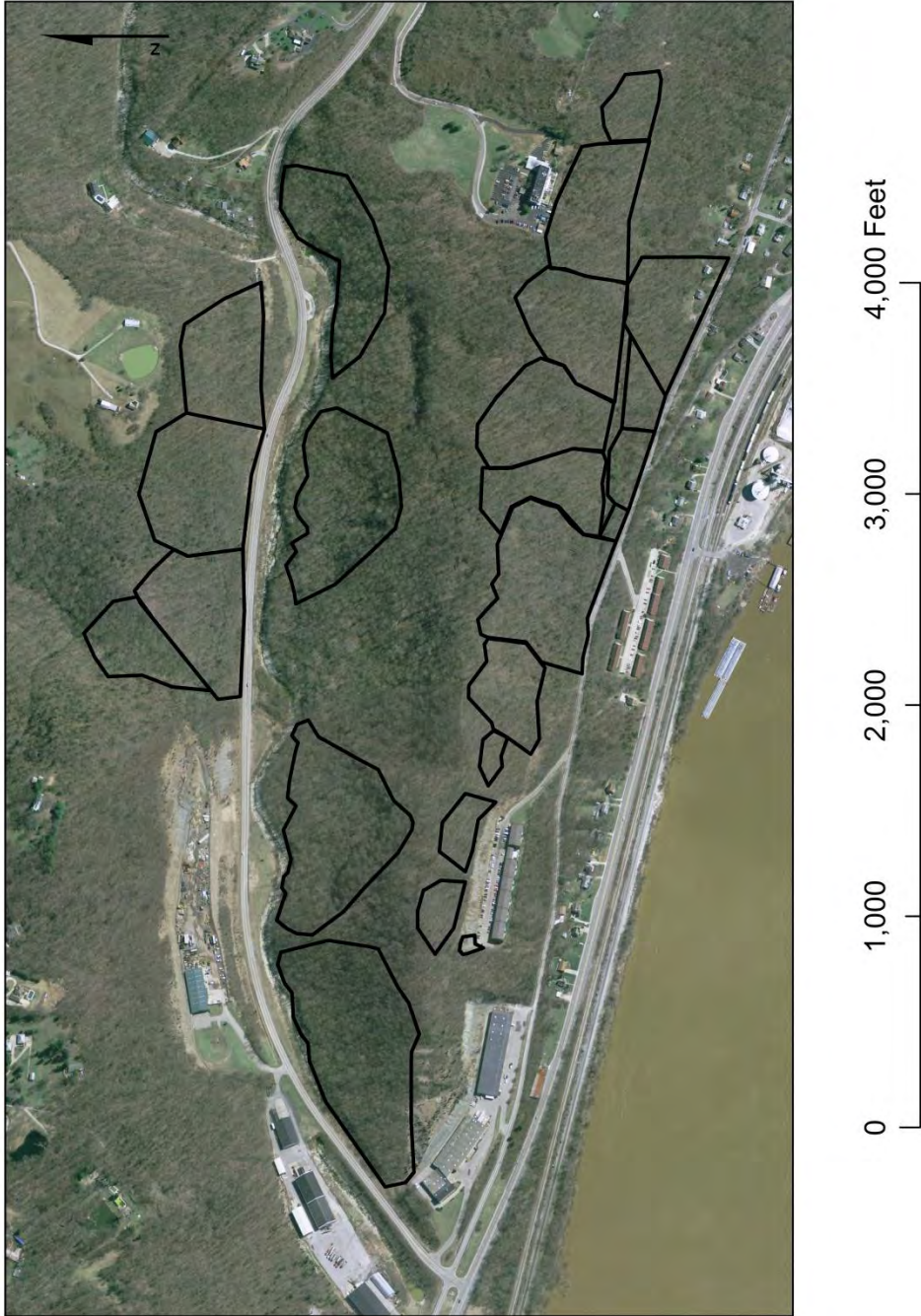
Figure AVI.34: DEM map of the Delhi Pike landslide.





Source: OIT (2007)  
Produced by: Michael P. Glassmeyer

Figure AVI.35: Topographic map of the Delhi Pike landslide.



Source: OIT (2007)  
Produced by: Michael P. Glassmeyer

Figure AVI.36: Aerial photograph of the Delhi Pike landslide.

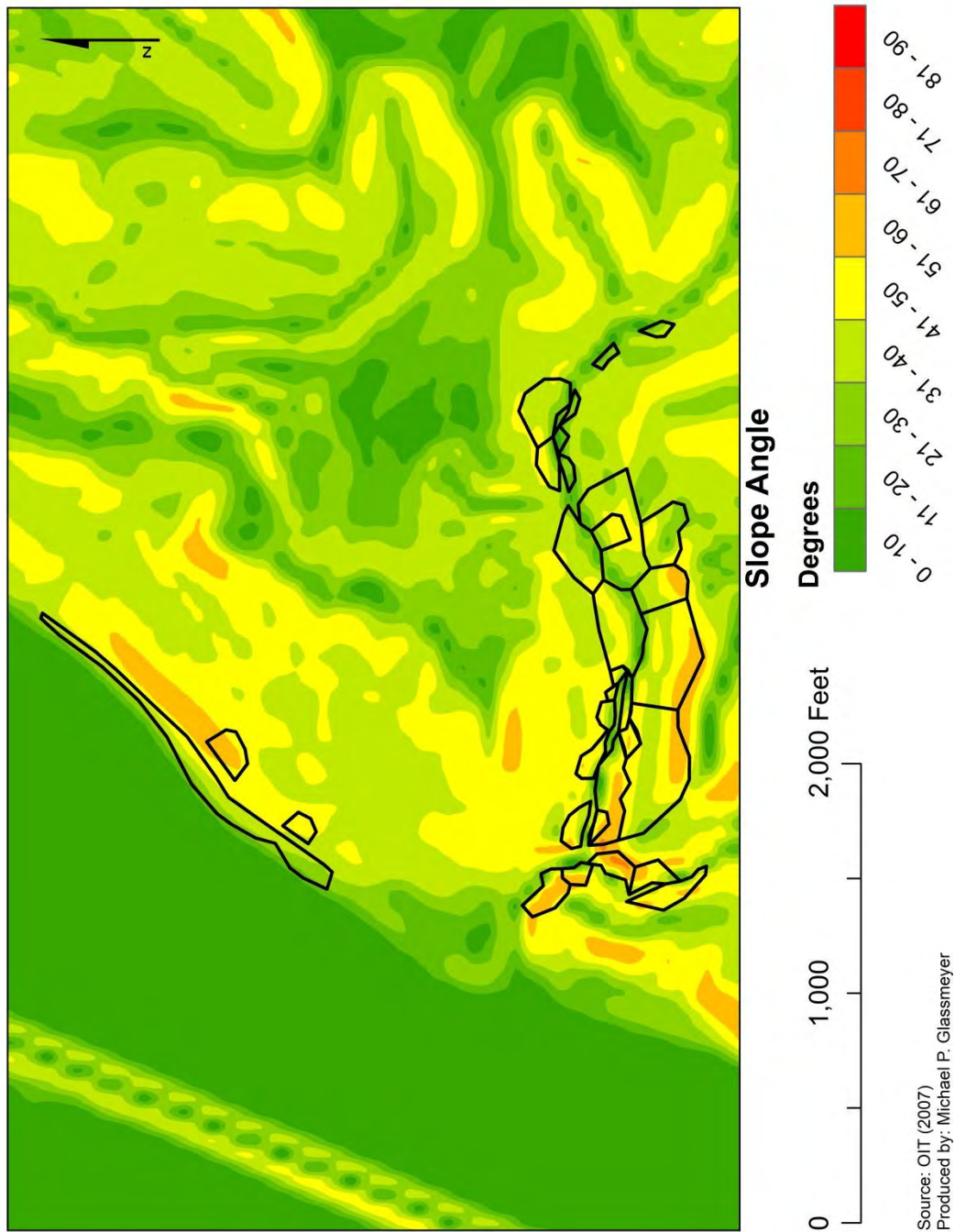
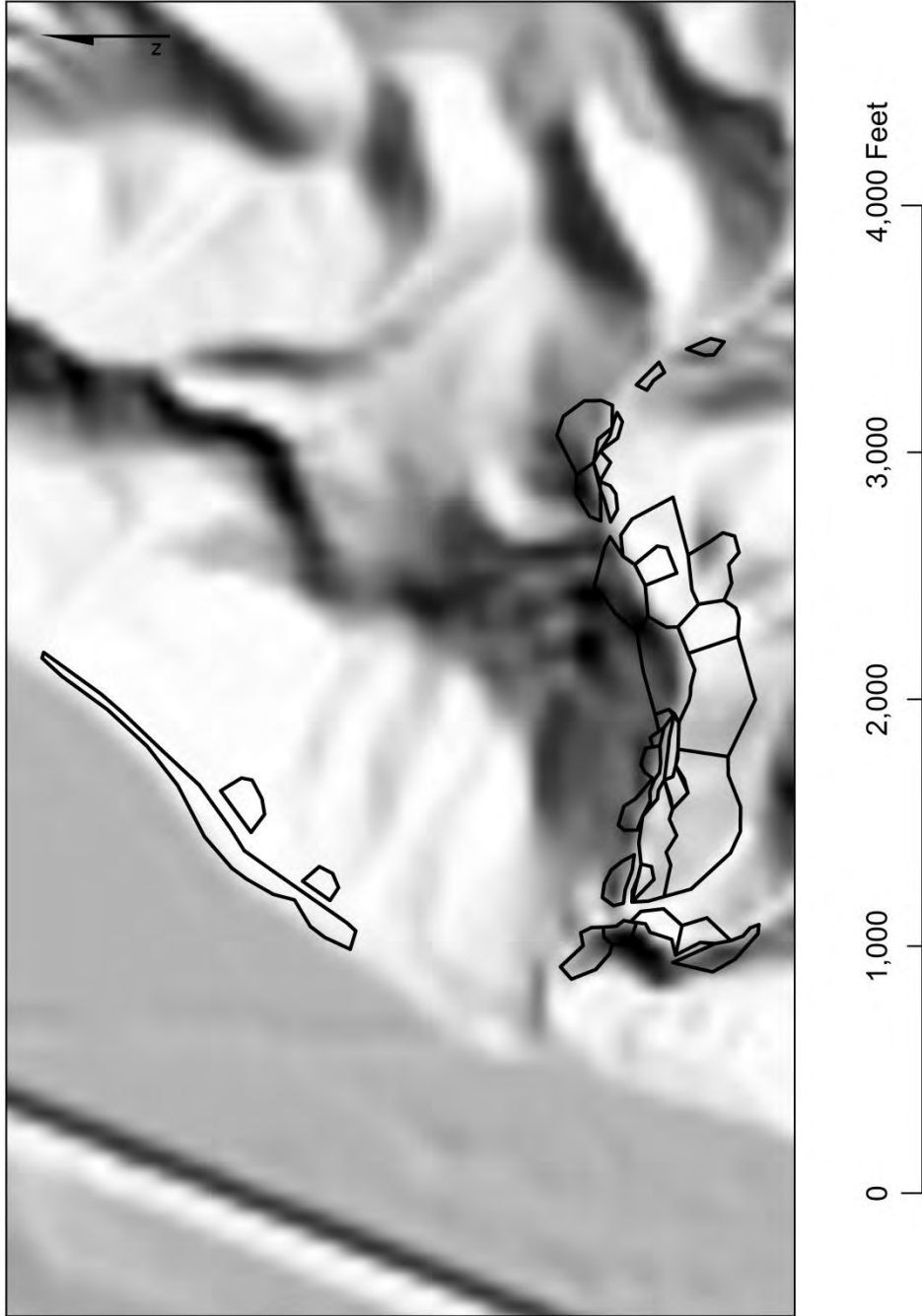


Figure AVI.37: Slope map of the Elstun Road landslide.



Source: OIT (2007)  
Produced by: Michael P. Glassmeyer

Figure AVI.38: Hillshade map of the Elstun Road landslide.



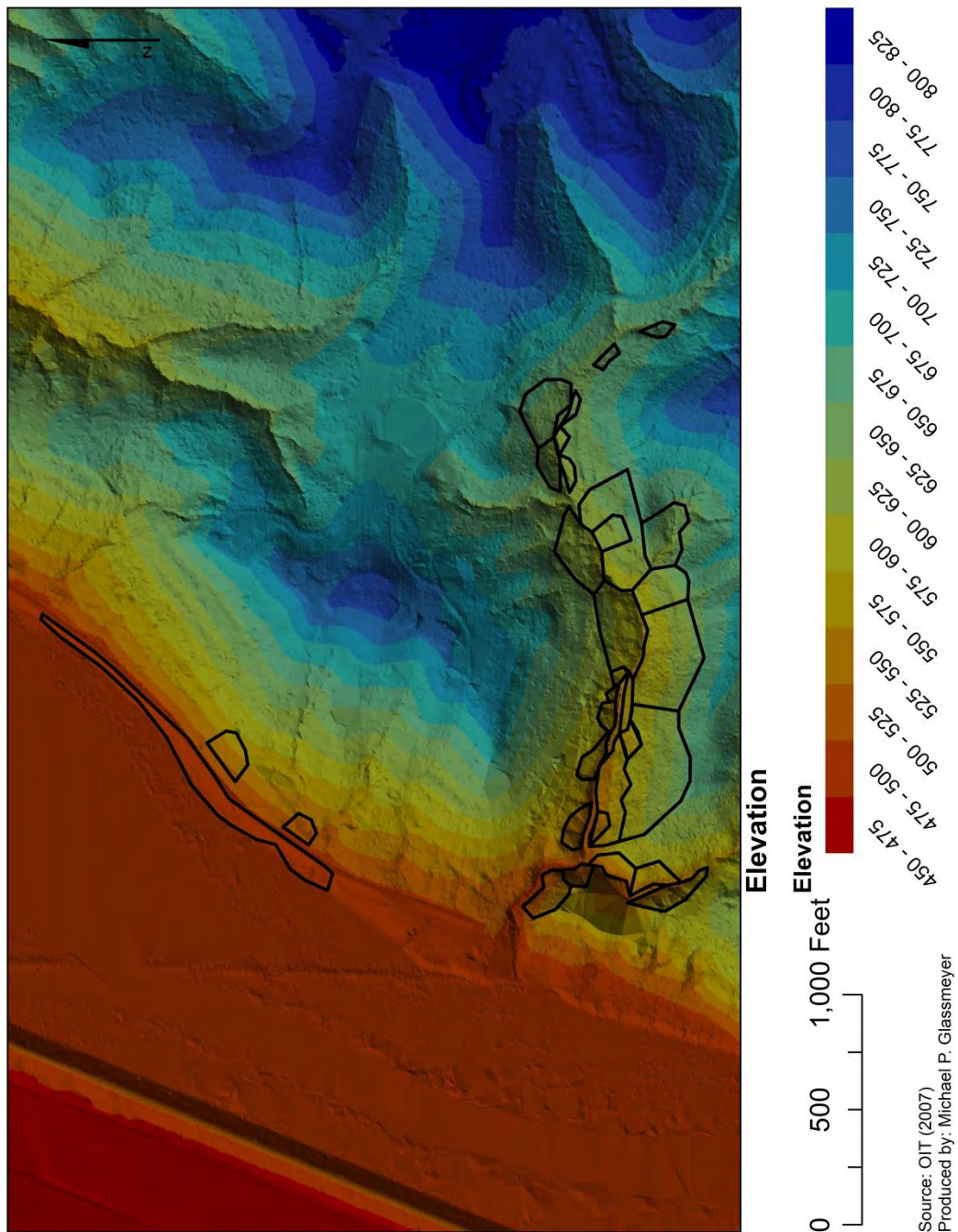


Figure AVI.39: Terrain map of the Elstun Road landslide.

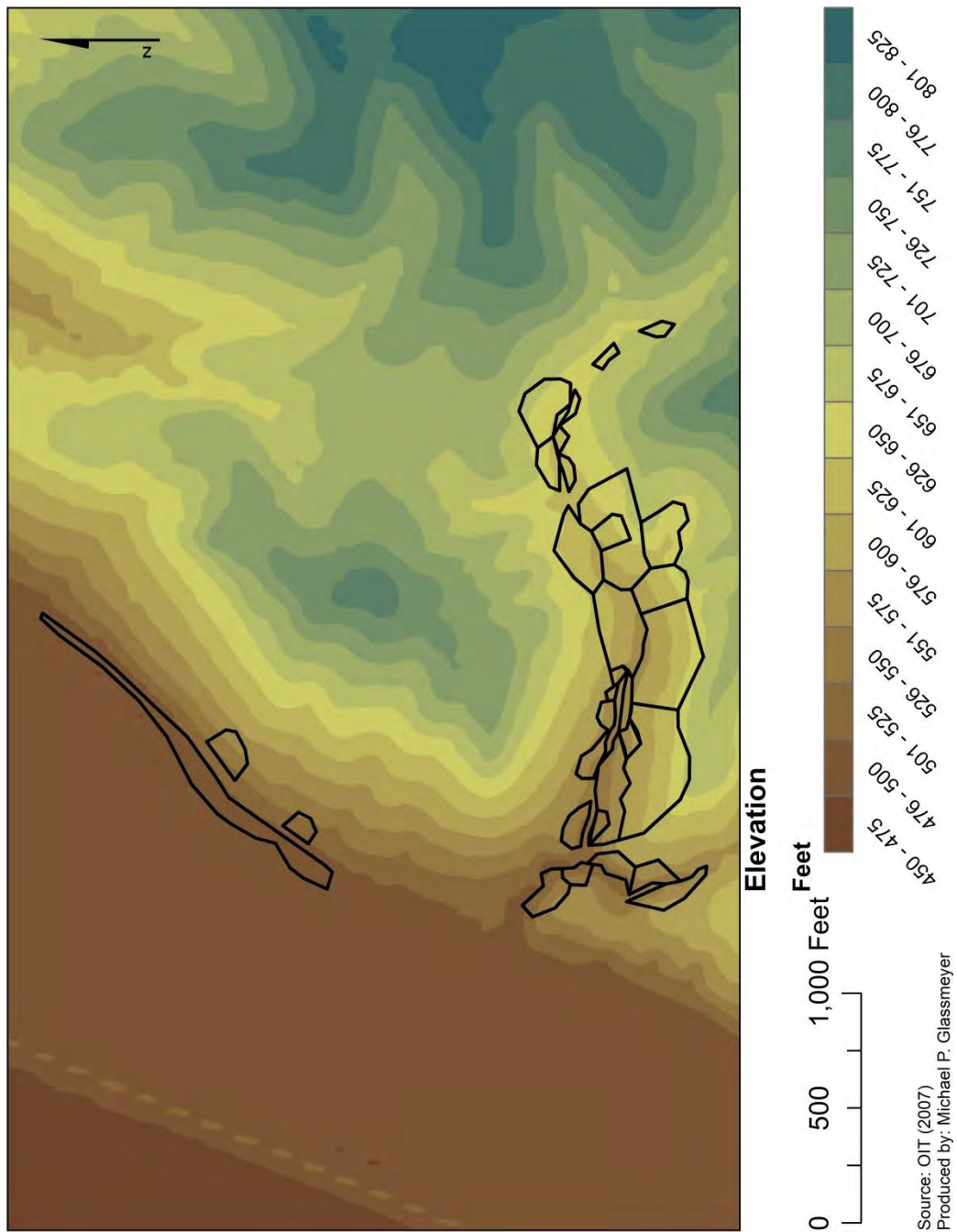
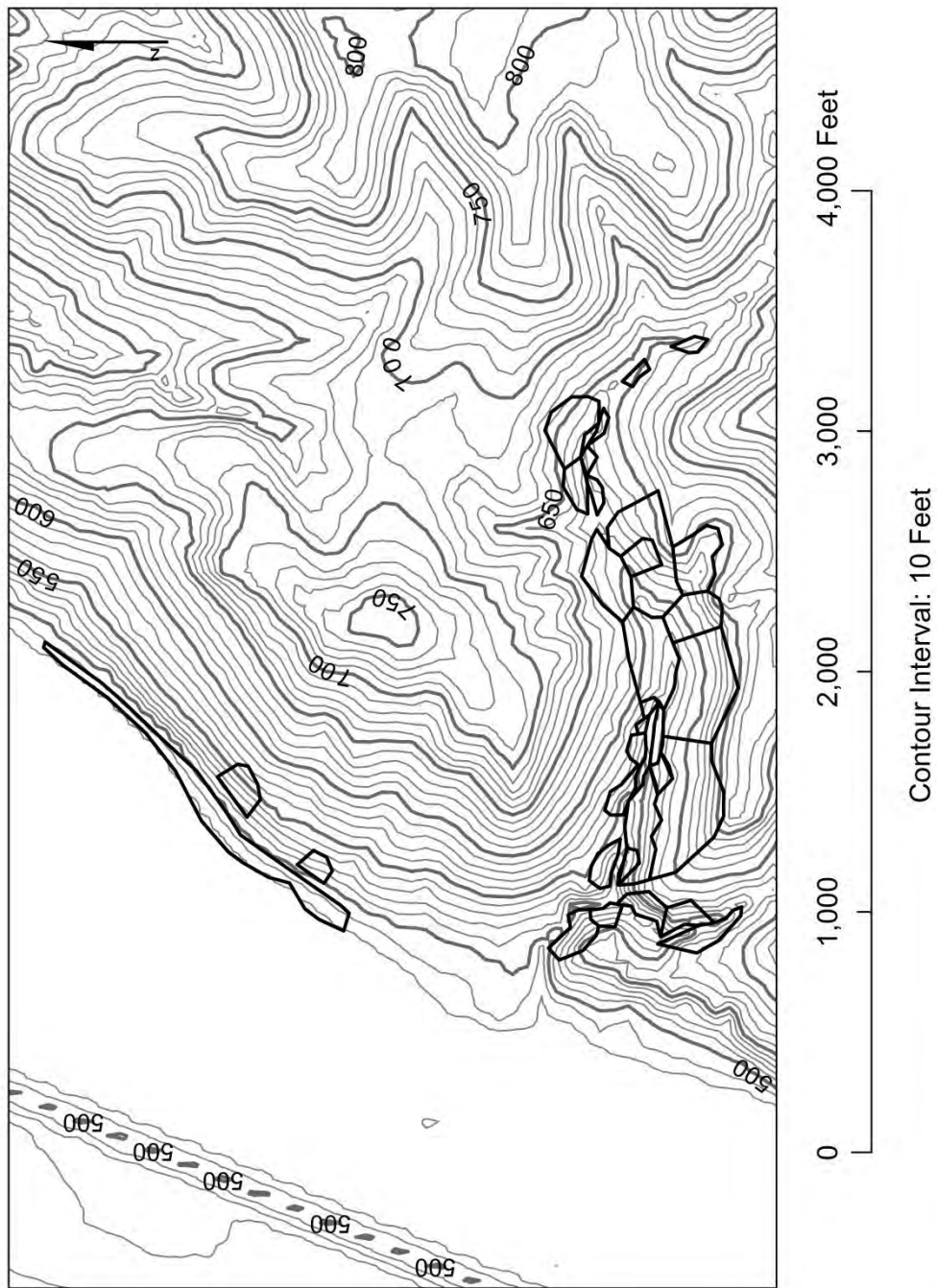


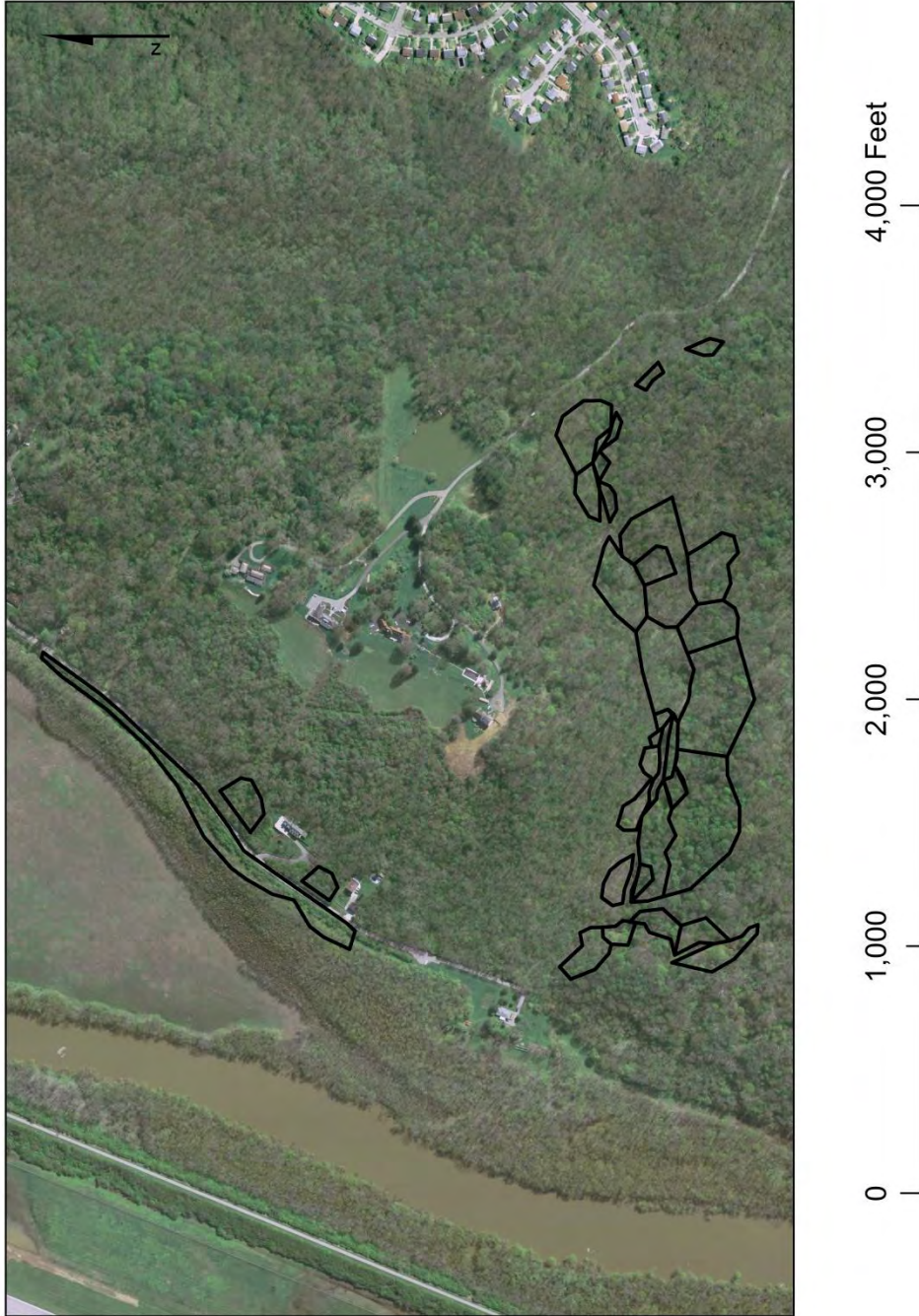
Figure AVI.40: DEM map of the Elstun Road landslide.





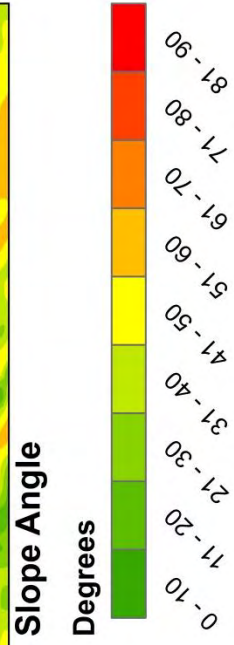
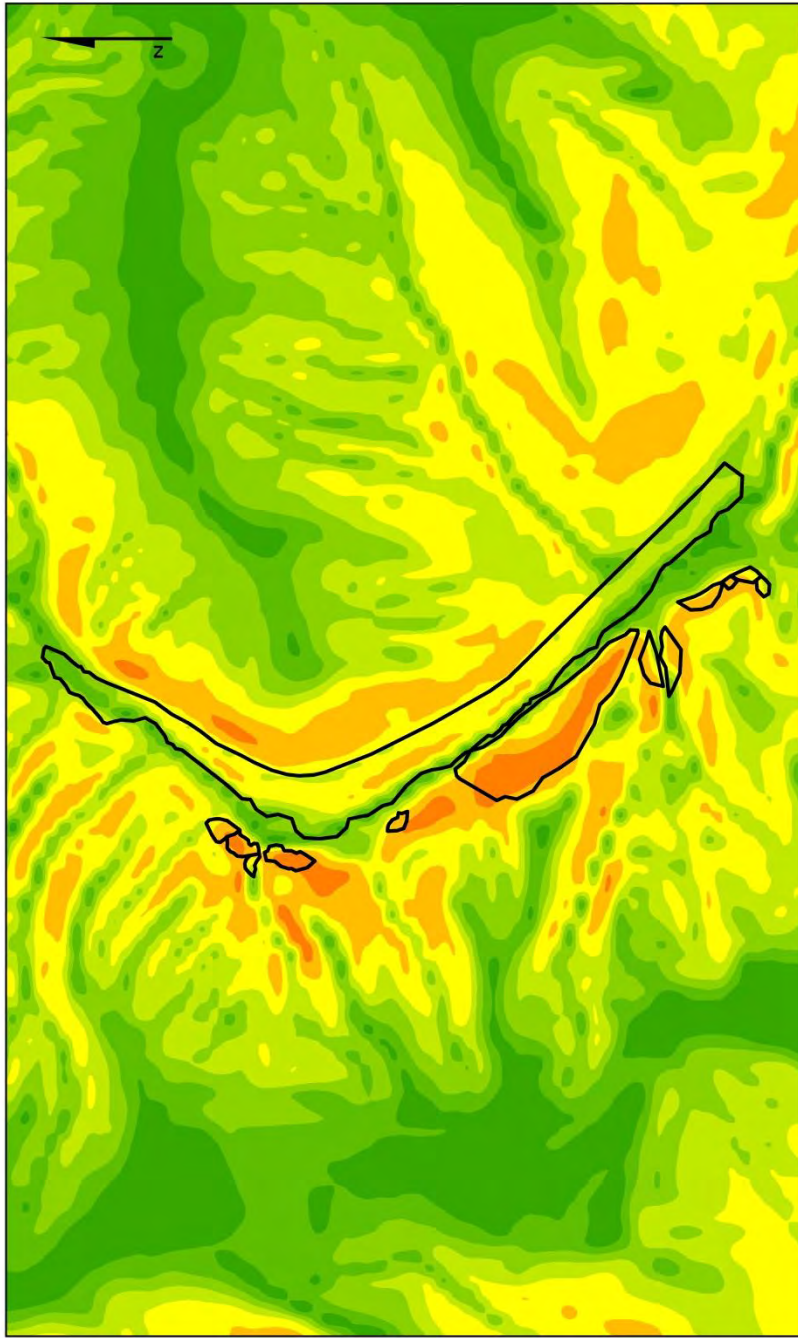
Source: OIT (2007)  
 Produced by: Michael P. Glassmeyer

Figure AVII.41: Topographic map of the Elstun Road landslide.



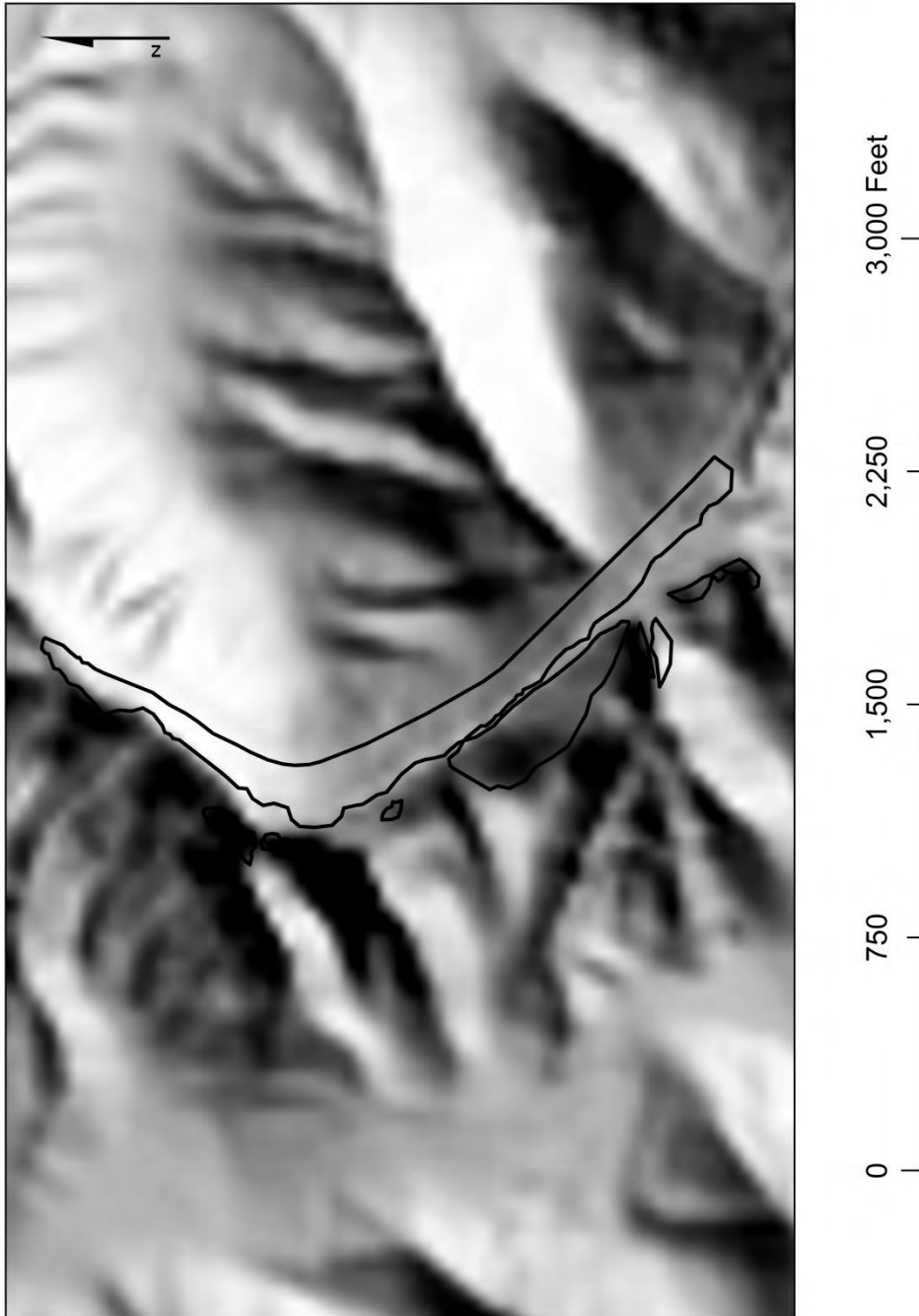
Source: OIT (2007)  
Produced by: Michael P. Glassmeyer

Figure AVI.42: Aerial photograph of the Elstun Road landslide.



Source: OIT (2007)  
 Produced by: Michael P. Glassmeyer

Figure AVI.43: Slope map of the Nordyke Road landslide.



Source: OIT (2007)  
Produced by: Michael P. Glassmeyer

Figure AVI.44: Hillshade map of the Nordyke Road landslide.



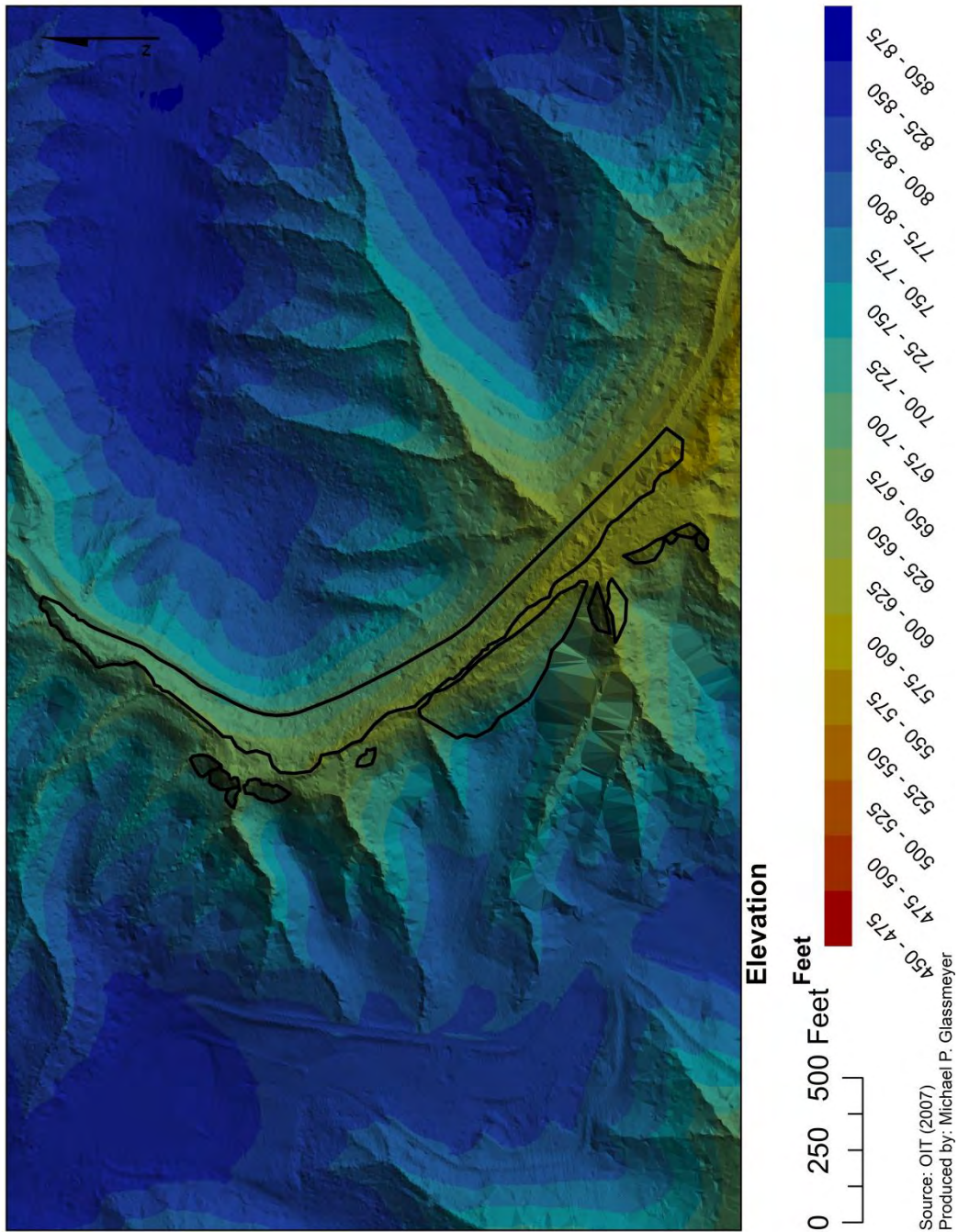


Figure AVI.45: Terrain map of the Nordyke Road landslide.

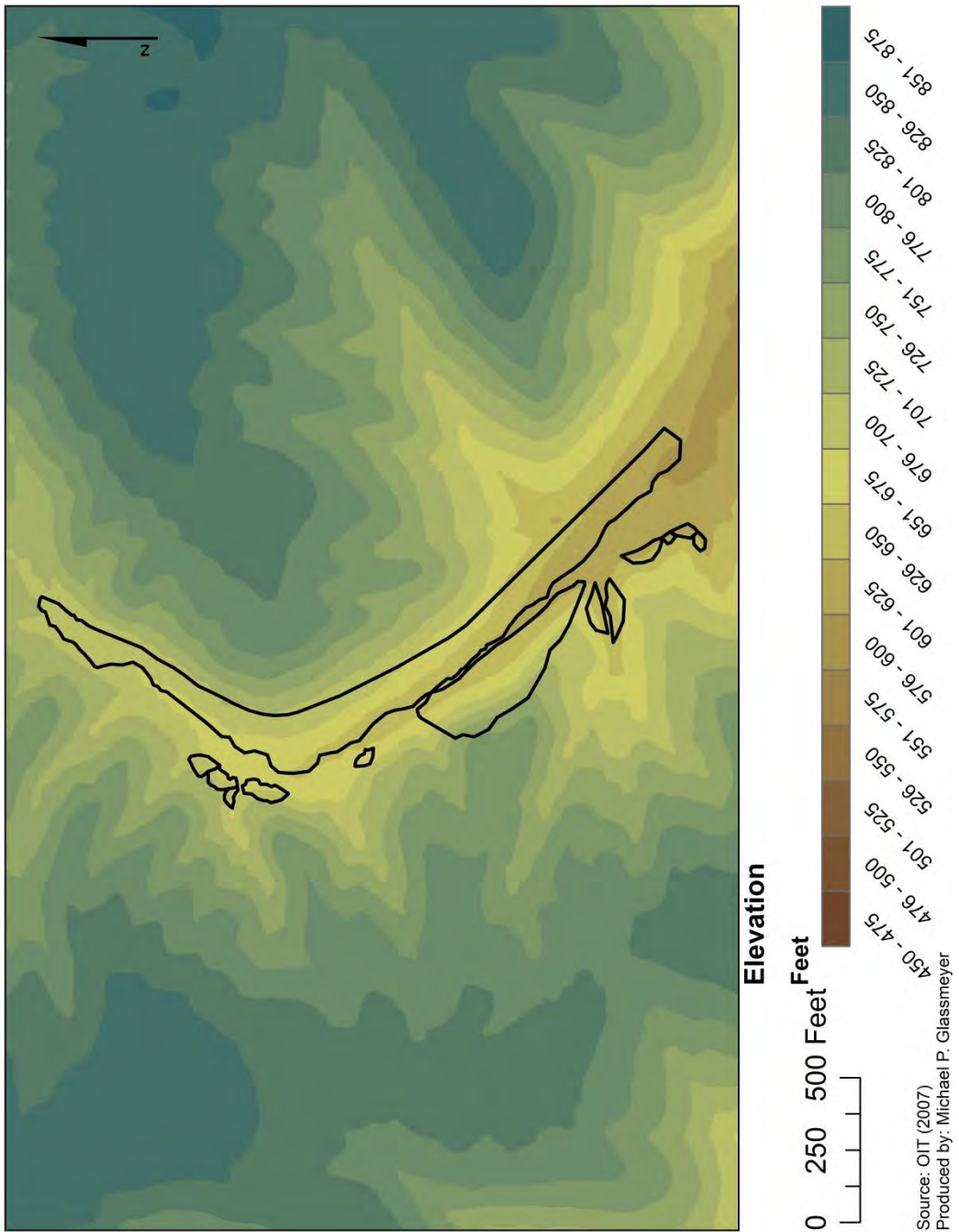
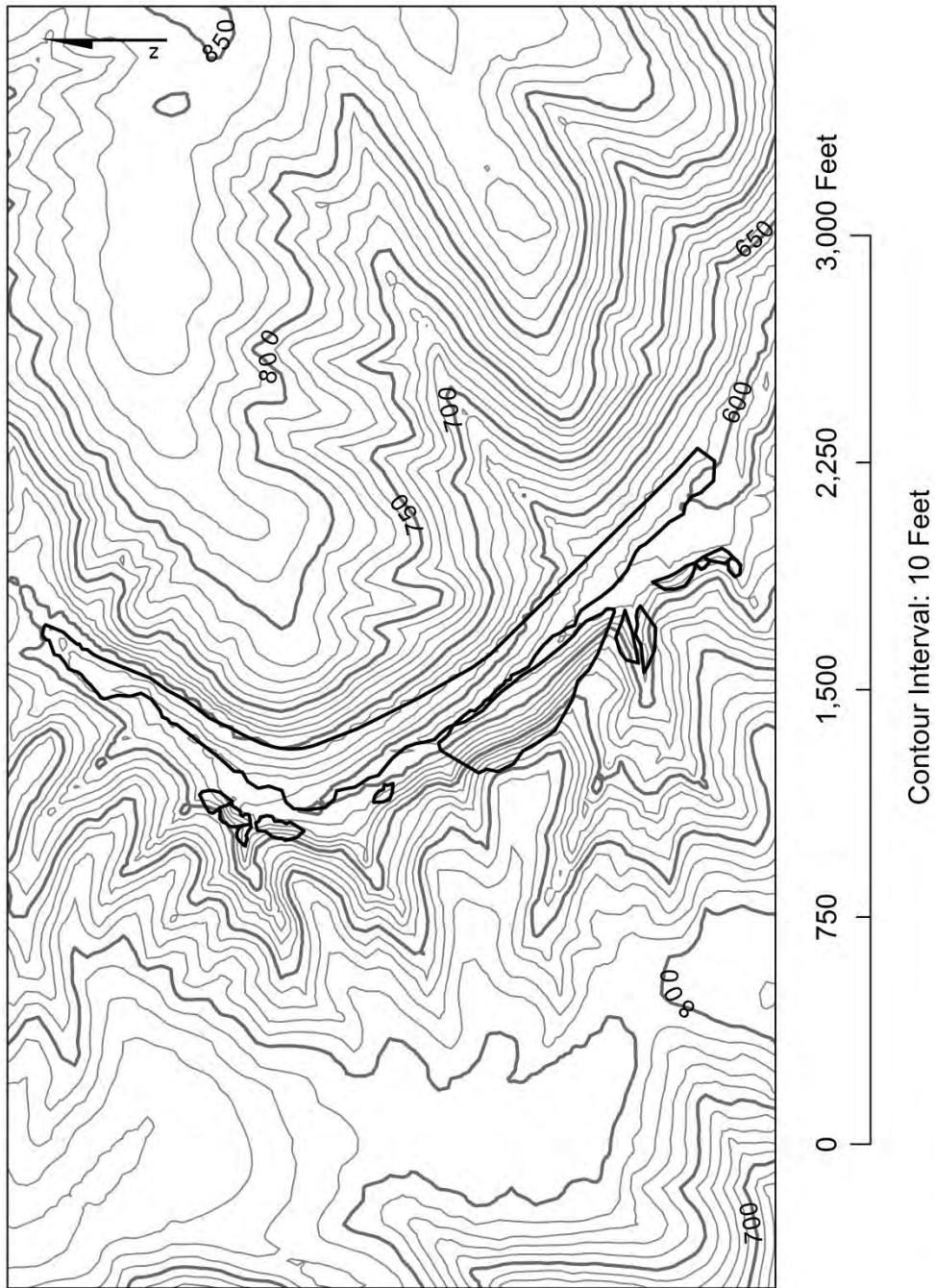


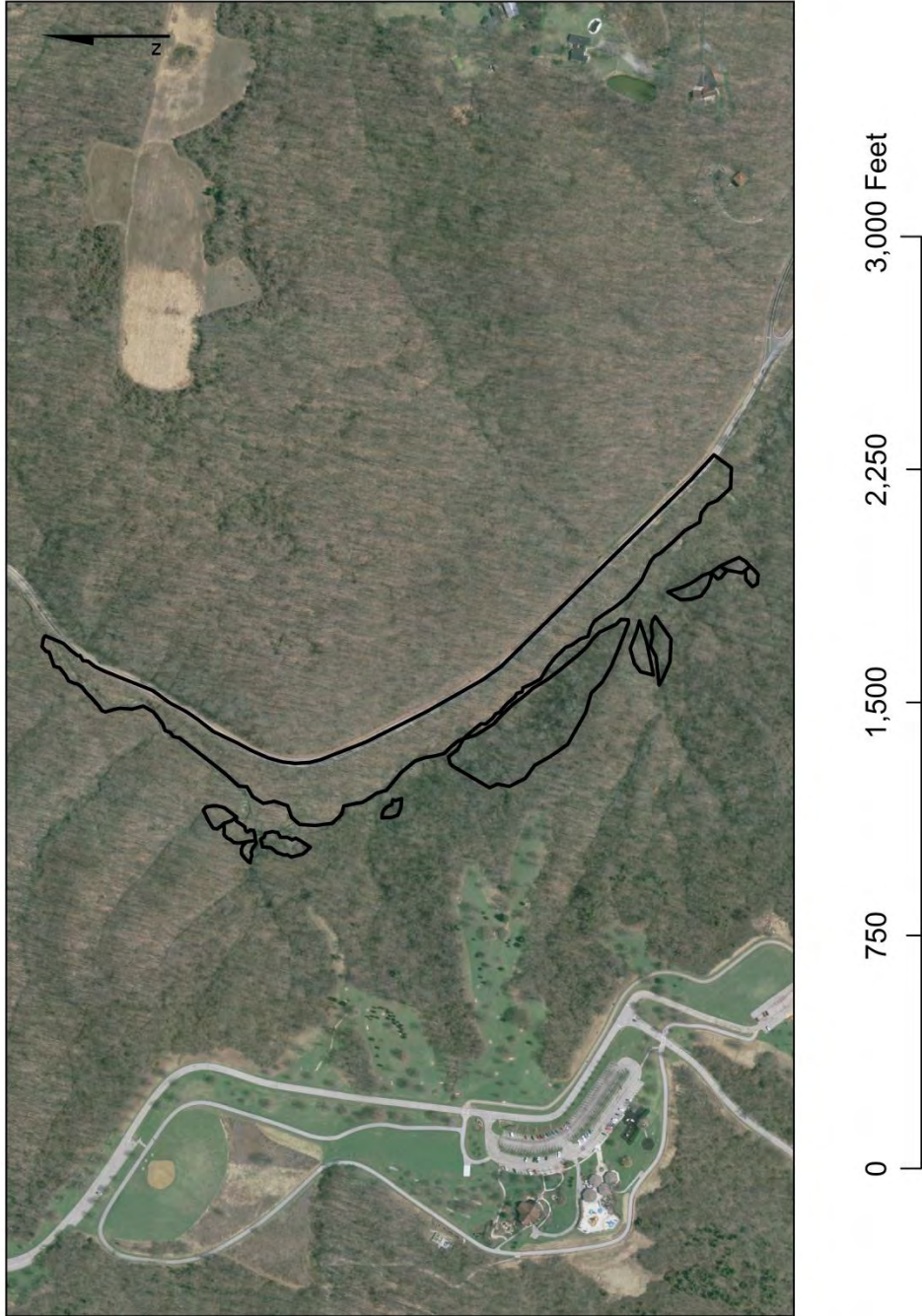
Figure AVI.46: DEM map of the Nordyke Road landslide.





Source: OIT (2007)  
 Produced by: Michael P. Glassmeyer

Figure AVI.47: Topographic map of the Nordyke Road landslide.



Source: OIT (2007)  
Produced by: Michael P. Glassmeyer

Figure AVI.48: Aerial photograph of the Nordyke Road landslide.

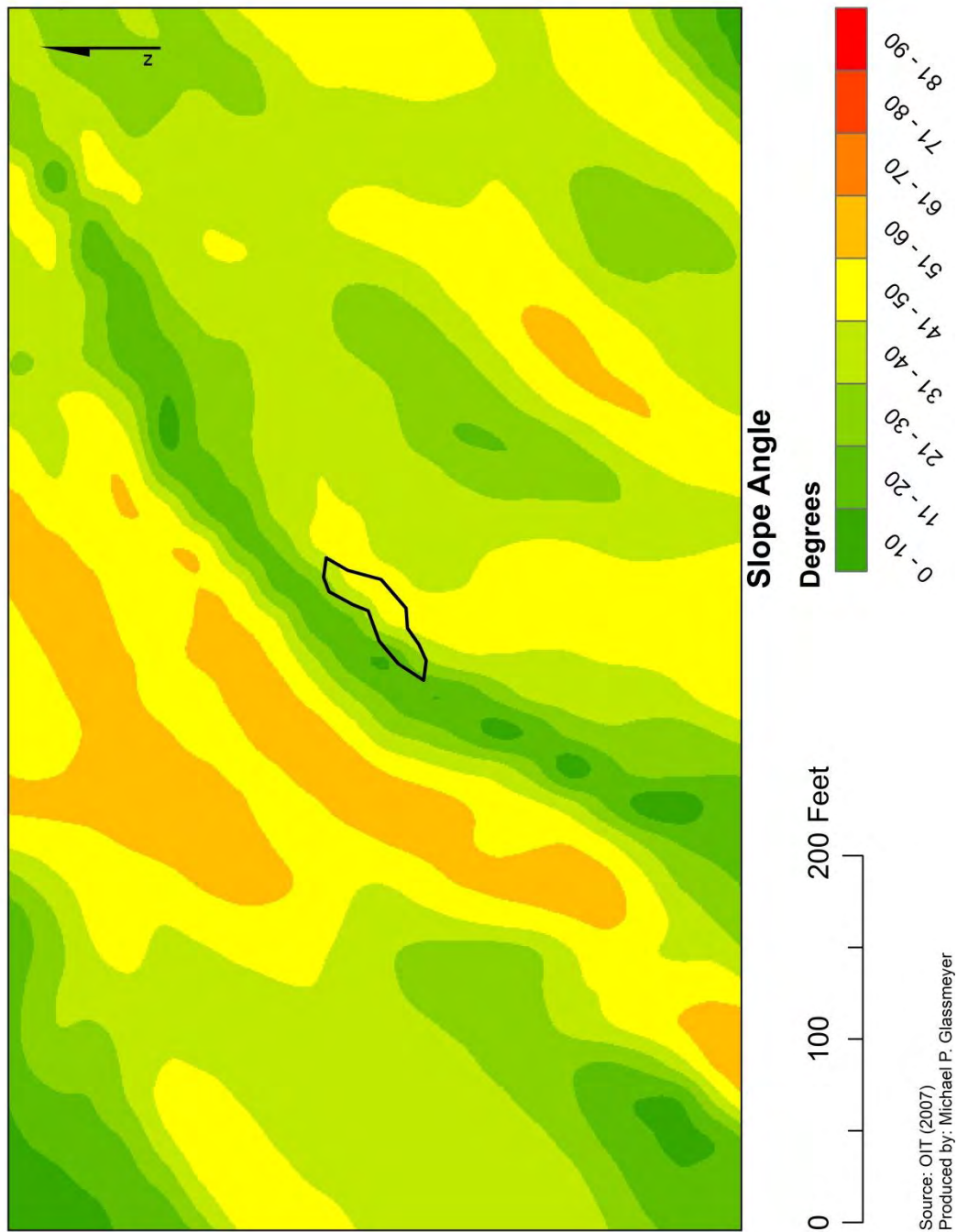


Figure AVI.49: Slope map of the Old US 52 landslide.

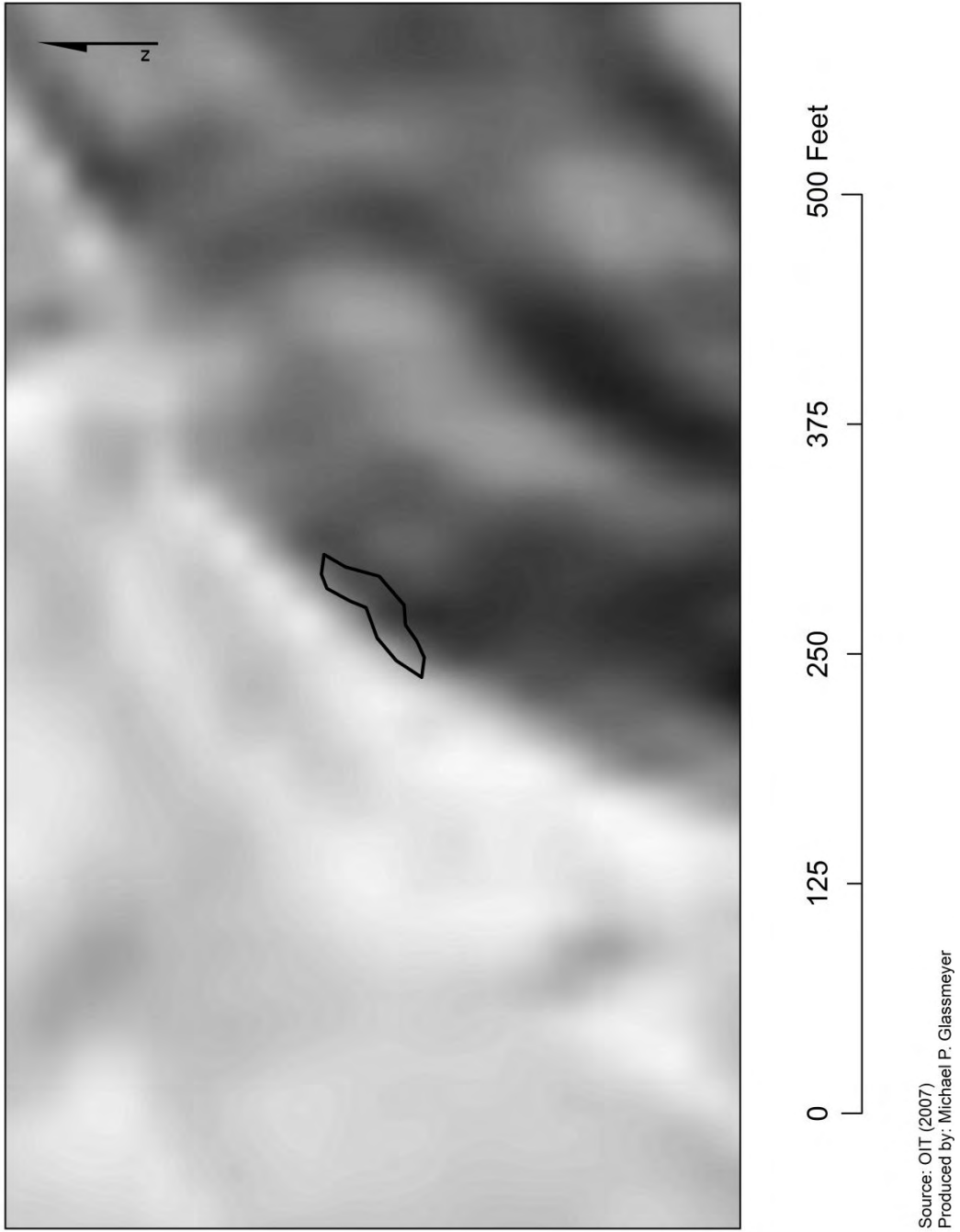


Figure AVI.50: Hillshade map of the Old US 52 landslide.



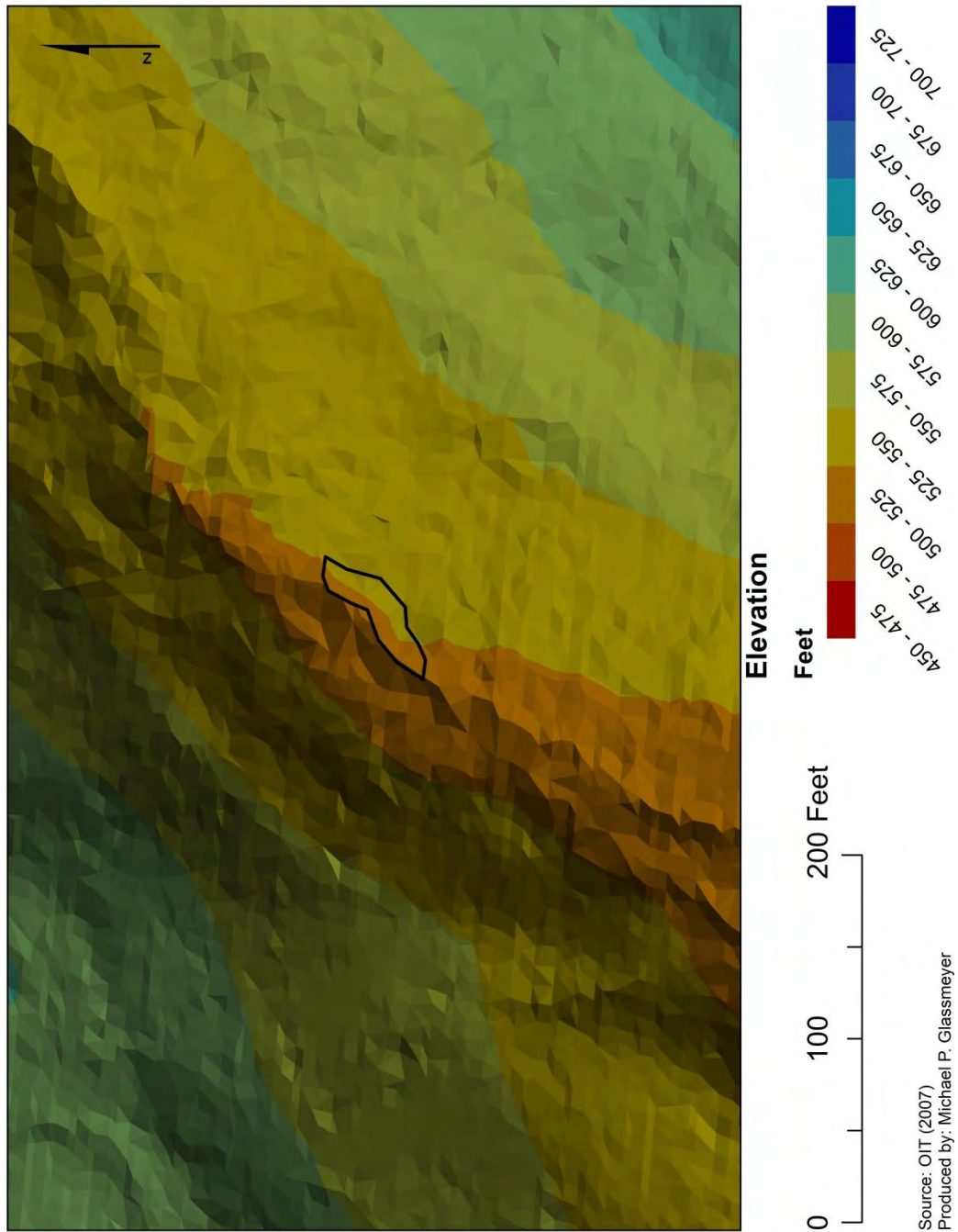


Figure AVI.51: Terrain map of the Old US 52 landslide.

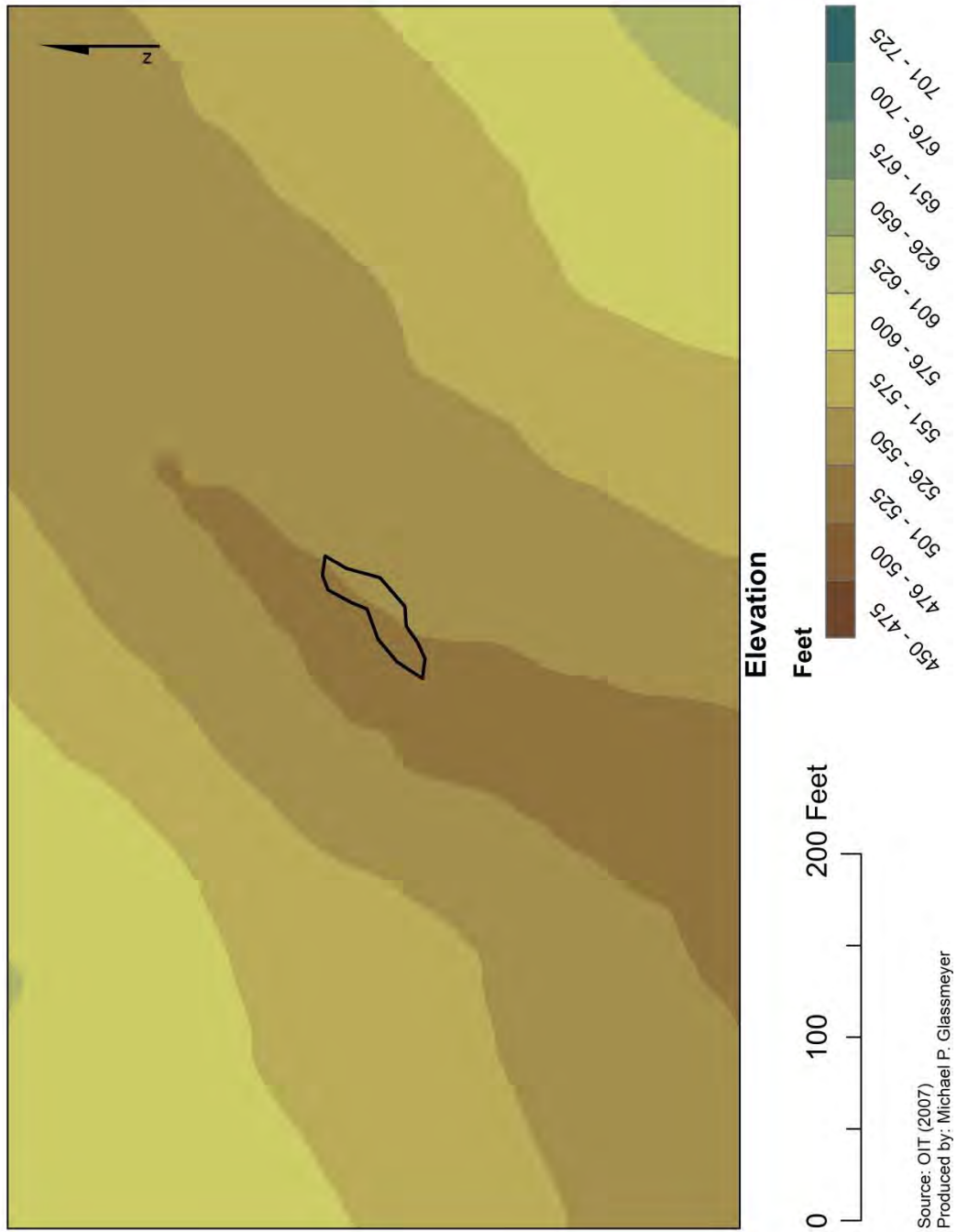
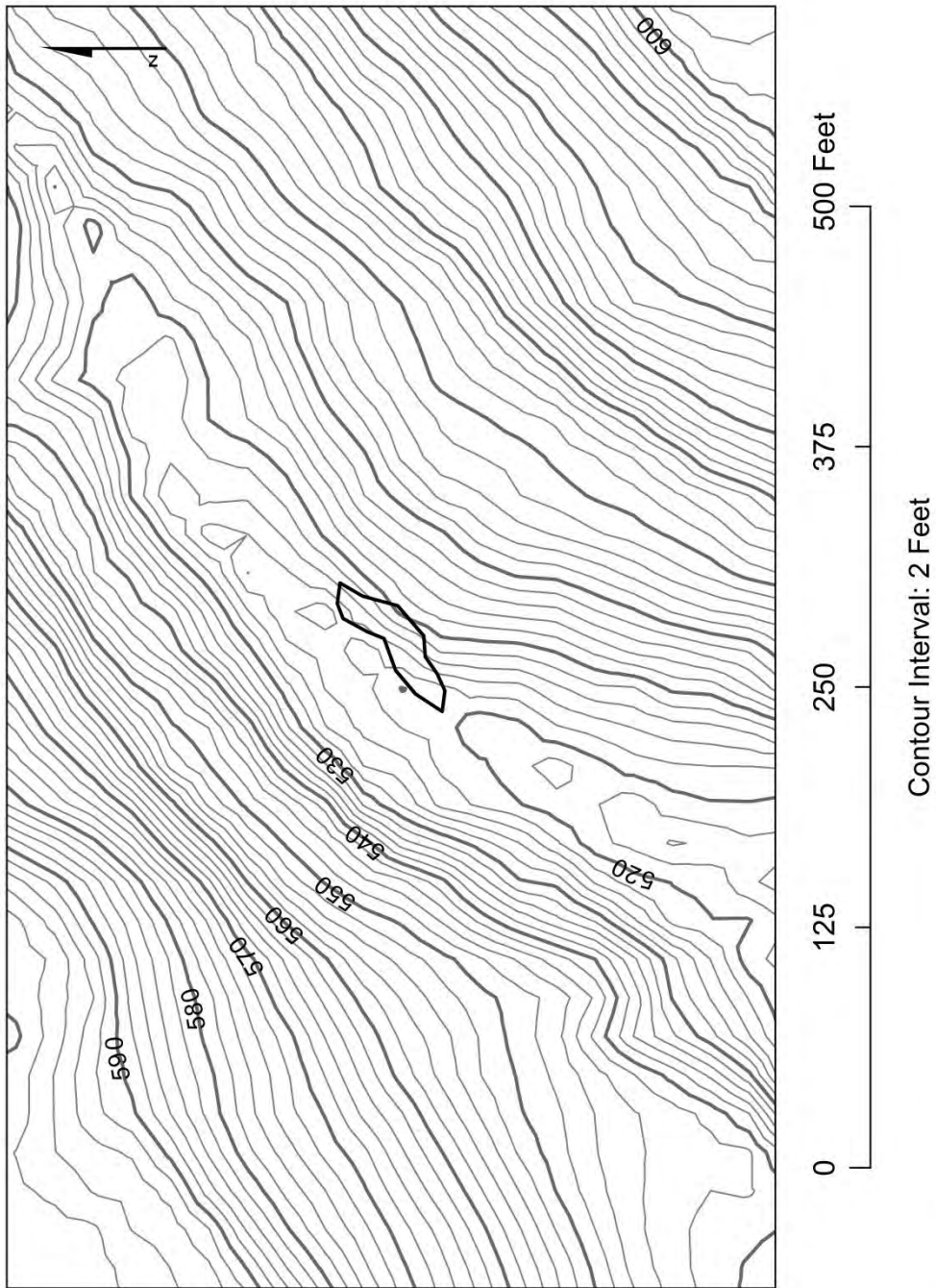


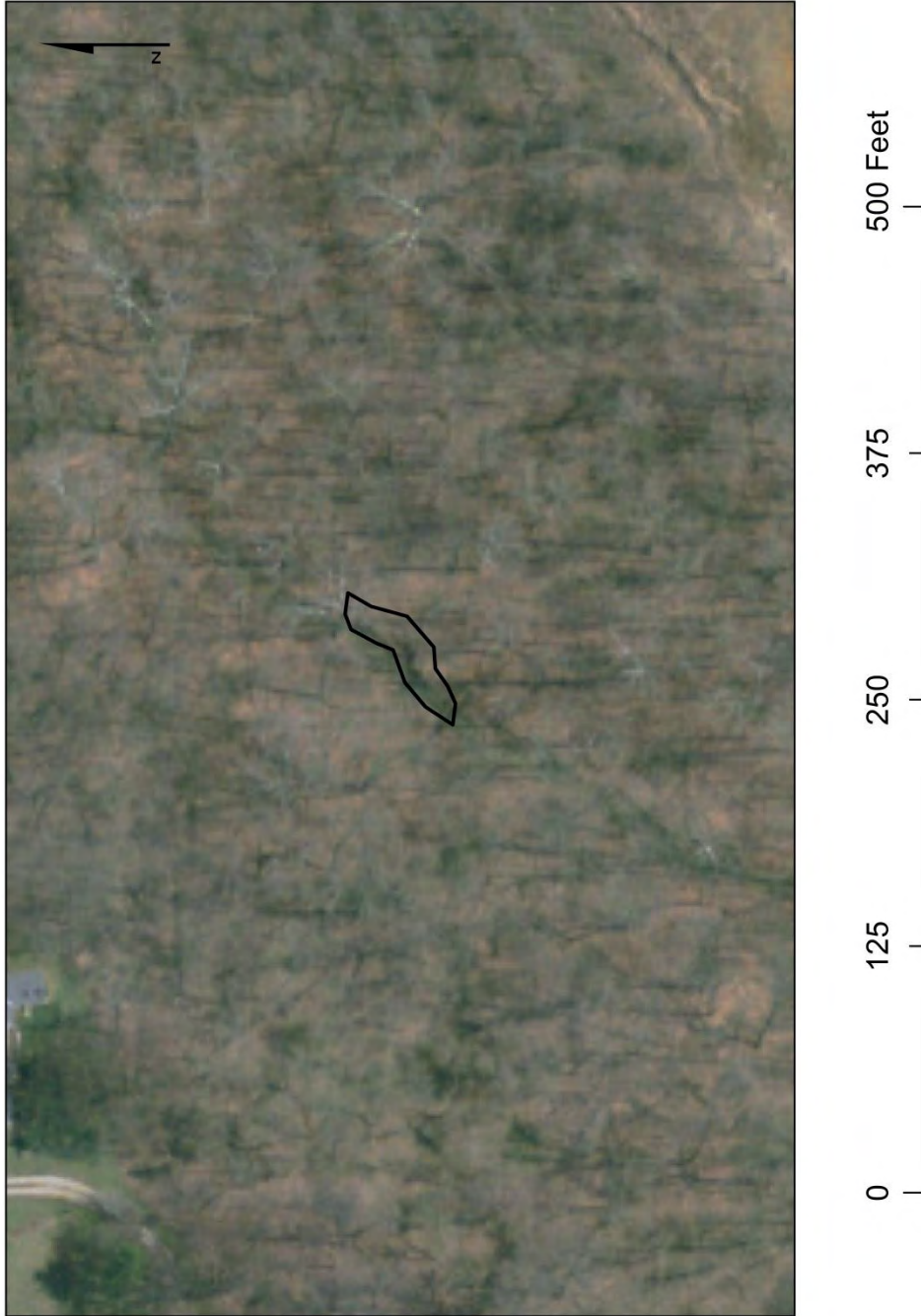
Figure AVI.52: DEM map of the Old US 52 landslide.





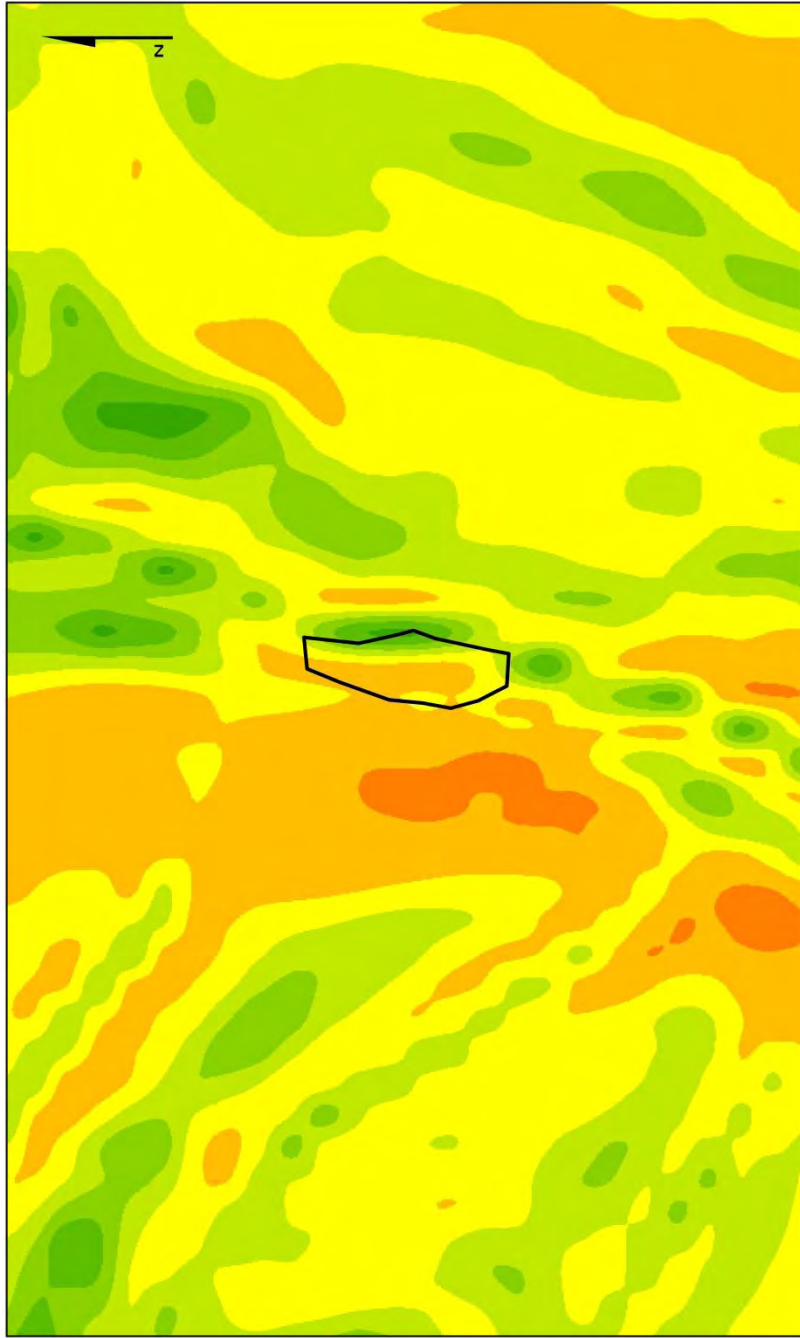
Source: OIT (2007)  
 Produced by: Michael P. Glassmeyer

Figure AVI.53: Topographic map of the Old US 52 landslide.



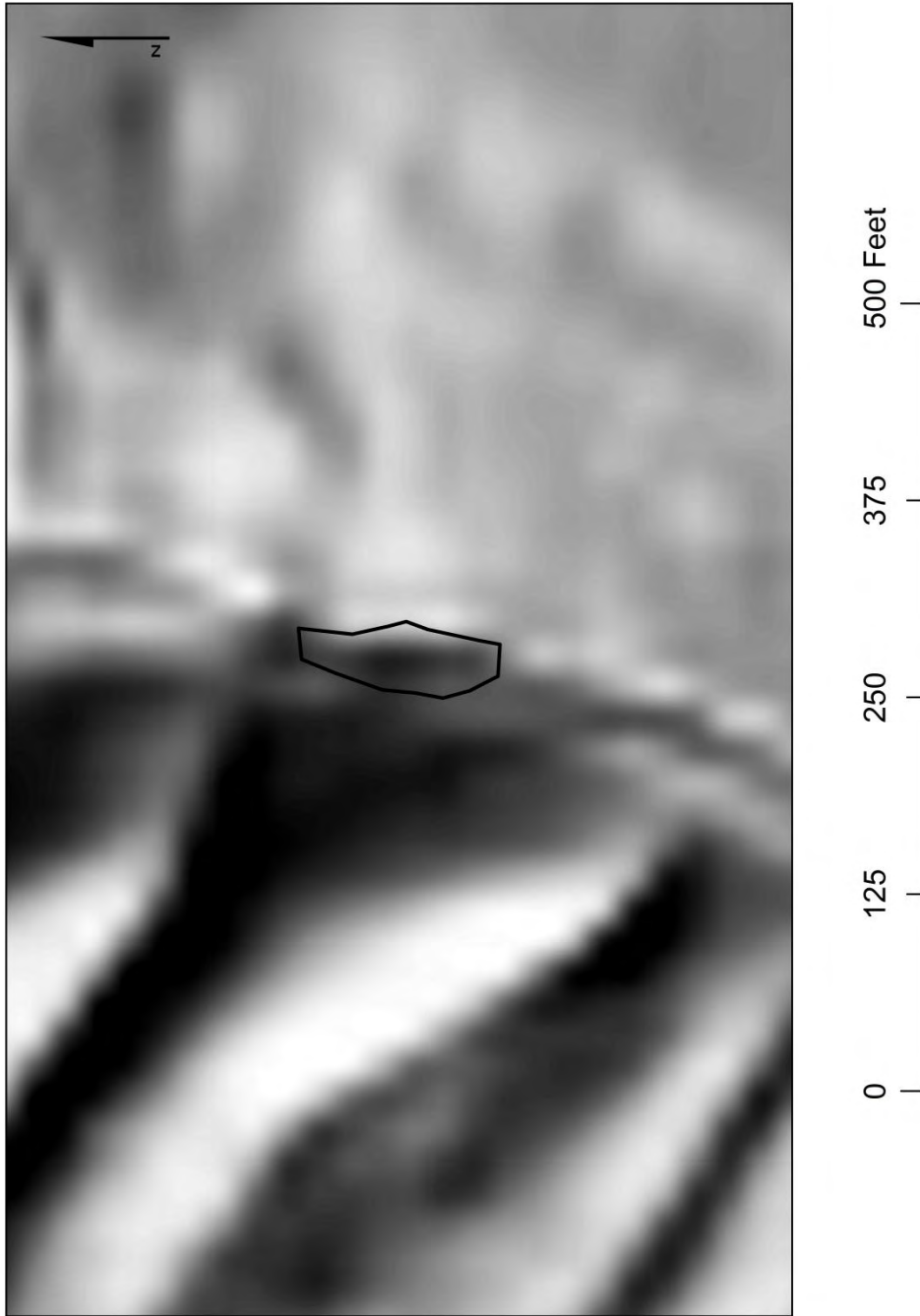
Source: OIT (2007)  
Produced by: Michael P. Glassmeyer

Figure AVI.54: Aerial photograph of the Old US 52 landslide.



Source: OIT (2007)  
 Produced by: Michael P. Glassmeyer

Figure AVI.55: Slope map of the Wagner Road landslide.



Source: OIT (2007)  
Produced by: Michael P. Glassmeyer

Figure AVI.56: Hillshade map of the Wagner Road landslide.



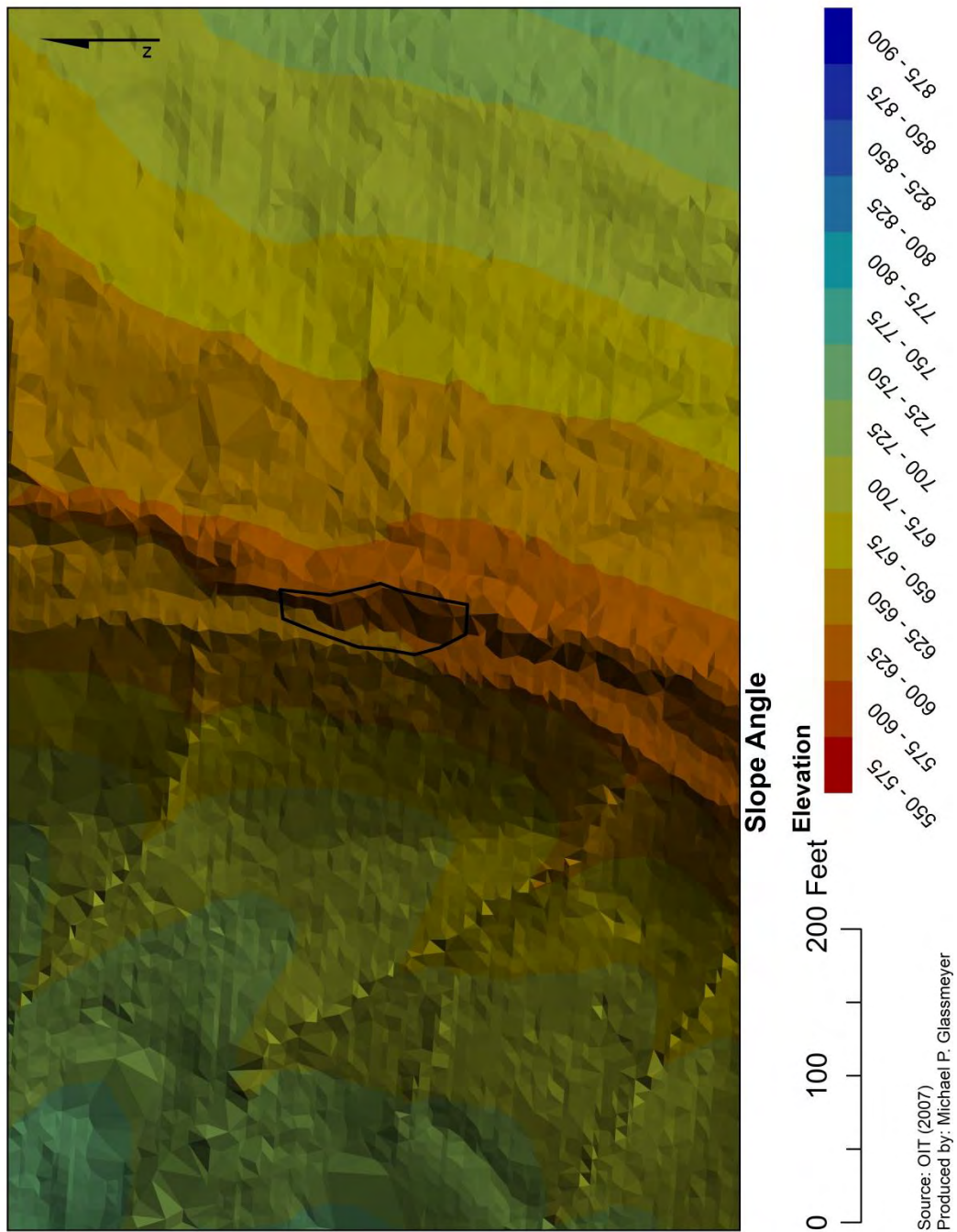


Figure AVI.57: Terrain map of the Wagner Road landslide.

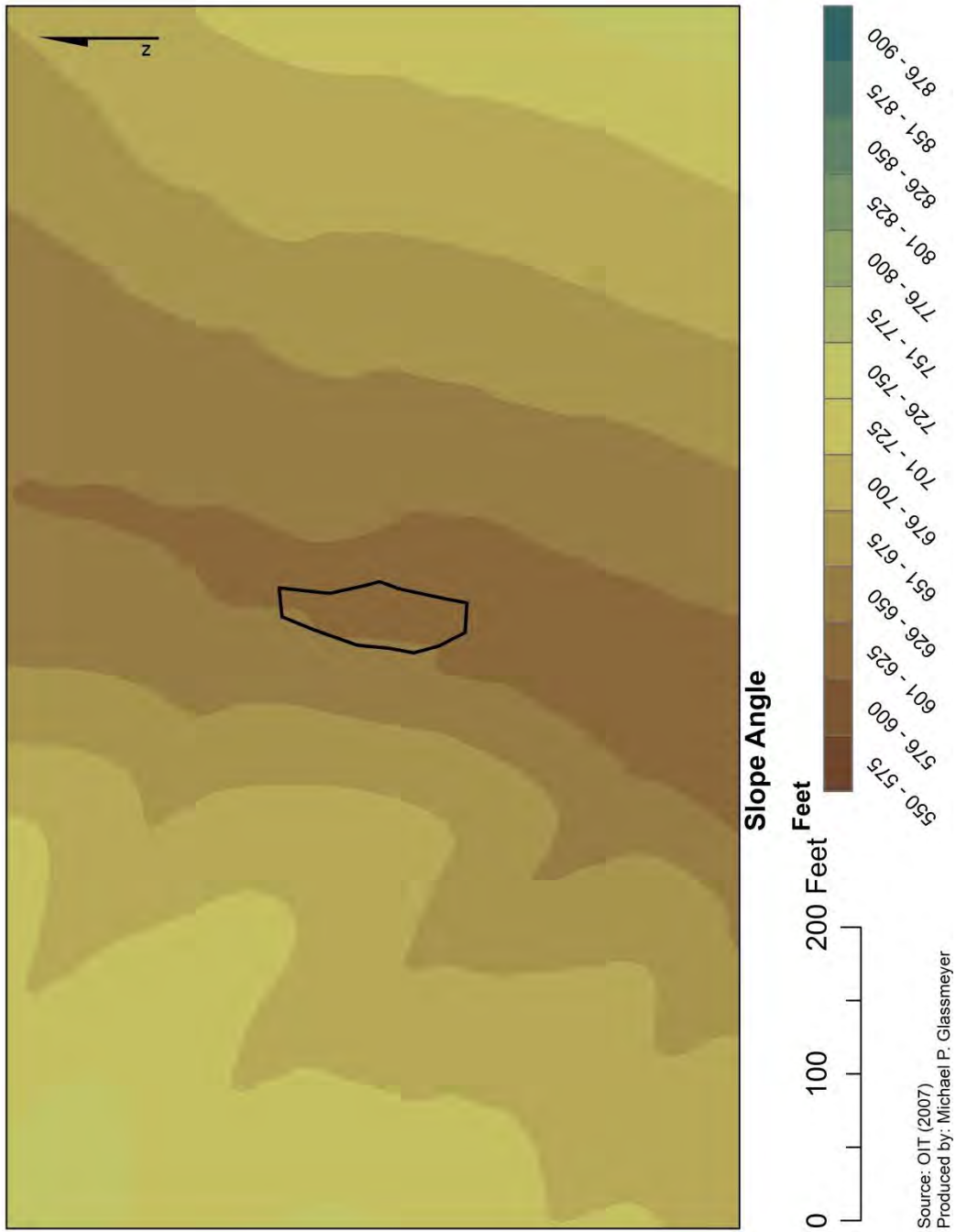
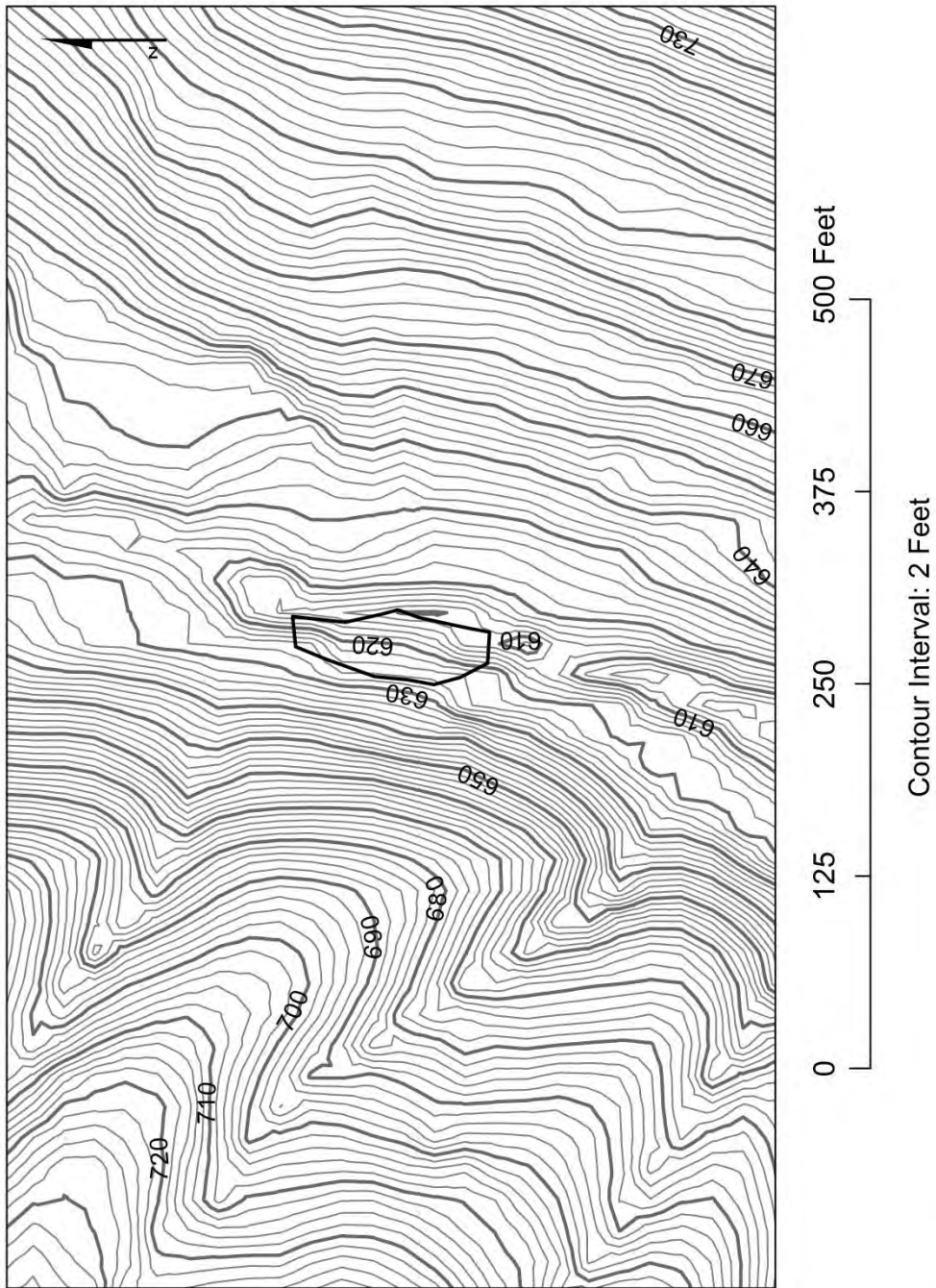


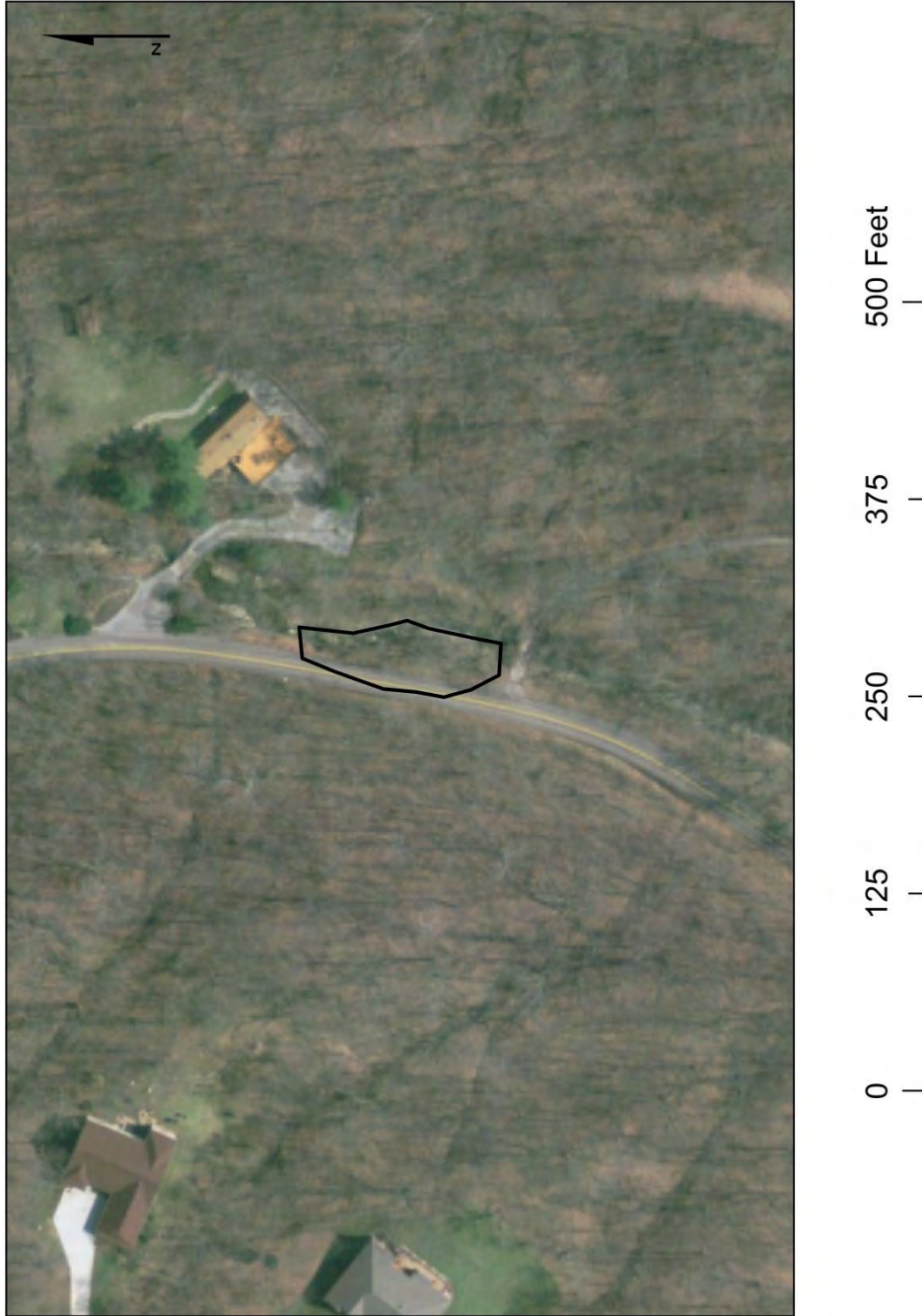
Figure AVI.58: DEM map of the Wagner Road landslide.





Source: OIT (2007)  
 Produced by: Michael P. Glassmeyer

Figure AVI.59: topographic map of the Wagner Road landslide.



Source: OIT (2007)  
Produced by: Michael P. Glassmeyer

Figure AVI.60: Aerial photograph of the Wagner Road landslide.

## APPENDIX VII

### Borehole Logs for the Wagner Road Landslide

LOG OF BORING NO. B-4										Page 1 of 1														
CLIENT <b>Clermont County Engineers</b>					ELEVATION REFERENCE <b>Interpolated from Site Topographic Plan</b>																			
SITE <b>Wagner Road Pierce Township, Clermont County, Ohio</b>					PROJECT <b>Wagner Road Landslide Stabilization</b>																			
Boring Location: As Shown on Boring Location Plan					SAMPLES		TESTS																	
GRAPHIC LOG	DESCRIPTION				DEPTH, ft.	USCS SYMBOL	NUMBER	TYPE	RECOVERY, %	BLOWS / 6in. (SPT - N)	WATER CONTENT, %	DRY UNIT WT pcf	UNCONFINED STRENGTH, psf											
	Approx. Surface Elev.: 626.69 ft																							
	0.5	<b>ASPHALT PAVEMENT</b>													626.2									
	1	<b>GRANULAR BASE</b> , sand and gravel, brown													625.7	1	SS	100	30					
	2.5														624.2	1a	SS	100	10-12				6000*	
	4	<b>FILL</b> , lean clay, trace limestone fragments, little sand, silt, brown, very stiff													622.7	CL	SS	100	6-5-7 (12)	23	102	5200		
	5	<b>LEAN CLAY</b> , little silt, trace limestone fragments, brown, very stiff													621.7									
		<b>LIMESTONE</b> , hard																						
	8	Interbedded <b>SHALE and LIMESTONE</b>													618.7									
		<b>SHALE</b> , brown, severely weathered, soft														1	NQ	93	CORED	@ 5.8" = 14			@ 5.8" = 10304 psf	RQD = 43%
		<b>LIMESTONE</b> , light gray, hard																						
		<b>SHALE</b> , with occasional limestone layers, moderately weathered, medium hard														2	NQ	96	CORED					RQD = 28%
	13	Boring Compelled @ 13'													613.7									

The stratification lines represent the approximate boundary lines between soil and rock types: in-situ, the transition may be gradual. \*Calibrated Hand Penetrometer


WATER LEVEL OBSERVATIONS, ft					BORING STARTED		4-27-11		
WL	∇	N/A	WD		∇	10	AB	BORING COMPLETED	4-27-11
WL	∇	BF	@		0 hrs	∇		RIG	Truck FOREMAN JJ
WL								APPROVED	DRK JOB # N1115091

Figure AVII.1: Borehole log of the Wagner Road landslide.



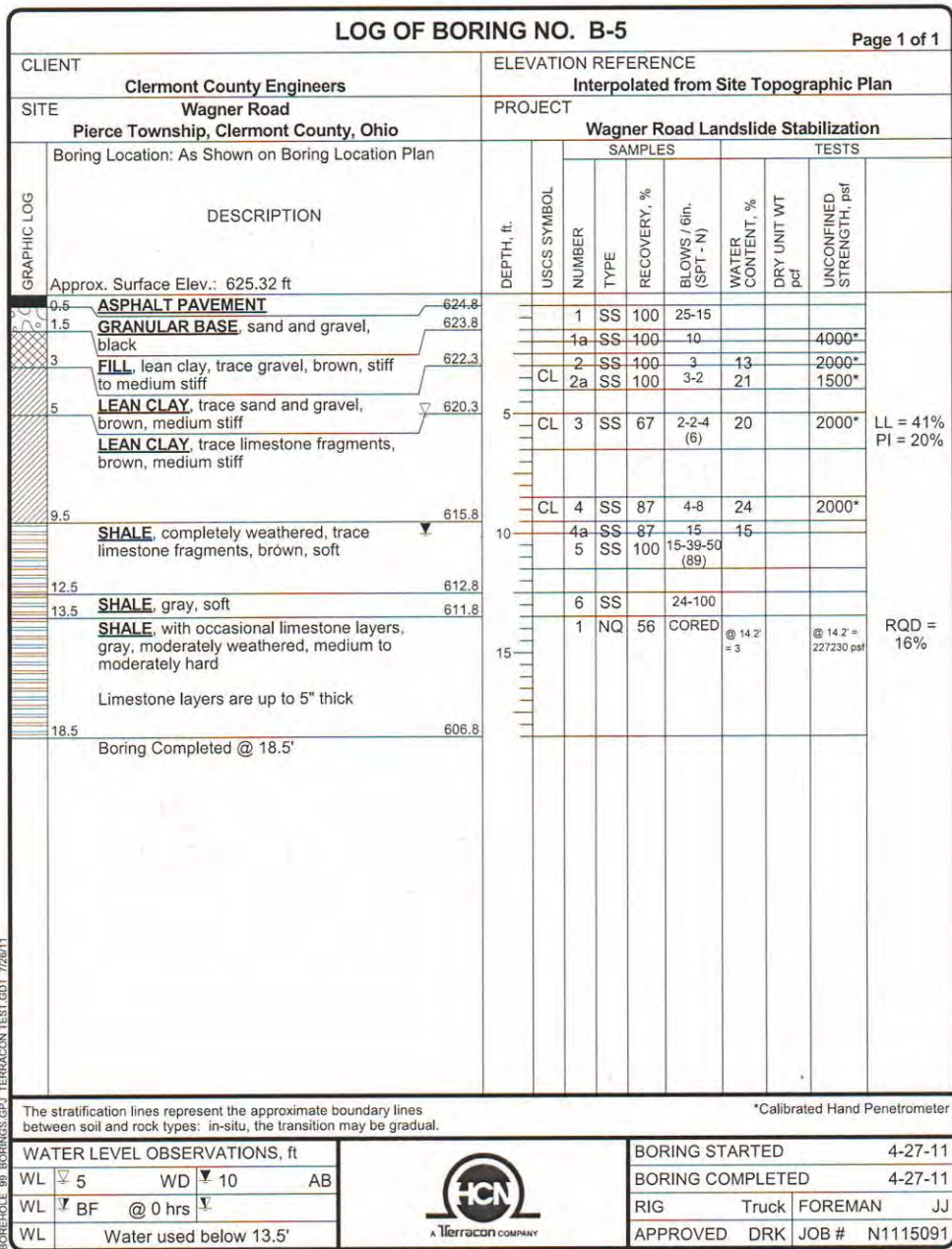


Figure AVII.2: Borehole log of the Wagner Road landslide.